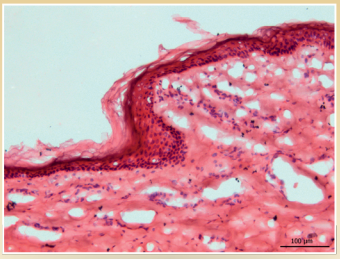

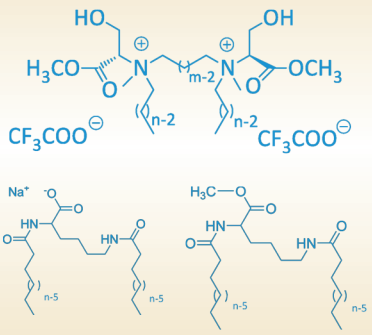

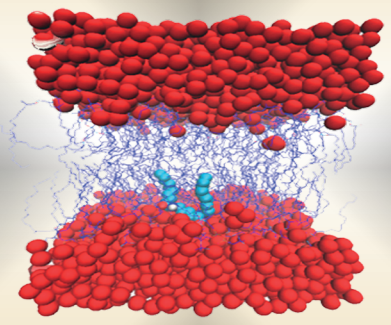

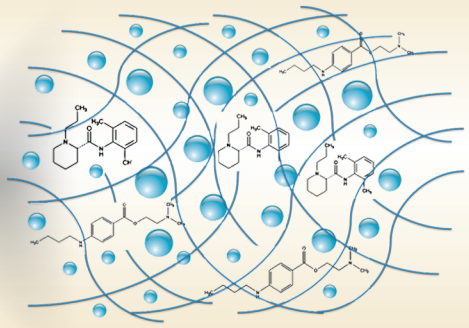

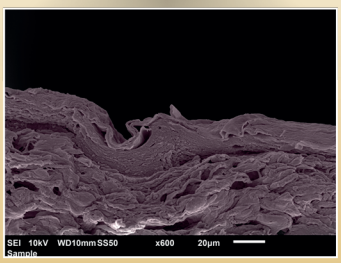

Raquel da Silva Teixeira

PHARMACEUTICAL DEVELOPMENT OF LOCAL ANESTHETICS FORMULATIONS FOR TOPICAL ADMINISTRATION

Tese de doutoramento em Farmácia, na Especialidade de Tecnologia Farmacêutica, orientada pelo Senhor Professor Doutor Francisco José Baptista Veiga e pela Senhora Professora Doutora Rita Cristina Sanches Oliveira e apresentada à Faculdade de Farmácia da Universidade de Coimbra

2014

· U C ·

UNIVERSIDADE DE COIMBRA

Pharmaceutical development of local anesthetics formulations for topical administration

Faculdade de Farmácia da Universidade de Coimbra

Raquel da Silva Teixeira

2014

Doctoral thesis submitted to the Pharmacy Faculty of University of Coimbra, in fulfillment of the requirements for the degree of Doctor of Philosophy in Pharmacy, specializing in Pharmaceutics Technology.

Tese de Doutoramento para obtenção do grau de Doutor em Ciências Farmacêuticas, especialidade de Tecnologia Farmacêutica e apresentada à Faculdade de Farmácia da Universidade de Coimbra.

The work presented in this thesis was carried out at the Center of Pharmaceutical Studies (CEF), Department of Pharmaceutics, Faculty of Pharmacy, University of Coimbra (Portugal), at the Chemistry Center, Chemistry Department, University of Coimbra (Portugal), at the Institute of Pharmaceutical Science, King's College, London, and funded by Fundação para a Ciência e Tecnologia (SFRH/BD/66968/2009), Lisboa, Portugal.

O trabalho apresentado nesta tese foi desenvolvido no Laboratório de Tecnologia Farmacêutica, Centro de Estudos Farmacêuticos (CEF) da Faculdade de Farmácia da Universidade de Coimbra (Portugal), no Centro de Química, Departamento de Química da Faculdade de Ciências e Tecnologia da Universidade de Coimbra (Portugal) e no Instituto de Ciências Farmacêuticas, King's College London (Inglaterra), e suportado financeiramente pela Fundação para a Ciência e Tecnologia (FCT), (SFRH/BD/66968/2009), Lisboa, Portugal.

Aos meus Pais, Avós e Irmão

Aos meus Familiares

Aos meus Amigos

Ao Sérgio

“*It always seems impossible until it is done*”

Nelson Mandela

Agradecimentos

Esta tese de doutoramento é o culminar de uma longa e árdua batalha. Confesso que foi difícil. Foi difícil para além de todo o trabalho e início da escrita da tese perceber que ainda faltava muito para conquistar o objectivo. Foi difícil gerir tudo, enfrentar adversidades e lidar com as frustrações. Foi difícil ficar longe da família e deixar para trás momentos que já não voltam mais. Mas ninguém me disse que ia ser fácil. Só me diziam que quanto maior o desafio maior a vitória. Por isso me esforcei, quebrei as barreiras, propus-me ao desafio, superei os meus limites tendo sempre em mente que entre muitos, poderia também ser a melhor.

Embora tenha sido uma luta minha, esta tese não seria possível sem a intervenção de pessoas que directamente ou indirectamente contribuíram para a sua realização. Em particular, gostaria de começar por agradecer de forma muito especial aos meus orientadores científicos que acreditaram em mim e me abriram portas para esta grande jornada. Ao Professor Doutor Francisco José Baptista Veiga, também na qualidade de director da Faculdade de Farmácia da Universidade de Coimbra, por ter reunido todas as condições necessárias à realização deste projecto. Agradeço especialmente todas as suas palavras amigas, a sua disponibilidade, conselhos, paciência e contínuo apoio ao longo de todo o meu doutoramento. Por todas estes motivos mas também pela crença nas minhas capacidades, permitiram-me enfrentar com mais força os desafios que o doutoramento colocou. À Professora Doutora Rita Sanches Oliveira da Universidade Fernando Pessoa, pelo projecto de doutoramento, correcções e sugestões científicas mas também por todo o incentivo, carinho e amizade demonstrados. Ao Professor Doutor Delfim Santos da Faculdade de Farmácia da Universidade do Porto, que me incentivou a abraçar este projecto.

Gostaria igualmente de agradecer ao Professor Doutor Alberto António Caria Canelas Pais e ao Professor Doutor Artur Valente do Departamento de Química da Universidade de Coimbra, que me ajudaram eximiamente no meu percurso de doutoramento. Gostava de expressar a minha eterna gratidão, por me terem acolhido, pelo apoio científico, análises críticas e discussões científicas. Mas especialmente gostava de expressar o

meu agradecimento pelo contínuo apoio e por terem sido incansáveis quando mais precisei. Aos meus colegas e amigos também do mesmo departamento, João Almeida pelo apoio e orientação no início do meu doutoramento e à Tânia Firmino pelo apoio, profissionalismo, dedicação aos estudos de simulação molecular mas especialmente por toda a sua amizade e incentivo. Ao Professor Doutor Eduardo Marques do Departamento de Química da Universidade do Porto, não só pela síntese dos tensioactivos à base de aminoácidos mas também pela oportunidade inovadora de os testar como promotores de permeação dos meus fármacos como também pela sua contribuição científica na discussão dos resultados obtidos.

Gostaria também de agradecer à Professora Doutora Teresa Rosete e à Doutora Ana Silva pela ajuda prestada durante os trabalhos que envolveram a cultura de células e avaliação de citoxicidade. À Professora Doutora Isabel Vitória e ao Fábio Branco pela ajuda prestada durante os estudos *in vivo.*

Agradeço aos meus colegas e amigos do departamento de Química, Andreia Jorge, Filipe Antunes, Luís Alves e Sandra Nunes, e da Faculdade de Farmácia, Amélia Vieira, Ana Fortuna, Ana Claúdia Santos, Ana Serralheiro, Carla Varela, Carla Vitorino, Daniela Gonçalves, Dulce Bento, Fátima Pina, Filipa Lebre, Ivo Múrias, Joana Almeida, Joana Bicker, Marisa Gaspar, Marlene Lopes, Sandra Jesus, Susana Simões, pela amizade e agradável convivência que ajudaram a ultrapassar melhor este desafio que todos igualmente partilhamos.. Agradeço também toda a ajuda, palavras amigas e assistência técnica prestada pela D. Gina.

Parte desta dissertação foi realizada em colaboração com o King's College London (Reino Unido), integrada no grupo de trabalho do Professor Doutor Stuart Jones agradecendo por me ter recebido no seu laboratório, por ter criado as condições necessárias ao desenvolvimento do trabalho e também todas as críticas, correcções e aconselhamento científico. Estendo os meus agradecimentos aos meus colegas com quem partilhei bons momentos em Londres, Richard Amison, Dania Hussein, Ricardo Inácio, Jasminder Chana, Aateka Patel, Julie Tzu-Wen, Nuelia Rubio, Giovanni Emma, Anna Poschl, Gian Luca, Magda Ska, Marie Defays e especialmente a Jesmine Cai e Marcelo da Silva por toda a amizade. Contudo, não poderia deixar de agradecer individualmente a duas pessoas que muito contribuíram para o meu bem-estar pessoal durante a minha longa e solitária estadia em Londres, a Swetha Monghra e Vicky Sheard. Embora fisicamente distantes a nossa amizade perdura e tem sido uma constante força de motivação ao longo da minha jornada.

À Fundação para a Ciência e Tecnologia (FCT, Lisboa, Portugal) entidade que financiou o meu projecto de doutoramento com a referência SFRH / BD / 66968 / 2009, deixo os meus votos de sincero agradecimento. A atribuição desta bolsa de doutoramento foi crucial para o desenvolvimento do trabalho quer em Coimbra, quer em Londres.

De forma especial quero agradecer à minha querida e estimada amiga, Leninha que infelizmente já não está fisicamente entre nós, deixo o meu agradecimento sentido por toda a amizade, apoio e boa disposição. Aos restantes amigos, Vânia Sá, Hugo Pereira,

Tó Zé, Ricardo Melo, João Silva, Nuno Lajes e Bruno Reis pela amizade e carinho sempre demonstrados.

Os meus agradecimentos não estariam completos se não agradecesse à minha família. Aos meus pais, ao meu irmão e avós pelo amor, apoio incondicional e amizade que contribuíram para o meu bem-estar emocional. Por último, mas não menos importante, presto o meu agradecimento ao Sérgio pelo companheirismo, confiança, sacrifício e dedicação. Compreendeu o quão valiosa esta etapa era para mim e por isso reuniu esforços para me ajudar e incentivar na escolha do melhor caminho. "*As pessoas entram na nossa vida por acaso, mas não é por acaso que permanecem nela*".

Para além de um considerável esforço pessoal na realização desta tese de doutoramento, pude contar com um número muito grande de contribuições, apoios, sugestões, comentários e críticas vindas de pessoas que referi. A sua importância assume uma valia tão preciosa que, sem elas, com toda a certeza, teria sido muito difícil chegar a qualquer resultado digno de menção.

Contents

List of figures

List of tables

Abbreviations

ACN	Acetonitrile
CD	Cyclodextrin
CER	Ceramides
CHO	Cholesterol
CMC	Critical micelle concentration
CPE	Chemical Permeation Enhancer
D	Translational diffusion coefficient
DLS	Dynamic light scattering
DMEM	Dulbecco's Modified Eagle Medium
DPPC	Dipalmitoylphosphatidylcholine
DSC	Differential scanning calorimetry
EE	Entrapment efficiency
ER	Enhancement ratio
FBS	Fetal bovine serum
H&E	Ellis Hematoxylin and Eosin
HEK	Human epidermal keratinocytes
HPLC	High performance liquid chromatography
HPMC	Hydroxypropylmethylcelulose
HP-β-CD	Hydroxypropyl Beta cyclodextrin
K	Apparent stability constants
LOD	Limit of detection
LOQ	Limit of quantification
LUV	Large unilamellar vesicles
Lys	Lysine
MD	Molecular dynamics

MDT	Mean dissolution time
MeOH	Methanol
MLV	Multilamellar vesicles
NMF	Natural moisturizing factor
NMR	Nuclear magnetic resonance
PBS	Phosphate Buffer Saline
PC	*L*-*α*-Phosphatidylcholine
PG	Propylene-glycol
PI	Polydispersity index
PME	Particle mesh Ewald
rdf	radial distribution function
ROESY	Rotating Overhauser effect spectroscopy
RPC	Ropivacaine
RSD	Relative standard deviation
S_0	Intrinsic solubility
SB	*Stratum basale*
S_C	Solubility of the inclusion complex
SC	*Stratum corneum*
Scd	Deuterium order parameter
SEM	Scanning electron microscopy
Ser	Serine
SG	*Stratum granulosum*
SL	*Stratum lucidum*
SPC	Simple point charge
SS	*Stratum spinosum*
SUV	Small unilamellar vesicles
TC	Tetracaine
TLE	Thin Layer Evaporation
UV/Vis	Ultra Violet visible spectroscopy
ZP	Zeta potential

Abstract

The work presented in this thesis reports the development of semi-solid anesthetics formulations, for topical application. Two different drugs were used: tetracaine and ropivacaine hydrochloride, an anesthetic with a fast and a slow onset of action, respectively.

The efficacy of a drug applied topically depends on its ability to cross the *stratum corneum*, the outermost layer of the skin, and reputedly its main barrier.

A detailed introduction to the work is presented on Chapter 1. Chapters 2, 3, 4 and 5 report in detail the development and characterization of systems and strategies with the purpose of improving the permeation of the two local anesthetics mentioned above. Chapter 6 describes the *in vivo* studies of TC and RPC loaded hydrogels and liposomal formulations optimized in the previous Chapters using the *tail-flick* test. The overall conclusions are summarized in Chapter 7.

The work presented in Chapter 2 focused on strategies to improve the solubility of tetracaine in aqueous formulations. Two different hydrophilic and ionizable cyclodextrins (*β*-CD e HP-*β*-CD) were used to improve tetracaine solubility, stability and bioavailability in aqueous environment. A wide set of solubility studies, fluorescence microscopy, nuclear magnetic resonance, *in vitro* release studies and kinetic studies were performed in order to gain new insights about the system. The results allowed the determination of the ideal concentration of cyclodextrin needed to solubilize the desired amount of tetracaine without compromising its release from the drug-loaded formulations.

Chapters 3 and 4 report in detail the evaluation of several aminoacids-based surfactants (lysine and serine, respectively) as chemical permeation enhancers for drugs delivered topically. The effects of these compounds were assessed by means of *in vitro* permeation studies, in Franz diffusion cells, across newborn porcine skin. The toxicity of the compounds and the morphological changes in the skin structure were also evaluated. Complementary molecular dynamic studies were carried out to obtain a mechanistic vision and to provide understanding on the mechanism of action of these molecules on lipid membranes.

In Chapter 3, the compounds evaluated were neutral and negatively charged surfactants, derived from the aminoacid lysine, with different alkyl chain lengths tails (10Lys10; 12Lys12; 14Lys14 and 16Lys16). In Chapter 4 the compounds under study were neutral and positively charged gemini surfactants, derived from the aminoacid serine, with structural differences both in the nature of the hydrophobic tails and spacer $(10Ser)_2N5$ $(12Ser)_2N5$ $(14Ser)_2N5$ $(12Ser)_2N10$). The results obtained show that these class of compounds were able to increase the permeation of both drugs, especially in the case of the hydrophilic drug ropivacaine hydrochloride. Optical microscopy and scanning electron microscopy studies showed that the use of this compounds and methodology did not determine major morphological changes in the skin structure. Cytotoxicity studies in human epidermal keratinocytes cell lines were performed to establish the relative toxicity of the compounds. The results obtained gave a positive indication about their future use in formulations to be applied topically.

Chapter 5 addresses the development of a liposome-based formulation as a strategy to improve the permeation across the skin, simultaneously, of two local anesthetics, aiming a sustained and prolonged therapeutic effect. Liposomes were prepared using various lipids, namely phosphatidylcholine and cholesterol, following thin layer evaporation methodology. In order to improve its properties and consequently, seeking to obtain higher drug permeation, some liposomes were modified by adding aminoacid-based surfactants previously optimized in Chapter 3 and Chapter 4. Liposomes were characterized for size, polydispersivity index, zeta potential and encapsulation efficiency. *In vitro* permeation studies across newborn pig skin were carried out from drug-loaded liposome formulations.

Additionally in Chapter 6, *tail-flick* test in Wistar rats was performed to determine the *in vivo* efficacy of the selected formulations, either hydrogels or liposomes compared with a

commercially available formulation (Ametop®). Chapter 7 compiles the most significant conclusions of the work presented in this dissertation.

Resumo

Em termos gerais, os trabalhos desenvolvidos nesta tese tiveram como principal objectivo o desenvolvimento de formulações anestésicas semi-sólidas de aplicação tópica que visam alcançar de um modo rápido e sustentado a analgesia. Para o efeito farmacológico pretendido foram utilizados dois tipos de anestésicos locais, um de acção rápida, a tetracaína e outro de acção farmacológica prolongada, a ropivacaína.

A eficácia clínica de um fármaco aplicado por via tópica depende da sua capacidade de ultrapassar o estrato córneo, a camada mais exterior da epiderme e reconhecidamente a sua principal barreira.

No capítulo 1 é feita uma introdução pormenorizada do tema que é desenvolvido nos capítulos seguintes. Os capítulos 2, 3, 4 e 5 abordam em pormenor o desenvolvimento e caracterização de sistemas e estratégias específicas com o objectivo de melhorar a eficiência da permeação dos dois anestésicos locais através da pele. O capítulo 6 descreve os estudos *in vivo* das formulações finais previamente optimizadas nos capítulos 3, 4 e 5. As conclusões gerais são apresentadas no capítulo 7**.**

O trabalho apresentado no capítulo 2 teve como objectivo a maximização da solubilidade da tetracaína em formulações aquosas. Duas ciclodextrinas hidrófilas e ionizáveis (*β*-CD e HP-*β*-CD) foram utilizadas com o objectivo de promover o aumento da solubilidade em meio aquoso, estabilidade e biodisponibilidade do fármaco. No âmbito deste trabalho foram realizados estudos de solubilidade, de microscopia de fluorescência, de ressonância magnética nuclear, estudos de libertação *in vitro* e de cinética e calculadas as constantes de estabilidade. Os resultados obtidos permitiram

determinar a quantidade ideal de ciclodextrina para solubilizar a tetracaína sem comprometer a sua libertação a partir das formulações.

Os capítulos 3 e 4 descrevem detalhadamente a avaliação em termos de eficácia e de citotoxicidade, de um conjunto de tensioactivos derivados de aminoácidos (lisina e serina, respectivamente) como promotores químicos da permeação dos fármacos através pele. O efeito destes compostos como promotores da absorção transdérmica, foi investigado através de ensaios de permeação *in vitro,* em células de difusão vertical de Franz, através de pele de leitão. Estudos de dinâmica molecular permitiram obter uma visão mecanicista e elucidar a acção destas moléculas sobre membranas lipídicas. No capítulo 3, o objecto de estudo foram tensioactivos neutros e carregados negativamente, derivados do aminoácido lisina, com cadeias alquílicas de diferentes comprimentos (dez, 10Lys10; doze, 12Lys12; catorze, 14Lys14 e dezasseis, 16Lys16 átomos de carbono). No capitulo 4 foram avaliados tensioactivos “gemini” neutros e carregados positivamente, derivados do aminoácido serina e com variações estruturais impostas no comprimento da cadeia e do espaçador ($(10Ser)_2N5$ $(12Ser)_2N5$ $(14Ser)_2N5$ $(12Ser)_2N10$). Os resultados obtidos demonstraram que ambas as classes de compostos foram eficazes e capazes de aumentar significativamente a cedência dérmica dos fármacos, especialmente no caso da ropivacaína, que por ser um fármaco hidrófilo, atravessa a pele em pequena extensão. Adicionalmente foram efectuados estudos de microscopia óptica e electrónica de varrimento para averiguar a integridade da pele utilizada após a sua utilização nos ensaios de permeação e potenciais efeitos tóxicos causados pelos promotores de absorção e metodologia utilizada. Ambas as técnicas demonstram a inexistência de alterações significativas do ponto de vista morfológico e estrutural. Foram também realizados estudos de citotoxicidade em linhas celulares de queratinócitos da epiderme humana, que permitiram estabelecer perfis de toxicidade relativa para os diferentes promotores. Estes resultados deram indicações positivas quanto à utilização segura destes compostos como promotores da absorção em formulações para administração tópica.

O capítulo 5 visa o desenvolvimento de uma formulação lipossomal como estratégia para promover a permeação conjunta dos dois anestésicos locais aumentando a sua biodisponibilidade e prolongando o seu efeito terapêutico. Os lipossomas foram preparados recorrendo a diversos lípidos (fosfatidilcolina e colesterol) e o método de preparação foi a evaporação em camada fina. Alguns lipossomas foram modificados com a adição de tensioactivos criteriosamente escolhidos (capítulos 3 e 4) de modo a torná-los mais flexíveis e por consequente aumentar os perfis de permeação. Os

lipossomas foram caracterizados relativamente ao tamanho, índice de polidispersão, potencial zeta e eficiência de encapsulação. No capítulo 6 são apresentados os resultados do estudo de farmacodinâmica recorrendo ao teste *tail-flick*, de modo a avaliar a biodisponibilidade *in vivo* das formulações optimizadas comparando com uma formulação de mercado (Ametop®). O capítulo 7 conjuga as principais conclusões deste trabalho.

Chapter 1

General introduction

In the last decades, many drug delivery systems for topical administration were developed. The work presented in this dissertation focused on the evaluation of novel biocompatible chemical permeation enhancers and liposomes to improve the delivery of two local anesthetics applied topically.

The selection of the variables explored in this thesis was based on the physicochemical properties of the drugs, biocompatibility and toxicity of the vehicles and chemical permeation enhancers used. The main objective was to improve the delivery of both drugs, in order to achieve sustained analgesic effects.

The structure, composition and different skin permeation strategies will be subsequently described in detail.

1.1. Topical administration

Topical administration is one of the most preferred administrations by patients with acute or chronic pain conditions since it is a noninvasive system of administration allowing a greater adherence to treatment. In addition, this route avoids the 1st hepatic effect and the degradation of the drug in the gastrointestinal tract among others adverse effects that occurs with other routes. However the skin is a biological membrane poorly permeable due to a layer, called *stratum corneum* (SC), with 15-20 μm of keratinized cells which is the mainly barrier to the passage of substances. It is thus important to have a background of the physiology and functions of a healthy human skin and the principal routes of administration, followed by a review of some of the chemical and technological modulation for topical and transdermal drug delivery.

1.1.1. The skin

Human skin is a unique organ that enables the body to interact most intimately with its environment. It is the largest organ of the human body, accounting for more than 10% of the body mass of an average person, and it covers an average area of 1.7 m^2 (Benson, 2011; Brown et al., 2006). Such large and easily accessible organ apparently offers ideal conditions and multiple sites to administer therapeutic agents for both local and systemic effect. However human skin is a highly efficient self-repairing barrier designed to keep 'the insides in and the outside out'.

1.1.2. Functions of the skin

Human skin constitute a sixth of the total weight of the body and it is constantly being regenerated. Numerous functions have been attributed to this highly complex organ. Skin can act as an environmental barrier providing physical, chemical and microbiological barrier protection crucial for terrestrial life (Benson, 2011; Elias, 2005; Madison, 2003a). Other functions of the skin are related to the neurosensory activity associated to pressure, pain and metabolism. Skin also plays an important role in the preservation of the homeostasis by regulating thermal hemodynamics. Basically, the body temperature is regulated by the constriction of the blood vessels that preserve heat and dilate to dissipate heat. Besides that, also hair helps thermal insulation, whereas

sweating facilitates heat loss by evaporation (Benson, 2011). Skin is also important as an immunological effector axis by having Langerhans cells process antigens and as an effector axis by setting up an inflammatory response to an external aggression. In addition skin is an endocrine organ and is a target for androgens that regulate sebum production, a complex mixture of lipids that function as antibacterial agents and for insulin, which regulates carbohydrate and lipid metabolism. The integument plays a role in metabolizing keratin, collagen, melanin, lipid, carbohydrate, and vitamin D as well as in respiration and in biotransformation of xenobiotics (Nancy, 2005). For the purpose of dermal drug delivery, the structure and composition of human skin will be described and will be categorized.

1.1.3. Structure and composition

With regard to its histology, skin is composed of three distinct tissue layers: the epidermis, the dermis and the hypodermis that is the dermis continuity. (Elias, 2005). There are also several associated appendages such as hair follicles, sweat ducts, apocrine glands and nails (Figure 1.1).

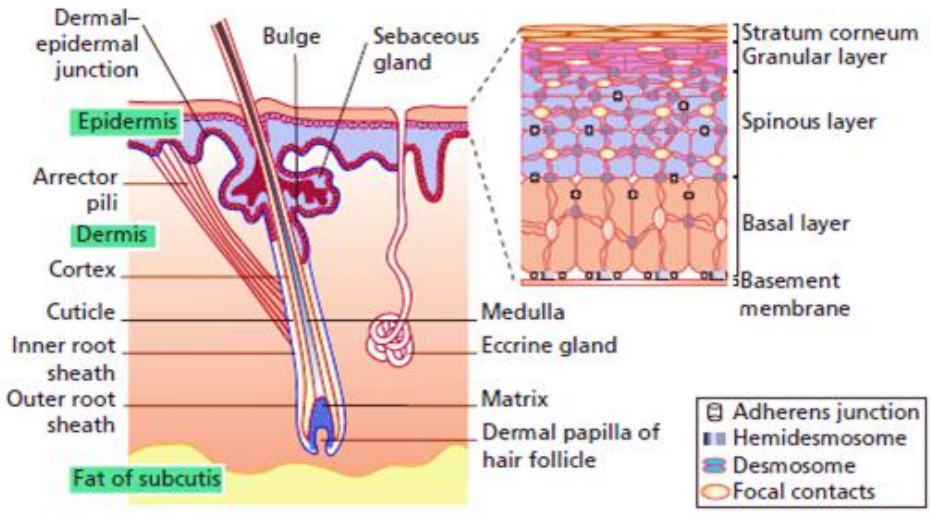

Figure 1.1 A diagrammatical illustration of the skin. The epidermis is the stratum surface coating formed by stratified squamous epithelium; the dermis is deeper stratum composed of dense connective tissue; and the hypodermis is the dermis continuity, rich in adipose tissue From reference (McGrath and Uitto, 2010).

1.1.3.1. Viable epidermis

The epidermis is itself a complex multiply layer membrane (Figure 1.2), whose thickness varies between 70 and 120 μm and is the most superficial and non-vascularized layer of

the skin. Due to the absence of blood vessels, and in order to maintain tissue integrity, the nutrients and waste products must diffuse across the dermo-epidermal layer. Also, molecules must cross this layer in order to reach the systemic circulation. Its structure is mainly composed of keratinocytes (95%), that go through a process of proliferation, differentiation and keratinization from the basal layer to the surface turning into corneocytes (Benson, 2011; Brown et al., 2006).

During the process of migration, cells undergo dehydration and flattening, the core disappears and the content of keratin increases. This process of cell renewal takes approximately 28 days (Walters, 2002b). The epidermis has other specialized cells such as melanocytes responsible for melanin synthesis, Merkel cells, associated with sensory nerve endings functions and Langerhans cells, dendritic cells with immune function (Foldvari, 2000).

The epidermis contains four histologically distinct layers which, from the inside to the outside, are the *stratum basale* or *germinativum*, *stratum spinosum*, *stratum granulosum* and the *stratum corneum*. A fifth layer, the *stratum lucidum*, is sometimes described but is more usually considered to be the lower layers of the *stratum corneum* (Figure 1.1).

1.1.3.1.1. Stratum Basale

Stratum basale is the deepest layer of the epidermis and is in contact with the germination membrane which is responsible for the renewal of the epidermis, forming the Malpighian body mucous. In this layer the cells contain typical organelles such as mitochondria, ribosomes, and the cells are metabolically active. Among other specialized cell types, this layer is composed mainly of keratinocytes that are undifferentiated cells with polyhedral shape, linked to each other by desmosomes and connected to the basal membrane (which separates the epidermis from the dermis) by hemidesmosomes. This layer is rich in aminoacids that origins the cysteine necessary for the biosynthesis of keratin which is a structural protein of skin (Woodley, 1987). Also, the melanocytes synthesize the pigment melanin from tyrosine and make surface contact with adjacent keratinocytes through dendritic connections, and this allows the pigment granules to pass from the melanocytes to the keratinocytes (Lai-Cheong and McGrath, 2009). Melanin provides protection against ultraviolet (UV) radiation and from free-radical scavengers (Benson, 2011). Langerhans cells are dendritic cells and can be also found within the *stratum basale*. Langerhans are recognized as the major antigen-presenting cells of the skin and plays an important role when allergic contact dermatitis occur

because the antigens readily bind to the cell surfaces (Lai-Cheong and McGrath, 2009). One other specialized cell type presented in this *stratum*, corresponds to the Merkel cells that are found mainly around the touch-sensitive sites of the body, such as lips and fingertips. These cells appear to be related in cutaneous sensation since are associated with nerve endings (Chilcott, 2008). The cells originated in the *stratum basale* migrate then upwards to the next layer.

1.1.3.1.2. Stratum Spinosum

The *stratum spinosum* is the thickest layer of the epidermis, consisting of two to six rows of keratinocytes that change morphology from columnar to polygonal cells maintaining their structural integrity. The spiky appearance is due to the abundance of desmosomes. Desmosomes connecting the cell membranes of adjacent keratinocytes are responsible for maintaining a distance of approximately 20 nm between the cells. Cells in this layer exhibit lipid-rich structures, the lamellar bodies (Odland bodies) and are richer in keratin filaments when compared to the cells in the *stratum basale* (Benson, 2011; Menon, 2002).

1.1.3.1.3. Stratum Granulosum

Stratum granulosum corresponds to 3-5 layers of flattened keratinocytes showing clearly granules of keratohyalin, particularly significant due to its major role in the aggregation and alignment of keratin filaments (Menon, 2002). In this layer the keratinocytes continue to differentiate, synthesize keratin and start to flatten. The enzymes present in this layer start a lysis phenomenon of cytoplasmic organelles that result from the activation of lysosomal enzymes (Egelrud, 1993). Numerous granulations are present such as the Odland bodies that, at this stage, are larger and more abundant. During the process of differentiation of keratinocytes, they enclose multiple lipidic lamellar units and hydrolytic enzymes, namely proteases, lipases and glycosidases. As the migration and differentiation takes place, Odland bodies migrate to the cell membrane, fusing with the plasma membrane next to the last layer of the epidermis and releases its lipid content to the outside, a fundamental process in the formation of the SC extracellular lipid matrix (Schmitz and Müller, 1991).

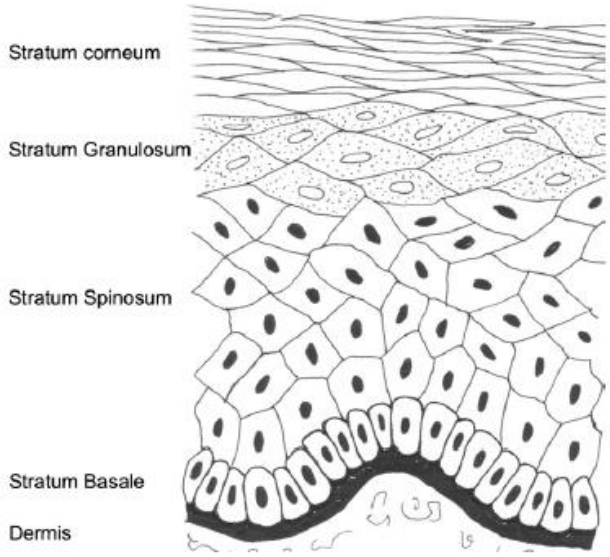

Figure 1.2 Representation of the epidermis (Wickett and Visscher, 2006). During the process of cell differentiation, epidermal cells move from the basal layer (SB) through the spinous layer (SS) and the granular layer (SG) towards the SC.

1.1.3.1.4. Stratum corneum

The *stratum corneum* and represents an effective barrier to penetration of substances due to its well organized structure, very high density and low hydration (10-30%) (Elias, 2005). This thin layer consists in dehydrated, anucleate and keratinized cells, the corneocytes. The corneocytes are the final product of the keratinocyte differentiation process that takes place along the epidermis and are continuously renewed, in a process denoted as desquamation, completing a total turnover in 2-3 weeks (Turesson and Thames). The corneocytes are connected by desmosomes (corneodesmosomes) and represent 12-25 layers of cells (Fartasch et al., 1993), embedded in a complex matrix of stacked intercellular lipids arranged similarly to a “brick and mortar” model (Elias, 1983; Nemes and Steinert, 1999). The lipid matrix allows for survival of terrestrial animals without desiccation. The SC also serves to regulate water loss from the body whilst preventing the entry of harmful materials, including microorganisms (Chilcott, 2008; Elias, 2007). Water plays a key role in maintaining SC barrier integrity and may mediate the activity of some hydrolytic enzymes since environmental humidity affects the activities of enzymes involved in the desquamation process. The barrier nature of the SC depends critically on its unique constituents and strongly defines the performance of the skin properties where 75-80% is protein and 5-15% is lipid with 5-10% unidentified on a dry weight basis (Bleck et al., 1999; Elias, 2005; Motta et al., 1995; Ponec et al., 1988; Robson et al., 1994). The protein is positioned mainly with the keratinocytes and basically is constituted by 70% of alpha-keratin with approximately 10% of beta-keratin

and a proteinaceous cell envelope (around 5%). 15% of the protein component consists in enzymes and other proteins where the cell envelope protein is highly insoluble and for that reason is very resistant to chemical attack. The lipid envelope is bound to the keratinocyte through glutamate moieties of the protein envelope. This surface keratinocyte protein plays an important role in structuring and ordering the intercellular lipid lamellae of the SC. Proteases have been demonstrated to degrade the desmosomal proteins (Egelrud and Lundström, 1991; Lundström and Egelrud, 1991; Suzuki et al., 1994), and it appears that hydrolysis of cholesterol sulfate also accompanies cell shedding (Long et al., 1985). The drug flux through the tissue is basically regulated by the mixture of lipids that constitutes the SC. Although varies between individuals and with body site (Lampe *et al.,* 1983a), these intercellular lipids are specially ceramides (CER) (45-50% by weight), cholesterol (CHO) (25%), free fatty acids (FFA) (10-15%) and cholesterol sulfate (<5%) ordered in a multiply bilayer lipid arrangement (Madison, 2003a). Some studies have been devoted to probing the lipid composition of the intercellular domains, particularly by Downing, Wenz, Elias and co-workers (e.g. Elias, 1983; Wertz *et al"* 1985). At least nine extractable ceramide subclasses (Ponec et al., 2003; Robson et al., 1994; Stewart and Downing, 1999; Wertz et al., 1985) present in the lipid matrix were extracted from human SC and are classified as CER1 to CER9 which, together with the fatty acids, CHO and cholesterol sulfate, provide the amphiphilic properties necessary to form lipid bilayers. Different classes of ceramides possess various functions in the stabilization of SC lipid bilayers. All of the ceramides and the fatty acids found in SC are rod-like or cylindrical in shape, and these physical properties make these lipids suitable for the formation of highly ordered gel phase membrane domains. Gel phase domains will be less fluid, hence, less permeable than their liquid crystalline counterparts. In addition CHO is a ubiquitous membrane lipid and is capable of either fluidizing membrane domains or of making them more rigid, depending on the physical properties of the other lipids and the proportion of cholesterol relative to the other components. The role of CHO in the epidermal barrier is probably to provide a degree of fluidity to what could otherwise be a rigid, possibly brittle membrane system. This may be necessary for the pliability of the skin (Wertz, 2000). In addition to the keratinocytes and lipid lamellae, water plays a key role by regulating enzymes that are involved in the generation of natural moisturizing factor (NMF). NMF is a highly efficient humectant synthesized and hence is located within the SC (Hachem et al., 2005). A proteolytic product from filaggrin, NMF is essentially a mixture of free aminoacids, aminoacid derivatives and salts; serine, glycine, pyrrolidone carboxylic acid, citrulline, alanine and histidine are the major components with lesser amounts of arginine,

ornithine, urocanic acid and proline. This hygroscopic mixture retains moisture within the SC and helps to maintain suppleness.

1.1.3.1.5. Stratum Lucidum

The stratum lucidum consists of some clear layers of flattened, compacted, anucleated cells, fully keratinized, whose nucleus and organelles undergone enzymatic digestion and is especially rich in eleidin, a product of keratohyalin and precursor of keratin transformation. This layer tends to be seen most clearly in relatively thick skin specimens, such as from the load-bearing areas of the body (soles of feet and palms). Indeed, some dermatologists question whether this layer is functionally distinct from the other epidermal layers, or if it is an artefact of tissue preparation, most researchers tend to view the *stratum lucidum* as the lower portion of the *stratum corneum* and hence bracket these two layers together (Benson, 2011).

1.1.3.2. Dermis

The dermis (or corium) is typically 3-5 mm thick and is the major constituent of human skin. It is composed of a dense connective tissue, rich in collagen fibrils providing support, elastic tissue providing flexibility and reticular fibers embedded in a mucopolysaccharide blend (Hussain et al., 2013). The dermis lies under the epidermis and is the principal mechanical support structure of the skin having also major roles in skin nutrition, thermal regulation and immune response. Adjacent to the epidermis is the papillary dermis which is a lax, vascularized and innervated *stratum* with free nerve endings (Lai-Cheong and McGrath, 2009). The extensive vasculature of the skin is essential for regulation of body temperature, delivering oxygen and nutrients to the tissue, removing toxins and waste products and plays an important role in wound repair. The rich blood flow, around 0.05 mL/min per mg of skin, is very efficient for the removal of molecules that have traversed the outer skin layers. In terms of transdermal drug delivery, this layer is often viewed as essentially gelled water, and thus provides a minimal barrier to the delivery of most polar drugs, although the dermal barrier may be significant when delivering highly lipophilic molecules. Furthermore, the blood supply thus maintains a concentration gradient between the applied formulation on the skin surface and the vasculature, across the skin membrane. It is this concentration gradient that provides the driving force for drug permeation (Benson, 2011; Ryman-Rasmussen et al., 2006). The main cells found in the dermis are the fibroblasts which produce the connective tissue components of collagen, elastin, and amorphous substance. There are

also cells with immune functions such as mast cells which are involved in the immune and inflammatory responses and melanocytes involved in the production of the pigment melanin. Other structures like blood and lymphatic vessels, sweat and sebaceous glands, sensory nerve endings and hair follicles are also found in this layer (Riviere, 2006; Walters, 2002a). The lymphatic system extends to the dermo-epidermal layer and promotes immunological responses to microbial assault and waste removal by regulating the interstitial pressure. The lymphatic vessels maintains the driving force for permeation removing the permeated molecules from the dermis (Cross and Roberts, 1993; Scheuplein and Ross, 1974). The skin surface pH is maintained around 5, due to the sebaceous gland associated with the hair follicle that secretes sebum composed of FFA, waxes and triglycerides. The appendages (hair follicles, sweat ducts) may offer a potential route for molecules to enter through the intact barrier provided by SC. These 'shunt routes' can be used by large polar molecules and for electrical enhancement. However, because the fractional area offered is so small, the predominant pathway for molecules to traverse the tissue remains across the bulk of the skin surface.

1.1.3.3. Hypodermis

Hypodermis or subcutaneous fat layer is the deepest skin structure, relatively thick, that links the overlying dermis and the underlying body constituents. This layer of adipose tissue insulates the body and provides mechanical protection against physical shock. Fibroblasts and macrophages are also present in this layer. However the predominant cells are the adipocytes, specialized in the storage of energy in the form of fat and providing a readily available supply of high-energy molecules, whilst the principal blood vessels and nerves are carried to the skin in this layer. (Riviere, 2006; Walters, 2002a)

1.1.4. Permeation skin pathways

The most of the molecules the *stratum corneum* is the principal barrier to the percutaneous absorption. Due to the high organization level of the skin, drug molecules applied on its outer surface must follow tortuous paths, crossing all the skin cell layers and intercellular lipids, in order to reach the circulatory system in the dermis (Hadgraft and Walters, 1994). There are essentially three pathways by which a molecule can traverse intact SC: via the appendages (via sweat glands and hair follicle); through the extracellular lipid domains (intercellular); or by a transcellular route (intracellular), where both are transepidermal pathways (Figure 1.3) (Trommer and Neubert, 2006).

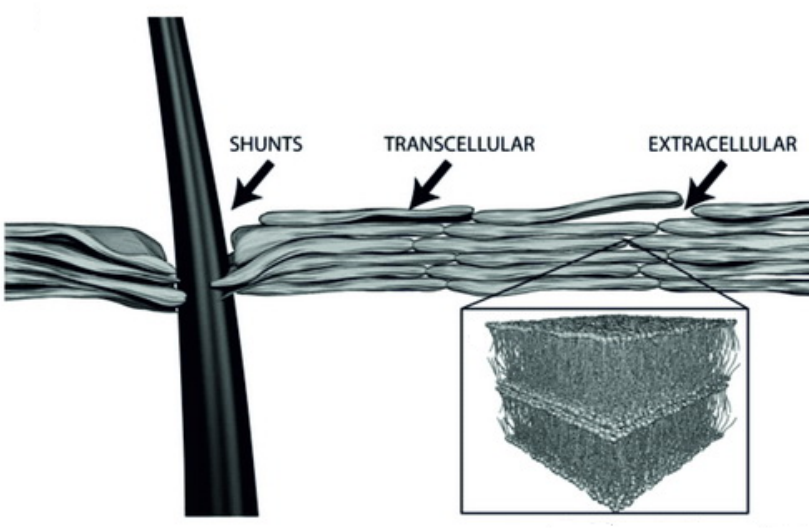

Figure 1.3 Illustration of possible drug transportation pathways through the *stratum corneum*. Adapted from (Simonsson, 2011).

The majority molecules probably will pass through the SC by a combination of these pathways. The relative contribution of each route depends on the solubility, partition coefficient and diffusivity of the drug. For that reason the relative contributions of these pathways to the flux will depend basically on the physicochemical properties of the permeant (Barry, 2001).

1.1.4.1. Transappendageal transport (shunt route transport)

The hair follicles and the sweat ducts possess pores that allow the transport of the drugs through the *stratum corneum*. This appendage area only occupies around 0.1 % of the total skin surface area (Moser et al., 2001; Scheuplein, 1967) and its contribution is negligible to the steady state drug flux, being particularly relevant for ions and large polar molecules that struggle to cross intact SC (Scheuplein and Blank, 1971). This route is important for delivering vesicular structures to the skin, and for targeting their contents to the pilosebaceous units, despite the extensive debate as to whether vesicles can traverse the SC intact (Lauer et al., 1996). The use of electrical charge to drive molecules to the skin (iontophoretic drug delivery) depends on this route, since the charge is carried through the SC via the path of least resistance and the shunt routes provide less resistance than the SC bulk.

1.1.4.2. Transepidermal routes

The transepidermal pathway involves the passage of the drug through the epidermis cells (transcellular or intracellular way) or by lipoprotein matrix existing between cells (intercellular way).

In both pathways, the drug penetrates the *stratum corneum* by diffusing through the intercellular lipid matrix (Boddé et al., 1989). However, the intercellular route appears to be predominant, and therefore many enhancement techniques aim to disrupt or bypass the molecular architecture of bilayers of the SC.

1.1.4.2.1. Intracellular route

This pathway is often regarded to provide a polar route for a molecule to traverse the *stratum corneum*. The highly hydrated keratin present in the cellular components (corneocytes) provides an effective aqueous environment that consequently increases the diffusion of hydrophilic molecules (Bolzinger et al., 2012). Since the keratin-filled cells are bound to a lipid envelope that connects to the intercellular multiply bilayer lipid domains, the apolar molecule faces numerous repeating hurdles to cross the intact SC (Wertz et al., 1987). The nature of the permeant influences the flux, for highly hydrophilic molecules the intracellular route predominates at pseudo-steady state. The multiply bilayer lipids that the molecule must traverse is the rate-limiting barrier for permeation via this route. The use of solvents can remove lipids from the SC and subsequently increases drug flux for even highly hydrophilic molecules. The intercellular pathway is an alternative for apolar molecules because the intercellular medium is rich in lipids arranged in bilayer (Marjukka Suhonen et al., 1999)

1.1.4.2.2. Intercellular route

The intercellular lipid route provides the principal pathway by which most small and uncharged molecules traverse the *stratum corneum* (Abraham et al., 1995; Roberts et al., 1996). The lipid bilayers represent 1% of the SC diffusional area and provides a continuous phase within the membrane with a great variety of ceramides (Trommer and Neubert, 2006). The composition of these bilayers is different to all other lipid membrane bilayers within the body, where phospholipids are absent and the SC lipids exist in a variety of states. The transdermal delivery of small molecules has been considered as a process of interfacial partitioning and molecular diffusion through the SC. A typical mathematical model considers the SC as a two-phase protein-lipid heterogeneous

membrane having the lipid matrix as the continuous phase (Elias, 1983; Elias, 1988; Michaels et al., 1975). Several theoretical skin-permeation models have been proposed which can predict the transdermal flux of a drug based on some of its physicochemical properties (Kirchner et al., 1997; Lee et al., 1997; Potts and Guy, 1992; Pugh and Hadgraft, 1994; Tojo, 1987). A domain mosaic model for the SC lipids has proposed by Forslind (Forslind et al., 1997). This model combines the heterogeneity of lipid packing with segregated areas of crystalline/gel domains with borders of more fluid liquid crystalline regions. This organization allows the water loss regulation allowing sufficient water to enter the tissue to maintain keratinocyte hydration. The lipid bilayers is the mainly limiting barrier to drug flux, where the intercellular transport is through the lipid domains and the intracellular permeation requires the lipid lamellae to be crossed and depends of the thickness of the *stratum corneum*. The intercellular route is extremely tortuous and the permeants needed to move through the continuous lipid domains between the keratinocytes. However the pathlength taken by the molecule is considerably greater than that of the SC thickness (Hadgraft, 2004).

1.1.5. Mathematical theoretical basis of percutaneous absorption

Human skin is a uniquely system with multiply layered and a heterogeneous biological tissue that is different between species. For that reason is impractical to describe this behavior with ideal mathematical models. Despite these complexities, Fick's first law of diffusion is a relatively simple mathematical that can be applied to data obtained from experiments.

1.1.5.1. Pseudo-steady state permeation (infinite dose):

Drug absorption across human skin is controlled by a passive diffusion mechanism and it can be described in physical terms, by the Fick's First Law of diffusion (Higuchi, 1960). Fick's first law of diffusion states that the rate of transfer of diffusing substance through unit area of a section is proportional to the concentration gradient measured normal to the section. In permeation experiments, Fick's first law is used to describe steady state diffusion and to analyze permeation data,

$$J = \frac{DC_0P}{h} \qquad (1.1)$$

where *J* stands for the steady-state flux per unit of area, i.e. the amount of a material passing through a unit area per unit time, *D* is the diffusion coefficient of the drug in the SC, C_0 represents the drug concentration in the vehicle, *P* is the partition coefficient between vehicle and the skin and *h* is the diffusional path length. Since the drug concentration applied (c_{app}) to the skin is much larger than the concentration under the skin (infinite dosing) Eq. 1.1 can be simplified to,

$$J = k_p \, c_{app} \tag{1.2}$$

where k_p is a permeability coefficient (= *DP* / *h*) and is a heterogeneous rate constant having the units, for example, cm h^{-1}. The parameter *h* cannot be accurately estimated as it is related to the tortuosity of the intercellular channels, which is imprecise (Guy and Hadgraft, 2003; Hadgraft, 2001).

The cumulative amount of drug permeating through the skin (Q_n) is given by Eq. 1.3,

$$Q_n = (C_n \times V_0 + \sum_{i=1}^{n-1} C_i \times V_i)/A \tag{1.3}$$

where C_n corresponds to the drug concentration in the receptor medium, C_i is the concentration in the sample, *A* is the diffusion area, V_0 and V_i stand for the volumes of the receptor compartment and the sample.

The concentration gradient is influenced by the ability of the drug to partition into the skin and its ability to partition out of the skin into the underlying tissues and should maintain the sink conditions that is defined as "*the volume of medium at least three times that required in order to form a saturated solution of drug substance*" when performing a dissolution procedure.

The steady-state flux can be calculated from the slope of the linear part of the permeation profile, extrapolated to the time axis and the value of the lag time is obtained by the intercept at Q=0 i.e., corresponding to a cumulative amount of drug permeating through the skin equal to 0. The lag time method is commonly used for analysis of the permeation data from *in vitro* experiments with an infinite dosing technique, that is, where the skin separates an infinite reservoir of drug on the donor side and a perfect sink as receptor. However, the lag time method could be subjective as it requires an evaluation to determine the linearity of the permeation profile (Banga, 1998).

1.2. Experimental design

1.2.1. *In vitro* vs. *in vivo* studies

The ideal situation to evaluate formulations for *in vivo* use is to employ and monitor drug delivery directly in human volunteers. Performing *in-vivo* studies has benefits such as the generation of realistic measures for the amounts of drug that would enter the skin or systemic circulation. However, due to experimental and ethical difficulties, most of the transdermal drug delivery studies tend to use skin *ex-vivo* (*in vitro*). *In-vitro* experiments can provide conditions to mimic the circulation and also can maintain the barrier properties of excised skin, however inherently reduce the natural complexity where the regeneration stops, immune responses cease and metabolic activity is usually lost in these studies, especially for the prolonged periods. Even though *in vitro* permeation studies are widely used to investigate the permeability of drugs, it should be noted that data obtained from excised skin may not translate directly to the *in-vivo* situation. Most of *in vitro* techniques are carried out using diffusion cells. This system has a donor compartment (where the vehicle containing the drug is placed) and a receptor chamber (containing receptor medium) separated by a membrane (e.g. skin), under controlled temperature conditions.

1.2.2. Membranes for *in vitro* studies

The most appropriate membrane for transdermal drug delivery studies is the human skin. However, due to ethical and legal restrictions on obtaining this kind of skin, alternative membrane models from animal sources or synthetic have been used with the same purpose. The use of model membranes can be useful for transdermal studies, but the results obtained, may not transfer directly to human skin either *in vitro* or *in vivo,* and results should be treated with careful. For formulation development, excised skin from different animal models (primates, pig, mouse, rabbit, rat, guinea pig and snake), can offer great value and are certainly more readily available and easier to store and handle. These types of membranes can be more reproducible than that from donated human tissue, because experiments can be performed *in vivo* and hence data concerning metabolism and distribution of absorbed materials can be obtained. The animal model choice depends on the similarity to human skin regarding physiological aspects such as blood perfusion, morphology and chemical composition. It has been reported that the

hairless mouse skin is an unacceptable model for predicting human skin permeation because mouse skin differs markedly from human tissue in terms of structure, lipid content that is greater than that in human *stratum corneum*, and because is thinner. In addition these tissue loses its integrity rapidly, whereas the human SC barrier remains intact for longer periods of time (Roberts and Mueller, 1990). Guinea pig SC can be an alternative to mimic human skin diffusion behavior, in terms of thickness, versatility and the skin behind the ears possesses no hair follicles or sebaceous glands, thus offering opportunities to study the role of shunt route permeation. In alternative to these models in terms of physiological responses and behavior, macaque monkey and dog skin has provided evidence for the efficacy of drugs as a model for the human membrane (Barbero and Frasch, 2009b; Bartek et al., 1972; Godin and Touitou, 2007; Reifenrath et al., 1984). However, the use of primates is restricted due to ethical concerns. Hereupon porcine skin seems to be the best model membrane to explore formulation modifications or for hazard evaluation, because the SC of the pig is similar to the human membrane in terms of thickness, lipid content and so it has remarkably similar permeability properties (Schmook et al., 2001). It is well documented that porcine skin has similar physiological properties and anatomical features of human skin and has an added advantage in that it may be relatively easy to acquire (Barbero and Frasch, 2009a; Davies and Trotter, 1981; Mowafy and Cassens, 1975; Schmook et al., 2001). Some studies designed to predict skin permeation in man reported that similar permeation values were obtained when porcine and human skin were tested under similar conditions *in vitro* (Bartek et al., 1972; Schmook et al., 2001). Also It has been reported that both the morphology of the epidermis and upper dermis vasculature and functions of endothelial cells (e.g. plasminogen activator) in the pig were similar to that in man (Forbes, 1969). Hence, in this work, porcine skin was selected to be used in substitution of human skin because it is functionally and structurally similar to the latter.

1.2.3. Artificial membranes

In some studies it is not necessary to use human and animal skin for comparison or optimization of formulations, since simple physicochemical rules govern permeation. More simplistic model membranes, like artificial “chemical” membranes have been widely used in drug delivery studies because offer the advantages of reproducibility and control. The membrane is isotropic, having no regional variability, and permeation can be described by simple mathematical rules. However, it has disadvantages in terms of poorly representing human tissue *in vivo* since there is no metabolism, there is minimal

variability, and the permeation process is simple permeation processes compared to the more complex multiple processes occurring in the heterogeneous human skin.

A great variety of synthetic membranes have been tested as model membranes in permeability studies (Hadgraft and Guy, 1992; Houk and Guy, 1988). Liquid membranes enclosing lipids as isopropyl myristate (Hadgraft and Ridout, 1987), dipalmitoyl phosphatidylcholine, linoleic acid and tetradecane (Hadgraft and Ridout, 1988) and others (Hadgraft et al., 1985) or polymeric membranes based on polymers or combination of polymers such as polydimethylsiloxane (Silastic®) (Pellett et al., 1994), poly-(2-hydroxyethylmethacrylate), cellulose acetate (Neubert et al., 1991; Neubert et al., 1995), silicone cellulose (Nastruzzi et al., 1993), silicone polycarbonate urethane (Carbosil®) (Russeau et al., 2009) are examples of artificial membranes used with the objective of reproducing SC barrier properties. The most popular artificial systems used to study percutaneous absorption are simple inert polymer membranes, most commonly, polydimethylsiloxane (silastic or PDMS membranes) that provides a 'non-porous' hydrophobic reproducible barrier and is used in formulation optimization studies and for testing physicochemical principles. In these work a dialysis membrane was selected as model membrane to evaluate and optimize the kinetics of the formulations using mathematics models (Chapter 2).

1.2.4. Diffusion cells for *in vitro* studies

The literature contains various designs of diffusion cells that range from the very simple to the highly complex. Diffusion cells can assume multiple aspects and different complexity levels, varying from two-compartment static diffusion cells (vertical or horizontal) (Franz, 1975a) to multi-jacketed ”flow-through” cells (Bronaugh and Stewart, 1985). Most simply Vertical Franz diffusion cells (Figure 1.4) are the most widely used *in vitro* percutaneous absorption studies and are usually made of glass (Franz, 1975b). These devices comprise two compartments with a membrane properly clamped between the donor (available for application of the permeant) and receptor compartment with a fixed volume. Such display allows the determination of a drug permeation profile across a specific membrane, to a receptor medium that is kept continuously stirring, most commonly with a magnetic bar stirrer at a controlled temperature (water bath, usually at 37°C to maintain surface skin temperature at 32°C as an *in-vivo* mimic). These cells are thus widely used for evaluating drug uptake into membranes, finite dose permeation or steady-state flux of a drug either alone or in formulations as the relatively large and open

donor compartment allows simple application of semi-solid formulations to the skin surface. The receptor compartment allows removal of receptor fluid at required time intervals for analysis with an appropriate analytical method (e.g. High Performance Liquid Chromatography - HPLC). Special attention must be taken while choosing the receptor medium. Ideally, it should simulate as accurately as possible the corresponding *in vivo* fluid (e.g. blood) and must ensure "sink conditions" for the drug under investigation (Skelly et al., 1987). Generally, *in vitro* methods allow a better control of the experimental conditions and are particularly useful during the earlier stages of research, limiting the number of expensive *in vivo* studies in humans and animals (Walters, 2002b).

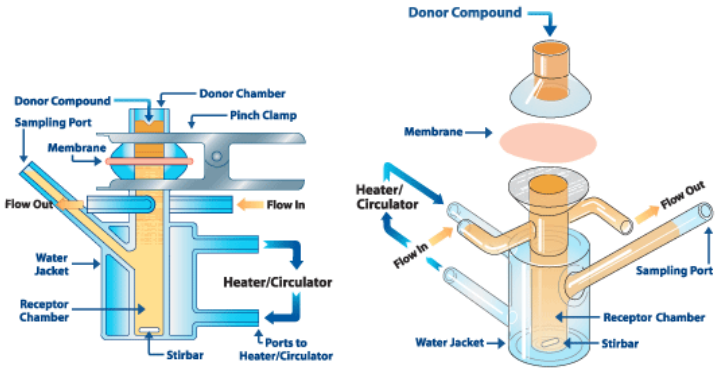

Figure 1.4 Schematic representation of a vertical Franz diffusion cell (PermeGear, 2012).

1.2.5. Formulation application considerations

1.2.5.1. Finite or infinite dose

The quantity of the preparation to be applied to the skin surface depends on the aim of the study. For example, when a cream is applied to the skin and thus permeation is from a finite dose, it is expected to deplete on the skin surface. In contrast, the application of an infinite dose to the skin surface is normally used to determine the fundamental permeation behavior of a material, because steady-state flux data and the effects of penetration enhancers on drug permeation through the skin are usually obtained. In this case, the permeant concentration in the donor phase should not fall by more than 10% from saturation during the experimental period. To avoid donor depletion, saturated drug solutions are used (Chantasart et al., 2013). In general terms, the experimental conditions including application dosages, exposure times and procedures should mimic as closely as possible the *in vivo* situation in order to provide appropriate data.

1.2.5.2. Vehicle effect

Depending on the experiments, the choice of vehicle to apply the drug can also differ, but it is desirable that it mimics the *in vivo* conditions as closely as possible. For example if the permeant is lipophilic and displays a low aqueous solubility, it will traverse the tissue relatively easily, and that, this donor depletion during the experiments can occur. The selection of vehicle for permeation studies is crucial to ensure that the vehicle does not interact with the membrane and if that happens should not affect the structure or integrity of the membrane. Usually a control formulation containing only the same vehicle for comparison of different formulations is used. Interactions between the drug and the vehicle or between the drug and other excipients in the formulation can also modify the permeation behavior of the penetrant (Williams et al., 1998).

1.2.6. Permeant detection

It is important to choose the most suitable method for detection of the permeant that traverses through the membrane. Chromatographic methodologies have the advantage of being versatile and adaptable to numerous permeants that across the skin. HPLC is commonly selected for analyzing the permeant in the receptor fluid. With appropriate selection of columns, mobile phases and detectors the compounds that permeate through the skin can be analyzed simultaneously, relatively rapid and easy. This technique is effective due to several features such high reproducibility, ease of selectivity manipulation and high recoveries. In one step the individual components of a mixture can be separated and quantified with excellent resolution. The separation depends on the interaction and the affinity of the molecules for the stationary phase. The process is based on the higher affinity of the molecules to the stationary phase that will be retained more than other molecules with low affinity for the stationary phase. The affinity degree is highly dependent on the structure and the interaction of the solute and the immobilized ligands. In the case of reverse-phase chromatography the mobile phase employed are mostly water-based solutions (polar) and separations are based on hydrophobic interactions where the stationary phase is hydrophobic. The aim of a successful separation protocol is the ability to manipulate the retention time of the molecule to quantify from other non-target compounds.

1.3. Skin permeation strategies

As was mentioned before, the *stratum corneum* is a highly efficient and effective barrier that possesses multiple bilayer lipids providing the principal pathway for permeation of drugs, especially small and moderately lipophilic molecules (Naik et al., 2000b). Efforts have been made to employ enhancement technologies to controllably, reversibly, and safely reduce the resistance of the SC and expand the range of molecules available for transdermal drug delivery. Some strategies include physical, biochemical and chemical methods. One of the strategies to enhance drug flux through the skin is based by working directly on SC barrier components, for example, the use of chemical permeation enhancers (CPE) or electroporation to disrupt the bilayer lipids. Alternative methods have been developed by some workers without directly altering the skin properties such modifying the thermodynamic activity of permeants in vehicles to alter the driving force for permeation and thus modified uptake into and flux through the membrane. On the other hand, in some studies the aim of permeation modification is to reduce permeant flux across the skin, such in cosmetic formulations or when designing a barrier cream to protect against pesticide exposure. The techniques that have emerged over the years can be generally categorized into passive or active (Figure 1.5). In order to choose the best strategies for each case it is important to understand the mechanism of action of a variety of chemical permeation modulation, and understand the advantages and disadvantages associated with each approach.

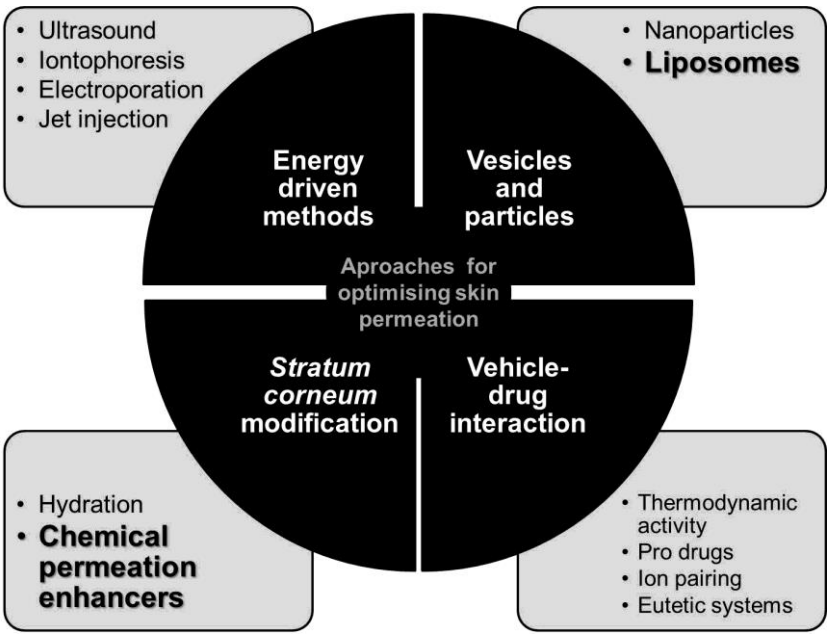

Figure 1.5 Passive and active methods for optimizing dermal drug delivery.

1.3.1. Passive enhancement of skin permeation

Based on Fick's first law, there are some permeation strategies that can increase the passive flux of a drug through the SC: by increasing the diffusion coefficient of the drug in the skin by increasing the drug solubility in the skin and by increasing the degree of saturation of the drug in the vehicle, often referred as the super saturation approach. While the latter is based on the interaction between the drug and the vehicle, the two first strategies involve an effect of the vehicle on the barrier properties of the skin. Therefore, the most recent dosage forms have been developed in order to enhance the driving force of drug diffusion (thermodynamic activity) and/or to increase the permeability of the skin. Such approaches include the use of chemical permeation enhancers (CPE) (Michniak et al., 2005; Michniak et al., 1998; Michniak et al., 1995; Teixeira et al., 2014a; Williams and Barry, 2004), supersaturated systems (Davis et al., 2002), prodrugs or metabolic approach (Elias et al., 2002; Tsai et al., 1996), liposomes and other vesicles that will be discussed in the section below (Bouwstra et al., 2003; Cevc, 2002, 2004; El Maghraby et al., 2008; Godin and Touitou, 2003; Heuschkel et al., 2008; Mezei, 1993; Schreier and Bouwstra, 1994; Sheihet et al., 2008; Touitou et al., 2000; Touitou et al., 1994).

1.3.2. Chemical penetration enhancers

Chemical penetration enhancers (or absorption promoters) facilitate the permeation of drugs through the skin. These chemical agents partition into the *stratum corneum*, interact with tissue components and reduce the barrier properties of the membrane temporarily and reversibly. An effective CPE may increase the diffusion coefficient of the drug in the SC, may increase the effective concentration of the drug in the vehicle, may improve partitioning between the formulation and the SC or can decrease the skin thickness. A chemical penetration enhancer to apply on human skin should have some desirable properties (Woodford and Barry, 1986). It should provide pharmacologically inert, non-toxic, non-irritating, non-allergenic and at the same time must be suitable for formulation into topical preparations and be compatible with drugs and excipients. It should provide a rapid onset of action, and the duration of effect should be predictable and reproducible. It should work in just one direction (i.e. should allow therapeutic agents into the body while preventing the loss of endogenous material) and when the CPE is removed from the skin, the barrier resistance should return fully and rapidly. Finally, and not less important, it should be cosmetically acceptable with appropriate skin feel

(odorless, tasteless, colorless), inexpensive and with good solvent properties (Barry, 1993).

The CPEs used in some topical and transdermal formulations rarely possess all the ideal properties. However there are an enormous range of compounds that have been evaluated and demonstrate some or several of the above characteristics such as sulfoxides (i.e. dimethylsulfoxide), laurocapram (commercially known as azone), pyrrolidones, fatty acids, alcohols, fatty alcohols, glycols, surfactants, urea, essential oils (i.e. terpenes and terpenoids), phospholipids and solvents. Some of these compounds will be summarize in the next section.

1.3.2.1. Azone

Azone (1-dodecylazacycloheptan-2-one or laurocapram) was the first molecule designed as a skin penetration enhancer and is a reference for comparison. Azone is a highly lipophilic molecule (log P close to 6.2) and for that reason it is compatible with most organic solvents, including alcohols and propylene glycol (PG). Azone has low irritancy, very low toxicity (oral LD_{50} in rat of 9 g/kg) and little pharmacological activity. Therefore, azone appears to possess many of the desirable qualities, and it is a potent and versatile enhancer for a wide variety of drugs including steroids, antibiotics and antiviral agents (Brown et al., 2006; Hadgraft et al., 1996; Lambert et al., 1989a; Riviere and Heit, 1997). Like other CPE, the efficacy of azone appears to be concentration dependent and is also influenced by the choice of vehicle from which it is applied (Srinivasan et al., 1989). Although azone has been in use for so many years, its mechanism of action is still controversial and object of study. Considering the chemical structure (possessing a large polar head group attached to a lipid alkyl chain), azone probably exerts its penetration enhancing effects through interactions with the lipid domains of the SC, causing the disruption of the bilayer lipids arrangement (Hadgraft et al., 1996; Jampilek and Brychtova, 2012; Lambert et al., 1989b). Surprisingly, azone is most effective at low concentrations (typically less than 10% in the formulations, and often at around 1-3%), although the amount of azone necessary to provide optimum enhancement varies between drugs and between formulations.

1.3.2.2. Surfactants

Surfactants (surface active agents) are present in many existing therapeutic, cosmetic and agrochemical preparations and usually are added to formulations used as

emulsifiers, wetting, solubilizing, and stabilizing agents. Therefore, and due to the great potential to solubilize/disrupt the lipid structure within the *stratum corneum*, they can be employed as CPE. Generally, surfactants are composed of a lipophilic alkyl or aryl fatty chain, linked to a hydrophilic head group, with amphiphilic properties. Surfactants are often described in terms of the nature of the hydrophilic moiety: the hydrophilic portion can be nonionic, ionic (anionic and cationic) or zwitterionic. The mechanism of action when applied in topical formulations is based on formation of diffusional paths for drug molecules, resulted of the interfacial defects and structure disruption and it is belief that can interact with the lipid molecules of skin, intercalating into lipid bilayers. Surfactants have generally low chronic toxicity, and most have been shown to enhance the flux of materials permeating through biological membranes. Some studies focus on the enhancement effect of surfactants on permeation of drugs through skin. The literature reports surfactant facilitated permeation of drugs such as diazepam, lorazepam, prazosin, piroxicam, hydrocortisone, lidocaine, etc. through various skin membranes, with significant flux enhancement (Cappel and Kreuter, 1991; Nokhodchi et al., 2003; Shin et al., 2001; Shokri et al., 2001; Walters et al., 1993b). Nevertheless depending on the amphiphilic structure and concentration employed local irritation of skin may be observed. Among the surfactant classes, the nonionic surfactants tend to be widely regarded as safe, while anionic and cationic surfactants are more likely to damage human skin. Most studies have focused on anionic and nonionic surfactants (Goreti Silva et al., 2012; Silva et al., 2013a; Silva et al., 2012). Anionic surfactants are negatively charged compounds that include sodium lauryl sulphate, and examples of cationic surfactants that exhibit positive charge are trimethylammonium bromide derivatives. The nonionic surfactants have modest enhancement effect in human skin whereas anionic surfactants can have a more pronounced effect

Some topical formulations, like creams that are stabilized by mixed emulsifiers contain ionic surfactants and their therapeutic efficacy depend, in part, on the penetration enhancement activity of the surfactants. These compounds are able to interact with skin constituents in many ways, for example, affecting proteins, and consequently inactivate enzymes and bind well within the SC. The anionic surfactants can swell the SC and modify the binding of water to the SC, probably by uncoiling the keratin fibers and altering the α-helices to a β-sheet conformation. Surfactants are also able to extract lipids from the SC by disrupting the lipid bilayer packing within the tissue. Surfactants can also modify the donor solution, altering the thermodynamics within the system to modify percutaneous drug delivery (Silva et al., 2013a). Gemini surfactants are a new class of surfactants, created to overcome problems such as irritancy and low

enhancement activity. The novel gemini surfactants derived from aminoacids such lysine and serine will be discussed in detail in Chapter 3 and 4.

1.3.2.3. Terpenes

Terpenes are essential oils and have been used as medicines, flavorings, fragrance agents and as penetration enhancers. Essential oils are complex mixtures of aromatic and aliphatic chemicals and the principal constituents are carbon, hydrogen and oxygen atoms. Terpenes are classified by their chemical structure, being based upon isoprene units (C_5H_8). The monoterpenes (C_{10}) contain two isoprene units, sesquiterpenes (C_{15}) have three and diterpenes (C_{20}) have four isoprene units. The application of monoterpenes and sesquiterpenes in topical and transdermal drug delivery has been extensively investigated by Barry and his co-workers (Cornwell and Barry, 1994; Williams and Barry, 1991). The principal terpene component of eucalyptus oil is 1,8-cineole, and this molecule was one of a series of 17 monoterpenes and terpenoids evaluated as enhancers for the 5-fluorouracil (a model hydrophilic drug) (Williams and Barry, 1989). Pre-treatment of human epidermal membranes with 1,8-cineole provided a near 100-fold increase in the permeability coefficient of 5-fluorouracil. Similar results were reported for the permeation of lipophilic molecule, indomethacin, traversing rat skin, also hydrocarbon terpenes, especially limonene, were as effective as azone in promoting drug flux. A synergistic effect for terpene efficacy has also been shown when PG was used as the vehicle (Williams and Barry, 1989). Terpenes also have the ability to modify drug diffusivity through the membrane and a reduction in the lag time for permeation is usually seen. Small-angle X-ray diffraction studies have indicated that d-limonene and 1,8-cineole disrupt SC bilayer lipids, whereas nerolidol (a long-chain sesquiterpene) reinforces the bilayers (Cornwell et al., 1996; Cornwell et al., 1994). Spectroscopic evidence has also suggested that, as with azone and oleic acid, terpenes could exist within separate domains in SC lipids.

1.3.2.4. Phospholipids

Phospholipids have been used as vesicles, to form liposomes that have the ability to carry drugs into and through human skin. However, some studies focus on using phospholipids in a non-vesicular form as penetration enhancers. For example, 1% egg phosphatidylcholine (PC) in PG (a concentration at which liposomes would not form) was used to enhance permeation of theophylline through hairless mouse skin. Likewise, the same phospholipid was used to enhance indomethacin flux through rat skin, and

hydrogenated soybean phospholipids have been reported to enhance diclofenac permeation *in vivo* through rat skin. The mechanism of action it is not well described. However considering the phospholipids physicochemical properties and structure, it is expected that they interact directly with SC lipid packing. Phospholipids can also occlude the skin surface and therefore improve tissue hydration allowing an increase on drug permeation. When phospholipid vesicles are applied, they fuse with the SC and the permeation is facilitated when the structure collapses and then releases the permeant into the vehicle in which the drug may be poorly soluble.

1.3.3. Chemical modulation of topical and transdermal permeation

1.3.3.1. Cyclodextrins

Cyclodextrins (CD) are known for nearly 100 years and are host molecules able to form inclusion complexes in solid and in solution phases (Del Valle, 2004). It was only during the last decades that CD have been used as potential drug carriers in delivery systems (McCormack and Gregoriadis, 1998). CD possess a cyclic structure containing six, seven or eight α (1–4) linked glucopyranose units designated by α, β and γ, respectively, and are called natural CD (Figure 1.6) (Szejtli, 1998). They take the shape of a truncated cone, instead of a perfect cylinder as a result of glucopyranose units in chair conformation (Loftsson and Brewster, 1996).

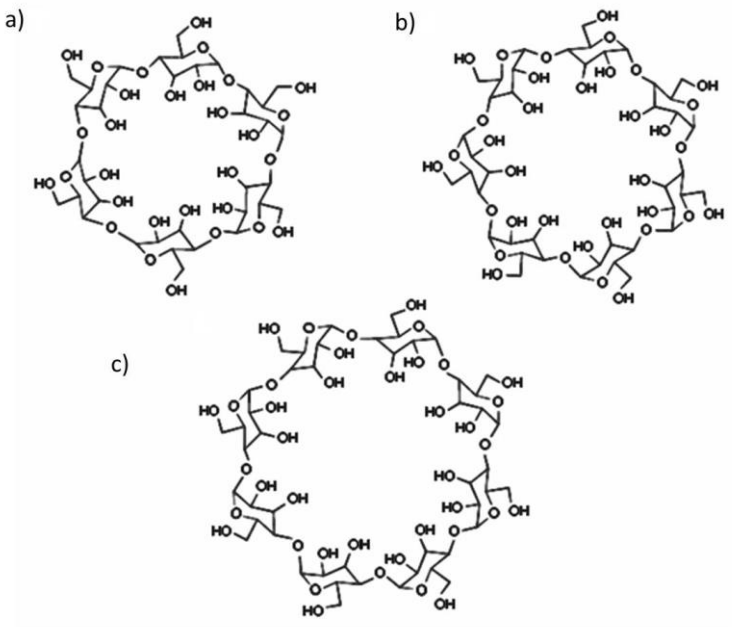

Figure 1.6 Schematic representation of α-CD (a), β-CD (b) and γ-CD (c). Adapted from (Davis and Brewster, 2004).

The hydroxyl groups are orientated to the exterior together with the primary hydroxyl groups of the glucose residues at the narrow edge of the cone and the secondary hydroxyl groups at the wider edge, resulting in a hydrophilic outer surface. The central cavity is lined by skeletal carbons and ethereal oxygens, which provides a lipophilic environment, thus allowing them to entrap apolar drugs (Arun Rasheed, 2008; Loftsson and Masson, 2001).

The use of CD is a practical and economical way to improve the physicochemical and pharmaceutical properties of administered drug molecules (Vyas et al., 2008). The traditional solubilizing agents such as organic co-solvents (ethanol and propylene glycol) and nonionic surfactants (Tween 80 or Cremophor®), or extreme pH conditions, may not be enough to solubilize drugs for their therapeutic efficacy (McCormack and Gregoriadis, 1998). So, an alternative approach to improve the water-solubility of drugs involve the use of CD which can form water soluble inclusion complexes with hydrophobic molecules (McCormack and Gregoriadis, 1998), (Uekama et al., 1998). Molecular encapsulations of the drug, in the appropriate CD, are able to overcome some problems and facilitate safe and efficient delivery of drugs (Vyas et al., 2008).

1.3.3.1.1. Derivatives

The naturally occurring CD and their complexes are hydrophilic but, however their aqueous solubility is rather limited, especially the *β*-CD (Loftsson et al., 2007). For that reason, many derivatives have been synthesized (Figure 1.7) and usually are produced by amination, esterification or etherification of the primary and secondary hydroxyl groups (Booij, 2009).

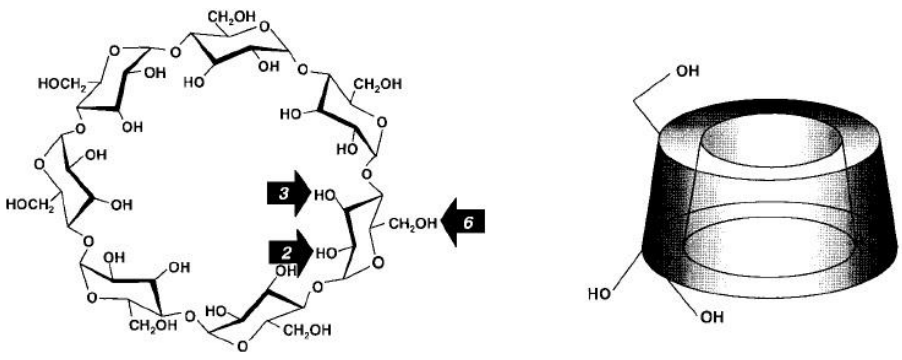

Figure 1.7 Location of the hydroxyl groups in the structure of β-CD (Uekama et al., 1998).

Depending on the substituent, the solubility of the CD derivatives will be different from that of their parent CD (Ventura et al., 2005). The most common CD derivatives currently used in drug formulations include hydroxypropyl-*β*-CD (HP-*β*-CD) used in this work, randomly methylated-*β*-CD (RM-*β*-CD), sulfobutylether-*β*-CD (SBE-*β*-CD), maltosyl-*β*-CD (ML-*β*-CD) and (2-hydroxypropyl)-γ-CD (HP-*γ*-CD). All of these five derivatives, as well the natural *α*-CD, *β*-CD and *γ*-CD, can be used in topical drug formulations (Loftsson and Masson, 2001). The aqueous solubility of these derivatives is usually 50–70% (w/v). Focusing on this aspect, the natural CD (*α*, *β* and *γ*) are the less hydrophobic CD and for example the HP-*β*-CD with the same cavity diameter as *β*-CD is less hydrophobic. On the other hand, 2,6 -dimethyl-*β*-CD (Dimeb) and 2,3,6-trimethyl-*β*-CD (Trimeb) have a deeper cavity and are more hydrophobic than *β*-CD (Piel et al., 2006).

1.3.3.1.2. Inclusion complexes

The most important property of CD is their ability to form complexes with a great variety of organic substances. The physicochemical properties of the included substances are altered upon complexation and CD are widely used for enhancement of aqueous solubility, stability and bioavailability of apolar drugs (Castronuovo and Niccoli, 2006; Mosher, 2002). The host-guest mechanism works like a dimensional fit between a guest molecule and the internal cavity. This lipophilic cavity has the appropriate environment for connecting the end of non-polar guest molecule, and during the formation of the inclusion complex, no covalent bonds are involved and drug molecules bound in the complex are in rapid equilibrium with free solubilized drug molecule (Figure 1.8) (Loftsson and Brewster, 1996; Loftsson and Duchêne, 2007).

The ability of a CD to form an inclusion complex with a guest molecule is a function of two key factors. The first is steric and depends on the relative size of the CD to the size of the guest molecule or certain key functional groups within the guest. The second critical factor is the thermodynamic interaction between the different components of the system (CD, guest, solvent) (Del Valle, 2004). In an aqueous environment, CD form inclusion complexes with many lipophilic drug molecules through a process in which water molecules located inside the central cavity are replaced by either the whole drug molecule or more frequently, by some lipophilic structure of the molecule. In this process, no covalent bonds are formed or broken and drug molecules located within the cavity are in a very dynamic equilibrium with free drug molecules out in the solution. In aqueous solutions drug/CD complexes are constantly being formed and broken at rates very close to the diffusion controlled limits (Stella and Rajewski, 1997).

In some cases, the complexation efficiency is not very high and, therefore relatively large amounts of CD are needed to complex small amounts of a certain drug (Loftsson and Masson, 2001). The drug molecule to be complexed with CD, it should have certain characteristics such has more than five atoms (C, P, S, N) forming the skeleton of the drug molecule, a melting point temperature below 250 ºC and solubility in water less than five condensed rings in its structure, a molecular weight between 100 and 400 (Szejtli, 1998, 2005; Vyas et al., 2008).

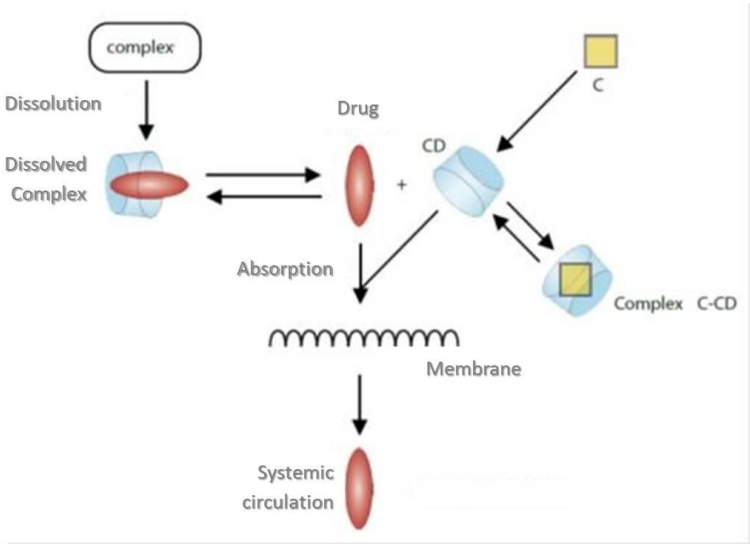

Figure 1.8 Scheme of drug complexation by CD and consequent release. Adapted from (Uekama et al., 1998).

1.3.3.1.3. Safety and stability of cyclodextrins on drug bioavailability

CD complexation has the advantage of promoting drug stabilization from hydrolyses, oxidation and photodecomposition (Loftsson and Brewster, 1996). The enhancement of drug stability induced by the CD is a result of inhibition of the drug interaction with vehicles and/or inhibition of drug bioconversion at the absorption site (Matsuda and Arima, 1999). The volatile components can also be stabilized by reducing liquids volatility or reducing the sublimation in the case of solids. Physical instabilities like sedimentation or recrystallization of substances may also be prevented or reduced by complexation with CD (Loftsson and Brewster, 1996). In addition CD has been used to prevent irritation caused by drugs that are irritant to the stomach, skin or mucous membranes by reducing drug toxicity and by making the drug effective at lower doses (Rajewski and Stella, 1996). The complexation with CD reduces the local concentration of free drug at the molecular level preventing their direct contact with biological membranes and thus reducing their side and local irritation with no drastic loss of therapeutic benefits (Challa et al., 2005; Scalia et al., 1999). With the dissociation of the complex, the drug is

absorbed by the body, always keeping the concentration of free drug within the desirable range (Rajewski and Stella, 1996)

1.3.3.1.4. Cyclodextrins as penetration enhancers

CD can also act as release enhancers contributing for the drug dissolution even if there is no complexation in the solid state (Challa et al., 2005). CD are also able to increase the permeability of hydrophobic drugs by increasing the drug solubility, dissolution and thus making the drug available at the surface of the biological barrier, from where it partitions into the membrane without disrupting the lipid layers of the latter. In such cases it is important to use just enough CD to solubilize the drug in the aqueous vehicle since excess may decrease the drug availability as will be discussed in Chapter 2. Also complexation with CD may increase drug concentration in aqueous vehicles, forming saturated solutions with a high thermodynamic potential, promoting the affinity of the drug to the SC and increasing the permeation flux. Nevertheless, only the free drug penetrates the skin and the promoting effect seems to be dependent on the amount of CD (Matsuda and Arima, 1999).

Due to CD high molecular weight (from 972 to over 2000 Da) and a low octanol/water partition coefficient (Log $P_{o/w}$ from less than - 3 to almost 0) it is not expected that they penetrate biological membranes. However it is believed that some hydrophilic CD with a Log $P_{o/w} < 3$, can penetrate lipophilic biological membranes such as the skin and gastrointestinal mucosa (Lipinski et al., 2001). Hydrophilic CD can modify the rate of drug release, which can be used for the enhancement of drug absorption across biological barriers, serving a potent drug carrier in the immediate release formulations (Dahan et al., 2009).

The use of CD in transdermal drug delivery is still controversial. Some authors found that CD and their derivatives can extract the lipids and some proteins from the SC (Legendre et al., 1995; Vollmer et al., 1994). In contrast other authors reported that there are no interactions with the skin components, although increased delivery for some materials could be explained though a solubilizing effect of the CD on drug in donor solutions. Further, excess of complexing host molecules in a formulation can reduce the flux of a permeant (Loftsson et al., 1994; Williams et al., 1998).

1.3.3.2. Production and characterization of cyclodextrin complexes

Cyclodextrin complexes are prepared by adding an excess of drug, to different concentrations of CD in the desired media. The solution is left stirring until reaching the equilibrium and then is filtered using nylon 0,22 µm filters. The concentration of the drug is determined using a UV spectrophotometer or HPLC. Data acquisition and analysis are performed using proper software. The concentration of drug is determined by comparison to a calibration curve make up in an equivalent media (Diane and Gerold, 2013).

1.3.3.2.1. Phase-solubility studies

The stability constant of the complex can be determined based on changes that occur during the process of complexation (Echezarreta-López et al., 2002). Phase solubility is the most common method used to determine the formation of the inclusion complex, the complex type and calculate their stability constant when the drug molecule is slightly soluble in water (Dittert et al., 1964). In this method, the solubility of the drug changes in the presence of increasing concentrations of CD. The thermodynamic equilibrium is achieved by stirring the samples at constant temperature and the results are presented graphically as solubility phase diagrams represented in Figure 1.9,

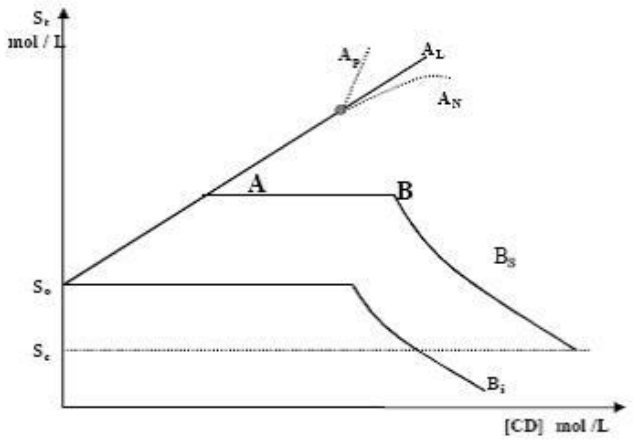

Figure 1.9 Solubility diagram types according to Higuchi and Connors (Siepmann and Peppas, 2011).

The solubility diagrams are divided into two groups: diagram type A that shows the formation of soluble complexes and diagrams type B that indicates the complex formation with intrinsic solubility less than the guest molecule solubility (S_0). In the diagrams of type A, the total apparent solubility of the guest molecule (S_t) increases linearly due to the formation of soluble inclusion complex of any concentration of

complexing agent. In the A_L type diagrams the total solubility of the substrate (S_t) depends on the linearity of the concentration of CD, obtaining complexes of first order. An A_P type diagram corresponds to the formation of complexes of higher molecular order with respect to CD, which means that the complexation of the guest molecule needs one or more molecules of CD, showing a positive deviation from linearity at higher CD concentrations. Systems that originate diagrams type A_N are related with a negative deviation of linearity at higher CD concentrations. It is one of the least observed in practice systems and their occurrence can be explained by self-association of the complexes in solution and by changing the nature of the solvent due to high concentrations of CD. The diagrams of type B indicate the formation of inclusion complexes with limited solubility. In the diagrams type B_S the solubility of the complex increases linearly due to the formation of soluble complexes. However, at point A, the solubility of the complex achieves the limit. The S_t of the guest molecule is constant between points A and B, indicating that the equilibrium is reached in the complex formation. After point B, since the guest molecule is completely consumed in the solid state with the addition of a larger amount of CD, the concentration of uncomplexed guest molecule in solution decreases, due to formation and precipitation of insoluble complex. This translates into a decrease in the solubility to a constant value corresponding to the solubility of the inclusion complex (S_C). The diagram of the type B_i is interpreted in the same way, with however the complex formed is so insoluble that the initial increase in solubility of the guest molecule is not detectable (Loftsson et al., 2005). The stability constant of the complex formed and the efficiency of complexation can be calculated based on the phase-solubility diagrams and equilibrium association and dissociation in the formation of inclusion complexes

$$K = \frac{Slope}{S_0\,(1-Slope)} \qquad (1.4)$$

where S_0 is the intrinsic solubility of the drug in the medium, obtained from the origin intercept and the slope is obtained from the linear regression of the data points.

1.3.4. Physical and technological modulation of topical and transdermal drug delivery

1.3.4.1. Liposomes

Encapsulation of drugs or cosmetics into vesicular systems has been used for various delivery systems especially in topical preparations. Liposomes were described for the first time in 1960 by Bangham and his co-workers (Schmid and Korting, 1996) but it was in 1988 that the first antifungal drug econazole topical formulation (Pevaryl Lipogel, Cilag Corp., Switzerland) was marketed (Schmid and Korting, 1996). Liposomes are characterized by concentric and microscopic vesicles in which an aqueous volume is entirely enclosed by a lipid bilayer membrane. This lipid bilayer is mainly composed of natural or synthetic phospholipids, with or without CHO, water and possibly electrolytes. The most common liposomes are prepared using lecithin of egg or vegetable origin (soy bean) and the lipids may be arranged in one or more bilayers (Barenholz, 2001; Meisner and Mezei, 1995). The choice of the lipid composition affects the liposome surface, that can be positive (stearylamine), negative (phosphatidic acid), or neutral (lecithin) (Meisner and Mezei, 1995) and the addition of relatively small amounts of CHO tends to stabilize the membrane and therefore the liposome tend to be more rigid (Schmid and Korting, 1996). Liposomes are amphiphilic molecules, with a hydrophilic head and a lipophilic tail, which means that they can incorporate hydrophilic molecules within their aqueous regions and lipophilic molecules within the membrane and hold them in route to their destination (McCormack and Gregoriadis, 1998; Meisner and Mezei, 1995).

Various methods have been proposed, but the most common is the thin layer evaporation method (TLE).

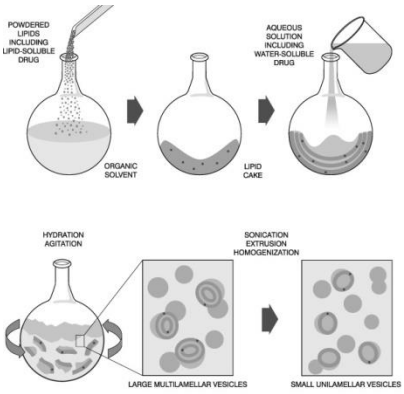

Figure 1.10 Preparation of lipid for hydration in TLE (adapted from Avanti polar lipids).

The TLE technique (Figure 1.10) is based on the evaporation of a volatile solvent containing the mixture of lipids to ensure the complete homogenization. After forming a thin film of lipids onto the walls of a vessel, this film is hydrated with the aqueous solution (water or buffer) containing the material to be entrapped. Depending on the method of preparation, on their size, on the lamellarity of liposomes they can be classified differently.

The unilamellar lipid vesicles are found when a single bilayer enclosing an aqueous compartment is obtained. According to their size, they are known as small unilamellar vesicles (SUV) or large unilamellar vesicles (LUV). If more bilayers occur, as they are called multilamellar vesicles (MLV) (Figure 1.11), (Meisner and Mezei, 1995). The MLV are typically 0.1 to 10/µm in diameter, they usually form spontaneously when the film is rehydrated at temperatures above the phase transition temperature of the lipids. Since the size and lamellarity of these MLVs are difficult to control, usually these structures are processed by sonication or extrusion through membrane filters that will considerably reduce the lamellarity to form LUV (generally 1 to 5/µm in diameter) or even SUV with 0.1 to 0.5/µm of diameter. To remove any free drug from the system, a filtration or dialysis step is considered after the preparation of encapsulated liposomal formulations (Vemuri and Rhodes, 1995).

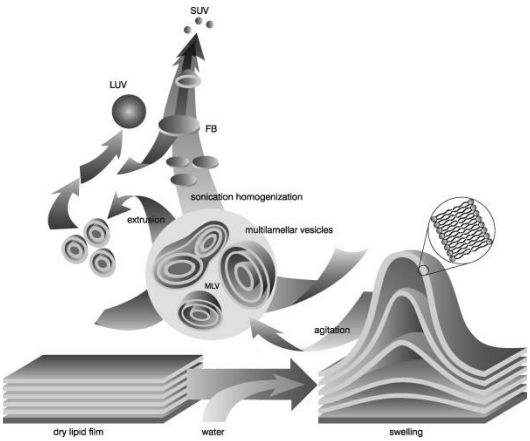

Figure 1.11 Mechanism of vesicle formation. The types of liposomes depend on size and number of lamellae.

1.3.4.1.1. Liposomal formulations

Liposomes are used to administer drugs by several routes such as the oral, parenteral and also promote dermal delivery of drugs which have to act topically, such as local anesthetics. In addition, they enhance transdermal delivery of drugs intended for

systemic use, being very effective in exploiting this non-invasive alternative route to oral administration (Maestrelli et al., 2006; Manosroi et al., 2004).

The liposomal formulations are widely used in the pharmaceutical field as drug delivery systems due to their versatility and clinical efficacy (Schmid and Korting, 1996). Besides, and compared to conventional formulations, drugs encapsulated in liposomes increase their effect, and liposomes are biodegradable and generally more effective and non-toxic than conventional topical formulations such as ointments, creams or lotions (Honzak et al., 2000a; Reimer et al., 1997).

It should be noted that the hydrophilic or lipophilic properties of the encapsulated drug affects the encapsulation efficiency of the drug in the liposomes (Glavas-Dodov et al., 2002). Among the substances that are able to be incorporated into liposomes, local anesthetics together with anticancer, antifungal and antibiotic agents are considered the most used, because they satisfy all the requirements necessary for topical application and localized drug delivery (Glavas-Dodov et al., 2002; Schmid and Korting, 1996).

Liposomes work like drug penetration enhancers into the skin and after topical application they can assume different functions. Usually they improve drug deposition into the skin at the site of action providing a local effect with little or no systemic activity and for that reason minimize side effects (Maghraby et al., 2006). The mechanism of action is not completely clear and consequently there is significant conjecture. However, most authors suggests that liposomes are effective on drug permeation and enhance clinical efficacy, due to the similarity to the biological membrane, which makes them suitable to encapsulate hydrophilic and lipophilic substances in their different phases. Furthermore, liposomes prepared with similar lipids to those found in the SC showed to be the most effective for topical drug delivery which penetrating the epidermal barrier to a larger extent thanother dosage forms (McCormack and Gregoriadis, 1994a; Verma et al., 2003a, b).

However there is a general problem concerning to the efficacy of topical drugs. It is necessary to reach the site of action and stay in an effective concentration for a certain time (Schmid and Korting, 1996). Another problem is that the permeability characteristics of the SC could be altered due to the fact that some lipids from the liposomes could penetrate into the latter and thereby modifying its endothermic profile (Weiner et al., 1994).

Classical liposomes (200-400 nm in diameter) are too big and unable to deform, for that reason they have some limitations as carriers for transdermal drug delivery as they do not penetrate skin deeply and thus are restricted to the outer layers of the SC (Elsayed et al., 2007). In order to target deeper the underlying skin tissue, intensive research led to the introduction and development of a new class of lipid vesicles, the highly deformable (elastic or ultraflexible) liposomes, which have been called Transfersomes® (Cevc and Blume, 1992).

1.3.4.1.2. Highly deformable liposomes

The possibility that intact vesicles can permeate through skin membranes and release the drug into the systemic circulation is still controversial. To overcome this problem, a new class of highly deformable liposomes namely transfersomes have been developed. These elastic and ultraflexible vesicles comprise a phospholipid (e.g. phosphatidylcholine) as main component together with 10 to 24 wt% of a surfactant added. The flexibility of the liposome is given by the high radius of curvature of the surfactant that acts as an 'edge activator' and some research has shown that it is able to squeeze through a pore of about 20 nm diameter (Cevc, 2002). The edge activator present in the formulation has the capability to accumulate at the high stress sites within the vesicles and form a highly curved area of the vesicle which, to maintain stability, will then move through narrow skin pores to the more hydrated environment within the deeper skin layers.

According to the inventors, these vesicles are able to penetrate intact into the deeper skin and even reach systemic circulation (Cevc et al., 1997; Cevc et al., 1996; Cevc et al., 1998). Whilst there is still some reservation and contradiction on the mechanisms by which ultra-deformable or highly flexible liposomes improve drug delivery, some workers proved that these vesicles can deliver increased amounts of therapeutic agents to and through the skin (Jianxin Guo, 2000; Maghraby et al., 2001a, b; van den Bergh et al., 2001). A lot of work has been developed to evaluate the influence of liposome fluidity on drug delivery of new therapeutic agents to be formulated (Cevc and Blume, 2001; Duangjit et al., 2013; Khan et al.; Nuria Perez-Cullell, 2000; Zhang et al., 2014).

1.3.4.2. Liposomes production and characterization

1.3.4.2.1. Size

Dynamic light scattering (DLS), also known as photon correlation spectroscopy is a technique for measuring the size of very small particles (Goldburg, 1999). The measure of the particle size is influenced by the fluctuation of the intensity of the scattered light of a laser beam caused by particle Brownian motion (Figure 1.12). The Brownian motion will be slower the larger is the particle, and the later will diffuse more slowly than the smaller ones. The velocity of the particle Brownian motion is defined by translational diffusion coefficient (*D*). Therefore the size of a particle is calculated from the translational diffusion coefficient by using the Stokes-Einstein relation

$$d(H) = \frac{K_B T}{3\pi\eta D} \qquad (1.5)$$

where *d(H)* corresponds to the hydrodynamic diameter, K_B to the Boltzmann's constant, *T* the absolute temperature, *η* the viscosity and *D* stands for the translational diffusion coefficient. This equation shows that, for large particles, *D* will be relatively small, and, thus, the particles will move slowly while for smaller particles, *D* will be larger and the particles will move more rapidly. Therefore, by observing the motion and determining the diffusion coefficient of particles in liquid media, it is possible to determine their size.

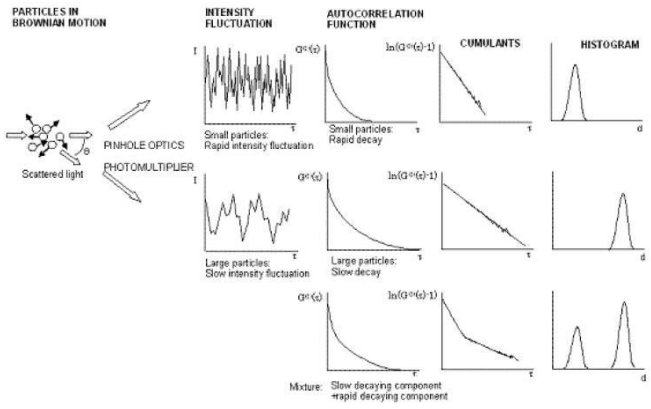

Figure 1.12 Determination of particle size by dynamic light scattering.

The diffusion coefficient is obtained by fitting the correlation function with a suitable algorithm, such as the cumulants analysis, which determines a mean size and polydispersity index (PI). The PI is a dimensionless measure of the broadness of the size distribution, ranging from 0 to 1. A PI value lower than 0.1 might be associated with a

high homogeneity in the particle population (monodisperse), whereas high PI values suggest a broad size distribution (polydisperse) or even several populations (plurimodal).The latter situations suggest potential problems with the stability of the formulation, and the probability of aggregation of the particles has to be considered.

1.3.4.2.2. Zeta potential

Zeta potential is a physical property exhibited by most colloidal particles when dispersed in liquids being related to its surface charge. This parameter predicts the stability of long term colloidal systems. The technique is based on the particles that move towards the electrode that has an opposite charge and an electric field is applied to the cell that contains the particle suspension. If zeta potential is high, the particles are stable due to high electrostatic repulsion between particles. On the contrary, a low zeta potential value (approaching zero) increases the probability of particles colliding and therefore, forming particle aggregates. Thus, zeta potential is used as an index of the dispersion stability of particles (Sudo et al., 2013).

1.4. Topical and transdermal formulations

Most preparations to be applied topically are semi-solids since they have good adhesion to the skin and can be used to deliver therapeutic agents over a period of time. Despite the various possibilities of vehicles used in dermal drug delivery systems, special emphasis will be given to gels, particularly water-based gels (or hydrogels) that were used in this work as vehicle as shown later.

1.4.1. Matrix formers

The physicochemical properties and the performance of the formulation depend of the nature of the matrix. For devices that incorporate the drug in a matrix, the composition of the latter can regulate permeant release. The matrices are usually prepared using simple polymer mixtures with the drug dispersed and then after forming the gel the permeant will be incorporated in the latter. Generally the degree of polymer cross-linking and the level of hydration of the gel control the diffusion of the permeant through the polymer matrix. Hydrogels are alternative matrices formed from a network of hydrophilic polymers that are waters swollen.

1.4.2. Hydrogels

Hydrogels are naturally formed by adding a thickness agent to a liquid phase exhibiting an intermediate behavior between solid and liquid materials. Hydrogels can be defined as three-dimensional, hydrophilic and polymeric network. The network is composed by a liquid phase that essentially forms a continuous phase where the solvent can be polar (water or alcohol) or non-polar. Numerous thickening agents are available and the selection is based on the physicochemical properties of the permeant. Simple gels can be prepared from water thickened with typically 1 and 5% in the formulation of natural polymers (carageenans or pectin) or synthetic polymers (hydroxypropylmethylcelulose - HPMC or Carbopol).

Hydrogels are biocompatible with proteins, as well as living cells and body fluids, due to their high water content and soft texture (Chandak and Verma, 2008b; Krishnaiah and Al-Saidan, 2008). For that reason, hydrogels are nowadays widely used in various therapeutic applications, e.g. tissue engineering, controlled drug delivery and diagnostic devices, e.g. medical and biological sensors, microarrays, diagnostic imaging. In terms of controlled drug delivery from gels, they have played a vital role as intelligent carriers. The continuous liquid phase allows free diffusion of molecules through the polymer scaffold, and hence release should be equivalent to that from a simple solution. Drug release from the polymer can be easily modulated by very large molecules (macromolecules), highly viscous gels and in particular, by permeants that bind to the polymer in the gel.(Roy et al., 2009).

1.4.2.1. Hydroxypropylmethylcellulose

HPMC has been tested as a matrix former in the design of patches of several drugs such as propranolol hydrochloride (Guyot and Fawaz, 2000), flurbiprofen (Verma and Murthy, 1997), tramadol (Chandak and Verma, 2008c), methotrexate (Chandak and Verma, 2008a), trimetazidine (Krishnaiah and Al-Saidan, 2008) and metformin (Jahan et al., 2011) widely used in oral and topical formulations. HPMC is a flexible hydrophilic polymer available in different grades and has been shown to yield clear films because of the adequate solubility of the drug in the polymer.

Matrices of HPMC without rate-controlling membranes have been observed to exhibit a burst effect during dissolution testing because the polymer was hydrated easily and swelled, leading to the fast release of the drug (Guyot and Fawaz, 2000). Moreover,

HPMC is also chemically unreactive and therefore it is compatible with all active and non-active ingredients.

Due to all reasons listed, HPMC was the polymer selected to be the matrix-former in the preparation of drug-loaded hydrogels in the permeation studies presented in the following Chapters of this thesis.

1.5. Drug information

Tetracaine (TC) (Figure 1.13) is a potent amino ester type local anesthetic, indicated for anesthesia before venipuncture or venous cannulation and is primarily used for surface anesthesia and spinal block (Covino, 1987). Due to its high systemic toxicity, the use in other anesthetic techniques is limited. Tetracaine has been shown to pass through the skin (Fisher et al., 1998; Romsing et al., 1999; Teixeira et al., 2014a). However adverse effects of its topical administration include mild erythema at the site of the application and less frequently slight edema, pruritus and blistering of the skin. This molecule is a white or light yellow, very slightly soluble in water and soluble in organic solvents and is stable under ordinary conditions. It has a pKa of 2.24 and 8.39 and a LogP of 2.79, which compared to the other anesthetics, makes this molecule a suitable candidate to undergone skin permeation. Tetracaine is commonly used as the hydrochloride form in solutions and creams and as the base form in ointments or gels. A 1% cream or a 0.5% ointment is normally used for topical anesthesia, while a 4% gel is employed for a percutaneous local anesthesia before venipuncture or venous cannulation. Tetracaine is reported to be about 15% bioavailable after application of a 4% gel to intact skin, with a mean absorption and elimination half-life of about 75 minutes (Berman et al., 2005; McCAFFERTY et al., 1989; Romsing et al., 1999; Schecter et al., 2005).

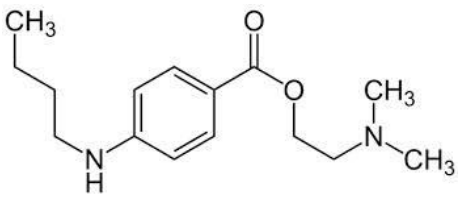

Figure 1.13 Chemical structure of tetracaine.

Ropivacaine hydrochloride (RPC) (Figure 1.14) it is a long-acting local anesthetic. Ropivacaine is used for epidural block, peripheral nerve block, infiltration anesthesia and field block, but is contra-indicated for obstetric paracervical block and for use in

intravenous regional anesthesia (Bier's block). At high doses ropivacaine produces surgical anesthesia, whereas at lower doses it is used for the management of acute pain such as labour pain and in postoperative analgesia. Ropivacaine has a differential blocking effect on nerve fibers and, at the lowest concentration used, there is good differentiation between sensory and motor block. The onset and duration of sensory block produced by ropivacaine is generally similar to that obtained with bupivacaine but the motor block is often slower in onset, shorter in duration, and less intense. Ropivacaine hydrochloride is administered in concentrations of 0.2 to 1%. The dosage depends on the site of injection and the procedure used, as well as the status of the patient. The dose of ropivacaine should be reduced in the elderly, and in acutely ill or debilitated patients. A test dose of lidocaine with adrenaline should be given before starting epidural block with ropivacaine to detect inadvertent intravascular administration (McClellan and Faulds, 2000; McCrae et al., 1995; Zink and Graf, 2004).

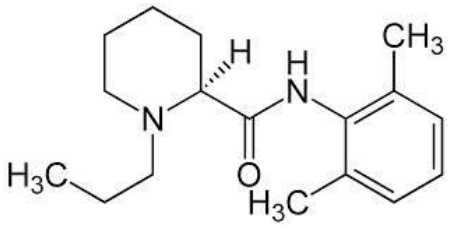

Figure 1.14 Chemical structure of ropivacaine.

1.6. Scope

The work presented in this thesis aims at the development of different formulations strategies to improve the efficacy and permeation of two distinct local anesthetics across the skin. The first part gathers a comprehensive set of data obtained from several complementary techniques regarding the nature of the association between two forms of TC and CD and how this interaction affects the transport across a model membrane. The second part is addressed in Chapter 3, 4 and 5, and consists of a detailed data of aminoacid-based surfactants and liposomes as chemical permeation enhancers for both local anesthetics. The final optimized formulations were subsequently tested *in vivo* and are presented in Chapter 6.

Chapter 2

Effect of cyclodextrins and pH on the permeation of tetracaine: supramolecular assemblies and release behavior

Tetracaine is a lipophilic molecule and cyclodextrins are known to increase the solubility of lipophilic molecules in water. This Chapter focuses on the interaction mechanism between tetracaine with different cyclodextrin (*β*-CD e HP-*β*-CD) and how such interaction affects the transport of the latter. The kinetics and mechanism of tetracaine release from HPMC gels was also discussed in this Chapter giving an insight on the role of cyclodextrin on the tetracaine transport. The present observations allow demonstrate that cyclodextrins increase the solubility of tetracaine in water which is successfully released from the formulations at a controlled rate.

2.1. Introduction

It is generally believed that the interaction of the anesthetic with membrane lipids and proteins leads to the inactivation of neuronal ion channel activity (Ragsdale et al., 1994). Tetracaine is reported to be about 15% bioavailable after application of a 4% gel to intact skin, with a mean absorption and elimination half-life of about 75 minutes (O'Brien et al., 2005). This drug can suffer hydrolysis, resulting in equilibria between three different absorbing species: tetracaine base form (TC) and tetracaine ionized forms (TCH^+ and TCH_2^{2+}) depending on the pH (Figure 2.1). The ability of this drug to cross biological membranes is also pH-dependent. It has been reported that tetracaine in its base form can permeate the skin (Liu et al., 2005). The ionic form (TCH^+), is dominant at physiologic pH of the skin (pH ~ 4.2 – 6.5) and it is generally accepted that the cationic form binds to the sodium channels on the nerve membrane, blocking the initiation and transmission of nervous impulses(Chekirou et al., 2012).

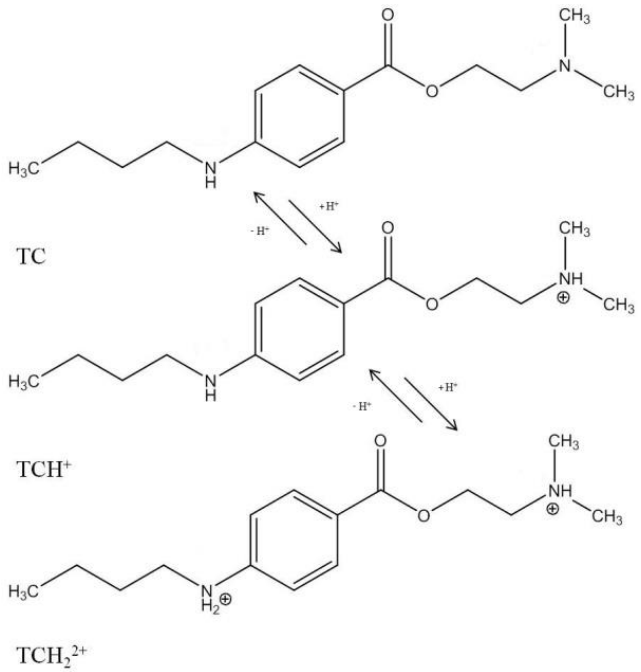

Figure 2.1 Schematic representation of ionization equilibrium of tetracaine, exhibiting two ionizable groups (pKa's 3.41 and 8.24) (Iglesias-García et al., 2010).

The bioavailability of most topically applied drugs is generally very low and various approaches have been developed to enhance drug diffusion across the skin (Hadgraft, 1999; Thomas and Finnin, 2004). One of them involves the use of cyclodextrins. These

compounds are known to have the ability to form complexes with a wide range of organic molecules, both in solution and in solid state (Másson et al., 1999; Ventura et al., 2006). CD have been recognized as promising drug carriers and delivery systems but how they function to modify topical administration has not as yet been fully elucidated (McCormack and Gregoriadis, 1998). Host-guest like complexes may improve the properties of the guest molecule, e.g. the drug, such as solubility enhancement (Loftsson and Brewster, 2012; Yuan et al., 2013) and stability improvement (Yuan et al., 2013). Additionally, CD act as efficient drug carriers, providing a controlled and sustained release, avoiding undesirable toxic effects (Castronuovo and Niccoli, 2006; Mosher, 2002). Although the naturally occurring CD (in particular the *β*-CD) and their complexes are hydrophilic, their aqueous solubility is limited. The synthesis of new CD derivatives (such as HP-*β*-CD) has allowed overcoming the solubility issue (Booij, 2009; Loftsson et al., 2007). As previously mentioned, the neutral TC permeates the skin, however that occurs at pH higher than 8, clearly above the skin physiological pH. This Chapter reports a comprehensive analysis regarding the transport of TC across a model membrane. Studies using a simple inert barrier model are very useful for optimization of formulations in earlier stages of research. The dialysis membrane was selected as a model membrane because it is isotropic and homogeneous (see section 1.2.3.). In these conditions, release data can be described by simple mathematical models. Essentially, this work focused on the complexation phenomenon occurring between aqueous solutions of two forms of tetracaine and *β*- and HP-*β*-CD and how the CD concentration on the formulation alters the release profile of tetracaine. *In vitro* release studies across dialysis membrane using different tetracaine formulations were carried out at two distinct pH values (4.1 and 9.0). The mechanism of release was evaluated on the basis of the interactions established between tetracaine and HP-*β*-CD.

Mathematical models appear as useful tools to correlate material properties, interaction parameters, kinetic events, and transport behavior within complex hydrogel systems (Korsmeyer et al., 1983; Siepmann and Peppas, 2001; Siepmann and Peppas, 2011).

Although the interactions between tetracaine and CD, at neutral pH, have already been reported elsewhere (Fernandes et al., 2007; Franco de Lima et al., 2012; Van Santvliet et al., 1998), no studies have been presented with acetate buffer at acidic pH (ca. pH 4). At this pH, the pKa of tetracaine in the presence of CH_3COO^- and the CD decreases, however the predominant structure remain the same. CD:TC complexes were characterized using different techniques: i) stoichiometry, association constants, and HPLC, fluorescence and nuclear magnetic resonance (NMR) spectroscopies to analyze

topology of complexation of the inclusion complexes. The tetracaine concentration during the experiments was kept below the critical micelle concentration - cmc (128 mM), as reported elsewhere (Dukhin, 2005). The results obtained were rationalized and the conclusions are new, significant and provide solid physicochemical knowledge of these systems that are crucial for future delivery studies with local anesthetics and cyclodextrins.

2.2. Experimental section

2.2.1. Materials

Tetracaine base, acetic acid, 3-(trimethylsilyl) propionic-2,2,3,3-d4 acid sodium salt (TSP), ammonium acetate, sodium acetate and *β*-CD were acquired from Sigma Aldrich (St. Louis, M. O. United States of America). Millipore water was used to prepare sodium acetate buffer aqueous solution. HP-β-CD with 97% of purity, with an average degree of substitution of 2 to 6 units of 2-hydroxypropyl (C_3H_7O) per glucose unit, and with an average molecular weight of 1380 g/mol, was purchased from Acros Organic (Geel, Belgium). Methanol (MeOH) and acetonitrile (ACN) HPLC grade were purchased from LiChroSolv Merck (Darmstadt, Germany). Phosphate buffer saline tablets (PBS) were purchased from TIC Gums (Belcamp, MD, USA). Dialysis membrane (Spectra/Por) with a 6-8.000MWCO, was bought from Spectrum Laboratories, Inc. (Broadwick St., Rancho Dominguez, US & Canada). Deuterated water (D_2O) (99.9%) for preparing NMR samples was purchased from Eurisotop (Saint-Aubin Cedex, France). HPMC - Methocel K15M Premium, 19%-24% methoxyl and 7-12% hydroxypropyl, M_w=4.3×10^5 Da) was a kind gift from Dow Chemical. All reactants were used as received.

2.2.2. Phase - solubility studies

Phase-solubility diagrams were carried out to assess the solubility of tetracaine and determine the association constants with the cyclodextrins. Phase solubility studies were performed according to the procedure reported by Higuchi and Connors and as mentioned in section 1.3.3.2.1. (Siepmann and Peppas, 2011). The studies were performed at room temperature, by adding an excess of TC base to deionized water (pH=9) and sodium acetate buffer aqueous solution (pH=4.1) containing increasing amounts of *β*-CD (1-15 mM) and HP-*β*-CD (1-45 mM), stirred during 72h. The solutions

were filtered using a MCE 0.45 µm filter syringe (Fioroni filters, Ingré, France) (n=3). An aliquot of solution was removed, diluted in a filtered and degassed mobile phase (MeOH, ACN and ammonium acetate) and quantified by using HPLC (Shimatzu LC-20AD) (see section 2.2.5.2. The apparent stability constants (K) of the complexes were calculated from the slope of the straight lines of the phase-solubility diagrams and the drug solubility in the medium using Eq. 1.4 (Connors and Mollica, 1966),

2.2.3. Fluorescence studies

Fluorescence spectrophotometry is usually the method of choice for quantitative analytical purposes, if applicable. It has assumed a major role in analysis, particularly the determination of trace contaminants in our environment, industries and bodies, because for applicable compounds fluorescence spectrometry gives high sensitivity and high specificity. The selectivity of fluorescence methods is greater than that of absorption methods, as fewer substances fluoresce than absorb radiation in the UV or visible region. Furthermore, fluorescence is more selective because both the emission and the absorption spectra can be obtained. Fluorescence is usually also more sensitive than absorption methods, as it is always easier to measure a small signal against a very small zero background than to measure a small difference between large signals. However, the phenomenon of fluorescence itself is subject to more rigorous constraints on molecular structure than is absorption.

In order to characterize the stability constants between TCH^+ and CD, the fluorescence emission spectra of TCH^+ were collected and analyzed. Changes in the intrinsic fluorescence of TC using different CD molar ratios of complexation were also investigated. A batch of buffered acetate aqueous solutions with a fixed concentration of TC (10 µM) were prepared (n=3) by adding increasing amounts of *β*-CD and HP-*β*-CD. The pH of each solution was fixed at 4.1 and maintained constant during the experiments. The solutions were subsequently mixed at 25°C during 72 h. The measurements were performed using a Horiba-Jobin-Ivon SPEX Fluorolog 3-22 spectrophotometer at 25°C. The excitation wavelength was fixed in 311 nm and the emission spectra were collected from 320 to 500 nm. The emission and excitation slits used were fixed at 5 nm.

2.2.3.1. Modeling stoichiometry and association constants

Assuming that a 1:1 complex between *β*-CD and HP-*β*-CD with ionized tetracaine, TCH^+ (a proof for this assumption will be presented in the section 2.3.1) is formed

$$CD + TCH^+ \overset{K}{\rightleftarrows} CD:TCH^+ \tag{2.2}$$

the stability of the complex $CD:TCH^+$ can be described in terms of an association constant, *K*,

$$K = \frac{\left[CD:TCH^+\right]}{\left[CD\right]_f \left[TCH^+\right]_f} \tag{2.3}$$

where $[CD]_f$ and $[TCH^+]_f$ represent the concentration of free (non-complexed) species, *β-CD* or HP-*β*-CD and ionized tetracaine, respectively, and $[CD:TCH^+]$ is the concentration of the 1:1 complex.

From Eq. 2.3 and the mass balance equations

$$\left[CD\right]_T = \left[CD:TCH^+\right] + \left[CD\right]_f \tag{2.4}$$

$$\left[TC^+\right]_T = \left[CD:TCH^+\right] + \left[TCH^+\right]_f \tag{2.5}$$

where $[CD]_T$ and $[TCH^+]_T$ represents the total (initial) concentrations of *β*-CD or HP-*β*-CD and TCH^+, respectively, the association constant, *K*, can be re-written as

$$K = \frac{f}{(1-f)\left(\left[CD\right]_T - f\left[TCH^+\right]_T\right)} \tag{2.6}$$

where *f* is the fraction of TCH^+ complexed with the *β*-CD and HP-*β*-CD.
Since the CD is not fluorescent, the observed fluorescence emission intensity, *F*, from free and complexed tetracaine is given by

$$F = k_1\left[TCH^+\right]_f + k_2\left[CD:TCH^+\right] \tag{2.7}$$

where k_1 and k_2 are constants. Considering F_0 and F_∞ the fluorescence intensity of TCH^+ in the absence and in excess of cyclodextrin, respectively, f can be represented by

$$f = \frac{F - F_0}{F_\infty - F_0} \tag{2.8}$$

Combining Eqs. (2.6) and (2.8) we obtain

$$F - F_0 = \frac{(F_\infty - F_0) K [CD]_T}{1 + K [CD]_T} \tag{2.9}$$

The experimental data (see Figure 2.7) can be perfectly fitted (R^2>0.9965) to Eq. (2.9), using a non-linear least-squares algorithm, to obtain the fitting parameters K and F_∞.

Eq. (2.9) can be simplified in order to have information on the stoichiometry of the association (Smith et al., 1991). Thus, a linear relationship of $(F-F_0)/[CD]_T$ as a function of $(F-F_0)$ is indicative of a 1:1 stoichiometry.

2.2.4. NMR/Rotating frame nuclear Overhauser effect spectroscopy (ROESY) studies

NMR spectroscopy (^{1}H-NMR), represents one of the most important technique in the study of supramolecular structures in solution such the inclusion complexes with CD. This technique provides information about stoichiometry, stability constants, energy process of complexation and complex structure of the drug/CD (Chao et al., 2004; Schneider et al., 1998). Although the phase solubility studies assess the solubility of the drug with CD, this technique only give an indication on the possible formation of inclusion complexes, however do not distinguish other external associations that may occur (Loftsson et al., 2004; Schneider et al., 1998). NMR spectroscopy is based on the polarity changes of the environment that results in alterations in the chemical shifts of the protons of the drug molecule and CD. Thus, the variation in chemical shifts is used for the characterization of those complexes (Schneider et al., 1998). The changes in chemical shifts ($\Delta\ \delta$) is calculated by the difference between the chemical shifts of the molecule in the presence of other complexing reagent δ (complex) and chemical shifts of the free molecule δ (free). Due to the change of its chemical environment, positive or negative changes occur representing a shift of the protons to lower or higher fields,

respectively (Loukas, 1997). Changes in chemical shifts on the H3 and H5 protons that are found in the internal cavity of CDs allow concluding the formation of an inclusion complex as well as its geometry. The protons deviations caused by the molecule which penetrates into the cavity of CD are due to anisotropic magnetic effects expressed in resonances deviations of higher fields (Ganza-Gonzalez et al., 1994; Veiga et al., 2001). Little or no changes in the chemical shifts occur in the protons that are located outside the ring (H1, H2, and H4). Usually the proton H6 of the CD, located on board of the narrower opening of the CD may suffer more or less change in their chemical shift depending on the type of inclusion of the drug molecule (Schneider et al., 1998). Changes in chemical shifts of the protons belonging to the CD or drug and the sensitivities and detection of the complex formation can be monitored by varying the proportion of the drug and CD in solution (Job 1928). Thus, it is possible to obtain information on the stoichiometry of the complex formed (Marangoci et al., 2011).

For more detailed information on the geometry of the complex, two-dimensional NMR spectroscopy technique can be used. The effects of nuclear Overhouser (NOE) in the steady-state are strongly dependent on a distance internuclear until 4Å, which becomes a difficulty to analyze CD complexes with a molecular weight of about 2000 g / mol. In these cases, the correlation of molecular parameters has values close to the unity leading to NOE low values. Nuclear Overhouser effect on the rotating frame (ROESY) can be used to overcome this drawback. This technique is based on the spin truncation (*spin-lock*) where an additional excitation pulse is applied changing the correlation times and the NOE becomes measurable (Amato et al., 1998; Schneider et al., 1998). The detection of spatial correlations between the protons of the drug and the CD, lead to the determination of the structure of the complex formed with sufficient precision in relation to the regions of the molecules involved in the process of complexation (Schneider et al., 1998).

^{1}H-NMR and ROESY experiments explore aspects of the geometry of the complex formed and provide robust evidence of the nature of the host-guest interaction. One-dimensional ^{1}H-NMR spectra for each different [CD]/[TC] ratios, *R*, were recorded using a 600 MHz Varian NMR spectrometer (Palo Alto, CA) at 25ºC using a 3 mm indirect detection NMR probe. The NMR samples were prepared using D_2O (99.9%) as solvent, and TSP, used as internal reference, at tracer amounts. Solutions were prepared by weighting different amounts of CDs to a fix TCH^+ concentration at room temperature and mixed for 12 h to achieve the equilibrium. Spectra were obtained with residual solvent (HOD) pre-saturation and the experimental parameters included 24k data points

covering a spectral width of 8 kHz, a radiofrequency excitation pulse was 45º and an interpulse delay of 10 seconds to allow complete nuclei relaxation.

Two-dimensional (2D) rotating frame overhauser effect spectroscopy (ROESY) experiments were performed using the same NMR spectrometer and probe. The spectra were collected using 2048 data points in the F2 dimension and 512 increments defining the F1 dimension. The spectral width was 7.2 kHz in both dimensions and 32 free induction decays were acquired per increment. ROESY spectra were processed using the VNMR 6.1 software (Varian Inc., Palo Alto, CA, USA). Zero-filling and apodization Gaussian functions were employed in both dimensions before Fourier transformation, to improve resolution and signal to noise ratios, respectively. The cross-peaks volumes were directly correlated with inter-nuclear distance, r, of the two observed protons, via the known r^{-6} dependence. The fixed and well-known intramolecular distances between two vicinal aromatic protons (2.48A°) of BZC – ortho and meta – were used for calibration.

2.2.5. Drug release studies

The *in vitro* release studies were conducted in vertical Franz diffusion cells (PermeGear, Inc., PA, USA) with a volume of 5.1 cm^3 and a surface area of 0.64 cm^2. The dialysis membranes were placed between the two chambers of the cell. The receptor compartment was filled with PBS solution (pH 7.4), maintained at 37 (± 0.1) ºC and under stirring during the diffusion experiments. Each donor compartment (n=3) was filled with different TC hydrogel formulations (95 mM), composed of different amounts of CD and immediately covered with Parafilm® to prevent evaporation. Samples were taken at predetermined times (0, 1, 2, 3.5, 5, 6, 16, 24, 32, 46, 73, 110 and 142 h) from the receptor compartment and replaced by fresh PBS solution. *In vitro* studies provided the release profiles of TC and TCH^+ in the presence of different amounts of HP-*β*-CD, as a function of time. It is worth noticing that the HP-*β*-CD derivative was selected because it promoted the highest increase in solubility of TC.

2.2.5.1. Composition and preparation of the HPMC gel

Drug-loaded HPMC hydrogels were prepared by adding 2.5% (w/w) of TC with different amounts of HP-*β*-CD in water and sodium acetate buffer aqueous solution to 1% (w/w) of dry polymer powder (HPMC), at room temperature. The polymer solutions were kept stirring for 24 h before use.

2.2.5.2. Drug quantification

Tetracaine quantification was carried out using a Shimatzu LC-20AD apparatus equipped with a quaternary pump, an autosampler unit, and a L2450 UV/visible dual wavelength detector. A Phenomenex (Torrance, CA, USA), reverse phase C_{18} column Luna (5µm pore size, 250mm x 4.6mm) with a guard column as the stationary phase, at 25°C was used to quantified tetracaine. The mobile phase was prepared by mixing methanol, acetonitrile and ammonium acetate solution on the proportions 7:7:6 respectively. The solution was subsequently filtered using a 0.45 µm Nylon membrane (Supelco Analytical, Bellefonte, USA) and sonicated for 1 h prior to use. The detection was at 311 nm, the injection volume was 25 µL and the mobile phase flow rate was set to 1.0 mL min^{-1}. In these conditions the retention time of tetracaine was ca. 6.5 minutes.

2.2.5.3. Data analysis in the release studies

The steady state flux (J, µg cm^{-2} h^{-1}) which represents the rate transfer of diffusion substance through unit area of a section (A) was calculated by

$$J = \frac{V}{A}\frac{dc}{dx} \tag{2.10}$$

where J is the cumulative drug amount permeated at time (t) calculated from the slope of the linear portion of the plot of cumulative drug amount permeated and V is the volume of the receptor compartment. Taking the Eq. 2.10 the permeability coefficient can be calculated by using

$$P = J\ \frac{l}{Q_0} \tag{2.11}$$

where Q_0 is the initial amount of drug in the donor compartment and l the thickness of the membrane.

The Q_6 express in µg/cm^2 refers to the cumulative drug amount present in the receptor compartment solution after 6 h and was calculated using Eq. (2.12)

$$Q_n = \left(C_n \times V_0 + \sum_{i=1}^{n-1} C_i\, x\, V_i\right)/A \tag{2.12}$$

where n is the number of aliquots collected during the 6 h period, C_n correspond to the drug concentration in the receptor medium, C_i is the concentration in the sample, A is the

diffusion area, V_0 and V_i stand for the volumes of the receptor compartment and the sample. Results are presented as mean ± standard deviation (SD).

2.2.5.4. Release Models

The release mechanism has been assessed using the power law equation (Korsmeyer et al., 1983).

$$C_t/C_\infty = kt^n \tag{2.13}$$

where C_t and C_∞ are cumulative concentrations of the drug released at time t and at infinite time, respectively, and k and n are fitting parameters, giving the latter useful information on the release mechanism; from Eq. (2.13), the mean dissolution time (*MDT*), which characterizes the drug release rate from a dosage form and to indicate the drug-release-retarding efficiency of the polymer (Sriamornsak and Sungthongjeeh, 2007) can be calculated using Eq. 2.14 (Möckel and Lippold, 1993).

$$MDT = \left(\frac{n}{n+1}\right)k^{-n^{-1}} \tag{2.14}$$

The application of Eq. (2.13) is restricted to a cumulative release below 60 %.The release kinetics was evaluated through first and second order rate law equations (Eqs. 2.15 and 2.16, respectively); we attempted to fit the experiments data to a zero order law equation but these fits were poor. For both cases the release rate is concentration-dependent.

$$\ln Q = \ln Q_0 - k_1 t \tag{2.15}$$

$$\frac{1}{Q} = \frac{1}{Q_0} - k_2 t \tag{2.16}$$

In equations (2.15) and (2.16), Q and Q_0 are the amount of drug remaining in the matrix at time t and at t=0, respectively, Q_∞ is the total amount of all released drug and k_0 and k_1 are first and second order rate constants. Both the release kinetics and the mechanism of release were analyzed by using the Weibull function (Eq. 2.17).

$$C_t = C_\infty[1-\exp(-k_W t)^d] \tag{2.17}$$

where k_W and d are constants related to the release rate and mechanism, respectively (Papadopoulou et al., 2006).

2.3. Results and Discussion

2.3.1. Physicochemical characterization of the complexes

The formation of complex with CD alters the physicochemical properties of the drug. In general by adding CD to a poorly soluble drug aqueous solution it will increase of its solubility (Marques et al., 1990). The solubility phase diagrams (Loftsson et al., 2005; Loftsson and Masson, 2004) were obtained for tetracaine/*β*-CD and tetracaine/HP-*β*-CD mixed aqueous solutions at a pH of 9.0, at this pH, tetracaine occurs in its neutral form.

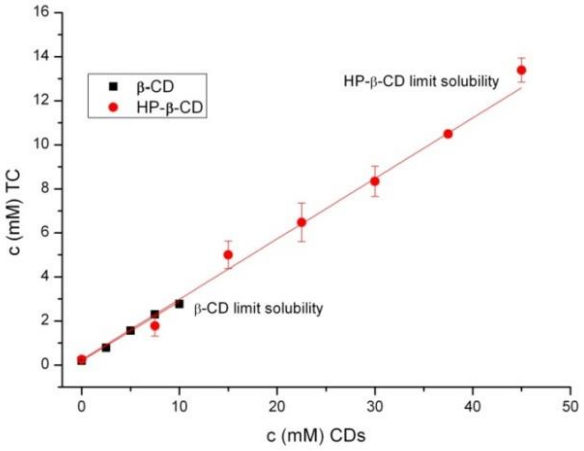

Figure 2.2 Solubility of tetracaine in water aqueous solution (pH 9) as function of CD concentrations at room temperature.

According with previous work an increase of either *β*-CD or HP-*β*-CD, leads to an increase in the concentration of TC dissolved in water (Sadlej-Sosnowska, 1997; Szejtli, 1998). Unionized TC is poorly soluble in water (51.4 µg/mL) and that the solubility was enhanced respectively by 14-fold and 69-fold respectively using *β*-CD (10 mM) and HP-*β*-CD (45 mM), as a consequence of formatting the drug-CD complexes (Connors and Mollica, 1966). The data shown in Figure 2.2 fitted to a straight linear Eq. (2.1) with a good correlation coefficient R^2=0.999. By applying the fitting parameters mentioned in Figure 2.2 into Eq. (2.1), the following stability constants, *K*, for the formation of TC:*β*-CD and TC:HP-*β*-CD complexes, in a 1:1 stoichiometry (Figure 2.3), were computed and are

equal to 1052 M^{-1} and 1051 M^{-1}, respectively. These results are in agreement to those reported by other authors (Franco de Lima et al., 2012; Loukas et al., 1998).

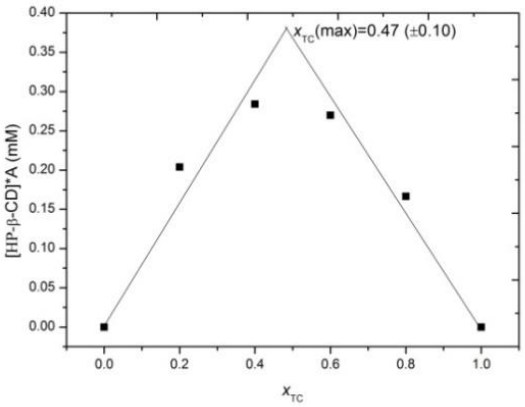

Figure 2.3 Job's plot analysis for tetracaine/HP-*β*-CD showing a maximum for a tetracaine molar fraction equal to 0.47 (± 0.10).

Table 2-1 Summarizes the association constants values (*K*), the maximum solubility and the efficiency of the complexation for TC:CD complexes, as computed from Figure 2.2.

Table 2-1 Effect of cyclodextrins on the solubility of tetracaine (TC) (n=3).

System	Solubility (μg/mL) a	Efficiency of the complex b	Slope =[TC]/[CD]	R^2	K (M^{-1})
TC: *β*-CD	734[c] ± 0.05	14	0.2671	0.9947	1052 ± 118
TC: HP-*β*-CD	3539[d] ± 0.14	69	0.2874	0.9923	1051 ± 46

[a] *Maximum of solubility of TC in the CD complexes.*

[b] *Ratio between TC solubility in the CD aqueous solution and the intrinsic solubility (51.4 μg/mL).*

[c] *Solubility computed by taking [β-CD]=10mM.*

[d] *Solubility computed by taking [HP-β-CD]=45mM.*

Both CDs forms have similar stability constants (Table 2-1), but the HP-*β*-CD significantly improves the solubility of TC due to its higher solubility in water (Mura et al., 1995). From the analysis of tetracaine ionization constants it was noted that only approximately 9% of the total amount of TC was protonated at pH 9. The proportion was calculated considering the pKa of TC and according to Henderson-Hasselbalch equation (Becker and Reed, 2012). In order to investigate the effect of the protonated form of tetracaine in CD interactions, similar experiments were carried out at pH 4.1. At the acid pH, TC solubilized even in the absence of CDs (Figure 2.4).

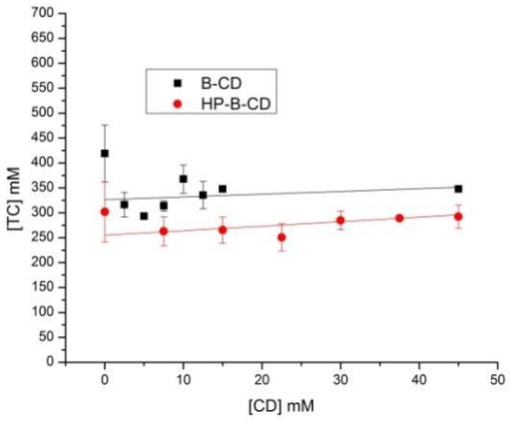

Figure 2.4 Solubility of tetracaine in buffer aqueous solution (pH 4.1) as function of CD concentrations at room temperature.

At pH 9, the higher solubility of TC observed in the presence of CD was due to a more efficient complexation of the neutral form of TC with CD when compared with its ionized form. However, at pH 4, TC was completely ionized, the concentration of dissolved TC only slightly change as a function of CD concentration, indicating a more limited interaction between TC and CD. Similar results regarding the effect of ionization of drugs and its affinity for CD have been reported elsewhere (Brewster and Loftsson, 2007).

2.3.2. Stoichiometry and association constant as seen by fluorescence spectroscopy measurements

In order to further understand the interactions of CD with ionized TC, fluorescence spectrophotometry of TC/CD mix solutions, at different molar ratios at pH 4.1, were carried out (Figure 2.5). Fluorescence spectroscopy is very sensitive to changes in the surrounding environment of the fluorophore. Therefore, this technique is able to provide accurate information of possible interactions occurring between TCH^+ and CD. This procedure has been reported in a previous study to calculate the concentrations of free (uncomplexed) ligands, needed for the calculation of the association constants (Sadlej-Sosnowska, 1997).

At pH 4.1 TCH^+ is the main species in solution although a small percentage of diprotonated tetracaine TCH_2^{2+} (ca. 16 %) is also present. Figure 2.5 shows the fluorescence emission spectra of TCH^+ at different TC/CD molar ratios. The relative fluorescence emission intensity of tetracaine, at 363 nm, increases in the presence of the cyclodextrins.

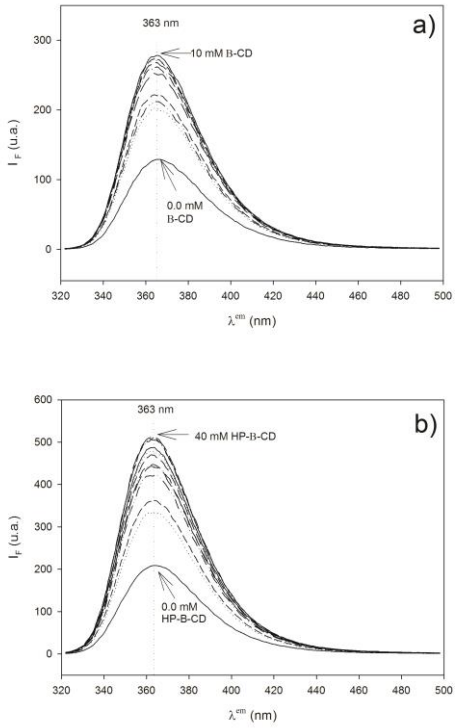

Figure 2.5 Fluorescence emission spectra of Tetracaine (1.0×10^{-5} M) in sodium acetate buffer aqueous solution pH = 4.1 at different a) *β*-CD (0.0mM -10 mM) and b) HP-*β*-CD concentration (0.0mM - 40 mM).

The emission enhancement can be used to determine the stoichiometry and the association constant of the TCH^+:CD complexes. Figure 2.5 shows the variation of the fluorescence intensity (*F*) as a function of CD concentration for solutions where the [TCH^+] concentration was kept constant and equal to 1.0×10^{-5} M. The experimental data of *F* can be fitted to Eq. (2.9) (see solid lines in Figure 2.6), using a non-linear least-square algorithm, to obtain the fitting parameters *K* and F_∞, assuming a 1:1 complex was formed.

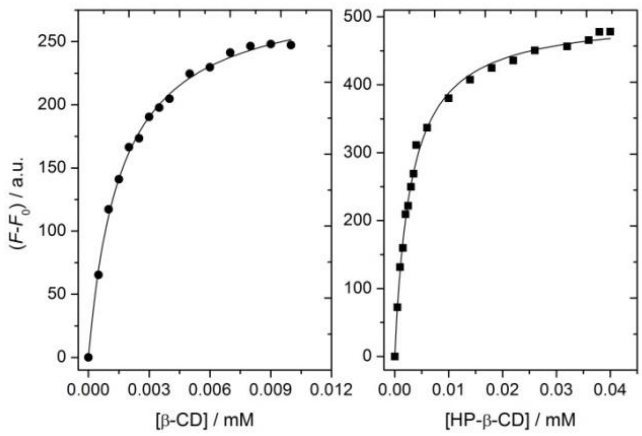

Figure 2.6 Relative fluorescence intensity of tetracaine in the presence of β-CD and HP-β-CD. [TCH^+]= 1.0×10-5 M. Solid lines were obtained by fitting the experimental data to Eq. (2.9).

Further support for the 1:1 association assumption is observed from the linear relationship of $((F-F_0)/[CD]_T)$ as function of $((F-F_0))$ for *β*-CD and HP-*β*-CD respectively, indicating that a 1:1 interaction stoichiometry is occurring Figure 2.7 (Smith et al., 1991). This stoichiometry was also in agreement with complexation studies between TCH^+ and CD reported elsewhere (Fernandes et al., 2007). The fitting parameters obtained by mapping the data to Eq. 2.9 (Figure 2.6) are: K=628 (± 24) M^{-1} and F_∞=292 (± 3), and K=337 (± 11) M^{-1} and F_∞=503 (± 4), for *β*-CD and HP-*β*-CD, respectively. It can be concluded from fluorescence spectroscopy studies, that TCH^+ form more stable complexes with *β*-CD than with HP-*β*-CD. Since both TCH^+ and HP-*β*-CD are highly soluble in water, it should be expected that a possible complexation would not cause a significant gain in the free energy of complexation. The same is not observed for *β*-CD, which can be justified by the relatively low solubility of this CD in water and consequently, the TCH^+ induces a stabilization effect on the *β*-CD in water interaction. These K values are lower than those obtained for neutral TC by using phase solubility diagrams but indicate that although interactions between CD: TCH^+ are weaker they should not be neglected. The TCH^+ structure could be incorporated inside CD cavity and if this was the case then the positive charge located at secondary amine induces a weak interaction between TCH^+ and CD (when compared with the corresponding neutral structure). Alternatively the TCH^+ may only interact with hydroxyl groups located at the extremities of the CD cavity. Although it is known that CD cavities can be penetrated by positive charged structures (Nilsson et al., 2008), the later hypothesis seems to be more reliable.

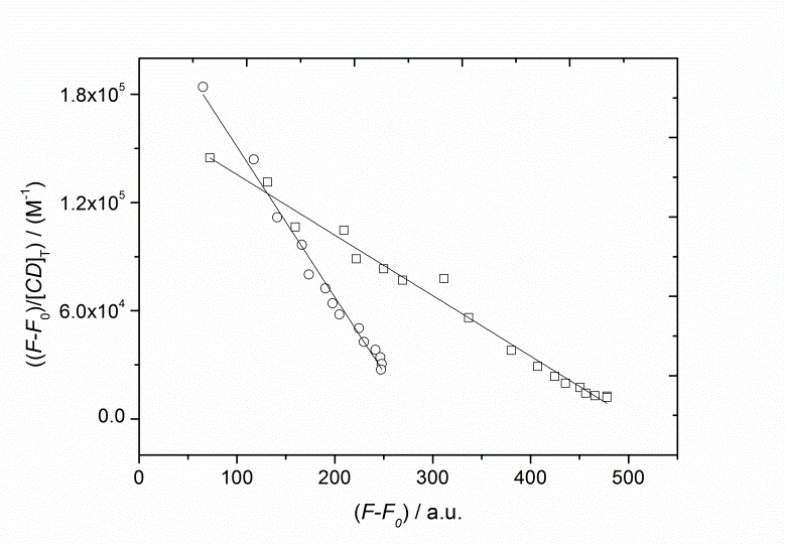

Figure 2.7 Effect of the normalized fluorescence relative intensity by the initial concentration of cyclodextrin as a function of fluorescence relative intensity for assessment on the stoichiometry of association. (o) *β*-CD and (□) HP-*β*-CD.

2.3.3. NMR analysis of TCH^+: CD complexes by ^{1}H-NMR and ROESY

In order to test if the TCH^+ did penetrate the CD cavity the interactions between TCH^+ and CD was characterized by ^{1}H-NMR and ROESY analysis on 1:1 and 1:2 TCH^+:CD mixtures. Figure 2.8 shows the ROESY spectrum for a 1:1 TCH^+:HP-*β*-CD mixture. The attribution of each resonance on the 1D ^{1}H-NMR spectrum is given on the projection. A full analysis of the cross-correlations present in the ROESY spectrum shows intramolecular nuclear Overhauser interactions between TCH^+ protons (dotted lines) and HP-*β*-CD protons (solid lines), but not even a single intermolecular interaction between TCH^+ and HP-*β*-CD protons. The absence of any intermolecular cross-correlation in ROESY spectra is evidence of the TCH^+ inclusion by the CDs at pH 4.1, thus the TCH^+ and CD interactions were assayed to the formation of fast equilibria hydrogen bonds.

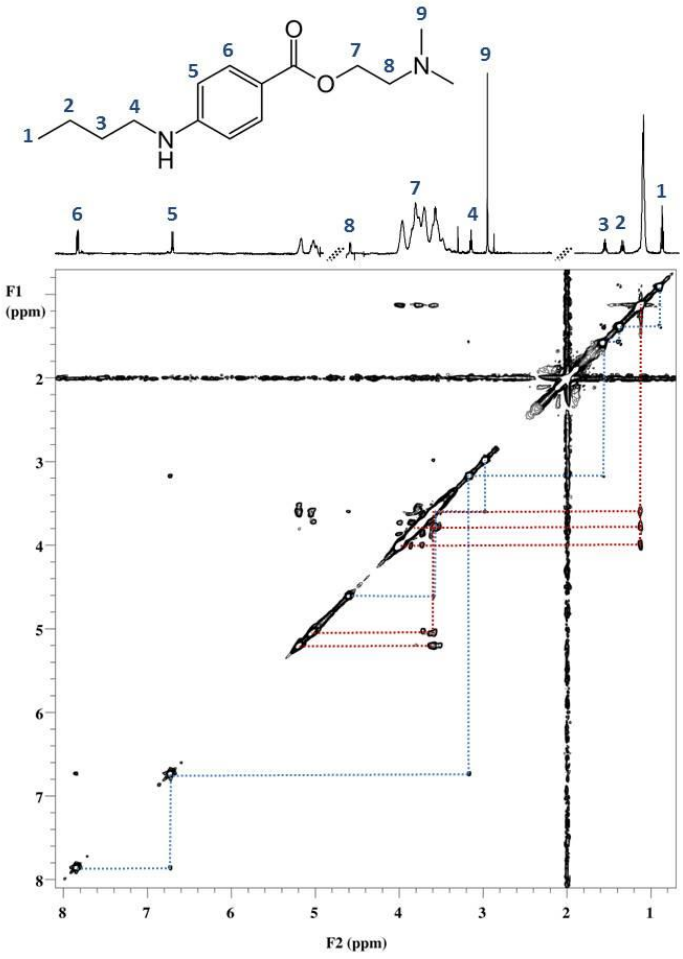

Figure 2.8 600 MHz 1H-NMR and ROESY spectra of a 1:1 complex of TCH+:HP-*β*-CD complex. Intramolecular nuclear Overhauser effects are detected for TCH+ (dotted lines) and HP-*β*-CD protons (solid lines). No intermolecular correlations are observed.

2.3.4. Effect of cyclodextrins on the tetracaine delivery: *In vitro* release studies

2.3.4.1. Steady-state transport

The transport of TC from the HPMC gels, in the presence of different amounts of HP-*β*-CD, across the dialysis membrane, shows a steady state flux in the first 6 h of the experiment (see inset in Figure 2.9). It can be seen that Q_6 (Table 2-2) decreases linearly with the increase of CD concentration, showing that CD controls the release of the drug.

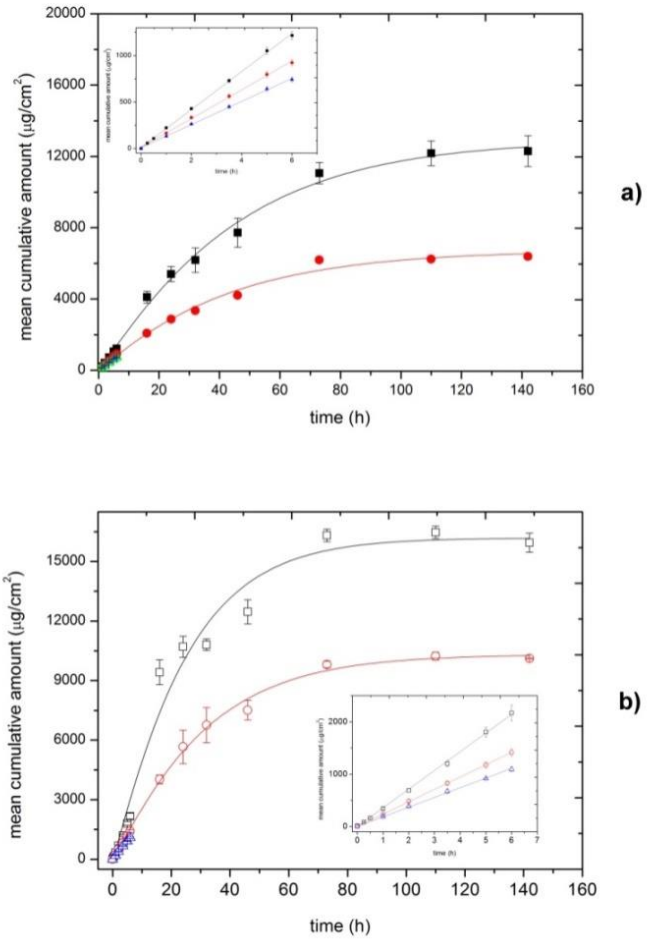

Figure 2.9 Cumulative release of neutral (a) and ionized (b) tetracaine across dialysis membrane as a function of time, at different initial cyclodextrin concentrations: (■,□) 190mM HP-*β*-CD, (●,○) 431mM HP-*β*-CD and (▲,Δ)518mM HP-*β*-CD. Solid lines show the fitting of eq. (2.10) to experimental data. Inset figures show the steady state flux of TC (A) and TCH^+ (B) occurring in the first 6 h of experiments.

Such effect can be ascribed to the corresponding formation of less mobile supramolecular structures (Loftsson et al., 2007), which might be explained by the

occurrence of complexation equilibrium between the drug molecules and hydroxyl groups located at both ends of cyclodextrins cavities.

The role of CD (either in the complex or free forms) on the transport of tetracaine can be assessed through the analysis of equilibria equations and the corresponding *K* values. Thus, for TC:HP-*β*-CD systems an increase of initial cyclodextrin concentration from 190 to 518 mM leads to an increase of free CD concentration from 96 to 406 mM, which corresponds to an increase of free CD from 51 to 81 %, respectively. On the other hand, such increase of CD concentration only leads to a decrease of free TC from 1 to 0.2 %, giving indication that for both systems the amount of complexed TC is higher than 99%. Similar values are obtained for the ionized TC system. Once TC aggregation can be ruled out, it can be hypothesized that the increase of free CD plays an important role on the depletion of TC flux.

Table 2-2 Effect of the HP-β-CD concentration on tetracaine delivery across dialysis membrane.

Formulation	J (μg cm^2 h-1)	Q_6 (μg cm^2)	P (10^{-3}cm^2 h^{-1})
TC: HP-*β*-CD (190mM)	203 ± 7	1215 ± 41	8.2 ± 0.3
TC: HP-*β*-CD (431mM)	152 ± 5	923 ± 34	6.1 ± 0.2
TC: HP-*β*-CD (518mM)	122 ± 5	740 ± 27	5.0 ± 0.2
TCH^+: HP-*β*-CD (190mM)	362 ± 22	2168 ± 146	14.5 ± 0.9
TCH^+: HP-*β*-CD (431mM)	234 ± 14	1415 ± 68	9.3 ± 0.6
TCH^+: HP-*β*-CD (518mM)	204 ± 6	1247± 41	8.1 ± 0.2

2.3.4.2. Release kinetic models

In the previous section we have found that the release of TC, either neutral or protonated, across the dialysis membrane, at short-range times, follows a steady-state flux. However, that is not valid for long-time range (i.e., for t > 6 h) (Figure 2.9). On the basis of the discussion carried out in the previous section it is expected that the release mechanism of TC can be described by a power law equation with the exponential factor around 1. In fact, taking into account the cumulative release of TC at equilibrium, and applying Eq. (2.13) in its linear form, we obtain *n* values ranging from 0.95 to 1.09 (Table 2-3), for TC:HP-*β*-CD (190 nm) and TCH^+:HP-*β*-CD (190 nm), respectively. Due to the cylindrical shape of the donor Franz cell compartment, those values are indicative of a complex mechanism, known as Super-Case II transport; such mechanism indicative of

coupling of diffusional and relaxational mechanism (Costa et al., 2011; Polishchuk and Zaikov, 1997), occurs for processes with *n* values higher than 0.89 (Costa et al., 2010)

Table 2-3 Fitting parameters of Eqs. (2.13) to (2.17) to experimental release data of tetracaine from HPMC matrices to receptor phase, at 37 ºC.

		TC: HP-β-CD 190 mM	**TC: HP-β-CD 431 mM**	**TCH^+: HP-β-CD 190 mM**	**TCH^+: HP-β-CD 431 mM**
	C_∞ (μM)	5801	4016	7521	7253
PL*	*N*	0.95 (± 0.05)	0.97 (± 0.04)	1.09 (± 0.03)	1.01 (± 0.04)
	K	7.94×10^{-6} ($\pm 3.12\times10^{-7}$)	5.09×10^{-6} ($\pm1.90\times10^{-7}$)	3.86×10^{-6} ($\pm 9.80\times10^{-8}$)	5.17×10^{-6} ($\pm 1.61\times10^{-7}$)
	R^2	0.9874	0.9888	0.9982	0.9945
	MDT (h)	31.6	41.1	13.9	22.3
FO	k_1 (h^{-1})	3.01×10^{-6} ($\pm 8.47\times10^{-8}$)	1.45×10^{-06} ($\pm 4.04\times10^{-8}$)	6.18×10^{-6} ($\pm 3.92\times10^{-7}$)	2.74×10^{-6} ($\pm 1.35\times10^{-7}$)
	R^2	0.99294	0.99304	0.9649	0.97843
SO	K_2 ($M^{-1}h^{-1}$)	4.37 ($\pm 0.18\times10^{-10}$)	1.76 ($\pm 0.03\times10^{-10}$)	1.32 ($\pm 0.13\times10^{-9}$)	3.794 ($\pm 0.128\times10^{-10}$)
	R^2	0.98539	0.99684	0.91521	0.98989
W	k_W (h^{-1})	6.51×10^{-6} ($\pm 3.02\times10^{-7}$)	4.75×10^{-6} ($\pm 2.1\times10^{-7}$)	1.13×10^{-5} ($\pm 1.16\times10^{-6}$)	8.61×10^{-6} ($\pm 4.23\times10^{-7}$)
	D	1.06 (± 0.09)	1.12 (± 0.086)	0.87 (± 0.134)	1.03 (± 0.093)
	R^2	0.9876	0.98827	0.96447	0.98798

** Fitting has been performed to cumulative release < 60%. R^2: correlation coefficient; PL: power law Eq. (2.13); FO: first order, Eq. (2.15); SO: second order, Eq. (2.16); Weibull function, Eq. (2.17).*

The *MDT* parameter characterizes the drug release rate from a dosage form, indicating drug release delaying efficiency of the polymer; the *MDT* of the drug increases with CD concentration, from 32 to 41 h when the drug is in the neutral form (TC) and from 14 to 22 h when it is in the ionized form (TCH^+). However, by comparing these two forms of tetracaine, the effect is more pronounced for TCH^+ (38 %) than for TC (23 %). It can be concluded from release data and mechanism analysis that TC release kinetics is dependent on the protonation state of TC and CD concentration. C_∞ was determined for each formulation. By fitting of first- and second-order kinetics equations (eqs. 2.15 and 2.16) to the experimental release data, we can conclude that, in general, good correlation coefficients were found for both cases. Assuming the analysis of those

correlation coefficients as a condition to conclude about what kinetics law characterizes a system, it was found that, for the release of TC in the presence of less concentrated CD, the release follows a first-order kinetics. However in the presence of the highest concentration of CD, the release of TC is characterized by a second-order kinetics law. This is close agreement with the previous discussion. When the CD increases from 190 to 431 mM, the percentage of free (not bound) CD decreases from 47 % to 24 % for TC-containing solutions (46 % to 23 % for TCH^+- containing solutions). Consequently, for the most concentrated mix solution, the release is controlled by free and complexed TC, whilst for solutions with 190 mM CD, the release kinetics seems to be only dependent on the TC concentration. Considering the analysis of the rate constants, they are in close agreement with such a CD concentration effect (by decreasing with an increase of CD concentration).

The equation that best fits the entire set of TC release data is the Weibull function (Eq. 2.17). This empirical equation provides, simultaneously, information on the mechanism (*d*) and rate k_W of release. *d* values are higher than 1 (except for TCH^+ with the lower CD concentration), characteristic of a sigmoid S-shaped, with upward curvature followed by a turning point concomitantly, and of a Super-Case II release. With respect to rate constants (k_W), they are quite similar to those calculated through a first order rate law equation. It is also worth noticing that the release rate constants for the whole time range follows the same trend than that found for the first 6 h. Consequently, the Weibull function seems to be reliable for an assessment of both mechanism (*d*) and rate k_W of release of TC.

2.4. Conclusion

The work presented in this Chapter focuses on the effects of CD on the transport of TC across a model membrane. The results obtained show that the interaction between CD and TC causes changes in water solubility (14 and 69-fold for *β*-CD and HP-*β*-CD, respectively) and release profile of the latter. HPLC and fluorescence spectroscopy data revealed that TC interacts with both CD (*β*-CD and HP-*β*-CD) on a 1:1 stoichiometry. An interesting finding arises from analysis of the stability constants between TC and both CD. These values are very similar for TC in its neutral form (1052 and 1051 M^{-1} for TC:*β*-CD and TC:HP-*β*-CD respectively) but different when TC is ionized (628 and 337 M^{-1} for TC:*β*-CD and TC:HP-*β*-CD respectively), indicating that the TC forms more stables complexes with CD than with TCH^+. Additionally, ROESY experiments provided specific

information concerning the non-inclusion nature of the interaction between TCH^+ and cyclodextrins. Despite the stability constant values are relatively low, *in vitro* studies data show that the flux of TC and TCH^+ across the dialysis membrane decreased with cyclodextrin concentration, following a Super-Case II transport mechanism. This work showed that such behavior does not depend on the formation of inclusion host-guest compounds, but due to the formation of weak supramolecular compounds. The conclusions obtained are very important as the CD concentration used was found to be critical; it should be sufficiently high to improve bioavailability of the drug, but not excessively as it could result in drug retention within the formulation.

Chapter 3

Lysine-based surfactants as chemical permeation enhancers for dermal delivery of tetracaine and ropivacaine

In this Chapter the studies between tetracaine and cyclodextrin (Chapter 2) are addressed, but now in a hydrogel formulation that includes new, biocompatible, lysine-based surfactants. The efficacy of these surfactants as chemical permeation enhancers for these two different drugs was investigated. The cytotoxicity profiles and the effect on skin integrity by light microscopy and scanning electron microscopy (SEM) was also investigated. Molecular dynamics simulation (*in silico*) results provided a rationale for the experimental observations, introducing a mechanistic view of the action of the surfactants molecules upon lipid membranes.

Based on the findings, this class of surfactants can be selected to influence the permeation of drugs without having significant deleterious effects upon the skin structure.

3.1. Introduction

As previously mentioned, the *stratum corneum* is the outermost layer of the skin and it is a highly organized structure that constitutes the major barrier to the permeation of drugs applied topically. In order to reversibly alter the barrier properties of the SC, and consequently increase the efficacy of the delivery of drugs across the skin, many strategies have been employed (Madison, 2003b). Chemical penetration enhancers are compounds that are known to have the ability of reducing the barrier properties of the SC and also increasing the partition of the drugs to the skin – see section 1.3.2.2. (Asbill and Michniak, 2000; Bach and Lippold, 1998; Finnin and Timothy M. Morgan, 1999). However, the practical use of CPE requires a careful balance between the toxicity to the skin and permeation enhancement benefits. Surfactants comprise a broad class of amphiphilic compounds, with surface-active properties, consisting of a lipophilic chain linked to a hydrophilic headgroup. These compounds are usually added to formulations to solubilize lipophilic active ingredients and therefore have a great potential to be used as permeation enhancers. Some surfactants are used alone as CPE, or in combination with other active methods (Ashton et al., 1992; Babu et al., 2005a; Cappel and Kreuter, 1991; Kitagawa et al., 2000; Nokhodchi et al., 2003; Shin et al., 2001; Shokri et al., 2001; Tan et al., 1993; Walters et al., 1993a). Surfactants have, in general, a low chronic toxicity (Williams and Barry, 2012), and the major concerns on its use in dermal delivery are associated to the possible occurrence of local irritation, erythema or itching, depending on the amphiphilic structure and concentration employed (Effendy and Maibach, 1995; Naik et al., 2000a; Scheindlin, 2004).

Surfactants have often been used either incorporated in a vehicle or dissolved in a solvent system, and their activity has been found to be dependent on its lipophilicity, charge and chain length (Karande et al., 2005). Nonionic surfactants are generally regarded as safe, but reputedly at least as irritating as cationic surfactants, a fact which has not excluded its use in cosmetic formulations. Nonionic surfactants have also been reported as possessing antibacterial properties (Schott, 1985; Shukla and Tyagi, 2006b).

Aminoacid-based surfactants, in particular, have attracted considerable interest because they are environmentally friendly due to their enhanced biodegradability (Brito et al., 2009; Infante et al., 2004) and low ecotoxicity (Perez et al., 2005), and also for displaying a moderate human cytotoxicity, as determined by their alkyl chain length and headgroup properties (Macián et al., 1996; Sanchez et al., 2006; Silva et al., 2013b). It has been

found that these class of surfactants exhibit lower toxicity when compared with conventional surfactants, making them promising alternatives to commercially available anionic and nonionic surfactants in pharmaceutical and cosmetic formulations (Sanchez et al., 2004, 2006; Vives et al., 1999; Vives et al., 1997). Additionally, these surfactants seem to be promising candidates to be used in topical pharmaceutical formulations, since they are less irritating and more biodegradable than the commercially available surfactants already tested (e.g., hexadecyltrimethylammonium bromide and sodium dodecyl sulphate) (Doi et al., 2001; Sanchez et al., 2004).

Unlike conventional surfactants that are composed by a single hydrophobic tail connected to a polar headgroup, the lysine-based surfactants employed in this work consist of double-chained amphiphiles (Brito et al., 2008; Brito et al., 2013). In fact, as can be seen in Figure 3.1a, the lysine side chain (a four-methylene group) acts as a spacer group between the two (dissimilar) polar regions, which imparts the surfactants with a dimeric type structure. The molecules used are either anionic sodium alkylcarboxylates with C10, C12, C14 and C16 long alkyl chains, or nonionic ester derivatives with C10 and C16 chains (Figure 3.1b).

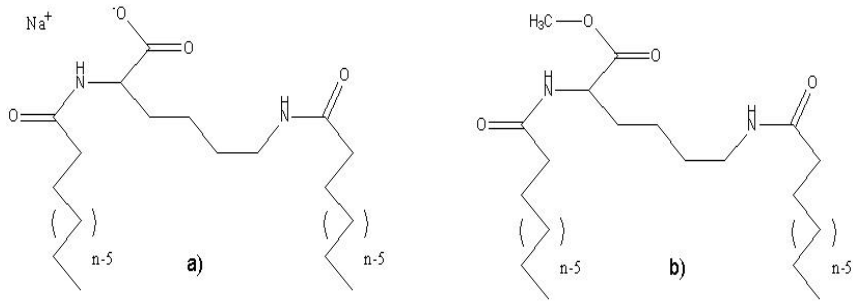

Figure 3.1 Structure of anionic lysine-based surfactants (a), *n*Lys*n*(-), where *n* is the alkyl chain length (n=10, 12, 14, 16) and nonionic lysine-based surfactants (b) *n*Lys*n*(0), where *n* is 10 and 16.

The efficacy of these lysine-based surfactants as CPE for tetracaine (non-ionized and hydrophobic) and ropivacaine hydrochloride (ionized and hydrophilic) across newborn porcine skin was investigated following a methodology reported elsewhere (Silva et al., 2012). The permeation in vitro studies were rationalized by molecular dynamics (MD) simulation, as a computational approach. Light microscopy and SEM techniques were employed to assess morphological changes of the skin in the presence of the CPE. Cytotoxic studies were subsequently performed in cultured human epidermal keratinocytes (HEK), establishing a concentration-toxicity response. Data collected from several complementary techniques provided new insight on the use of novel lysine-based surfactants as penetrations enhancers, which is crucial for their prospective use as delivery agents.

3.2. Experimental section

3.2.1. Materials

TC, ammonium acetate, PG (Reagent Plus, 99%), sodium bicarbonate, glucose, penicillin G potassium salt and streptomycin were purchased from Sigma Aldrich (Saint Louis, MO, USA). RPC was a kind gift from AstraZeneca (London, United Kingdom), and HPMC K15M a kind gift from Dow Chemical Company (Midland, MI, USA). HP-*β*-CD with 97% of purity, with an average degree of substitution of 2 to 6 units of 2-hydroxypropyl (C_3H_7O) per glucose unit, and with an average molecular weight of 1380 g/mol, was purchased from Acros Organic (Geel, Belgium). MeOH and ACN HPLC grade were purchased from LiChroSolv Merck (Darmstadt, Germany). PBS was purchased from TIC Gums (Belcamp, MD, USA). Newborn porcine skin tissue was obtained from young pigs (3 weeks, ~5 kg, acquired at a local slaughterhouse). The lysine-based surfactants used in this study were synthesized and purified according to a method described in previous works (Brito et al., 2006; Gomes et al., 2008). The purity of the compounds was determined by NMR, elemental analysis, surface tension and differential scanning calorimetry (DSC) (Brito et al., 2006; Brito et al., 2008; Gomes et al., 2008). The anionic lysine based surfactants, comprising 10, 12, 14 and 16 carbon atoms are referred in this manuscript as 10Lys10(-), 12Lys12(-), 14Lys14(-) and 16Lys16(-), in an obvious notation, while the nonionic ones are referred as 10Lys10(0), 16Lys16(0). The Tissue-Tek® O.C.T™ compound was purchased from VWR international (Radnor, Pennsylvania, USA). Formaldehyde solution min. 37% was purchased from Merck (White House Station, NJ, USA). The Dulbecco's Modified Eagle Medium (DMEM), fetal bovine serum (FBS) and trypsin were purchased from Invitrogen™ (Carlsbad, CA, USA). HEK were obtained from DKFZ (Im Neuenheimer Feld, Heidelberg, Germany). Finally, the Alamar-Blue® Cell Viability reagent was obtained from Thermo Scientific (Waltham, MA, USA). All reactants were used as received.

3.2.2. Porcine skin preparation

Newborn porcine skin tissue used as skin model, was excised and dermatomed using a Padgett® Model B Electric Dermatome (Integra LifeSciences, Plainsboro, NJ), Figure 3.2. The skin samples with 700 µm thickness were stored at −20ºC for no more than 3

months. Prior to the experiments, skin samples were thawed at room temperature, before immersion in PBS (pH=7.4) for 1 h, for equilibration.

Figure 3.2 Dermatomed newborn porcine skin using a dermatome.

3.2.3. Composition and preparation of the hydrogels and enhancer solutions

Tetracaine hydrogel contained 2.5% (w/w) TC, mixed with appropriate amounts of HP-*β*-CD (Teixeira et al., 2014b), 1% (w/w) HPMC K15M and deionized water. Ropivacaine hydrogel was composed of 2.5% RPC, 1% (w/w) HPMC and deionized water. The polymers solutions were kept stirring for 24 h before use at low speed (50 rpm) to ensure complete homogenization. The enhancer solutions were prepared at a concentration of 0.15 M in PG by stirring at room temperature until complete solubilization. Generally, the compounds were soluble in PG at the concentration used, and produced clear solutions. However, when necessary, some samples were heated prior to use.

3.2.4. *In vitro* permeation studies

In vitro permeation studies were performed for 24 h using Franz diffusion cells (PermeGear, Inc., PA, USA) (Figure 3.3) with a diffusion area of 0.64 cm^2 and a receptor compartment of 5.1 mL filled with PBS solution (pH=7.4). Dermatomed porcine skin pieces (0.70 mm thickness) were placed between the donor and receptor compartments, with the epidermal side up. The receptor medium was maintained at 37.0 ± 0.1 ºC and stirred at 600 rpm during the permeation experiments. The drug loaded hydrogel was placed in each donor compartment, and immediately covered with Parafilm® to prevent evaporation. At predetermined time points (0, 2, 4, 6, 8, 18, 20, 22 and 24 h) 300 µL samples were collected from the receptor compartment and immediately replaced with

300 µL of fresh PBS solution. Samples were kept in the refrigerator prior to HPLC analysis. All the skin samples, except the ones used in control, were pretreated with 60 µL of the various enhancer solutions, for 1 h, prior to the application of the drug loaded hydrogel in the donor compartment (t = 0).

Figure 3.3 Franz diffusion cells (PermeGear, Inc., PA, USA) with a diffusion area of 0.64 cm2 and a receptor compartment of 5.1 mL.

3.2.4.1. Drug quantification

All samples were analyzed using HPLC. The system consisted of a Shimadzu LC-20AD apparatus equipped with a quaternary pump, an autosampler unit, and a L2450 UV/visible dual wavelength detector. The quantification of TC and RPC were carried out using a reverse-phase C_{18} column (250 x 4.6 mm C18 (2) 100 A Luna 5 µm, Phenomenex® (Torrance, CA, USA) with a guard column as the stationary phase, at 25°C. The mobile phase was prepared by mixing methanol, acetonitrile and ammonium acetate solution on the proportions 7:7:6 respectively. The solution was subsequently filtered using a 0.45 µm Nylon membrane (Supelco Analytical, Bellefonte, USA) and sonicated for 1 h prior to use. The flow rate was set to 1.0 mL/min and the injection volume was 25 µL. TC was detected at 311 nm and the retention time was ca. 6.9 minutes. The method showed a linear response in the 0.1–100 µg range (R^2 = 0.9999) with a daily relative standard deviation (RSD) < ± 5.0%. RPC was detected at 210 nm and the retention time was ca. 9 minutes. The method showed a linear response in the 0.1-50 mg/mL (R^2=0.9998) with a daily RSD < ± 6.0%.

3.2.4.2. Data analysis in the permeation studies

According to Fick's first law of diffusion, the steady state flux (µg cm^{-2} h^{-1}), *J*, can be expressed by Eq. 3.1

$$J = \frac{DC_0P}{h} \qquad (3.1)$$

where D is the diffusion coefficient of the drug in the SC, C_0 represents the drug concentration applied in the donor compartment, P is the partition coefficient between vehicle and the skin and h is the diffusional path length. The flux J can be calculated from the slope of the linear portion of the plot of cumulative drug amount permeated per unit area. Also calculated was Q_{24}, the cumulative drug amount present in the receptor compartment solution after 24 hours, expressed in μg/cm^2 (Eq. 3.2)

$$Q_n = (C_n \times V_0 + \sum_{i=1}^{n-1} C_i \times V_i)/A \quad (3.2)$$

where C_n corresponds to the drug concentration in the receptor medium, C_i is the concentration in the sample, A is the diffusion area, V_0 and V_i stand for the volumes of the receptor compartment and the sample. The enhancement ratio (ER) for flux was calculated using Eq. 3.3

$$ER = \frac{\text{flux for treated skin with enhancer}}{\text{flux for untreated skin (control)}} \quad (3.3)$$

Results are presented as mean ± standard deviation (n), where n is the number of replicates. Differences between flux values were examined for significance using unpaired Student's t-test. The p value was set to 0.05, with $p < 0.05$ indicating statistical significance in the differences between control and enhancers tested.

3.2.5. Simulation details

The effect of the introduction of the lysine-based surfactants on a fully hydrated dipalmitoylphosphatidylcholine (DPPC) bilayer was studied by molecular dynamics simulation. DPPC is a relatively common lipid often chosen to monitor membrane structure and dynamics when exposed to external agents (Almeida et al., 2010; Bennett et al., 2009; Kukol, 2009). This simple and well-characterized model has been used specifically in studies similar to that described in this work, so as to assess effects on the permeation and membrane behavior (Almeida et al., 2011; Cerezo et al., 2011; Gurtovenko and Anwar, 2007; Kyrikou et al., 2004; Notman et al., 2006). DPPC and SPC (simple point charge) water were described using the original definitions of the GROMOS 53a6 force field (Schuler et al., 2001). This force field and variants have been extensively used for modeling membrane properties along with a variety of organic molecules (Bennett et al., 2009; Piggot et al., 2012; Poger and Mark, 2009; Schuttelkopf and van Aalten, 2004). Supported on this force field, topology for each surfactant was generated

using the ATB (Malde et al., 2011) platform. A DPPC bilayer, consisting of 128 phospholipid molecules equally distributed by two leaflets and 3655 SPC water molecules was used, as made available by Kukol (Kukol, 2009). In each system, a single molecule of surfactant was considered. This was found suitable for studying the interaction of each solute with the surrounding lipids, as well as assessing the preferential positioning and respective action on the bilayer. The system was solved using the GROMACS package, version 4.5.5 (Hess et al., 2008; van der Spoel et al., 2012). All MD simulations were carried out in the NPT ensemble and under periodic boundary conditions. A standard time step of 2 fs was used for both the equilibration and production runs. Non-bonded interactions were computed on the basis of a neighbor list, updated every 10 steps. Long-range electrostatic contributions were computed using the particle mesh Ewald (PME) method. For Lennard–Jones energies, a cut-off of 1.4 nm applied. Temperature and pressure were coupled to the Berendsen external baths, maintained at 325 K and 1 bar, with coupling constants of 0.1 and 0.5 ps, respectively. To obtain the starting configuration, each system was firstly subjected to an energy minimization step. The systems were then left to evolve for up to 80 ns, using the LINCS algorithm (Hess et al., 1997). The first 20 ns were considered sufficient to attain equilibration, while the last 60 ns of the production runs were subsequently subjected to standard analysis, including the determination of order parameters, mean square displacements (MSD), density probability distributions and radial distribution functions (rdf). MD trajectories were visualized, and configuration images extracted using the VMD 1.9 software (Humphrey et al., 1996).

3.2.6. Skin integrity evaluation

After the permeation studies, skin samples were rinsed with deionized water, dried and stored at -20ºC. These samples were later investigated for the occurrence of morphological changes caused by the CPE and methodology employed.

3.2.6.1. Histology- light microscopy studies

Skin samples used in the permeation studies were carefully cut in small pieces and fixed with 10 % of buffered formalin during 24 h at room temperature. They were subsequently dehydrated with different volumes of ethanol (50 %, 75 %, 95 %, and 100 %) for 1 h each, and embedded in Tissue-Tek® O.C.T. and frozen (Hoppert, 2003). Cross-section

slices of 7 μm thickness were obtained using a cryostat (Figure 3.4) SLEE medical GmbH (Carl-Zeiss, Mainz, Germany).

Figure 3.4 Cryostat for the cross-section slices.

The samples were subsequently stained following the Ellis Hematoxylin and Eosin (H&E) staining protocol (Ellis, 2010) and were analyzed using a Nikon Eclipse 50i light microscope (Melville, NY, USA) at 10, 20 and 40 magnifications. A Nikon Digital Camera (Model DS-FI 1) equipped with a Digital Sight DS-U2 microscope camera controller was used to capture images. Images were processed using NIS-Elements Imaging Software.

3.2.6.2. Scanning Electron Microscopy studies

SEM analysis was performed in order to investigate the morphological characteristics of the skin that could not be observed using conventional light microscopy. After the *in vitro* studies, the skin samples were placed in a plastic former, were submerged in Tissue-Tek® O.C.T. and frozen. Cross-section slices of the frozen samples were cut (10 μm thickness) using a cryostat SLEE medical GmbH (Carl-Zeiss, Mainz, Germany).

Skin samples were defrosted, washed and fixed with formalin for 1.5 h and subsequently rinsed and placed in deionized water, at room temperature, for 2 h. They were subsequently dehydrated using solutions of 30 %, 50 %, 75 %, and 95 % ethanol in water for 25 minutes and finally, were put in two changes of absolute ethanol (100 %) for 2 h, at room temperature. Prior to analysis, the sample was placed on a double-side carbon tape mounted onto an aluminum stud, and dried in a desiccator. The sample was then coated with gold in order to make it conducting. Surface and cross-sections pictures of the samples were taken using SEM – JEOL, model JSM-6010LV/6010LA.

3.2.7. Cytotoxicity studies

Cell viability was evaluated by the Alamar Blue assay protocol. Alamar Blue cell viability assay is a colorimetric method used to determine the number of viable cells in cytotoxicity assays, widely reported in the literature for similar systems (O'Brien et al., 2000). Viable cells are able to reduce the resazurin compound [7-Hydroxy-3H-phenoxazin-3-one-10-oxide sodium salt] (a non-fluorescent blue dye) into resorufin (pink colored and fluorescent). The number of viable cells is directly proportional to the quantity of resorufin product formed as measured by the absorbance at 570 and 600 nm (alamarBlue® Cell Viability Assay Protocol). The levels of resorufin formed were quantified using a Microplate Power Wave X Scanning Spectrophotometer (Bio-TEK Instruments, Inc. Winooski, VT, USA). Cytotoxicity studies were carried out in cultured human keratinocyte cell line HaCaT with a density of $0.1x10^5$/mL, in a final volume of 0.2 mL/well under sterile conditions. Subculturing was performed by splitting cells at ratios between 1/5 and 1/10 and cells were used after reaching 70–80 % confluence. HaCaT was seeded in 96-well plates in 200 μL/well of DMEM® medium supplemented with sodium bicarbonate (3,7 g/L), glucose (25 mM), 10% heat inactivated FBS, 100 U/mL penicillin, and 100 μg/mL streptomycin and were incubating for 24 h at 37 ºC, 5 % CO_2 and 90 % R.H. After seeding, the culture medium was removed and cells were exposed to medium (control) and various concentrations, 1600 (S1), 160 (S2), 16 (S3), 1.6 (S4), 0.16 (S5) μM of 10Lys10(-), 12 Lys12(-), 14 Lys14(-), 16Lys16(-), 10Lys10(0), 16Lys16(0) solutions in PG, diluted in culture medium and were placed in the incubator for another 24 h in the same environmental conditions. After 20 h of reagents exposure, 50 μM of resazurin solution (in sterile PBS) was added to each well and the plates were read after 4 h. Results are presented as % cell viability (mean ± standard deviation, n=3), *C.V.* calculated according to Eq. 3.4

$$C.V. = \frac{\text{abs read in treated cells}}{\text{abs read in control (untreated) cells}} \times 100 \qquad (3.4)$$

3.3. Results and Discussion

3.3.1. *In vitro* permeation studies using lysine-based surfactants

Firstly, the focus is the analysis of six lysine-based surfactants as CPE. Each of these surfactants will be, in turn, used for the two drugs employed in this study.

3.3.1.1. Percutaneous drug delivery of tetracaine

Surfactants were dissolved in PG at a concentration of 0.15 M. The respective solutions were applied to the epidermal side of dermatomed porcine skin placed between the donor and receptor compartments of Franz diffusion cells for 1 h prior to the application of tetracaine loaded hydrogels. The tetracaine permeation results obtained are presented in Table 3-1 while the permeation profiles are shown in Figure 3.5.

Table 3-1 Effect of the chemical permeation enhancers on percutaneous permeation of tetracaine across porcine skin samples. Data are presented as means ± S.D. (4≤N≤6).

Penetration modifier	Flux / μg cm^{-2} h^{-1}	Q_{24} / μg cm^{-2}	ER
Control - PG	19.83 ± 2.47	417 ± 53	-
0.15 M 10Lys10(-)	15.31 ± 0.61	335 ± 16	0.77
0.15 M 12Lys12(-)	19.88 ± 0.58	429 ± 15	1.00
0.15 M 14Lys14(-)	20.32 ± 0.91	449 ± 15	1.02
0.15 M 16Lys16(-)	25.21 ± 2.52	563 ± 44	1.27
0.15 M 10Lys10(0)	20.75 ± 0.67	463 ± 16	1.05
0.15 M 16Lys16(0)	26.31 ± 2.68	620 ± 71	1.33

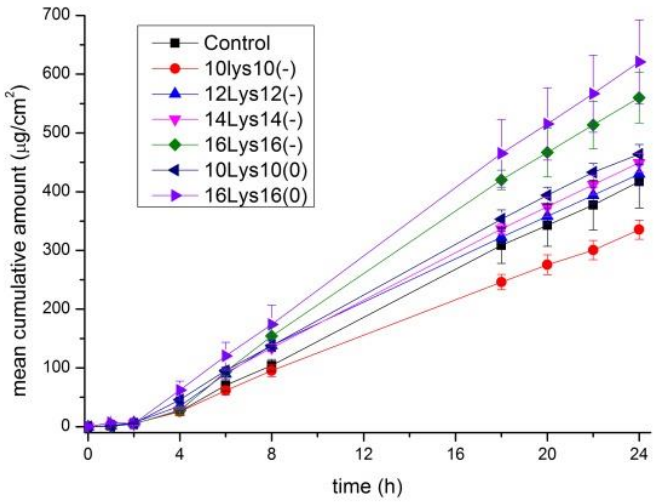

Figure 3.5 Cumulative amount of tetracaine permeated across porcine skin as a function of time. Skin was pretreated for 1 h with enhancer solutions in PG, prior the start of the permeation experiments.

The lysine-based surfactants tested, generally caused an increase on tetracaine permeation, when compared to the control as measured by the flux (19.83 μg cm^{-2} h^{-1}),

with the exception of 10Lys10(-), which displayed a value of 15.31μg cm^{-2}. Surfactant 16Lys16(0) has shown to be the most effective permeation enhancer, resulting in a 1.33-fold increase of the ER, closely followed by 16Lys16(-) (ER = 1.27). In contrast, lysine-based surfactants with shorter alkyl chains (10Lys10(0), 10Lys10(-); 12Lys12(-) and 14Lys14(-)) did not promote a significant increase in terms of drug permeation.

3.3.1.2. Percutaneous drug delivery of ropivacaine

The results obtained with ropivacaine in its salt form are summarized in Table 3-2 and Figure 3.6. It should be noted that the overall effect of the surfactants on the percutaneous drug delivery of ropivacaine is clearly different from that of tetracaine (base form). All anionic surfactants statistically increased the ropivacaine permeated after 24 h, when compared to control. In contrast, nonionic surfactants did not affect significantly the ropivacaine permeation.

Table 3-2 Effect of the chemical permeation enhancers on percutaneous permeation of ropivacaine across porcine skin. Data are presented as means ± S.D. (6≤N≤9).

Penetration modifier	Flux (μg cm^{-2} h^{-1})	Q_{24} (μg cm^{-2})	ER
Control – PG	1.94± 0.10	36.87 ± 0.67	-
0.15 M 10Lys10(-)	3.95* ± 0.24	86.63* ± 4.32	2.03
0.15 M 12Lys12(-)	5.46 ± 0.34	103.57 ± 6.43	2.81
0.15 M 14Lys14(-)	8.27* ± 0.48	172.75* ± 11.40	4.26
0.15 M 16Lys16(-)	11.89* ± 0.55	237.49* ± 17.03	6.12
0.15 M 10Lys10(0)	1.64 ± 0.13	31.02 ± 1.70	0.89
0.15 M 16Lys16(0)	1.79 ± 0.10	34.45 ± 2.14	0.92

** Statistically significant difference between enhancer and control at p < 0.05 (Student's t-test)*

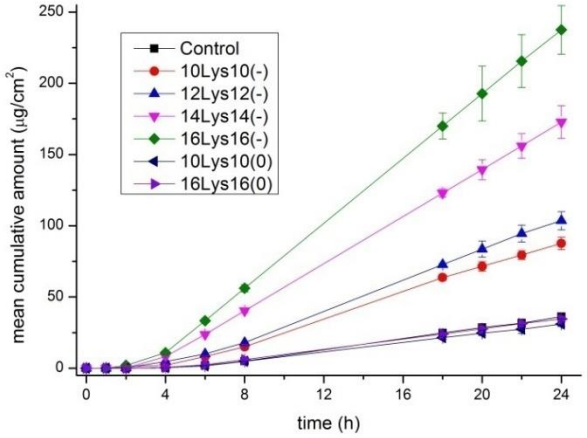

Figure 3.6 Cumulative amount of ropivacaine permeated across porcine skin as a function of time. Skin sample was pretreated for 1 h with enhancer solutions in PG, prior the start of the permeation experiments.

The anionic 16Lys16(-) surfactant was the most effective CPE with a 6-fold increase in the flux, followed by 14Lys14(-), with a value of 4, 12Lys12(-), with 3, and 10Lys10(-), with 2. In contrast, both nonionic surfactants (10Lys10(0) and 16Lys16(0)) have shown a modest performance in terms of penetration enhancement, causing only a slight increase in the value of the flux of ropivacaine permeated, which is not statistically significant. In terms of the amount of drug permeated in 24 h (Q_{24}), it was observed that the anionic surfactants also performed better, with a significant increase in Q_{24} (36 to 238 µg/cm^2).

3.3.1.3. Overall behavior

It is known that the effect of surfactants on the skin are complex and the mechanisms are based on different factors that affect permeability (Torchilin, 2001). The protective lipid barrier of skin is composed of highly organized lipid layers located between the cells of SC. Surfactants may interact with the lipid bilayers, disorganizing them and therefore altering the skin barrier function. However, these effects depend on the surfactant structure, since both the hydrophobic alkyl chain and the hydrophilic headgroup exhibit some influence. It was observed that the most effective CPE are those with the longest alkyl chains.

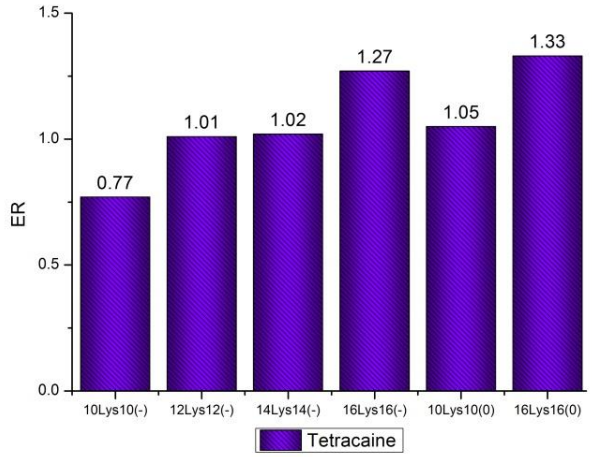

Figure 3.7 ER obtained pretreating the skin using the various CPE for tetracaine.

In the case of tetracaine (Figure 3.7) the maximum ER was found with the nonionic lysine surfactant with 16 carbons (16Lys16(0), ER=1.3), while the least effective was the anionic compound with the shortest chain (10Lys10(-)). However, the trend changes when the drug is in ionized (cationic) form. In the case of ropivacaine (Figure 3.8) the anionic surfactant 16Lys16(-) was clearly the most effective CPE accounting for a 6-fold increase in the flux. The effects of both 16Lys16(0) and 10Lys10(0) were found negligible in comparison with the control.

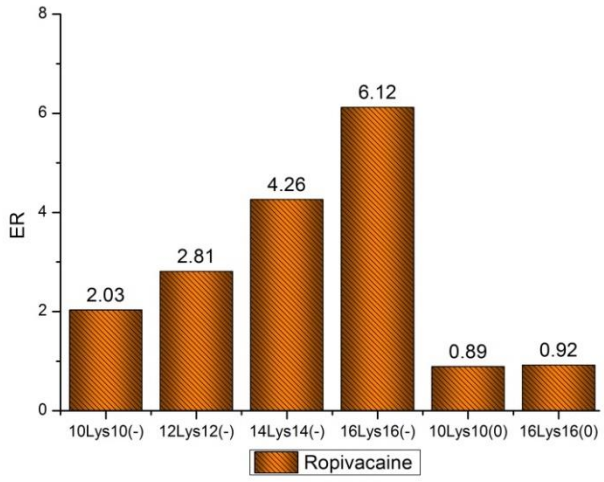

Figure 3.8 ER obtained pretreating the skin using the various CPE for ropivacaine.

The anionic surfactants are likely to strongly interact with both keratin and lipids, producing large alterations in the barrier properties (Rieger and Rhein, 1997). An additional mechanism involves the hydrophobic interaction of the alkyl chain with the skin

structure, which leaves the end carboxylate group of the surfactant exposed, creating additional sites in the membrane where the drug may permeate. This may result in the development of repulsive forces that separate the protein matrix, uncoil the filaments, and expose more water binding sites, hence increasing the hydration level of the skin (Froebe et al., 1990) (see next section). Anionic surfactants may cause a larger enhancement than nonionic surfactants, but the effects probably are dependent on the exposure time (Williams and Barry, 2012).

Another related effect to be taken into account is that the anionic headgroup of the n(Lys)n(-) compounds may promote electrostatic interactions with the ropivacaine molecules in their cationic form (HCl salts). In fact, once inserted in the skin bilayer membranes, the anionic surfactants might well enhance surface binding and overall permeation of the drug owing not only to direct coulombic anionic-cationic interactions but to the entropy increase associated with counterion release (sodium and chloride ions in this case). These findings are consistent with previous work in which terpenes and alkylammonium C_{12}-Gemini surfactants were used as CPE for drugs with different hydrophobicities and charge (El-Kattan et al., 2001; Silva et al., 2013a).

3.3.2. Molecular dynamics simulations

In an attempt to provide molecular-level insight into the permeation effects induced by the lysine-based surfactants, MD simulations were carried out. The procedure described in Section 3.2.5. was applied to five systems, a neat DPPC bilayer, as reference, and four other systems comprising DPPC and one molecule of lysine-based surfactants, both anionic and nonionic, with different tail lengths. The latter were denoted DPPC/10Lys10(-), DPPC/16Lys16(-), DPPC/10Lys10(0), DPPC/16Lys16(0), in an obvious notation. The vertical positioning of some key groups relative to the membrane center was firstly analyzed, resorting to the probability density functions. This analysis provides relevant information about the structural modifications induced on DPPC bilayers as a consequence of the surfactant molecule incorporation.

Figure 3.9 depicts the density profiles of these groups across the bilayer, namely the positioning of the P and N atoms of the headgroups and the terminal methyl groups of DPPC. The nitrogen atom of the surfactant headgroups and the respective end methyl groups of the surfactant tails were also considered. The distributions of the SPC water molecules and the polar heads of DPPC, represented by the nitrogen atom, are symmetrical around the center of the z-coordinate, being depicted in both sides of the

bilayer. On the other hand, the distribution of the terminal methyl groups of DPPC appear as a single curve with its maximum at Z=0, indicating a clear overlapping of the terminal part of both leaflets.

Additionally, the distributions concerning the nitrogen atom of the surfactants reflect the presence of only one molecule. Also included in the representations is the center of mass of each molecule. The profile of characteristic groups referring to the single-component DPPC system, shown in Figure 3.9 - panel (a), agrees with the data reported in the literature (Vitorino et al., 2013). The incorporation of the surfactant molecules (Figure 3.9 - panel (b) to (e)) introduces some modifications in the bilayer structure. From panels (d) and (e) it is seen that the lysine-based nonionic surfactants are mostly embedded in the hydrophobic region, while anionic molecules (panels (b) and (c)) are preferentially positioned close to the interface, as can also be seen in Figure 3.10, in which four representative snapshots are presented.

The anionic surfactants, as a consequence, interact more strongly with the lipid polar heads, displaying a reduced probability of crossing the center of the bilayer. Additionally, the polar heads of both anionic surfactants (represented by the nitrogen atoms) are fully embedded in the membrane. The more hydrophilic nature and the smaller tail length of the anionic 10Lys10(-) molecule prevent the terminal methyl groups from reaching the center of the bilayer. In contrast, the end methyl groups of the anionic 16Lys16(-) surfactant tails are almost leveled with those of DPPC, fully reaching the inter-leaflet region. As it was already observed for the shortest anionic surfactant, the polar heads are placed below those of DPPC. In panels (d) and (e) of Figure 3.9, the wide distribution of the surfactant polar heads indicates that the mobility into the membrane is high, and even the polar heads are fully embedded in the inter-leaflet region of the DPPC membrane (Figure 3.9 - panel d).

The nonionic 10Lys10(0) molecule, panel (d), is likely to be found at the inter-leaflet region, easily switching between the two leaflets, as suggested by the MSD profile of DPPC obtained from the simulation trajectories (Figure 3.11). Based on the MSD results, the anionic 10Lys10(-) molecule is, among the lysine-based surfactants under study, the one that promotes the highest lateral diffusion of DPPC molecules.

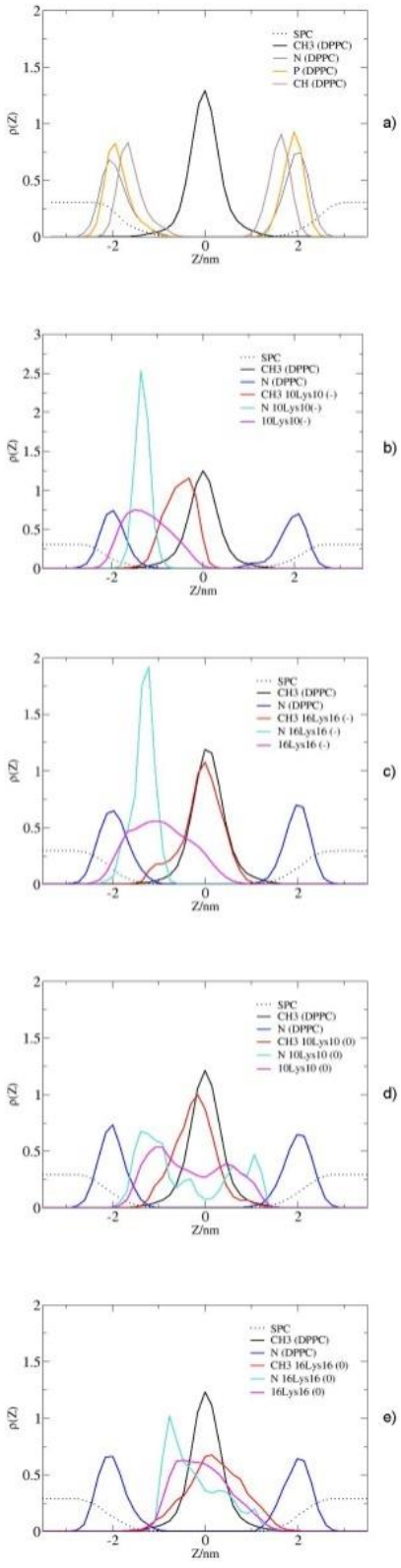

Figure 3.9 Probability density profiles of key atom/groups relative to the Z-axis, extracted from the MD simulations carried out at 50°ºC for (a) single DPPC, (b) DPPC/10Lys10(-), (c) DPPC/16Lys16(-), (d) DPPC/10Lys10(0) and (e) DPPC/16Lys16(0) systems. SPC water groups (••); DPPC groups - ammonium nitrogen (dark blue), and end methyl groups of tail chains (black); surfactant groups – ammonium nitrogen atoms (blue) and terminal methyl groups of both tails (red). The Z-coordinate represents the normal to the bilayer plane.

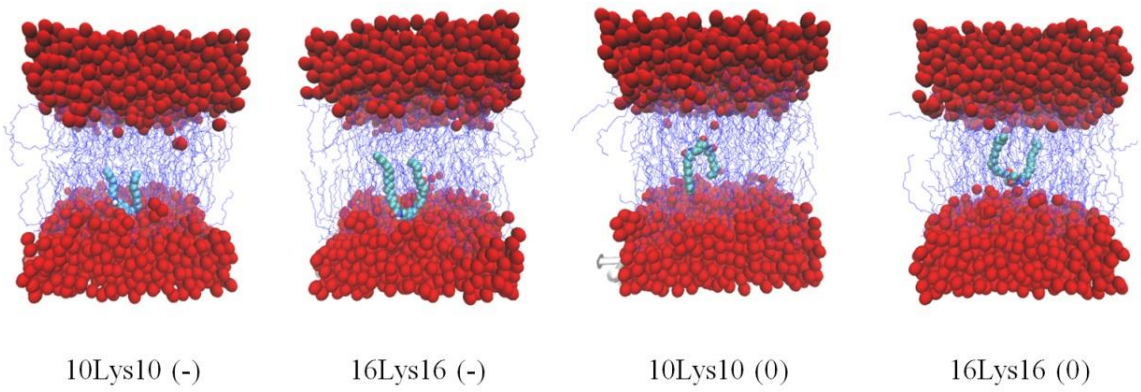

Figure 3.10 Representative configurations, showing the positioning of lysine-based molecules embedded in the bilayer. Water, surfactant molecules and DPPC are represented in red, light and dark blue, respectively.

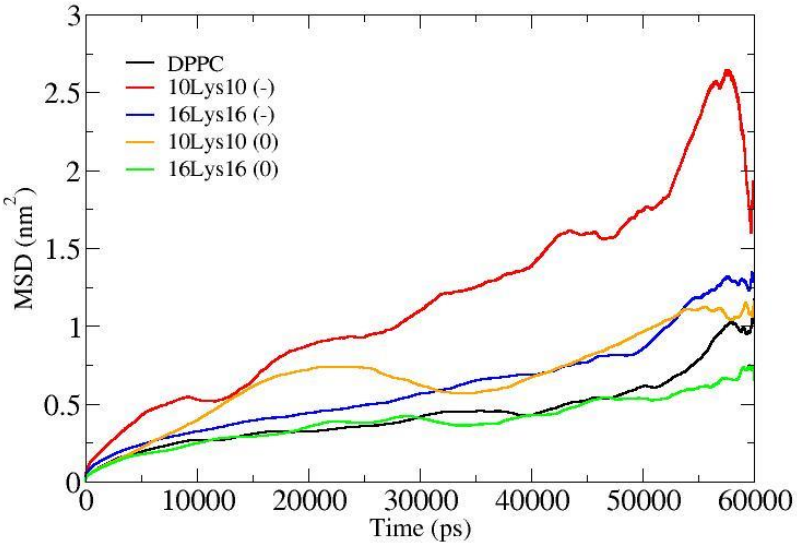

Figure 3.11 Mean square displacements of DPPC molecules, calculated from the MD simulations for the DPPC/lysine-based systems.

A more detailed analysis on the order of the membrane is presented from the estimated order parameter, S_{CD}, for the carbon atoms in DPPC tails (Figure 3.12). All the surfactants, with the exception of the longest anionic molecule, 16Lys16(-), induce a similar disordering effect close to the interface. A strongest action is observed for the nonionic 16Lys16(0) and 10Lys10(0) surfactants in comparison to that of 16Lys16(-). For the internal part of the carbon tails, the main differences appear between carbons 5 and 10. The effect of the longest anionic surfactant (16Lys16 (-)) increases, while the effect of its nonionic homologous decreases. On the most internal part of the membrane, the shortest tail nonionic surfactant (10Lys10(0)) presents a higher disorder effect, with a

behavior similar to that of both anionic molecules and nonionic 16Lys16 for the terminal carbon.

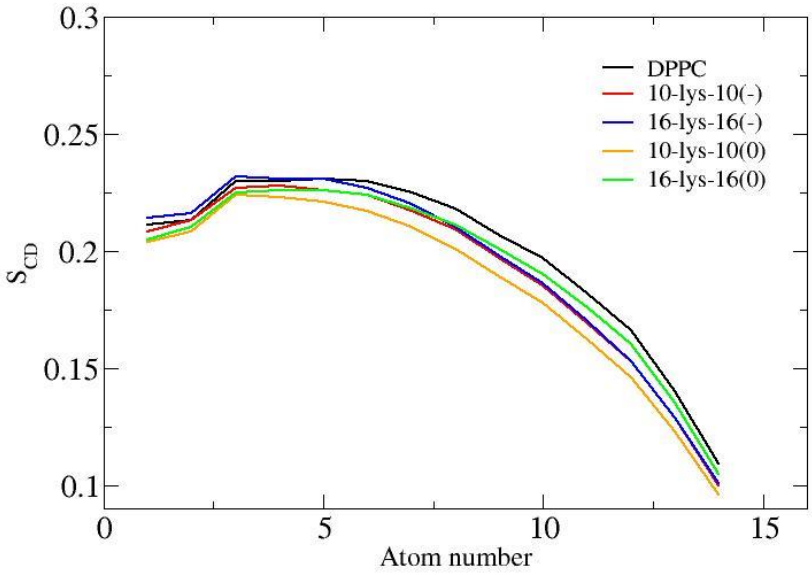

Figure 3.12 Deuterium order parameter, SCD, estimated from the MD simulations, along the bilayer depth for DPPC chains, averaged over sn-1 and sn-2 chains, in the presence of the lysine-based surfactants.

Changes in the hydration level were also assessed by the analysis of rdfs of SPC water molecules around the polar heads of both DPPC and surfactants, represented by the ammonium groups (Figure 3.13). In what concerns the polar heads of DPPC, Figure 3.13 - panel (a), it is observed that the presence of the surfactants molecules promotes a decrease in the amount of water accessible. However, no significant differences were found in terms of the hydration of the ammonium groups of DPPC in the presence of the different surfactant structures. Conversely, for the surfactant polar heads, panel (b), the same analysis indicates an increased solvation of the anionic molecules. Figure 3.14 presents the rdfs of SPC water molecules relative to the carbonyl-ester atoms of DPPC chains (panel (a)) and the surfactants polar heads. No significant differences were found in terms of the hydration of the carbonyl-ester atoms of DPPC tails, corresponding to the upper part of the hydrophobic region. From panel (b), an increase in the amount of water is observed in the proximity of the anionic molecules. In contrast, panel (c) shows the absence of water close to the nonionic molecules. Such behavior is compatible with the previous analysis: nonionic molecules are fully embedded in the inter-leaflet region of the DPPC membrane, which may explain their reduced action upon permeation.

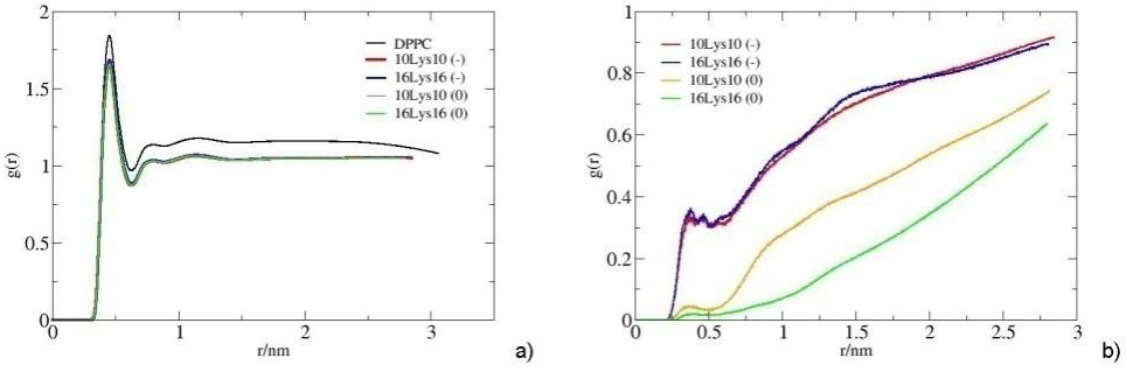

Figure 3.13 Radial distribution function of water molecules relative to DPPC (panel (a)) and lysine-based surfactants (panel(b)) ammonium groups, calculated from the MD simulations carried out at 50°C.

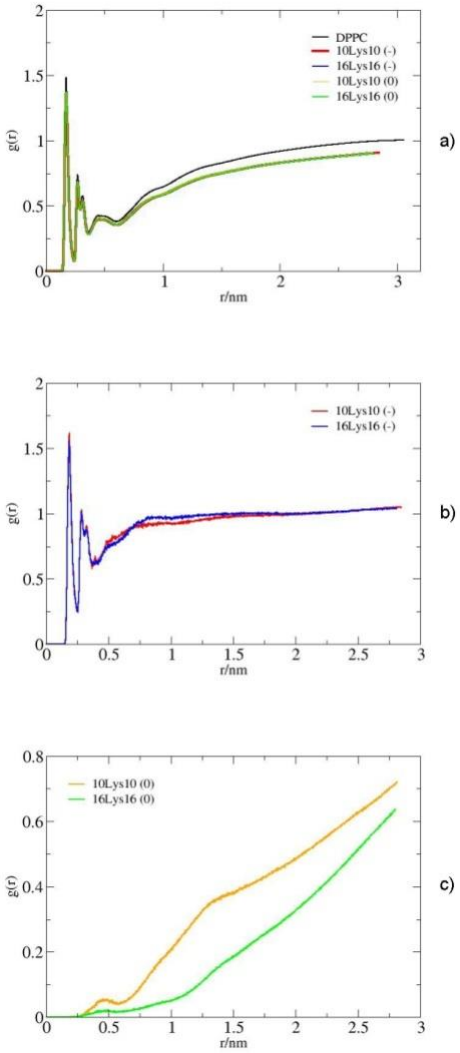

Figure 3.14 Radial distribution functions of water molecules around the carbonyl-ester atoms for the sn1 and sn2 chains of DPPC (panel (a)) and the polar heads for both anionic (panel (b)) and nonionic (panel (c)) lysine-based surfactants.

3.3.3. Skin integrity

Histology-light microscopy and SEM were used to visualize potential morphological changes and effects on the skin after the *in-vitro* studies caused by the use of the chemical penetration enhancers and formulations.

3.3.3.1. Histological studies

After the permeation studies, the skin samples pretreated with various lysine-based surfactants were stored at -20ºC. Prior to use, the samples were defrosted and submitted to histological procedures for observation using light microscope at different magnifications (10x, 20x and 40x).

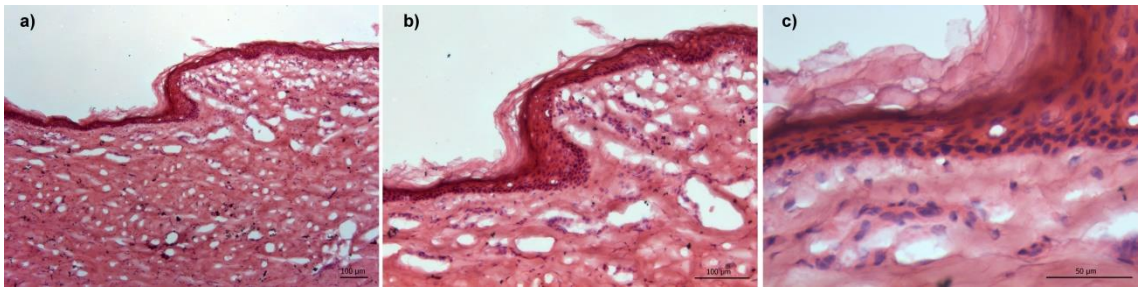

Figure 3.15 Pictures of control porcine skin sample taken in an optical light microscope at different magnifications: 10x - a), 20x - b), 40x - c).

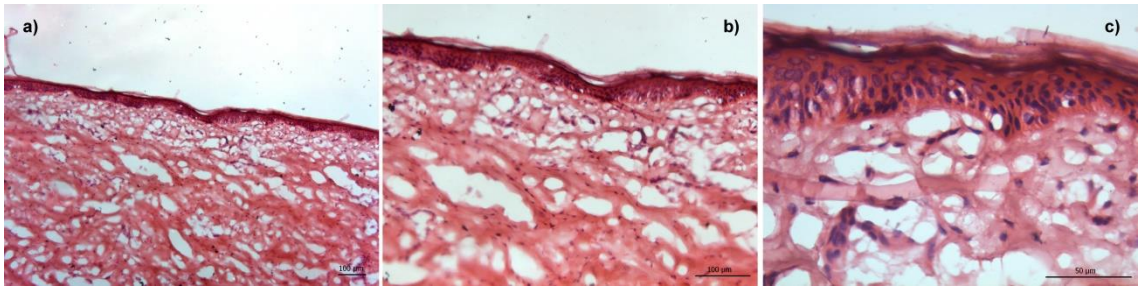

Figure 3.16 Pictures of porcine skin sample used in the permeation studies, taken at different magnifications: 10x - a), 20x - b), 40x - c) after permeation experiments employing (16Lys16(-)), the most effective CPE.

It can be observed that no significant morphological or structural changes have been detected when comparing the control samples (Figure 3.15) with the surfactant treated ones (Figure 3.16). Although minor changes were visible regarding cell cohesion, with some areas of the SC detaching or peeling off from the adjacent layer. However this effect can be related to the sample handling, since this is also observed in the control skin samples.

3.3.3.2. Scanning Electron Microscopy studies

Skin integrity evaluation was further analyzed by using SEM studies after the drug permeation experiments in order to observe the occurrence of potential harmful effects caused by the use of CPE. This technique has a large depth of field compared to conventional light microscopy and for that reason the images obtained have a three-dimensional appearance, high-resolution at high magnifications, revealing details of the surface of the skin.

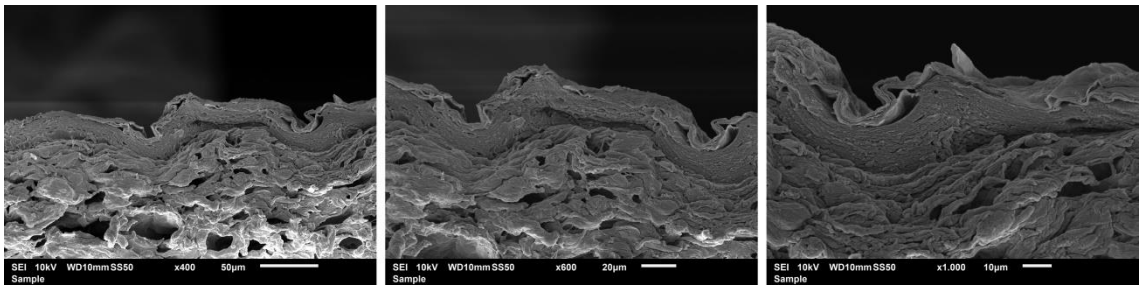

Figure 3.17 SEM cross section of control porcine skin sample at 400x, 600x and 1000x magnification.

From the images it can be seen the details of the skin structure with different layers such as the SC (the outermost multi-layered structure), viable epidermis (the darker area) and dermis (the thicker structure mostly composed of connective tissue under the viable epidermis). Unlike the control samples shown in Figure 3.17 presented for comparative purposes, the pictures presented in Figure 3.18 were obtained from skin samples previously used in the permeation studies, reported in section 3.2.4. It can be observed that some SC cells are naturally shedding however this effect can be seen both in the control and treated samples. Also noticed is some expected variability between the samples analyzed, mostly regarding the thickness of the SC, but changes or damage to the skin structure caused by the CPE used that could result in permanent alterations or loss of integrity are not detected.

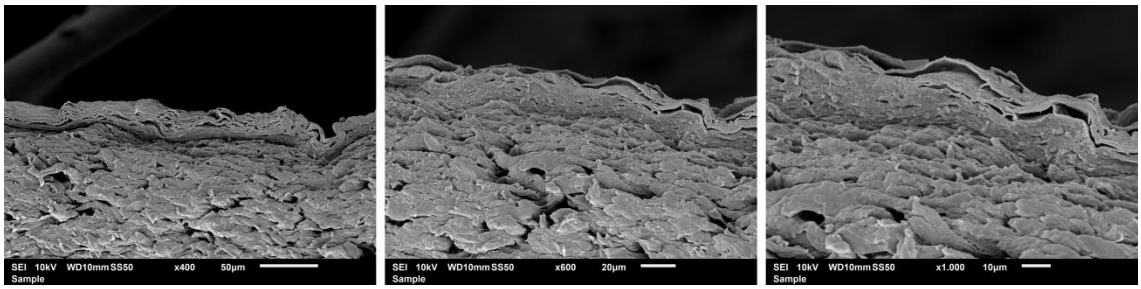

Figure 3.18 Skin samples treated with the anionic surfactant 16Lys16 at 400x, 600x and 1000x magnification taken after permeation studies.

3.3.4. Cytotoxicity studies

Skin irritation is a reversible inflammatory reaction produced by the arachidonic acid cascade and cytokines in the viable skin cells like keratinocytes and fibroblasts. To determine the cytotoxicity profiles of all CPE used in this work, cultured human epidermal keratinocytes (Figure 3.19) were exposed to various concentrations of the lysine based surfactant, following the Alamar assay protocol (O'Brien et al., 2000).

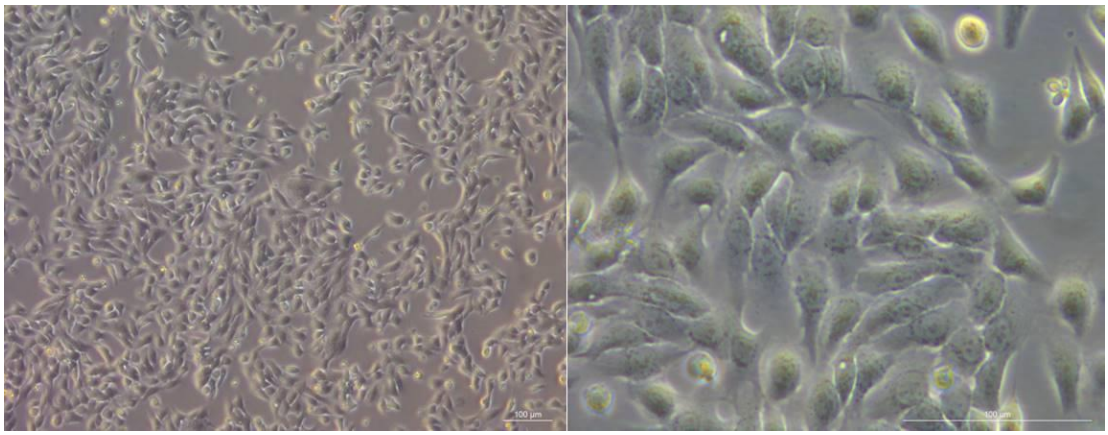

Figure 3.19 Pictures of cultured HEK 20x (on the left) and 40x (on the right), seeded at 10.000 cells/well in appropriate culture medium, prior to the start of the Alamar Blue assay.

To ensure the linearity of the Alamar Blue assay method used, standard plots for HEK (R^2 = 0.975) were constructed based on the absorbance readings at 570 and 600 nm for 0, 10.000, 20.000, 40.000, 60.000 cells/well. Although, the groups of cells cultured for the alamar assay is noticeably less complex in number and in cell types when compared to the skin tissue, the results are a good indication of potential, relative toxicity and irritation of these compounds to the skin cells. The results obtained in the Alamar Blue assays are presented in Figure 3.20.

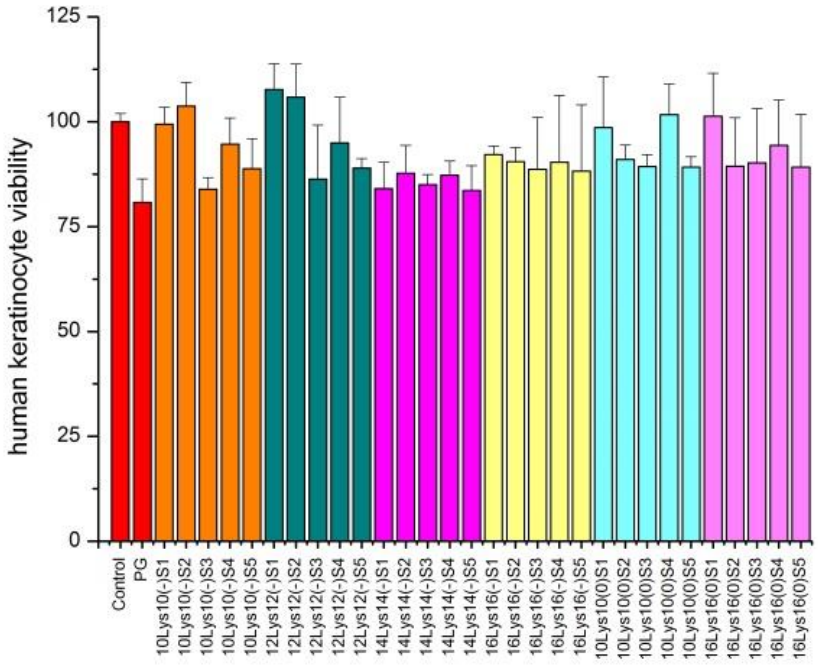

Figure 3.20 Alamar Blue assay results for HEK. The bars represent the cell viability (%) for each permeation modifier and concentration tested. The error bars represent the standard deviation (n=6).

The results summarized in Figure 3.20, demonstrate that HEK show a good tolerance to the presence of all the CPE tested, as the cell viability is similar to the control. PG exposure resulted in a slight reduction in HEK viability (20 %), yet not statistically significant from the control. It can be concluded that all the concentrations tested are not considered harmful to the cells, as the cell viability is always close to PG. Note that the presence of an hydrogel in the actual formulations has probably some impact on the diffusion of the molecules under scrutiny, but it is not likely to promote an overall change in the respective effect upon living cells. A global analysis of the Alamar assay results obtained with HEK suggests that the cytotoxicity of the surfactants studied it is not dependent on the alkyl chain length.

3.3.5. Analysis of trends and effects

In this work it is observed that all the surfactants act as chemical permeation enhancers, with different degrees of efficacy. The simulation results sum up to the experimental data, including data on, e.g., the order parameter and diffusion, both indicating a certain degree of membrane perturbation. The experimental results pointed out to a more pronounced effect of the anionic surfactants, a result that is also observed in the molecular dynamics studies. The incorporation of the nonionic surfactants in the interior

of the lipid membrane, should promote the permeation of hydrophobic drugs (albeit marginally) and, in contrast, preclude that of ionic drugs, as indeed experimentally observed. In terms of the variation in effect due to chain length, there is no visible correlation between experimental and simulation data. All the surfactants employed seemed to promote a limited degree of membrane disruption, as computationally extracted, which is in direct agreement with the absence of cytotoxicity found for the concentrations employed. As previously discussed, in the case of ropivacaine, one cannot discard electrostatic effects by the anionic surfactants, which should favor binding and thus enhanced permeation of the cationic drug (an effect particularly significant for the C16 compound).

3.4. Conclusions

This work presents a systematic approach to the use of a series of lysine-based surfactants as permeation. The two classes of lysine-based molecules, anionic and nonionic, possess varying alkyl chain length, comprising 10, 12, 14 or 16 carbon atoms for the anionic and 10 and 16 for the nonionic. It was observed that the most effectives CPE were the compounds with the longest alkyl chain (16Lys16) for both drugs. The highest enhancing effect was achieved for ropivacaine, presumably due to a combination of membrane perturbation, surface exposure of the anionic surfactant headgroups and ensuing favorable electrostatic interactions with the drug. In this case, the 16Lys16(-) was the most effective (ER=6.12), while in the case of tetracaine this was observed for 16Lys16(0), likely due to a combined perturbation/hydrophobic effects (comparatively weaker, in any case, than the electrostatic effect mentioned above). Results thus suggest that lysine-based surfactants are promising candidates to increase drug transport, especially for hydrophilic drugs, through the SC without changing the skin tissue morphology and with the advantage of being non cytotoxic. Molecular dynamics simulations have proved to be a useful tool for a mechanistic rationalization of the system behavior.

Chapter 4

Serine-based gemini surfactants: a comprehensive study on structure-activity relationships, molecular dynamics and skin penetration enhancement of local anesthetics

This Chapter provides new insights on the efficacy of biocompatible, serine-based gemini surfactants as CPE for tetracaine and ropivacaine. *In vitro* permeation and *in silico* studies combined with cytotoxicity profiles were performed to obtain relevant data on the permeation of both drugs and how such interactions affect the skin integrity. Results show that the selected permeation enhancers do not have significant deleterious effects on the skin structure and do not cause relevant changes on cell viability. Cationic chemical enhancers with long alkyl chain and shorter spacer showed to be the most promising chemical permeation enhancers for both drugs. Molecular dynamics simulation results provided a mechanistic view of the action of the surfactants molecules on lipid membranes that essentially corroborated the experimental observations.

4.1. Introduction

The principal goal in the development of dermal drug delivery systems is the temporary disturbance of the skin barrier without causing negative effects such as erythema, itching and local irritation (Effendy and Maibach, 1995; Naik et al., 2000b).

Surfactants are amphiphilic molecules that are employed in a wide range of technical applications, such as cosmetic, drug delivery and food formulations, and in fundamental studies as models for biological membranes. Surfactants have also been used as chemical permeation enhancers (CPE) because they are able to improve drug permeation across the skin due to a combination of various mechanisms, including increasing the diffusivity and/or in the solubility of drugs in the skin and by reversible change of the lipid organization of the stratum corneum (SC), with a consequent reduction in the diffusional resistance (Almeida et al., 2010; Karlsson et al., 2002; Kirby et al., 2003). The use of this class of compounds must be carefully monitored as local irritation of the skin may occur, depending on the nature and concentration employed. Intense efforts have been made to solve this problem, including the incorporation of natural amino acids, sugars, and fatty acids in the surfactant structure (Blunk et al., 2006; Clapés and Rosa Infante, 2002; Moran et al., 2004). As a result of the search for novel surfactants with higher efficiency, better biocompatibility and biodegradability profiles, gemini surfactants have been extensively explored (Borde et al., 2008; Infante et al., 2010; Menger and Littau, 1993; Tehrani-Bagha et al., 2007; Zana et al., 1991). Unlike conventional monomeric surfactants, which are usually composed by one or two hydrophobic tails connected to a single polar head group, gemini surfactants consist of two hydrophilic headgroups linked covalently by a spacer and two hydrophobic main chains (Menger and Littau, 1991). The chemical nature of the polar headgroups can be varied, as well as the length of the main alkyl chains. Considering that the spacer may also possess different characteristics, namely it can be made short or long, flexible or rigid, polar or nonpolar, a significant structural diversity and variable physico-chemical behavior can be obtained for this class of compounds. The enhancement of skin permeability is generally related to the ability of the surfactant molecules to penetrate in the hydrophobic domains of the SC, and therefore increasing the fluidity of the lipid structures (Walters et al., 1993b; Zana, 2002b). Recent studies have been performed to evaluate the potential of some alkyl surfactants as CPE for numerous drugs (Ashton et al., 1992; Babu et al., 2005b; Tan et al., 1993; Walters et al., 1993b) and have focused

on the influence of the alkyl chain length in the efficacy of the surfactants. It was reported that the highest enhancer activity was found for surfactants with C_{12} alkyl chains (López et al., 2000). Because of the enhanced interfacial properties of gemini surfactants, these molecules are more efficient and safe for delivery of drugs across the skin. Furthermore, it has been observed for a series of *n-s-n* bis-quat gemini that these properties are considerably influenced by the spacer length, *s* (Brun et al., 2003; Menger et al., 1999; Shukla and Tyagi, 2006a; Tehrani-Bagha et al., 2007; Zana, 2002a, b; Zana and Talmon, 1993). Gemini surfactants based on sugars, peptides and, particularly amino acids based on lysine and arginine derivatives, have been recently synthesized to overcome toxicity and biocompatibility issues (Blunk et al., 2006; Colomer et al., 2012). This class of surfactants is more environmentally friendly and less toxic to human cells (specially the lysine-based derivatives) (Teixeira et al., 2014a; Yang et al., 2010). Although the nonionic surfactants are reportedly the least irritant (Effendy and Maibach, 1995), cationic gemini surfactants have recently attracted significant attention due to their biocompatibility, very important for applications in the biomedical field and have been suggested as highly promising in gene therapy and drug delivery (Badea et al., 2005; Cardoso et al., 2011; Kirby et al., 2003; Vieira and Carmona-Ribeiro, 2006; Viscardi et al., 2000). However their toxicity represents a limitation to the respective use in skin formulations, due to the irritancy potential to eyes and skin. More recently, a novel group of cationic gemini surfactants containing serine residues as the polar headgroup have been synthesized and characterized physicochemically (Silva et al., 2013b).

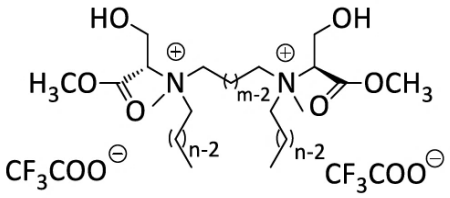

Figure 4.1 Molecular structure of the cationic serine-based surfactants [(nSer)$_2$Nm]; n is number of C atoms in the main alkyl chain (n=10, 12, 14) and m is the number of methylene groups included in the spacer (m = 5). Nonionic surfactants possess non-quaternized N atoms in the polar head groups. For both families, a longer spacer, m = 10, was also considered.

The objective of the present study was to evaluate the potential of a series of novel gemini surfactants, nonionic and cationic, as CPE for tetracaine and ropivacaine, across newborn porcine skin, following a similar methodology to that previously reported by the authors and using a systematic variation in the structure of the gemini surfactants (Silva et al., 2013a; Silva et al., 2012; Teixeira et al.). The choice of the serine-based surfactants used in this work was dictated by the optimal toxicological profile presented by these compounds in previous work on various cationic monomeric surfactants (Brito et al., 2009; Silva et al., 2013b; Silva et al., 2009). A series of nonionic (non-quaternized

N) and cationic (quaternized N, as shown in Figure 4.1) serine-based gemini surfactants of the amine series compounds were designed and synthesized, by imposing variations in the type of linkage of the spacer to the quaternary N atom (amine, ester or amide linkage), spacer length (number of methylene groups) and main chain length. For both families the spacer length is kept constant (*m* = 5) and the main alkyl chain length (*n*) is varied between 10, 12 and 14 carbon atoms, allowing to study both the influence of charge and main chain length on the enhancement efficacy. Furthermore, for the *n* = 12 compound a longer spacer, *m* = 10, was used allowing to assess also the influence of spacer length. The two local anesthetics drugs were chosen based on their distinct physical-chemical properties where tetracaine is non-ionized and hydrophobic while ropivacaine is ionized and therefore hydrophilic. Tetracaine is of the ester type, and possesses a logP of 2.79, which compared to the other anesthetics, makes this molecule a suitable candidate for topical administration (Covino, 1987; Fisher et al., 1998). Ropivacaine hydrochloride is a long-acting local anesthetic with a slower onset of action, shorter in duration and less intense, reason why it is well tolerated for regional anesthesia (Becker and Reed, 2012). However it is a hydrophilic molecule and, consequently, poorly absorbed through intact skin (McClellan and Faulds, 2000; Zink and Graf, 2004).

The effects on the skin structure of these CPE were later evaluated using SEM. The analysis of the *in vitro* results also relied on the insight provided by molecular dynamics simulation studies. Additionally, the cytotoxicity profiles of both nonionic and cationic serine-based surfactants in HEK) was assessed and compared. Data collected from different techniques provided new information about novel serine-based surfactants and their potential use as to be used as CPE in transdermal formulations.

4.2. Experimental section

4.2.1. Materials

The eight nonionic and cationic serine-based surfactants used in this study were synthesized and purified according to a method previously developed and reported by some of the authors (Goreti Silva et al., 2012; Silva et al., 2013b; Silva et al., 2009). The purity of the compounds was determined by NMR, high resolution mass spectroscopy and surface tension measurements. The nonionic serine-based surfactants, comprising 10, 12 and 14 carbon atoms with 5 carbon atoms as spacer and 12 with 10 as spacer,

respectively referred in this Chapter as $(10Ser)_2N5(0)$, $(12Ser)_2N5(0)$, $(14Ser)_2N5(0)$, $(12Ser)_2N10(0)$ and the cationic ones are referred as $(10Ser)_2N5(+)$, $(12Ser)_2N5(+)$, $(14Ser)_2N5(+)$ and $(12Ser)_2N10(+)$. RPC was a gift from AstraZeneca (London, United Kingdom) and HPMC K15M a gift from Dow Chemical Company (Midland, MI, USA). TC, ammonium acetate, PG (Reagent Plus, 99%), sodium bicarbonate, glucose, penicillin G potassium salt and streptomycin were purchased from Sigma Aldrich (Saint Louis, MO, USA). HP-*β*-CD with 97% of purity, with an average degree of substitution of 2 to 6 units of 2-hydroxypropyl (C_3H_7O) per glucose unit, and with an average molecular weight of 1380 g/mol, was purchased from Acros Organic (Geel, Belgium). PBS was purchased from TIC Gums (Belcamp, MD, USA). MeOH and acetonitrile ACN HPLC grade were purchased from LiChroSolv Merck (Darmstadt, Germany). HEK were purchased from DKFZ (Im Neuenheimer Feld, Heidelberg, Germany). Alamar-Blue® Cell Viability reagent was purchased from Thermo Scientific (Waltham, MA, USA).Tissue-Tek® O.C.T™ compound was purchased from VWR international (Radnor, Pennsylvania, USA). Formaldehyde solution min. 37 % was purchased from Merk (White House Station, NJ, USA). DMEM, FBS and trypsin were purchased from Invitrogen™ (Carlsbad, CA, USA). All reactants were used as received.

4.2.2. Drug delivery studies

In vitro studies were used to determine the permeation profile of each drug through the skin and were carried out using Franz diffusion cells (PermeGear, Inc., PA, USA) with a diffusion area of 0.64cm^2. The receptor compartment of 5.1 mL was filled with PBS solution (pH=7.4) kept at 37.0 ± 0.1 °C and stirred at 600 rpm during the entire permeation experiments. Dermatomed newborn porcine skin pieces (section 4.2.2.1.) were placed between the donor and receptor compartment, with the epidermal side facing up. All the skin samples, except the control, were pretreated with 60 μL of the various serine-based surfactant enhancer solutions prepared in section 4.2.2.3., for 1 h prior to the application of the formulations in the donor compartment (t = 0). Drug loaded hydrogel formulations (500 μL) prepared in section 4.2.2.2 were placed in each donor compartment and were occluded with Parafilm® to prevent evaporation. Subsequently 300 μL of each Franz Cell receptor compartment samples were collected at 0, 2, 4, 6, 8, 18, 20, 22 and 24 h, and immediately replaced with the same volume of fresh PBS solution. The samples were placed in 0.350 mL inserts supported by adequate vials and storage at -20 ºC.

4.2.2.1. Porcine skin preparation

The skin model used in the permeation studies was newborn porcine skin tissue (3 weeks, ~5 kg) acquired from a local slaughterhouse. The tissue was then removed with a scalpel and dermatomed using a Padgett® Model B Electric Dermatome (Integra LifeSciences, Plainsboro, NJ) Figure 3.2. The skin with 650-750 µm thickness was cut in small pieces and stored at −20 ºC no longer than 3 months. Prior to use, skin samples were defrosted at room temperature and submerged in PBS (pH=7.4) during 1 h to promote equilibration.

4.2.2.2. Composition and preparation of hydrogels formulation

Tetracaine HPMC hydrogel was composed of 2.5% (w/w) TC mixed with appropriate amount of HP-*β*-CD (Teixeira et al., 2014b), 1% (w/w) HPMC K15M and deionized water. Ropivacaine hydrochloride HPMC hydrogel was prepared by adding 2.5% (w/w) RPC to 1% (w/w) HPMC K15M and deionized water. The polymers solutions were kept stirring at low speed (50 rpm) during 24 h to ensure complete solubilization.

4.2.2.3. Preparation of the serine enhancer solutions

After obtaining the synthesized and purified serine-based surfactants, all enhancer solutions were added to PG to a final concentration of 0.15 M and left stirring overnight at room temperature until homogenization. Generally the compounds produced clear solutions, however in some cases the solutions needed to be heated prior to use.

4.2.2.4. HPLC quantification of tetracaine and ropivacaine

All samples were quantified by HPLC using a Shimadzu UFLC apparatus with SPD-M20A UV/visible dual wavelength detector. The quantification of both drugs were carried out at 25°C using a reverse-phase C_{18} column (250 x 4.6mm C18 (2) 100 A Luna 5 µm, Phenomenex® (Torrance, CA, USA) with a guard column as the stationary phase. A methanol, acetonitrile and ammonium acetate solution on the proportions 7:7:6 respectively, was used as mobile phase. The prepared mixing solution was filtered using a 0.45 µm Nylon membrane (Supelco Analytical, Bellefonte, USA) and sonicated during 1 hour prior use. The injection volume (25 µL) and the flow rate (1.0 mL/min) was maintained constant during all the analysis. Tetracaine was detected at 311 nm with a retention time of ca. 6.9 minutes. The method showed a linear response in the 0.01–100

μg range (R^2 = 0.9998) with a daily relative standard deviation (RSD) < ± 5.0%. Ropivacaine was detected at 210 nm and the retention time was ca. 9.1 minutes. The method showed a linear response in the 0.01-500 mg/mL (R^2=0.9973) with a daily RSD < ± 6.0%.

4.2.2.5. Data analysis in the permeation studies

The cumulative amount of tetracaine and ropivacaine present in the receptor compartment solution after 24 hours of permeation experiment (Q_{24}) was calculated by Eq. 3.2.

The steady state flux (μg cm^{-2} h^{-1}), *J*, that describes the amount of drug passing through a unit area per unit of time was also calculated according to Fick's first law of diffusion, resorting to Eq. 3.1.

The enhancement ratio (ER) for flux was calculated for comparison among formulations using Eq. 3.3.

Results are presented as mean ± SD (*n*), where *n* is the number of replicates. The significance of differences between the flux values of different formulations was evaluated using Student's t-test at the probability level of 0.05.

4.2.3. Skin integrity evaluation after permeation studies

Skin samples were rinsed with deionized water and, subsequently dried, to evaluate morphological changes caused by the CPE after the permeation studies.

4.2.3.1. Scanning Electron Microscopy studies

Skin samples were analyzed by SEM to evaluate if any morphological changes occurred after the *in vitro* studies. The samples were placed in a plastic mold and were submerged in Tissue-Tek® O.C.T. compound. Cross-section slices of frozen samples were cut with 10 μm of thickness using a cryostat SLEE medical GmbH (Carl-Zeiss, Mainz, Germany). The samples were defrosted, rinsed with deionized water and fixed with 4% formaldehyde during 1.5 h. Afterwards skin samples were rinsed and placed in deionized water during 2 h at room temperature. Skin samples were subsequently dehydrated using different solutions of ethanol in water (30 %, 50 %, 75 %, and 95 %) for

25 minutes each. Finally, skin samples were placed in two changes of absolute ethanol (100 %) for 2 h at room temperature and placed on a double-side carbon tape mounted onto an aluminum stud. The samples were coated with gold and the respective pictures were taken at 600x and 1000x magnification using a SEM – JEOL, model JSM-6010LV/6010LA.

4.2.4. Simulation details

Molecular dynamics simulations were performed on systems containing novel serine-based gemini surfactants, nonionic and cationic, in a fully hydrated DPPC bilayer, consisting of 256 lipid molecules (128 per leaflet). DPPC/surfactant systems have been proven to be adequate models to investigate the mechanisms of enhancement of drug permeation through inspection of the effects induced by the drug in this type of membranes (Almeida et al., 2011; Cerezo et al., 2011; Gurtovenko and Anwar, 2007; Kyrikou et al., 2004; Notman et al., 2006; Teixeira et al.). DPPC and SPC water (3655 molecules) were described using the original definitions of the GROMOS 53a6 force field, which has been shown previously to accurately reproduce the experimental area per lipid, lateral self-diffusion constant, and deuterium order parameters for the acyl chains of DPPC bilayers in solution (Kukol, 2009; Piggot et al., 2012; Poger and Mark, 2009; Schuttelkopf and van Aalten, 2004). In each system, a single molecule of surfactant was considered. This was shown to be sufficient to provide a rationale for the experimental results. The interaction of each solute with the surrounding lipids and the preferential positioning and respective action on the bilayer was assessed.

Equilibrium properties, structure, and dynamics for the various DPPC/surfactant systems were calculated over the 80ns simulation runs using GROMACS package, version 4.5.5 (Hess et al., 2008; van der Spoel et al., 2012). To maintain the stability of the lipid system, all simulations were performed above the experimental liquid-crystalline phase transition temperature (325 K) for pure DPPC as reported by Curtis and Hall (Curtis and Hall, 2013).

4.2.4.1. Simulations parameters

All MD simulations were carried out in the NPT ensemble under periodic boundary conditions. A standard time step of 2 fs was used for both the equilibration and production runs. Non-bonded interactions were computed on the basis of a neighbor list, updated every 10 steps. Long-range electrostatic contributions were computed using the

PME method as recommended for charged polymer simulations. For Lennard–Jones energies, a cut-off of 1.4 nm was applied. The Berendsen thermostat was used to keep the temperature and pressure constant at 325 K and 1 bar, respectively, throughout the simulation with time constants of 0.1 ps and 0.5 ps, respectively. To obtain a starting configuration each system was firstly subjected to an energy minimization step. The systems were subsequently left to evolve up to 80 ns, using the LINCS algorithm (Hess et al., 1997). The first 20 ns were considered sufficient to attain equilibration, while the last 60 ns of the production runs were subsequently subjected to standard analysis, including the determination of density probability distributions, order parameters, mean square displacements and rdf. Throughout the GROMACS simulation the coordinates of each atom were written to an output trajectory file every 1 ps. MD trajectories were visualized, and configuration images extracted using the VMD 1.9 software (Humphrey et al., 1996).

4.2.5. Cytotoxicity studies

Cytotoxicity was assessed by the Alamar Blue assay, a colorimetric cell viability method that has been widely reported in the literature for similar systems (O'Brien et al., 2000). The objective was to evaluate the toxic effects of the serine-based surfactants on cultured HEK, and establish a concentration-toxicity response. The number of viable cells is directly proportional to the quantity of resorufin (a pink colored and fluorescence compound) that is a product of reduction of resazurin [7-Hydroxy-3H-phenoxazin-3-one-10-oxide sodium salt] (a non-fluorescent blue dye). The levels of resorufin formed were quantified by absorbance readings at 570 and 600nm (alamarBlue® Cell Viability Assay Protocol) using a Microplate Power Wave X Scanning Spectrophotometer (Bio-TEK Instruments, Inc. Winooski, VT, USA). Cytotoxicity studies were carried using a skin cell line HaCaT seeded at $10x10^5$ cells/well in 96-well plates, under sterile conditions. Before this, HEK were seeded in 200μL/well of DMEM® medium supplemented with sodium bicarbonate (3,7 g/L), glucose (25 mM), 10% heat inactivated FBS, 100 U/mL penicillin, and 100 μg/mL streptomycin and were incubating for 24 h at 37ºC, 5 % CO_2 and 90 % R.H. After seeding the cells were exposed to medium (control), PG and various concentrations (160 (S1), 16(S2), 1.6(S3), 0.16(S4) μM) of cationic and neutral serine based-surfactant solutions diluted in culture medium. Subsequently, well plates were placed in the incubator for another 24 h in the same conditions. 4 h before the absorbance measurements, cells were exposure to the resazurin compound and

returned to the incubator. The 96-well plates were read, and the results presented as % cell viability (mean ± standard deviation, n=6), *C.V.*, calculated according to Eq. 4.4

$$C.V. = \frac{\text{abs read in treated cells}}{\text{abs read in control (untreated) cells}} \quad (4.4)$$

4.3. Results and Discussion

4.3.1. *In vitro* permeation studies using serine-based surfactants

4.3.1.1. Percutaneous drug delivery of tetracaine

All serine-based surfactants were dissolved in PG in a final concentration of 0.15 M. Prior to the permeation experiments 60 μL of each serine enhancer solution was applied to the epidermal side of dermatomed porcine skin placed between the donor and receptor compartments of Franz diffusion cells. 500 μL of tetracaine loaded hydrogel was applied. The permeation parameters (Flux, Q_{24} and ER) presented in Table 4-1 and the permeation profiles shown in Figure 4.2 were determined using the equations described in section 4.2.2.5.

Table 4-1. Effect of the chemical permeation enhancers on percutaneous permeation of tetracaine across porcine skin. Data are presented as means ± S.D. (4≤N≤6).

Penetration modifier	Flux (μg cm^{-2} h^{-1})	Q24 (μg cm^{-2})	ER
Control – PG	19.83 ± 2.47	417 ± 53	-
0.15M (12Ser)2N10(0)	18.03 ± 1.34	402.98 ± 34	0.9
0.15M (10Ser)2N5(0)	20.22 ± 0.94	425.32 ± 18	1.02
0.15 M (12Ser)2N5(0)	22.91 ± 1.24	477.21 ± 34	1.15
0.15M (14Ser)2N5(0)	24.67 ± 0.71	526.52 ± 13	1.24
0.15M (12Ser)2N10(+)	24.84 ± 5.15	537.39 ± 103	1.25
0.15M (10Ser)2N5(+)	22.35 ± 0.62	515.18 ± 18	1.13
0.15 M (12Ser)2N5(+)*	28.25 ± 2.94	618.83 ± 79	1.42
0.15M (14Ser)2N5(+)*	37.08 ± 1.85	690.14 ± 42	1.87

** Statistically significant difference between enhancer and control, at p < 0.05 (Student's t-test)*

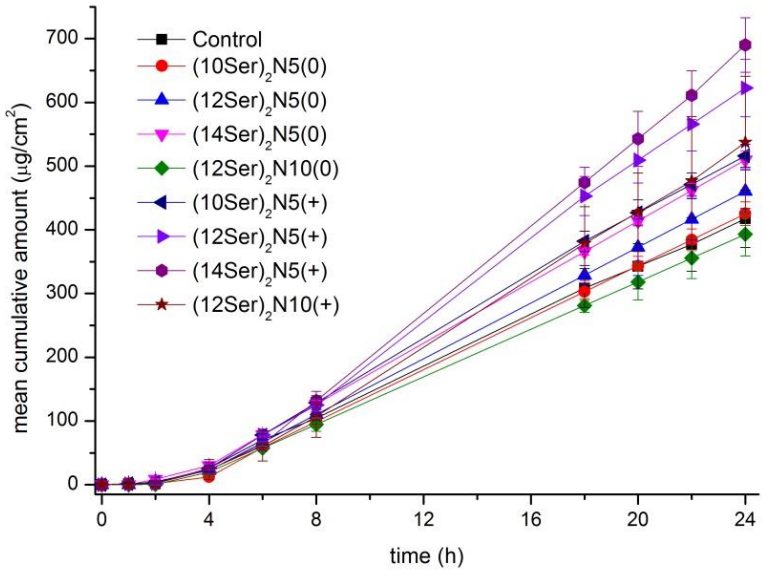

Figure 4.2 Cumulative amount of tetracaine permeated across porcine skin as a function of time. Skin was pretreated for 1 hour with enhancer solutions in PG, prior the application of the drug hydrogel in the donor compartment of the franz cells (t=0).

Serine-based surfactants promote an increase on the flux and Q_{24} values of tetracaine, with exception of $(12Ser)_2N10(0)$. However, only the results for $(12Ser)_2N5(+)$ and

$(14Ser)_2N5(+)$ cause a statistically significant difference ($p<0.05$) in tetracaine permeation.

It is clear that the highest values of flux and Q_{24} were achieved when the cationic compounds where applied. It is also interesting to note that the compound with the longest alkyl chain and shortest spacer, $(14Ser)_2N5(+)$, was the most effective permeation enhancer, resulting in a 1.9-fold increase of the flux, closely followed by $(12Ser)_2N5(+)$ (ER = 1.4). In contrast, serine-based surfactant with a longer spacer $(12Ser)_2N10(0)$ displayed a modest performance when compared with the control.

4.3.1.2. Percutaneous drug delivery of ropivacaine

The permeation profiles and permeation parameters (Flux, Q_{24} and ER) of ropivacaine permeated across the newborn porcine skin, during 24 h are presented in Figure 4.3 and in Table 4-2.

Table 4-2 Effect of the chemical permeation enhancers on percutaneous permeation of ropivacaine across newborn porcine skin. Data are presented as means ± S.D. (6≤N≤9).

Penetration modifier	Flux (μg cm^{-2} h^{-1})	Q24 (μg cm^{-2})	ER
Control - PG	1.94 ± 0.02	36.9 ± 1.6	-
0.15M $(12Ser)_2N10(0)$	1.31 ± 0.08	27.9 ± 2.3	0.68
0.15M $(10Ser)_2N5(0)$	1.87 ± 0.15	40.5 ± 2.5	0.96
0.15M $(12Ser)_2N5(0)$	2.60 ± 0.43	42.8 ± 2.7	1.34
0.15M $(14Ser)_2N5(0)$*	5.14 ± 0.24	102.4 ± 3.1	2.65
0.15M $(12Ser)_2N10(+)$	1.44 ± 0.05	19.9 ± 1.8	0.74
0.15M $(10Ser)_2N5(+)$	1.54 ± 0.06	21.8 ± 2.3	0.79
0.15 M $(12Ser)_2N5(+)$*	4.86 ± 0.74	82.9 ± 9.8	2.50
0.15M $(14Ser)_2N5(+)$*	5.74 ± 0.74	105.4 ± 15	2.96

** Statistically significant difference between enhancer and control at $p < 0.05$ (Student's t-test)*

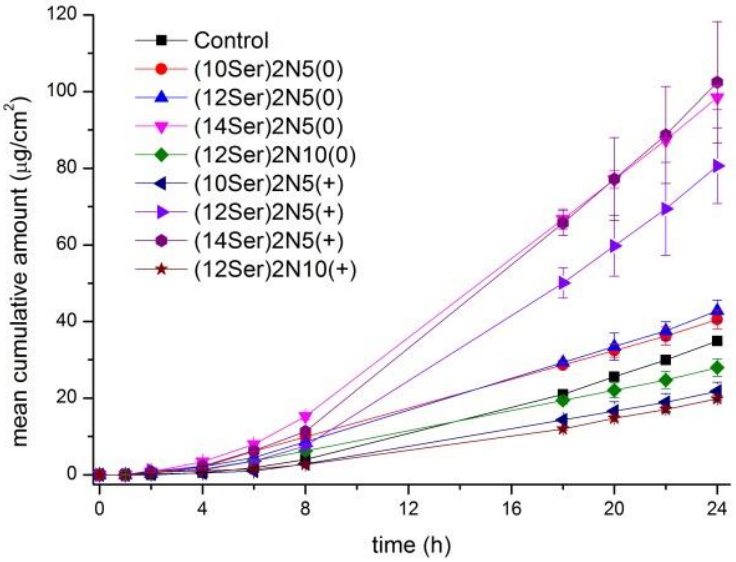

Figure 4.3 Cumulative amount of ropivacaine permeated across porcine skin as a function of time. Skin was pretreated for 1 hour with enhancer solutions in PG, prior the start of the permeation experiments.

Skin samples treated with all the serine-based surfactant tend to increase the permeation of ropivacaine, but statistical significance was only observed for $(14Ser)_2N5(+)$, $(12Ser)_2N5(0)$ and $(12Ser)_2N5(+)$. Results showed that the highest ropivacaine permeation was attained when serine-based surfactants with longer alkyl chain and shorter spacer were employed, resulting in a 3-fold increase for $(14Ser)_2N5(+)$, 2.7-fold for $(14Ser)_2N5(0)$ and 2.5 for $(12Ser)_2N5(+)$ increase in the flux values. The effect of the spacer is also remarkable, as the compounds with longer spacer ($(12Ser)_2N10(+)$ and $(12Ser)_2N10(0)$) showed a lower permeation of ropivacaine HCl, compared with the control, with values of ER of 0.74 and 0.68, respectively.

4.3.1.3. General trends

Overall, the steady-state permeation was obtained after a period not exceeding 8 hours, and maintained for the full period of observation of 24 h. It can be seen that the most effective CPE are the cationic compounds with longer alkyl chain and shorter spacer length, namely $(14Ser)_2N5(+)$, resulting in a 2-fold and 3-fold permeation enhancement for tetracaine (Figure 4.4) and ropivacaine (Figure 4.5), followed by $(12Ser)_2N5(+)$, with a ER of 1.4 and 2.5, respectively. In contrast, the CPE with the longer spacer, $(12Ser)_2N10(+)$ and $(12Ser)_2N10(0)$, and shorter alkyl chain, $(10Ser)_2N5(+)$; $(10Ser)_2N5(+)$, are the least effective for both drugs. In these cases, the effect of charge/ionization was found to be negligible.

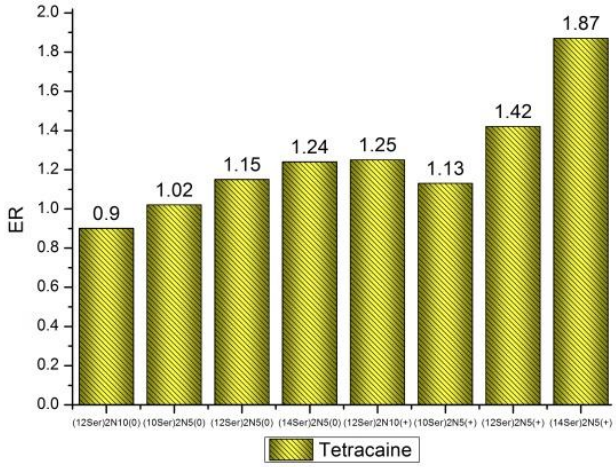

Figure 4.4 ER obtained pretreating the skin using the various CPE for tetracaine.

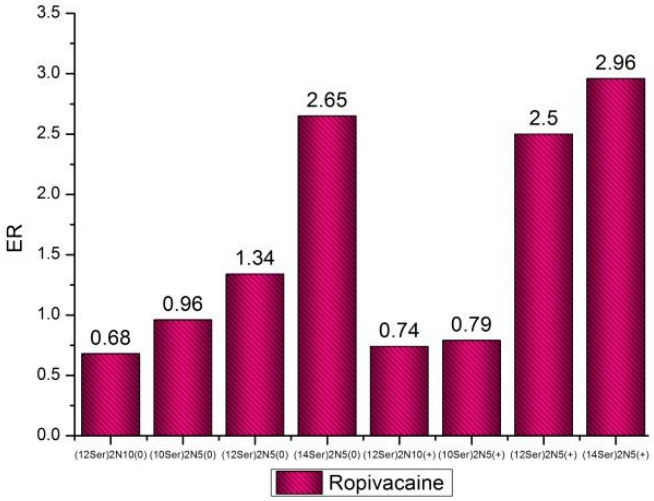

Figure 4.5 ER obtained pretreating the skin using the various CPE for ropivacaine.

Since tetracaine is a lipophilic molecule and permeates the SC more easily, the results obtained indicate that the effects of the CPE are especially relevant in the case of ropivacaine, which is a charged and hence hydrophilic molecule. These results are in agreement with previous work, where CPE were tested for drugs with different hydrophobicities (El-Kattan et al., 2000; Silva et al., 2013a; Teixeira et al., 2014a).

4.3.2. Skin integrity evaluation

After the *in vitro* permeation experiments, skin samples were rinsed with water and further analyzed by light microscopy and SEM to evaluate if any skin damage or morphological changes occurred during the *in vitro* permeation experiments.

After the *in vitro* permeation experiments, skin samples used in the permeation experiments and pre-treated with serine based-surfactant were rinsed with water and further analyzed by SEM to evaluate if any skin damage or morphological changes occurred during the *in vitro* permeation experiments. Figure 4.6 shows untreated newborn porcine skin (control) and Figure 4.7 represents the skin sample treated with the most effective enhancer in terms of drug permeation $(14Ser)_2N5(+)$. Details of skin layers such as the SC (the outermost multi-layered structure), viable epidermis and dermis (the thickest structure mostly composed of connective tissue under the viable epidermis) are visible due to the large depth of field of this technique.

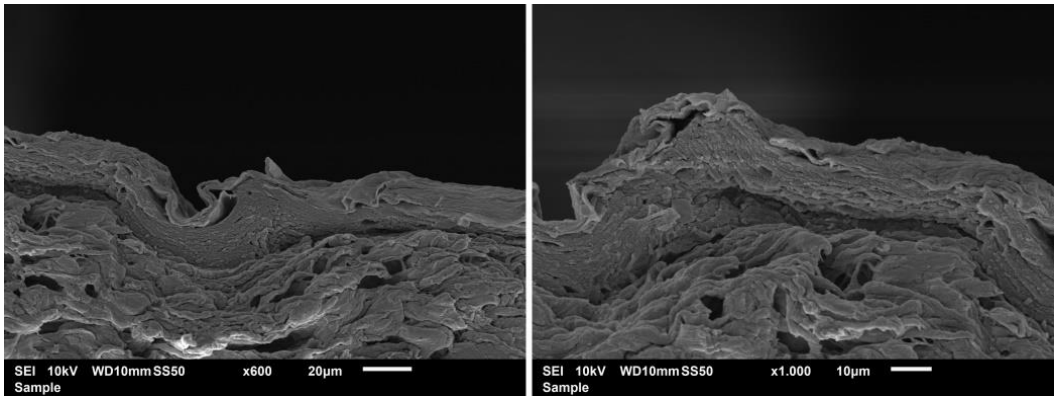

Figure 4.6 SEM cross section of untreated porcine skin (control) at 600x and 1000x magnification. This skin sample was not subjected to permeation studies.

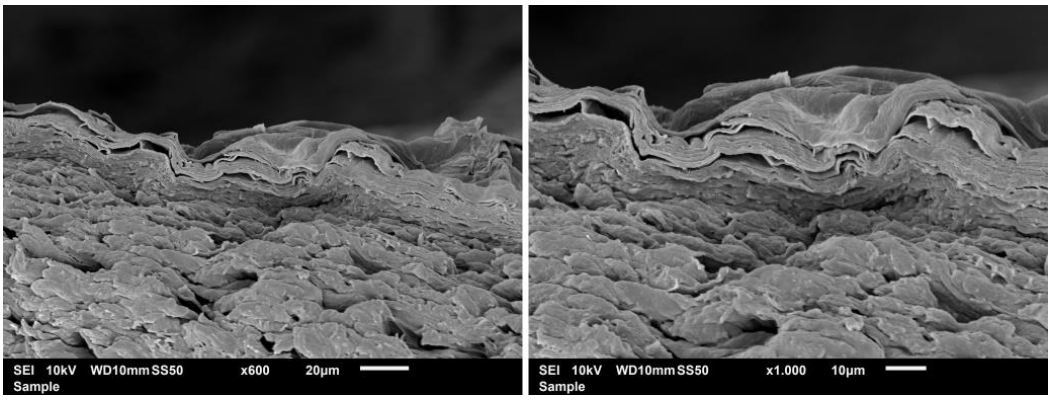

Figure 4.7 Skin samples treated with the cationic surfactant (14Ser)2N5(+) at 600x and 1000x magnification taken after permeation studies.

The tissue of the skin samples remains compact, consolidated and organized. Although no major morphological or structural changes are detected when comparing with the control samples, minor changes in cell morphology and cohesion can be seen, at the level of organization of the tissues, and also some areas of the SC seem to be separated from the subsequent layer. However, this occurrence is probably the result of natural peeling or sample handling since this effect was also observed in the untreated samples.

Overall, SEM studies confirmed that there are no significant changes on the skin tissue when comparing the CPE treated samples with the untreated one (control). The use of these compounds does not cause permanent alterations or loss of integrity.

4.3.3. Simulation results

Molecular dynamics simulations were performed on seven systems, a neat DPPC bilayer, taken as reference, and six other systems each comprising DPPC and one molecule of six different serine-based bis-quat gemini surfactants [$(nSer)_2Nm$] (Goreti Silva et al., 2012), both nonionic and cationic, with different lipophilic alkyl chain and spacer lengths. The latter were denoted DPPC/$(10Ser)_2$N5(0), DPPC/$(12Ser)_2$N5(0), DPPC/$(10Ser)_2$N5(+), DPPC/$(12Ser)_2$N5(+), DPPC/$(14Ser)_2$N5(+) and DPPC/$(12Ser)_2$N10(+).

The structural characteristics of the DPPC bilayers with gemini incorporation were firstly analyzed using the probability density functions, that reflect the vertical positioning of key groups relatively to the membrane center (defined as the central plane between the bilayer leaflets).

Figure 4.8 depicts the density profiles of these groups across the bilayer, namely the positioning of the P and N atoms of the head groups and the terminal methyl groups of DPPC. The nitrogen atom of the gemini head groups and the respective end methyl groups of the gemini tails were also considered. The distribution of the terminal methyl groups of DPPC appear as a single curve, with its maximum at Z=0, indicating a clear overlapping of the terminal part of the leaflets. Additionally, the distributions concerning the nitrogen atom of the gemini surfactants reflect the presence of only one molecule.

On the other hand, the distributions of the SPC water molecules and the polar heads of DPPC, represented by the nitrogen atom, are symmetrical around the center of the z-coordinate, being depicted in both sides of the bilayer.

The profile of key groups pertaining to the single-component DPPC system, shown in Figure 4.8 panel (a), is correlated with the profiles previously reported (Teixeira et al., 2014a). The incorporation of the gemini molecules (Figure 4.8 panels (b) to (g)) introduces some modifications in the bilayer structure. From Figure 4.8 panels (f) and (g) it is seen that the serine-based nonionic molecules are mostly embedded in the hydrophobic region, while cationic molecules (Figure 4.8 panels (b) to (e)) are preferentially positioned close to the interface, as can also be seen in Figure 4.9, in which six representative configurations are presented. The cationic molecules, as a consequence, interact more strongly with the lipid polar heads, displaying a reduced probability of crossing the center of the bilayer. Both $(10Ser)_2N5(+)$ and $(12Ser)_2N5(+)$ cationic surfactants (Figure 4.8 panel (b) and (c), respectively) are, among the six gemini surfactants under study, the ones that interact more strongly with the lipid polar heads, with evidence of establishing hydrogen-bonding. The $(14Ser)_2N5(+)$ and $(12Ser)_2N10(+)$ cationic molecules have a similar behavior, but the strong interaction with the lipid polar heads becomes less pronounced. The more hydrophilic nature and the smaller tail length of the cationic gemini surfactants prevents the terminal methyl groups from reaching the center of the bilayer. In contrast, the terminal methyl groups of the $(14Ser)_2N5(+)$ cationic gemini tails (see panel (d), Figure 4.8) are almost leveled with those of DPPC, reaching the inter-leaflet region.

In Figure 4.8 panel (f), the wide distribution of the gemini terminal methyl groups of the $(12Ser)_2N5(0)$ nonionic surfactant indicates that the mobility of the tails within the membrane is high, with the chains easily switching between the two leaflets. It is also seen that the polar heads are fully embedded in the inter-leaflet region of the DPPC membrane (see Figure 4.9) and are less mobile, as suggested by the MSD profile in Figure 4.10.

The above observations are compatible with the fact that serine-based bis-quats $[(nSer)_2Nm]$ contain hydrogen bonding donor and acceptor groups. A more detailed analysis on the order of the membrane is presented from the estimated order parameter, S_{CD}, for the carbon atoms in DPPC tails. A summary of these S_{CD} values obtained for the DPPC tails is presented in Figure 4.11. A typical membrane profile was obtained for the neat DPPC system. As one moves towards the end of the tails, the high ordering found in the first carbons, close to the interface, gives place to a decreased order, with a minimum degree found in the terminal carbons.

Both $(10Ser)_2N5(0)$ and $(12Ser)_2N5(0)$ nonionic molecules induce an increased organization near the interface. An opposite effect, although weaker, is found close to the bilayer center. All the cationic molecules, with the exception of the longest molecule, $(14Ser)_2N5(+)$, induce a similar disordering effect close to the interface. The strongest effect is observed for the $(12Ser)_2N10(+)$ cationic molecule in comparison to that of $(14Ser)_2N5(+)$. For the internal part of membrane, a stronger action is observed for the $(12Ser)_2N5(+)$, $(12Ser)_2N10(+)$ and $(10Ser)_2N5(+)$ cationic molecules, with emphasis in the former. The $(12Ser)_2N5(+)$ cationic surfactant promotes a larger disorder, with a behavior similar to that of both $(12Ser)_2N10(+)$ and $(10Ser)_2N5(+)$ cationic molecules for the terminal carbon. As stated before, no pronounced effect is found for both the nonionic molecules ($(12Ser)_2N5(0)$ and $(10Ser)_2N5(0)$).

The MSD analysis performed from the simulation trajectories and reported in Figure 4.10 allows observing relevant structural modifications in comparison to the well-ordered DPPC system for only one molecule of surfactant. MSD results are well correlated with the previous analysis. Figure 4.10 clearly shows that the incorporation of $(12Ser)_2N5(+)$ cationic surfactant is responsible for a significant increase in the DPPC lateral diffusion, when compared to its nonionic homologues, and the shortest cationic molecule ($(10Ser)_2N5(+)$). The $(12Ser)_2N5(+)$ cationic molecule is, among the serine-based surfactants under study, the one that promotes the highest lateral diffusion of DPPC molecules. Based on the membrane perturbation MD results, $(12Ser)_2N10(+)$ and $(12Ser)_2N5(+)$ cationic molecules are identified as the most effective and both nonionic, $(12Ser)_2N5(0)$ and $(10Ser)_2N5(0)$, as the least effective permeation enhancers of the study. In general, the MD results corroborate the experimental observations, both in what pertains to the deuterium order parameters and mean-square displacement values. The experimental ER values are in the order $(10Ser)_2N5(0)$, $(12Ser)_2N5(0)$, $(12Ser)_2N10(+)$ and $(12Ser)_2N5(+)$, corresponding to a decrease in order and an increase in displacement. This confirms, in general, both chain length and charge effect.

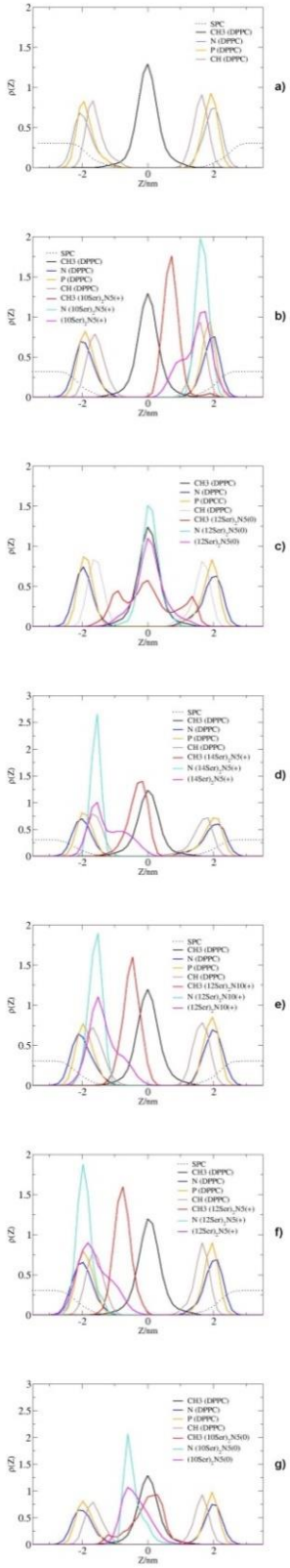

Figure 4.8 Probability density profiles of key atom/groups relative to the Z-axis, extracted from the MD simulations carried out at 50°C for (a) single DPPC, (b) DPPC/(10Ser)2N5(+), (c) DPPC/(12Ser)2N5(+), (d) DPPC/(14Ser)2N5(+), (e) DPPC/(12Ser)2N10(+), (f) DPPC/(10Ser)2N5(0) and (g) DPPC/(12Ser)2N5(0) systems. SPC water groups (··), DPPC groups - ammonium nitrogen (dark blue), and end methyl groups of tail chains (black); gemini groups – ammonium nitrogen atoms (blue) and terminal methyl groups of both tails (red). The Z-coordinate represents the normal to the bilayer plane.

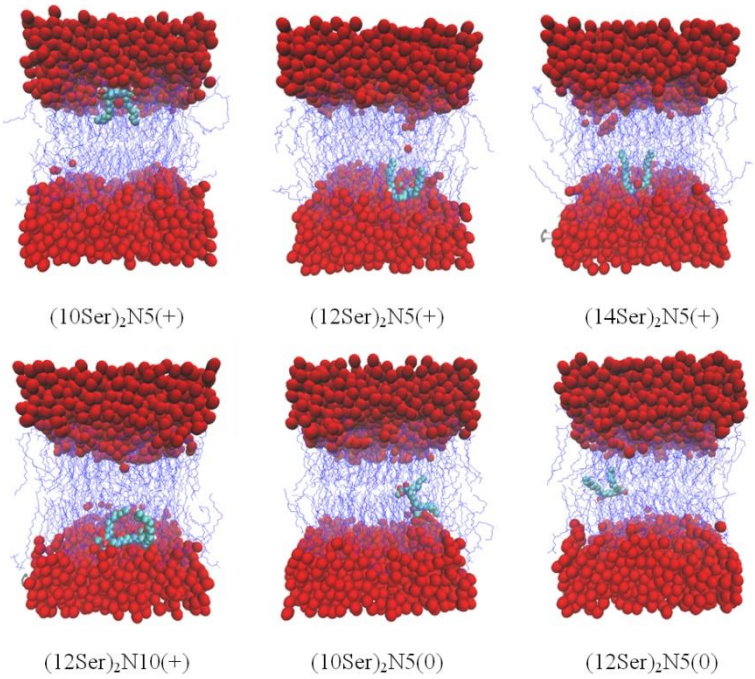

Figure 4.9 Snapshots of the typical positioning of serine-based molecules embedded in the bilayer. Water, surfactant molecules and DPPC are represented in red, cyan and blue, respectively.

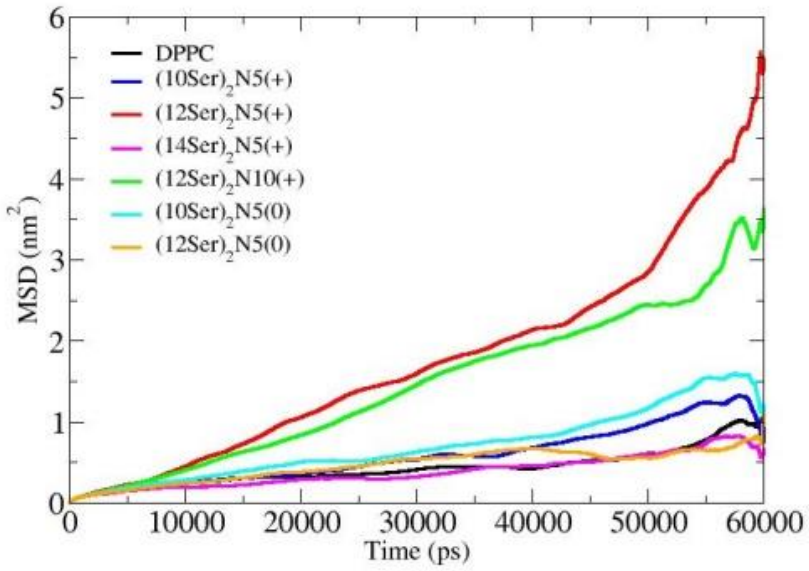

Figure 4.10 Mean square displacement of DPPC molecules, calculated from the MD simulations for the DPPC/serine-based systems.

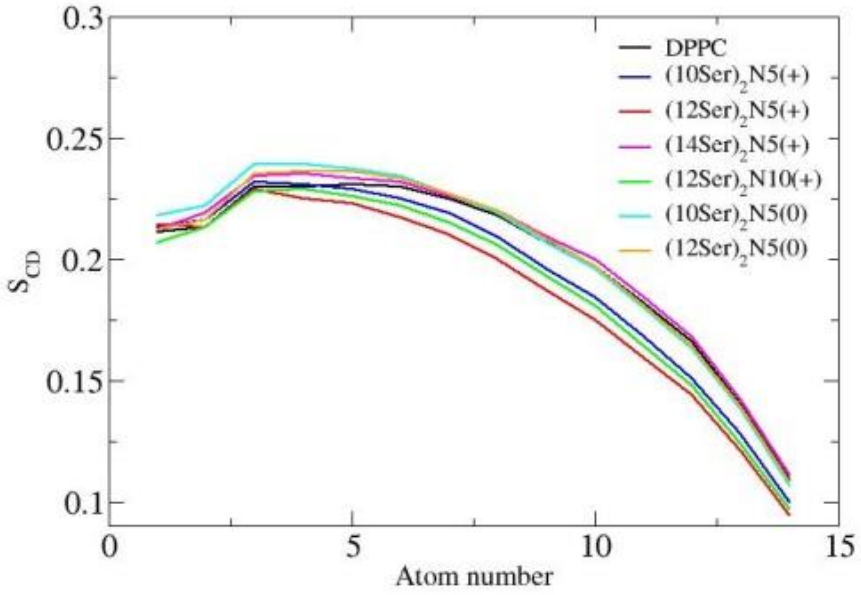

Figure 4.11 Deuterium order parameter, SCD, estimated from the MD simulations, along the bilayer depth for DPPC chains, averaged over sn-1 and sn-2 chains, in the presence of the serine-based surfactants.

Radial distribution function analyses of SPC water molecules around the polar heads of both DPPC and gemini surfactants, displayed in

Figure 4.12, were also used to inspect changes in the hydration level. In what concerns the polar heads of DPPC, represented by the ammonium groups,

Figure 4.12 panel (a), it is observed that the presence of the gemini surfactants promotes a decrease in the amount of water accessible. However, no significant differences were found in terms of hydration of the ammonium groups of DPPC in the presence of the different gemini structures. On the other hand, for the gemini polar heads, also represented by the ammonium groups,

Figure 4.12 panel (b), the same analysis indicates an increased solvation of the cationic surfactants, with a pronounced effect for the $(12Ser)_2N5(+)$ molecule.

Figure 4.13 presents the rdfs of SPC water molecules relative to the (i) carbonyl atoms of DPPC chains (Figure 4.13 panel (a)) and surfactants polar heads (Figure 4.13 panel (b)), (ii) carbonyl-ester (Figure 4.13 panel (c)) and (iii) hydroxyl atoms (Figure 4.13 panel (d)) for both cationic and nonionic surfactants polar heads. The profiles displayed in Figure 4.13 panel (a) indicate more accessible water in the presence of the $(12Ser)_2N5(+)$

cationic molecule, while no significant differences were found in terms of the hydration of the carbonyl atoms of DPPC tails in the presence the remaining structures, corresponding to the upper part of the hydrophobic region. Panel (b) of Figure 4.13 shows an increase in the amount of water in the proximity of the cationic molecules. The absence of water near the nonionic molecules is a common pattern in Figure 4.13 panels (b), (c) and (d). Such behavior is compatible with the membrane perturbation analysis: nonionic molecules are fully embedded in the inter-leaflet region of the DPPC membrane. From these profiles it is also seen that the longer spacer cationic surfactant $(12Ser)_2N10(+)$ induces some decrease of the respective solvation. In addition to the charge effect, the gemini tail length is relatively important in this regard, with the shorter tail cationic surfactant $(10Ser)_2N5(+)$ promoting a more pronounced hydration effect.

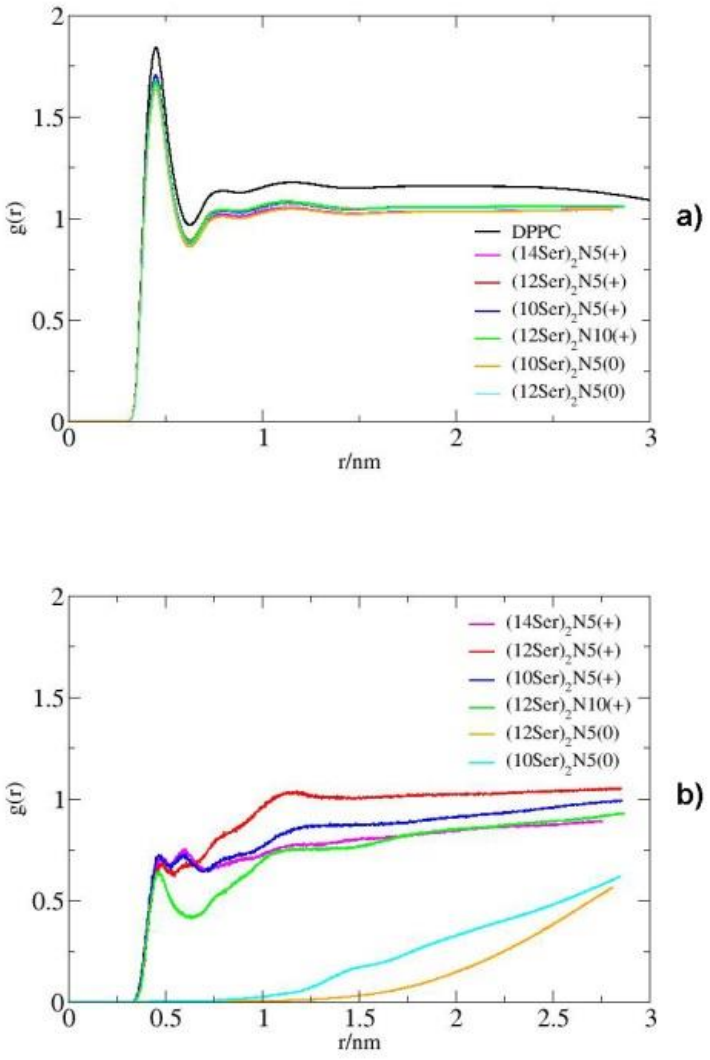

Figure 4.12 Radial distribution function of water molecules relative to the DPPC (panel (a)) and gemini (panel(b)) ammonium groups, calculated from the MD simulations carried out at 50°C.

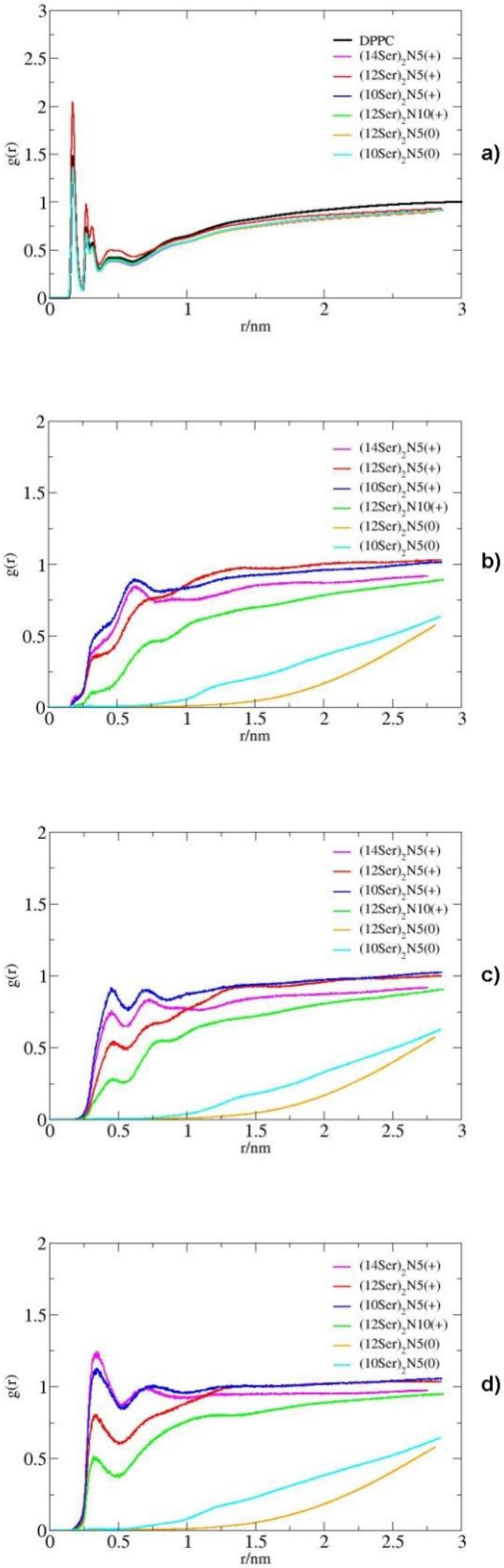

Figure 4.13 Radial distribution functions of water molecules around the carbonyl atoms for the sn1 and sn2 chains of (a) DPPC and the polar heads for (b) both cationic and nonionic molecules, and (c) carbonyl-ester and (d) hydroxyl atoms for the polar heads of the serine-based gemini surfactants.

4.3.4. Cytotoxicity studies

The cytotoxicity profiles of each serine based-surfactant were determined in HEK (Figure 4.14).

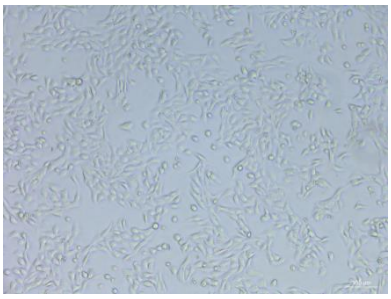

Figure 4.14 Pictures of cultured HEK 10x, seeded at 10.000 cells/well in appropriate culture medium, prior to the start of the Alamar Blue assay.

A calibration curve was performed based on the absorbance readings of standards plots of HEK (R^2 = 0.975) with 0, 10.000, 20.000, 40.000, 60.000 cells per well, in order to ensure the linearity of the Alamar Blue assay method used. The results obtained in the Alamar assay are displayed in Figure 4.15.

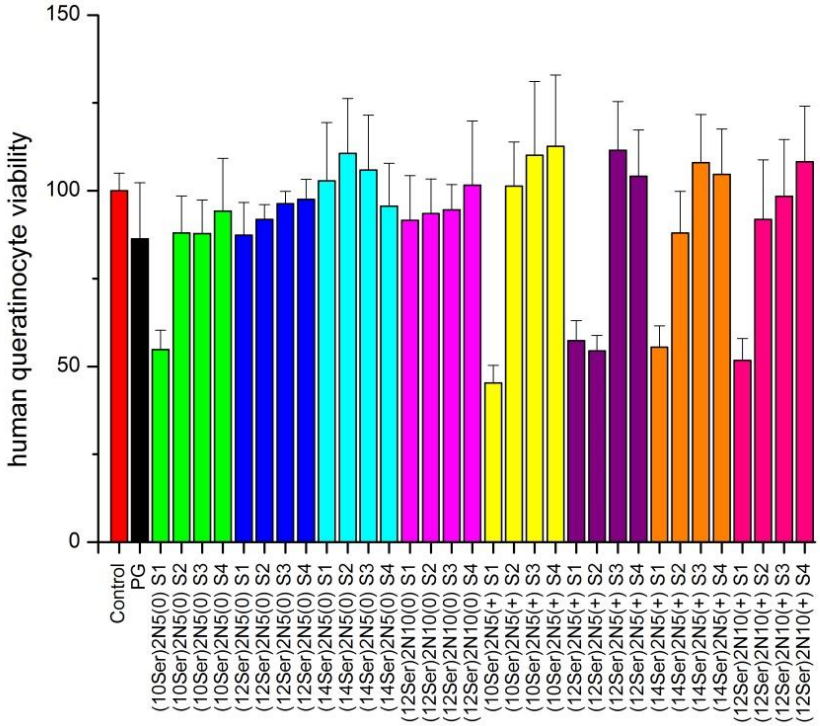

Figure 4.15 Alamar Blue assay results for nonionic and cationic serine-based surfactant. The bars represent the cell viability (%) for each permeation modifier and concentration tested. The error bars represent the standard deviation (n=6).

The cytotoxicity assay revealed that, in the range of concentrations studied, generally nonionic compounds are less toxic than the cationic ones and the PG exposure resulted in a slight reduction in HEK viability, yet not statistically different from the control. Nonionic surfactants tested did not cause a significant reduction in HEK viability, when compared to the control, except for (10Ser)2N5(0) (S1). When this compound was applied to the cells, it was observed that approximately 50 % cell death occurred.

The results for cationic serine-based surfactants are slightly different from those obtained with the nonionic counterparts. The exposure of HEK to higher concentrations of $(10Ser)_2N5(+)$, $(12Ser)_2N5(+)$, $(14Ser)_2N5(+)$ and $(12Ser)_2N10(+)$ (S1) caused approximately 50% cell death. However, the presence of a concentration not higher than 16 µM (S2) of any CPE did not have a negative effect in the HEK viability, except for $(12Ser)_2N5(+)$ (S2). In this case cell viability was reduced in approximately 50 % when HEK were exposed to a concentration of 16 µM (S2).

A global analysis of the Alamar assay results obtained with HEK suggests that the cytotoxicity of the serine-based gemini surfactants studied is dependent on the charge of the compounds, since HEK showed a higher tolerance to the nonionic compounds. In fact, $(10Ser)_2N5(0)$, $(12Ser)_2N5(0)$, $(14Ser)_2N5(0)$ and $(12Ser)_2N10(0)$ were found to be less toxic to HEK when compared to $(10Ser)_2N5(+)$, $(12Ser)_2N5(+)$, $(14Ser)_2N5(+)$ and $(12Ser)_2N10(+)$.

4.4. Conclusions

This work presents a systematic study on the use of a series of serine-based gemini surfactants as permeation enhancers for drugs from the same therapeutic group, with different ionization state and hydrophobicity. The two classes of serine-based molecules, nonionic and cationic, possess different alkyl chain length, comprising 10, 12, 14 or 16 carbon atoms. It was observed that the most effective CPE for both drugs were cationic, with longer alkyl chains. The highest permeation of ropivacaine was achieved when the cationic surfactant with the longest alkyl chain $(14Ser)_2N5(+)$ was employed (ER = 3). Interestingly, in the case of tetracaine, the cationic surfactant with the longest alkyl chain $(14Ser)_2N5(+)$ (ER=1.9) was also the most effective CPE followed by $(12Ser)_2N_5(+)$ (ER= 1.4). These results suggest that serine-based surfactants are suitable, safe and promising candidates to increase drug transport across the skin, especially for

hydrophilic/ionized drugs. Molecular dynamics simulations provided results in accordance with the experimental observations.

Chapter 5

Novel vesicular liposomes systems containing aminoacid-based surfactants for topical administration of tetracaine and ropivacaine

This Chapter addresses a study that, again, aims the improvement of a formulation containing tetracaine and ropivacaine, for topical administration, now using liposomes, prepared with aminoacid-based surfactants (previously reported in Chapter 3 and in Chapter 4). Liposomes were prepared following thin layer evaporation method and were characterized regarding its size, zeta potential and encapsulation efficiency. A conventional liposomal formulation was prepared with L-α-phosphatidylcholine, cholesterol and both drugs, following the same methodology and was used as the control. *In vitro* permeation studies were performed in Franz diffusion cells to assess the efficacy of liposomal formulations prepared with aminoacid-based surfactants on drug permeation.

5.1. Introduction

One of the most important requirements for the intrinsic anesthetic potency of a drug is its lipid solubility. The duration of anesthetic effectiveness is related to the extent of the protein binding that are located within lipids of the cell membrane (Alster, 2013). Tetracaine is considerably more lipophilic and intrinsically more potent than ropivacaine due to the binding of the latter to a butyl group and the aromatic group. In order to increase the onset of action of both drugs, especially ropivacaine, liposomes were the selected strategy.

Liposomes are concentric vesicles in which an aqueous volume is entirely enclosed by a lipid bilayer (Barenholz, 2001; Meisner and Mezei, 1995) (Figure 5.1). Liposomes are able to encapsulate hydrophilic drugs in their aqueous compartment, while lipophilic drugs are encapsulated in their lipid bilayer and retained until their destination. The accommodation of lipophilic compounds in the lipid phase can be problematic as some drugs may interfere with bilayer formation and stability, limiting the range and amount of drugs that can be formulated with liposomes (Gillet et al., 2009; McCormack and Gregoriadis, 1998).

Liposomal formulations are commonly used in the pharmaceutical field as drug delivery systems namely for oral and parenteral routes, due to their versatility and clinical efficacy (Maestrelli et al., 2006). Liposomes have been intensively studied as carriers for dermal and transdermal administration of drugs and skin care products since it is a non-invasive alternative to the oral route (Maestrelli et al., 2006). Liposomes act as penetration enhancers for the active ingredient into the skin. Liposomes can improve drug deposition within the skin at the site of action, providing a local effect with little or negligible systemic activity, desirable in the case of local anesthetics minimizing the occurrence of side effects (Manosroi et al., 2004). Liposomes can also provide targeted delivery to skin appendages in addition to their potential in transdermal delivery (Glavas-Dodov et al., 2002; Maghraby et al., 2006). Compared to conventional formulations, drugs encapsulated in liposomes generally exhibit improved efficacy and less negative effects than conventional topical formulations such as ointments, creams or lotions (Honzak et al., 2000b; Reimer et al., 1997).

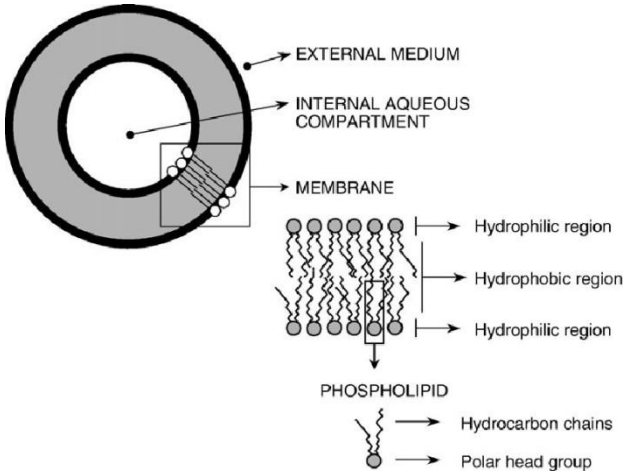

Figure 5.1 Schematic representation of a liposome. Adapted from (Lopes et al., 2013).

Despite some controversy in the literature about possible vehicle-mediated phenomena of skin uptake, the majority of authors agree that liposomes contribute to an effective drug penetration and enhance clinical efficacy, due to the similarity with a biological membrane. Moreover, liposomes are similar to the epidermis in terms of lipid composition, reason why liposomes are able to permeate into the epidermal barrier to a greater extent than other dosage forms (Verma et al., 2003a, b).

The biggest challenge of topically applied drugs is that, in order to be effective, drugs must reach the site of action above the therapeutic concentration, for a certain period of time (Schmid and Korting, 1996). Another issue arises from the fact that some lipids of the liposomes may penetrate into the *stratum corneum* cause a modification on the its structure and altering its barrier properties (Weiner et al., 1994).

Some classical liposomes have little interest as carriers for transdermal drug delivery as they do not penetrate into the deeper layers of the skin, but instead remain confined to its upper layers (Elsayed et al., 2007). Intensive research led to the introduction and development of a new class of lipid vesicles capable of reaching deeper layers of the skin, highly deformable (elastic or ultraflexible) liposomes, known as Transfersomes® (Cevc and Blume, 1992).

These elastic and ultraflexible vesicles comprise a phospholipid (e.g. phosphatidylcholine) as its main component, and 10 to 24 weight percent of a surfactant. The flexibility of the liposome is given by the high radius of curvature of the surfactant that acts as an 'edge activator'. Some data on the literature, has shown that these vehicles are able to squeeze through a pore of approximately 20 nm diameter (Cevc, 2002). The ‘edge activator’ present in the formulation has the ability to accumulate at the

high stress sites of the vesicles forming a highly curved area which will eventually move through narrow skin pores to a more hydrophilic environment of the deeper layers of the skin. There is still some controversy about the mechanisms involving skin penetration of ultra-deformable or highly flexible liposomes, however some workers have shown that these vesicles can clearly improve the delivery of therapeutic agents to and across the skin (Jianxin Guo, 2000; Maghraby et al., 2001a, b; van den Bergh et al., 2001). Cevc and his co-workers claimed that these vesicles can penetrate intact into the deeper skin and even to systemic circulation (Cevc et al., 1997; Cevc et al., 1996; Cevc et al., 1998).

This Chapter reports the evaluation of the efficacy of liposomal formulations prepared with different aminoacid-based surfactants previously selected in Chapter 3 and 4. The mentioned formulations are referred in this Chapter as LPS-LP $(14Ser)_2N5$; LPS-LP 10Lys10(0) and LPS-LP 16Lys16(0). A conventional liposomal formulation referred as LPS-LP was prepared with phosphatidylcholine, cholesterol, tetracaine and ropivacaine and was used as the control. The liposomal formulations were characterized regarding solubility, size, zeta potential, stability and encapsulation efficiency. *In vitro* studies conducted in Franz Cells were performed in order to investigate the effect of the combination of the aminoacid-based surfactant and conventional liposomes on tetracaine and ropivacaine delivery across porcine skin.

5.2. Experimental section

5.2.1. Materials

TC, ammonium acetate, L-α-phosphatidylcholine (PC), chloroform and CHO were purchased from Sigma Aldrich (Saint Louis, MO, USA). RPC was a kind gift of AstraZeneca (London, United Kingdom) and HPMC K15 M was a kind gift from Dow Chemical Company (Midland, MI, USA). HP-*β*-CD with 97% of purity, with an average degree of substitution of 2 to 6 units of 2-hydroxypropyl (C_3H_7O) per glucose unit, and with an average molecular weight of 1380 g/mol, was purchased from Acros Organic (Geel, Belgium). MeOH and ACN HPLC grade were purchased from LiChroSolv Merck (Darmstadt, Germany). Deionized water was purified (Millipore®) and filtered through a 0.22 µm nylon filter before use. PBS was purchased from TIC Gums (Belcamp, MD, USA). Newborn pig skin (3 weeks, ~5 Kg) was purchased from a local slaughter (Condeixa-a-Nova, Portugal) and was used as skin model. Nonionic lysine (10Lys10; 16Lys16) and cationic serine-based gemini surfactants ($(14Ser)_2N5$) were synthesized

and purified according to a standard method at the Department of Chemistry, Porto University (Porto, Portugal) (for details see Chapter 3 and 4) (Goreti Silva et al., 2012; Silva et al., 2013b). All other chemicals were used as received.

5.2.2. Liposome composition and preparation

Liposomes containing PC, CHO, lysine (10Lys10; 16Lys16) and serine-based surfactant ($(14Ser)_2N5$) were prepared following the TLE method (Bangham et al., 1965). The lipids were dissolved in a small quantity of chloroform which was subsequently removed under vacuum using a Buchi - Rotavapor R-210 with a vaccum pump V-700 and a vaccum controller V-850. The temperature was set at 55 ºC using a Buchi Heating Bath B-491 (Figure 5.2). 20 % of $(14Ser)_2N5$, 10Lys10 and 16Lys16 were added to the lipid phase. Evaporation continued for 2 h to ensure complete solvent removal. After the dry lipid appeared on the flask wall, drug-loaded liposomes composed of 2.5 % (w/w) of TC and RPC were prepared following two different methodologies. In the first method (LPS-LP), TC was directly dissolved in the lipophilic phase, and the hydrophilic phase constituted by water and RPC was subsequently added. In the second method (LPS-AP), the aqueous phase constituted by water, TC, HP-*β*-CD and RPC was used to hydrate the lipid phase (PC and CHO). An alternative liposomal formulation without the aminoacids-based surfactants was prepared and used as control (LPS-LP).

Figure 5.2 Buchi - Rotavapor R-210 with a vaccum pump V-700 and a vaccum controller V-850.

After adding the hydrophilic phase, the suspension was alternately shaken using a vortex mixer and sonicated using a bath sonicator, (Clifton Ultrasonic Bath, London, United Kingdom) at 55 ºC during 30 min to allow vesicle formation. In order to obtain a homogeneous size distribution, the liposomes suspension was extruded through a 100 nm polycarbonate membrane using a LipoFast extrusor Avestin® (Mannheim, Germany). To obtain viscosity values adequate for dermal application, a 1% (w/w) hydrogel of 15 M

HPMC was prepared and left to hydrate at lower speed (50 rpm), during 24 h, to ensure complete homogenization.

5.2.3. Liposome characterization

5.2.3.1. Solubility studies and HPLC quantification

The solubility of TC and RPC was determined for the conventional liposomes and for the liposomes containing $(14Ser)_2N5$, 10Lys10 and 16Lys16. In brief, an excess of each drug was added to the different vesicles prepared as mentioned in section 5.2.2. The samples were subsequently centrifuged for 60 min at 13229 rpm in a Minispin® (Eppendorf Ibérica S.L., Madrid, Spain). A small portion of the suspension was diluted with mobile phase and quantified. Drug quantification was carried out in a Shimadzu UFLC with SPD-M20A UV/visible dual wavelength detector. The quantification was carried out at 25 °C using a reverse-phase C_{18} column 250 x 4.6mm C18 (2) 100 A Luna 5 μm, Phenomenex® (Torrance, CA, USA) with a guard column as the stationary phase. The mobile phase was prepared with methanol, acetonitrile and ammonium acetate solution on the proportions 7:7:6 respectively, filtered using a 0.45 μm Nylon membrane (Supelco Analytical, Bellefonte, USA) and sonicated during 1 h prior use. Samples of 25 μL were injected at a constant flow rate of 1.0 mL/min. Tetracaine was detected at 311 nm with a retention time of ca. 6.9 minutes. Ropivacaine was detected at 210 nm and the retention time was ca. 9.1 minutes. Both methods showed a linear response in the 0.01-500 mg/mL with a daily RSD < ± 6.0%.

5.2.3.2. Particle size analysis

Liposome size distribution was measured by DLS that provides the mean particle size (Z-average), and the PI. Measurements were performed in a Delsa Nano C Submicron (Beckman Coulter, Krefeld, Germany) apparatus, at 25 °C, with a fixed angle of 160°.Sizes are expressed as average values of the liposomal hydrodynamic diameter. To avoid multi-scattering phenomena, liposome suspensions were diluted with ultrapurified water. Samples were analyzed 24 h after preparation. The PI is a measure of a unimodal size distribution. A value of PI < 0.1 indicates the existence of a homogenous population, while a PI > 0.3 indicates a higher heterogeneity. Results are presented as mean ± SD, extracted from the cumulate algorithm (Goll and Stock; Kaszuba et al., 2008).

5.2.3.3. Zeta Potencial

Zeta potential of diluted liposomal dispersions was determined from electrophoretic mobility measurements using a Delsa Nano C Submicron (Beckman Coulter, Krefeld, Germany) at 25 °C. The Zeta Potential was calculated using the Helmholtz–Smoluchowsky equation (Lyklema and Overbeek, 1961).

5.2.3.4. Liposome encapsulation efficiency

Liposome encapsulation efficiency is defined as the ratio between the masses of original drug added to solution and the drug encapsulated in the liposome formulation, and was determined indirectly. The ultrafiltration-centrifugation method was carried out across centrifugal filters (Amicon® Ultra-4, Millipore, Germany) with a 100 kDa molecular weight cut-off. The samples were centrifuged during 60 min at 13229 rpm using a Minispin® (Eppendorf Ibérica S.L., Madrid, Spain). Non-entrapped drug obtained from the supernatant solution was quantified by HPLC. The encapsulation efficiency (EE %) was calculated according to the equation (5.1),

$$EE\% = \frac{[Qt-Qs]}{[Qt]} \times 100 \qquad (5.1)$$

where the *Qt* is the theoretical amount of each drug that was initially added to the system and *Qs* is the amount of each drug detected in the supernatant.

5.2.4. *In vitro* permeation studies

The *in vitro* permeation studies were carried out in vertical Franz diffusion cells (PermeGear, Inc., PA, USA), with an average volume of 5.1 cm^3 and an average surface area of 0.64 cm^2. Prior to the experiments, skin samples (prepared as mentioned in section 5.2.4.1.) were submerged in PBS (pH=7.4) during 1 h for equilibration and placed between the donor and receptor compartments, with the epidermal side up. The receiver chamber was filled with PBS with 1 % of CD to ensure sink conditions. Each chamber jacket was maintained at 37 ºC ± 0.1 and kept stirring at 600 rpm during the permeation experiments. 0.5 mL of drug-loaded liposome in hydrogels optimized as mentioned in section 5.2.3, were placed in each donor compartment and immediately covered with Parafilm® to prevent evaporation. At predetermined time points (0, 2, 4, 6, 8, 18, 20, 22 and 24 h) 300 μL samples were collected from the receptor compartment and

immediately replaced with the same amount of PBS solution. Samples were kept in the refrigerator prior to HPLC analysis.

5.2.4.1. Porcine skin preparation

Newborn porcine skin tissue used as skin model, was excised and dermatomed with 700 µm of thickness using a Padgett® Model B Electric Dermatome (Integra LifeSciences, Plainsboro, NJ) and frozen at -20ºC. Prior to the experiments, the frozen skin samples were thawed at room temperature, immersed in PBS (pH=7.4) for 1 h, for equilibration.

5.2.4.2. Data analysis in the permeation studies

The cumulative drug amount present in the receptor compartment solution after 24 h (Q_{24}) and expressed in µg/cm^2 was calculated as before. Flux and enhancing ratio also followed the procedures described in previous Chapters 3 and 4.

Results are presented as mean ± standard deviation (*n*), where *n* is the number of replicates.

5.2.4.3. Statistical analysis

Differences between flux values were examined for significance using unpaired Student's *t*-test. The *p* value was set to 0.05, with $p < 0.05$ indicating statistical significance in the differences between control and enhancers tested. This analysis was performed using Origin® graphing and analysis (OriginLab Corp, Northampton, USA).

5.2.5. Stability studies

Particle size, zeta potential values and entrapment efficiency were monitored during a period of 6 months to evaluate the stability of the formulation LPS-LP 16Lys16(0).

5.3. Results and Discussion

Preliminary solubility studies were performed to select the best method to prepare the liposomes. The formulations were optimized according to size, zeta potential and encapsulation efficiency described below.

5.3.1. Solubility studies

The choice of PC and CHO was based on previous data available in the literature (McCormack and Gregoriadis, 1994a, b, 1998). PC is considered a skin permeation enhancer, whose effects are attributed to an intercalation into the structured lipids of the SC and disturbance of the lipid packing (Williams and Barry, 2012). The solubility of the drugs in different vesicles is presented in Table 5-1.

Table 5-1. Solubility of both drugs in different liposomal formulations. Data are expressed as mean ± SD, n=3.

Formulation	Tetracaine solubility (mg/mL)	Ropivacaine solubility (mg/mL)
LPS-LP	24.6 ± 1.7	3.8 ± 0.2
LPS-AP	21.3 ± 1.6	1.4 ± 0.1
LPS-LP (14Ser)2N5	20.7 ± 2.3	4.1 ± 0.3
LPS-LP 10Lys10(0)	20.3 ± 1.4	3.5 ± 0.2
LPS-LP 16Lys16(0)	24.6 ± 1.6	5.8 ± 0.5

According to the results presented in Table 5-1, the method LPS-LP, where TC was directly dissolved in the lipophilic phase and the RPC in the hydrophilic phase, was selected because it provided maximal solubility for both drugs. The liposomes prepared with aminoacid-based surfactant, namely lysine-based surfactant 16Lys16(0), showed higher solubility particularly in the case of RPC. The solubility of the drugs in the lipid phase is known to be an important condition to obtain a satisfactory encapsulation efficiency (Jannin et al., 2008). Based on these results, the concentration of lipid phase was adjusted to obtain the maximal solubility for both drugs.

5.3.2. Liposomes characterization

Encapsulation efficiency, size and zeta potential of liposomes with different lipid composition were determined. The influence of the liposomes preparation methods was also evaluated. The results are presented in Table 5-2.

Table 5-2 Mean particle size (PS), average polydispersitivity index (PI), zeta potential (Zeta) and encapsulation efficiency (EE). Samples identified with an LPS-LP were prepared by directly dissolving the drug in the lipid phase. LPS-AP refer to samples in which TC-CD complexes were pre-dissolved in the aqueous solution used to hydrate the lipid film.

Formulation	Molar Ratio	PS (nm)	PI	Zeta Potential (mV)	EE/% TC	EE/% RPC
LPS-LP	70:30	201.3 ± 2.8	0.184	33.99 ± 0.31	56.1 ± 0.3	64.2 ± 0.1
LPS-AP	70:30	205.5 ± 5.3	0.192	49.31 ± 0.16	61.3 ± 0.2	43.1 ± 0.3
LPS-LP	60:40	178.6 ± 1.9	0.170	63.33 ± 0.21	59.6 ± 0.3	67.4 ± 0.4
LPS-AP	60:40	206.5 ± 1.0	0.203	64.13 ± 0.28	74.2 ± 0.2	63.0 ± 0.1
LPS-LP	50:50	174.4 ± 2.0	0,175	31.47 ± 0.18	47.6 ± 0.4	64.3 ± 0.2
LPS-AP	50:50	210.9 ± 2.6	0.265	45.12 ± 0.24	62.7 ± 0.5	42.4 ± 0.2
LPS-LP $(14Ser)_2N5(+)$	60:30:10	149.8 ± 1.2	0.137	33.16 ± 0.39	65.1 ± 0.2	61.4 ± 0.3
LPS-LP 10Lys10(0)	60:30:10	176.0 ± 3.7	0.145	30.43 ± 0.38	66.7 ± 0.3	62.3 ± 0.1
LPS-LP 16Lys16(0)	60:30:10	151.6 ± 1.8	0.124	32.66 ± 0.17	75.3 ± 0.4	73.1 ± 0.1

All liposomal formulations showed a satisfactory PI (below 0.3), which indicates reasonable size homogeneity of the liposomes. The mean diameter of the various liposomal suspensions ranged from 150 to 210 nm. The average zeta potential stayed within the stability limits (> 30 mV) in all formulations. According to the results, the increase the amount of L-α-phosphatidylcholine in the liposomes (LPS-LP) caused an increase in the mean particle size and in the polydispersitivity index. In contrast, the entrapment efficiency did not vary significantly. 60PC:40CHO formulations showed the highest absolute value of the zeta potential indicating an excellent stability (> 60 mV).

Results obtained showed that the most efficient encapsulation and smallest particle size were achieved when TC was directly dissolved in the lipophilic phase and RPC in the aqueous phase (LPS-LP). The formulation (60mol PC: 40mol CHO: 10mol 16Lys16(0)) showed to be a promising formulation for drug delivery, since it combines a good stability with a good EE %. This formulation was selected to proceed in the *in vivo* studies (Chapter 6) and its stability was evaluated for a period of 6 months

5.3.3. In vitro permeation studies

5.3.3.1. Percutaneous drug delivery of tetracaine

The focus of this Chapter was the evaluation of the permeation of TC and RPC from the liposomal formulations. Prior to the *in vitro* permeation studies, formulations were previously optimized, as described in section 5.3.2. The formulations selected were applied to the epidermal side of dermatomed porcine skin placed between the donor and receptor compartments of Franz diffusion cells. The results obtained are presented in Table 5-3, and the permeation profiles shown in Figure 5.3.

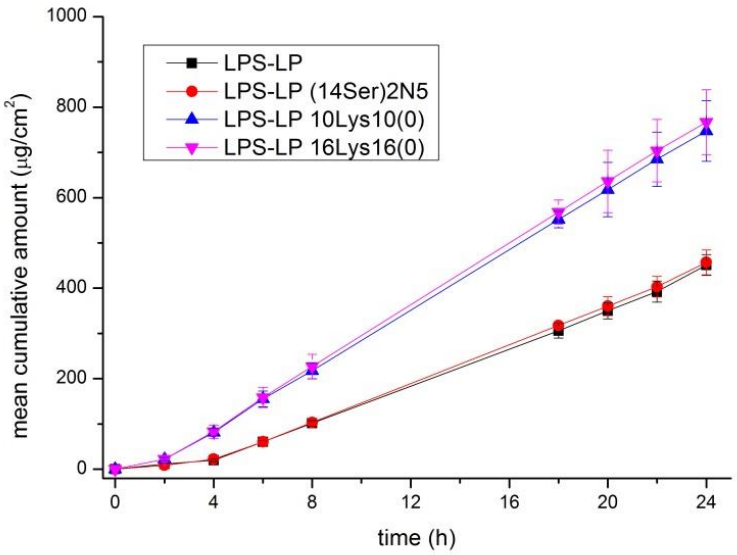

Figure 5.3 Cumulative amount of tetracaine permeated across porcine skin as a function of time.

The liposomes prepared with lysine-based surfactant caused a significant increase ($p < 0.05$) on tetracaine permeation when compared to control. The surfactant with longer alkyl chain (16Lys16(0)) was the most effective permeation enhancer, resulting in higher flux (34 µg/cm^{-2}/h, control 29 µg/cm^{-2}/h), a higher value of Q_{24} (767 µg/cm^{-2}, control 451 µg/cm^{-2}) and a significantly lower lag time (1.4 h, control 4.4 h). In contrast, the liposomes prepared with serine-based surfactant determined a slight reduction in the permeation flux (26 µg/cm^{-2}/h) and lag time of 3.7 h.

Table 5-3 Tetracaine percutaneous permeation from liposome formulations across porcine skin. Data are presented as means ± S.D. (4≤N≤6).

Liposomal formulation	Flux / µg cm^{-2} h^{-1}	Q_{24} / µg cm^{-2}	Lag Time / h^{-1}	ER
Control	29.09 ± 1.39	451 ± 23	4.41 ± 0.21	
LPS-LP $(14Ser)_2N5$	26.06 ± 2.43	457 ± 27	3.74 ± 0.17	0.90
LPS-LP 10Lys10(0)	32.80* ± 2.88	747* ± 66	1.94* ± 0.24	1.14
LPS-LP 16Lys16(0)	33.71* ± 2.82	767* ± 71	1.41* ± 0.34	1.16

** Statistically significant difference between Control and liposomes, at p < 0.05 (Student's t-test)*

5.3.3.2. Percutaneous delivery of ropivacaine

The results obtained with ropivacaine are presented in Table 5-4 and the permeation profiles shown in Figure 5.4.

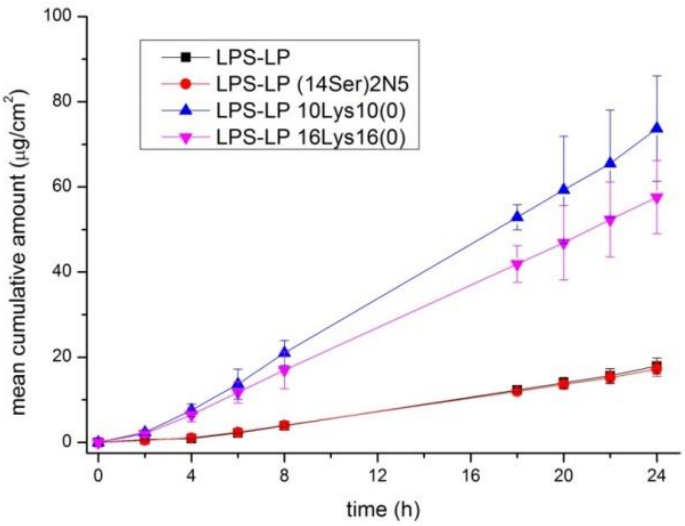

Figure 5.4 Cumulative amount of ropivacaine permeated across porcine skin as a function of time.

Similarly with the previous results, obtained with TC, the liposomal formulations prepared with lysine-based surfactant with longer alkyl chain 16Lys16(0) showed a higher flux 3 µg/cm^{-2}/h (1.4-fold higher than control). The value of Q_{24} obtained (76 µg/cm^{-2}) was also significantly higher than the control (18 µg/cm^{-2}). The lag time was significantly reduced to 1.2 h (control 4.1 h). Liposome formulation containing serine-based surfactant (LPS-LP(14Ser)2N5) exhibited a permeation profile very similar to the control.

It is worthy of note that the incorporation of the lysine-based surfactants in the liposomal formulation clearly determined an increase in the flux of ropivacaine, however, the

absolute values of permeation attained are generally small. This result is due to the hydrophilic nature of the drug. In this case, it is seen that the composition of the liposomes strongly influences the permeation of RPC. Clearly, the liposomes containing lysine-based surfactants resulted in higher values of permeation.

Table 5-4 Ropivacaine percutaneous permeation from liposome formulations across porcine skin liposome on percutaneous permeation of tetracaine across porcine skin. Data are presented as means ± S.D. (4≤N≤6).

Liposome formulation	Flux / μg cm^{-2} h^{-1}	Q_{24} / μg cm^{-2}	Lag Time / h^{-1}	ER
Control	1.40 ± 0.12	17.95 ± 1.84	4.12 ± 0.17	
LPS-LP (14Ser)2N5	1.23 ± 0.14	17.25 ± 1.72	3.45 ± 0.25	0.90
LPS-LP 10Lys10(0)	2.61 ± 0.34	59.58 ± 8.6	1.18 ± 0.12	2.12
LPS-LP 16Lys16(0)	2.97* ± 0.35	75.72* ± 12.36	1.23 ± 0.30	2.14

** Statistically significant difference between control and liposomes, at p < 0.05 (Student's t-test)*

5.3.3.3. Overview and comparison

In this Chapter, the incorporation of a chemical permeation enhancer in a conventional liposome formulation (previously optimized in section 5.3.1. and 5.3.2.) was thoroughly investigated. Generally, the incorporation of lysine-based surfactant promoted higher fluxes of tetracaine and ropivacaine when compared to the liposomal formulations containing serine-based surfactant. The synergistic effect of lysine-based surfactants has already been addressed in this thesis (Chapter 3). The permeation of both drugs significantly increased when the lysine-based surfactant with higher alkyl chain were employed, yielding a flux enhancement for TC and RPC (1.16 and 2.14-fold) compared to the formulation considered as control, followed by (LPS-LP 10Lys10(0)) with a ER of 1.14 and 2.12 for TC and RPC respectively (Table 5-3 and Table 5-4).

According to findings addressed in Chapter 4, serine-based surfactant with longer alkyl chain ($(14Ser)_2N5$) led to an increase in the tetracaine permeation. This was the reason why the ($(14Ser)_2N5$) was selected for this study. However, when the latter was incorporated in the liposome formulation the differences on the flux observed was negligible. This behavior is probably related to the limited solubility of the ($(14Ser)_2N5$).

Focusing now on the differential behavior of the co-encapsulated drugs, the slower permeation observed with tetracaine can be attributed to a difference in the solubility of the drugs in the lipid phase. Additionally, the lag time for TC and RPC was reduced when lysine-based surfactant was incorporated in the liposomes but no significant difference

was found when (14Ser)2N5 was used. These results are quite relevant, particularly with of local anesthetics, where the onset of the therapeutic response depends on short lag times.

5.3.4. Stability studies

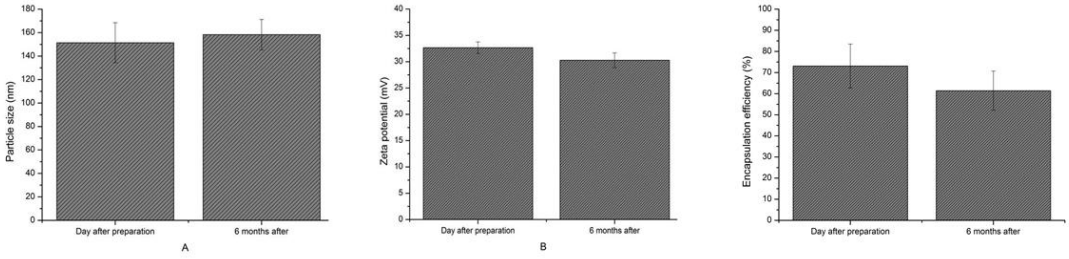

Figure 5.5 Particle size, zeta potential and efficiency encapsulation of optimized formulation (LPS-AP 60:30:10 16Lys16(0)) after preparation and after six months (n=3) results are presented as means ± S.D.

The results presented refer to the physicochemical stability of the formulation with better permeation profile (LPS-AP 16Lys16(0)). Data showed that the size, zeta potential and encapsulation efficiency of the liposomes was not significantly influenced during a period of 6 months (Figure 5.5).

5.4. Conclusions

This study shows that liposomal formulations were able to efficiently deliver tetracaine and ropivacaine. The highest encapsulation efficiency and smallest particle size were achieved when TC was directly dissolved in the lipophilic phase and RPC in the hydrophilic phase (LPS-LP). The combination of liposomes (L-α-phosphatidylcholine, cholesterol) with lysine-based surfactant with the longer alkyl chain LPS-LP 16Lys16(0) resulted in the highest permeation, with a marked synergistic effect. These results suggest that these liposome formulations are promising and versatile vehicles for the concomitant dermal delivery of tetracaine and ropivacaine.

Chapter 6

In vivo studies using *tail-flick* analgesic test

This Chapter describes the *in vivo* pharmacodynamic studies of TC and RPC loaded hydrogels and liposomal formulations previously optimized (Chapters 3, 4 and 5). The goal was the evaluation of the performance of the above mentioned formulations, applied topically in Wistar Rats. The *in vivo* studies were performed using the *tail-flick* test that is the most frequently method used to measure pain levels and assess the effect of anesthesia.

6.1. Introduction

Often, data obtained from *in vitro* studies may not directly be translated in terms of biological equivalence. The differences in the therapeutic responses may be related to the active substance and/or its pharmaceutical form or due to the inter-individual variability. *In vivo* studies are used to evaluate formulations and to monitor drug delivery after administration in animals or human volunteers. *In vivo* studies have advantages such as the generation of realistic measures of the amount of drug that permeate into the skin and reach the systemic circulation.

Various methods have been employed to observe the effect of local anesthetics (Kokubu et al., 1990). The *tail-flick* (TF) test is the most frequently used perception test for measuring the severity of acute or chronic pain. The *in vivo* pharmacodynamics studies were conducted in Wistar rats using the TF technique, in order to examine the ability of the formulations to reduce the responsiveness of the animals after increasing the temperature (Cargill et al., 1985). The TF equipment consists of a restraining cage, a light source with adjustable intensity and a light sensor. The ensemble is connected to a chronograph that is triggered at the same time as the light source. The referred light sensor stops the timer at the first beam of light it receives. The animal's tail is positioned above the sensor and exactly below the light source, thus, its withdrawal or flick sets off the timer by activation of the sensor. The tail flick test is the most frequently used method to measure pain levels and assess the effects of anesthesia. The pain evaluation, by means of the latency time, depends on the intensity of the stimulus. The withdrawal latency, for the animal, shall be set accordingly and might be in the range of 5 – 10 s (Barrot, 2012). In order to avoid tissue damage the cut-off time must be set to not overpass approximately 3 times the baseline and the latter must be set in order to obtain a regular response in the animal, thus differing hypo or hyperalgesic animals from the control (EUMODIC, 2014). The test must be performed by an experienced person in a calm and quiet space without any external influences. Room temperature and humidity must also be taken into consideration. It is important to notice that the stress caused by the environment change and the manipulation of the animals may result in misleading results (Barrot, 2012; Le Bars et al., 2001). This technique does not require a surgical procedure to administer the local formulations anesthetics and the duration of action can be easily assessed with a standard *tail-flick* apparatus.

Various passive methods have been used to potentiate drug transport across the skin (Alexander et al., 2012). The chemical permeation enhancers and the combination of the latter with liposomes have emerged as promising strategies to improve skin permeation of drugs (Cevc and Blume, 2001; Cevc et al., 1997; Cevc et al., 1998).

This Chapter encompasses the physiological effects of a series of selected anesthetic formulations. The selection was based on *in vitro* release studies results addressed in Chapter 3, 4 and 5. Here it is reported the assessment of the efficacy of hydrogels and liposomes based formulations of tetracaine and ropivacaine prepared with lysine-based surfactants. The analgesic response was compared with a commercial formulation (Ametop®) and the influence of the concentration of drugs was also evaluated.

6.2. Experimental section

6.2.1. Materials

TC, PC, chloroform and CHO were purchased from Sigma Aldrich (Saint Louis, MO, USA). RPC was a kind gift from AstraZeneca (London, United Kingdom), and HPMC K15M a kind gift from Dow Chemical Company (Midland, MI, USA). HP-*β*-CD with 97% of purity, with an average degree of substitution of 2 to 6 units of 2-hydroxypropyl (C_3H_7O) per glucose unit, and with an average molecular weight of 1380 g/mol, was purchased from Acros Organic (Geel, Belgium). The nonionic lysine (10Lys10(0) and 16Lys16(0)) and serine-based surfactant $(14Ser)_2N5$ used in this study were synthesized and purified according a method previously developed and reported by some of the authors (Goreti Silva et al., 2012; Silva et al., 2013b). The purity of the compounds was determined by NMR, elemental analysis, surface tension and DSC. Ametop® (4 mg/mL) was purchased from Smith&Nephew (Kingston upon Hull, London, UK). The Wistar rats were purchased from Charles River (Barcelone, Spain). All materials were used as received.

6.2.2. Animal selection for *in vivo* studies

The study has been approved by the ethics committee of the Faculty of Pharmacy, University of Coimbra. Wistar rats (Figure 6.1) weighing 417 g ± 29.5 were kept under controlled temperature (22 ± 1˚C) and humidity (55 %) during all the experiments. The

animals were acclimatized in wire cages in a 12/12 h light/dark cycle and were separated in groups of eight prior to start of the experiments (n=8). The animals had free access to food (pellets diet) and tap water during the experimental. All procedures were conducted in Faculty of Pharmacy, University of Coimbra.

Figure 6.1 Wistar rat used in the *in vivo* experiments.

6.2.3. Optimized formulations for *in vivo* studies

6.2.3.1. Composition and preparation of tetracaine and ropivacaine hydrogels

The optimized hydrogels formulations of tetracaine, ropivacaine and its combinations (Chapter 3) were mixed with the permeation enhancer (16Lys16(0)) and were prepared according to Table 6-2.

Table 6-1 Hydrogel formulation preparation.

	HPMC (%)	**TC (mM)**	**RPC (mM)**	**CPE (mM)**
Hyd_0	1	-	-	-
Hyd_TC	1	0.095	-	-
Hyd_RPC	1	-	0.091	-
Hyd_TC:RPC	1	0.095	0.091	-
Hyd_L_0	1	-	-	0.0031
Hyd_L_TC	1	0.095	-	0.0031
Hyd_L_RPC	1	-	0.091	0.0031
Hyd_L_TC:RPC	1	0.095	0.091	0.0031

The hydrogel containing 2.5 % (w/w) TC was mixed with appropriate amounts of HP-*β*-CD (Teixeira et al., 2014b), 1 % (w/w) HPMC K15M, 16Lys16(0) and deionized water.

Ropivacaine hydrogel was composed of 2.5 % (w/w) RPC, 1 % (w/w) HPMC, 16Lys16(0) and deionized water. These formulations were referred in this Chapter as Hyd_L_TC; Hyd_L_RPC; Hyd_L_TC:RPC. A control hydrogel formulation containing TC, RPC and its combinations, referred as Hyd_TC; Hyd_RPC; Hyd_TC:RPC was prepared without 16Lys16(0). An alternative hydrogel formulation without drug (Hyd_0) was used as placebo. The polymers solutions were kept stirring for 24 h at low speed (50 rpm) before use to ensure complete homogenization. The compounds were soluble in the hydrogel at the concentration used.

6.2.3.2. Preparation of liposomal formulation by TLE method

Liposomal formulations for *in vivo* studies were prepared by TLE method (Bangham et al., 1965) according to Table 6-2.

Table 6-2 Liposomal formulation preparation.

	HPMC (%)	TC (mM)	RPC (mM)	CPE (mM)	PC (mM)	CHO (mM)
Lip_0	1	-	-		0.029	0.014
Lip_TC	1	0.095	-	0.0031	0.029	0.014
Lip_RPC	1	-	0.091	0.0031	0.029	0.014
Lip_TC:RPC	1	0.095	0.091	0.0031	0.029	0.014

The formulation LPS-LP 16Lys16(0) optimized as reported in Chapter 5 was selected to proceed with *in vivo* studies due to the maximal enhancement permeation, size and zeta potential. The lipids (PC: CHO) and lysine-based surfactant (16Lys16) were dissolved in a small quantity of chloroform and was afterwards removed under vacuum (Buchi - Rotavapor R-210 with a vaccum pump V-700 and a vaccum controller V-850) at 55ºC (Buchi Heating Bath B-491). Evaporation was carried out for a period of 2 h to ensure that all the traces of solvent were removed. After the dry lipid appeared on the flask wall, three different liposomal formulations composed of 2.5 % of TC and RPC were prepared. Firstly, the TC was directly dissolved in the lipophilic phase, and the hydrophilic phase was constituted only by water (Lip_TC). Secondly, the aqueous phase constituted by RPC was added to the lipophilic phase containing TC (Lip_TC:RPC). Finally, a water solution containing RPC was used to hydrate the lipid content (Lip_RPC). A placebo liposomal formulation prepared without drug and is referred as Lip_0. Note that the quantities of both drugs were chosen to ensure maximization of the amount within suitable entrapment efficiency, as established from preliminary tests (Chapter 5). After

adding the hydrophilic phase, the suspension was alternately shaken using a vortex mixer and sonicated using a bath sonicator (Clifton Ultrasonic Bath, London, United Kingdom) at 55 ºC, during 30 min to allow vesicle formation. The liposome suspension was extruded through a 100 nm polycarbonate membrane using a LipoFast extrusor Avestin®. In order to obtain viscosity values adequate for dermal application, a hydrogel of 1 % (w/V) of 15 M HPMC was added to the formulation mentioned above at low speed (50 rpm) during 24 h to ensure complete homogenization.

6.2.4. Experimental protocol

The anesthetic effect of 2.5 % (w/w) of tetracaine, 2.5% (w/w) of ropivacaine and its combinations was tested in Wistar rats using the *tail-flick* analgesic test (D'AMOUR and SMITH, 1941). The hydrogels formulations were prepared according to Table 6-2 and the liposomal formulation was prepared according to Table 6-2. The effects of the anesthetic formulations were compared with a commercially available product (Ametop® 4mg/mL) and the placebos (Hyd_0; Hyd_P_0; Lip_0).

Prior to the experiments, the animals were brought from their housing and left to acclimatize for 15 min. For each set of experiments (n=8), at time 0 h, 100 µL of each formulation was applied to the skin on the proximal third of the tail (1.5 cm from the root of the tail).

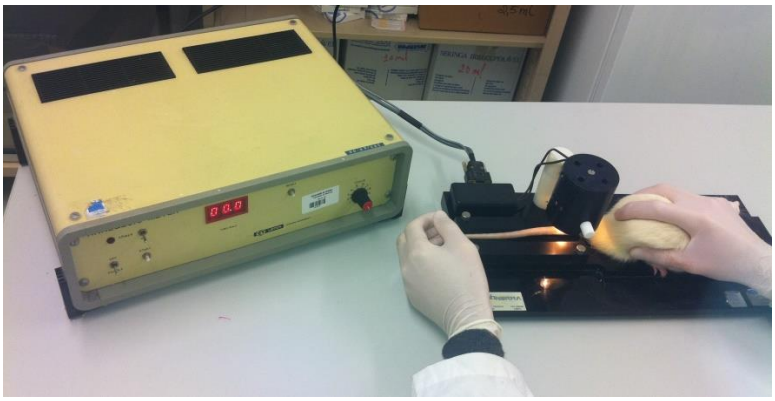

Figure 6.2 *Tail-flick* analgesimeter apparatus.

Rats were restrained on the *tail-flick* analgesimeter Letica (Scientific instruments, Barcelona, Spain) – heat stimulus and chronograph were triggered at the touch of a button. Each animal was positioned in the restraining cage and left it still for some moments. The luminous heat stimulus and time counter stopped when the exposed rat's tail flicked and cut-off time was set to 30 s to avoid tissue damage. The tail was

positioned on the equipment's groove and the light was turned on; automatically the chronograph started to count and at the first flick of the tail the counter was stopped (Figure 6.2).

The animal was removed from the restraining cage when the heat source was cut off. The anesthetic effect, as well as the formulations without drugs and the blank group (no formulation), was tested hourly during a period of 6 h.

6.2.4.1. Statistical analysis

Differences between the values obtained at the chronograph were recorded and examined for significance using unpaired Student's *t*-test. The *p* value was set to 0.05, with $p < 0.05$, indicating statistical significance in the differences between formulations tested and the commercial formulation.

6.3. Results and discussion

In vivo pharmacodynamics studies were performed in Wister rats, in order to evaluate the efficiency of selected formulations. All animals were able to move their tails at random during the experiments. The dosage of the positive control (commercial) was of 4 mg/mL and tested formulations had 2.5 mg/mL of tetracaine and ropivacaine. The results obtained are represented in Figure 6.3.

Generally, the response of drugs starts 1 h after the application of the formulations. However, a noticeable anesthetic effect reached a maximum at 3 to 4 hours after the skin application of the formulation. The effect was maintained for 2 h more and then decreased at approximately 6 h. For this reason, the results are shown for the 3rd and 4th hour.

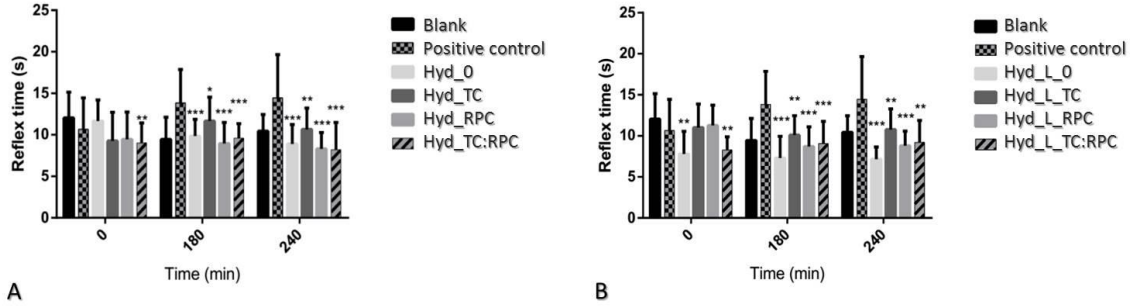

Figure 6.3. Response time for each different formulation with 2.5 % of the respective drug and their combination on the *tail-flick* analgesimeter. Formulation A was a hydrogel; B formulation was a hydrogel containing 16-Lys-16 as CPE. t-student test was carried out to evaluate statistical difference between the formulations A and B and the commercial formulation (positive control) * $p < 0.05$; ** $p < 0.01$; *** $p < 0.001$.

The results showed that a small change in the reflex time was noticed in rats which were exposed to the developed formulations. The reflex time values were higher for formulations containing tetracaine than for formulations containing ropivacaine. The main reason for this might be related to RPC properties: on its hydrochloride form, this molecule is ionized and hydrophilic and, consequently, poorly absorbed across the skin.

The results revealed that the duration of the anesthetic effect increased with the hydrogels formulations containing lysine-based surfactant (16Lys16) when compared with the hydrogel formulation without lysine-based surfactant (Figure 6.3). These findings are in agreement with the *in vitro* skin permeation studies data, reported in Chapter 3. There are no statistical differences between the formulations except Hyd_TC exhibiting a prolonged duration of the anesthetic effect compared to Hyd_RPC. However the duration of RPC clearly increase when the lysine-based formulation is added to the hydrogel.

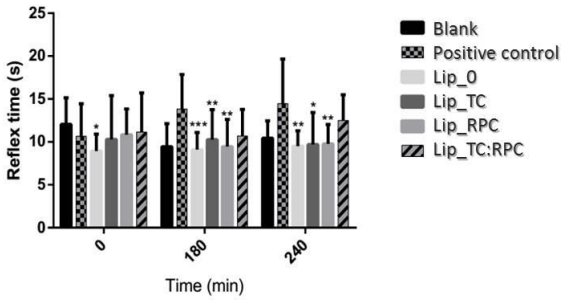

Figure 6.4 Response time for each different formulation with the respective drug and their combination on the *tail-flick* analgesimeter. The formulation was a liposome. t-student test was carried out to evaluated the statistical difference between the proposed formulations A and B and the positive control (commercial formulation (positive control) * $p < 0.05$; ** $p < 0.01$; *** $p < 0.001$.

The dermal administration to rats resulted in steady-state levels reached at approximately 3 h and maintained for a period of 6 h. The statistical analysis performed show that Lip_TC:RPC was the only formulation that showed no significant statistical difference ($p > 0.05$) when compared to the positive control (commercial formulation) (Figure 6.4). These findings are also in agreement with the *in vitro* results, where the flux was higher for liposomes (34 and 3 µg cm^{-2} h^{-1} for TC and RPC respectively) than in the hydrogel formulation (26 and 1.7 µg cm^{-2} h^{-1}). The main advantage of liposomal formulations is the faster onset of analgesia when compared to hydrogels formulations. Despite the promising results obtained with the liposomal formulation, the anesthetic effect is lower than the anesthetic effect obtained with the commercial formulation Ametop®, probably due to the lower tetracaine content (2.5 % (w/w) vs 4 % (w/w) in Ametop®). The differences between *in vitro* and *in vivo* studies can also be attributed to the skin model used; rat versus newborn pig skin. The animals may likewise have suffered from test adaptability due to the repetitive measuring (Shin et al., 2004). It is important to note that the skin integrity, maintained practically unalterable after formulation removal with the exception of the commercial formulation that in some causes caused damage in the skin of the tail.

6.4. Conclusion

The results clearly demonstrate increases in the local analgesic responses of the selected formulations. The *in vivo* experiments in rats correlated partially the *in vitro* findings and revealed that the hydrogels combined with lysine-based surfactants, results in an anesthetic effect higher than the hydrogel without CPE. However the liposomal formulations showed a higher analgesic response exhibiting a better *in vivo* performance compared to any hydrogel formulations. Based on data obtained it as concluded that this formulation was the most similar to the commercial formulation (Ametop®) regarding the analgesic effects produced. These findings support the use of liposomal formulation may be an efficient approach for topical application, for the concomitant administration of tetracaine and ropivacaine.

Chapter 7

Concluding remarks and future work

The work reported in this thesis highlight the importance of combining different strategies to increase the permeation of two distinct local anesthetics across the skin, without causing skin irritation or damage. It relies on fundamental approaches for the study of the formulation, based on HPMC hydrogels, including systems containing cyclodextrins, aminoacid-based gemini surfactants and liposomes.

Chapter 2 provides a clear indication of the effect of TC protonation on the aqueous solubility in the absence and presence of *β*-CD and HP-*β*-CD and how such interactions affects the transport of TC, at different concentrations, across a model membrane. UV-Vis and fluorescence spectroscopy data revealed that TC interacts with both CD on a 1:1 stoichiometry and the presence of latter increase the solubility of TC. However the release of TC decreases by increasing the CD concentration, being more effective in the protonated form. This work showed that such behavior does not depend on the formation of inclusion host-guest compounds, but due to the formation of weak supramolecular assemblies. The kinetics and mechanism of TC release from HPMC gels was also evaluated providing an insight on the role of CD on the TC transport. This Chapter demonstrated that both forms of TC were successfully released from the formulations at a controlled rate, following a Super-Case II transport mechanism and the transport of TC can be tuned by using CD, especially the HP-*β*-CD.

In what concerns the study reporting the evaluation of a series of nonionic and anionic lysine-based surfactants as CPE (Chapter 3), it was found that the most effective CPE

for both drugs was the compound with the longest alkyl chain comprising 16 carbon atoms (16Lys16). The highest enhancing effect was achieved for ropivacaine, a drug that is does not easily administered cross the *stratum corneum*, attaining an approximately 6-fold enhancement, certainly due to a combination of effects such as membrane perturbation, resulting from surface exposure of the anionic surfactant headgroups and favorable electrostatic interactions with the drug. In this case, the 16Lys16(-) was the most effective (ER=6.12), while in the case of TC this was observed for 16Lys16(0), probably due to a combine perturbation/hydrophobic effects (comparatively weaker, in any case, than the electrostatic effect mentioned above). Molecular dynamics simulations have shown to be a useful tool for a mechanistic rationalization of the system behavior. MD data results also suggested that lysine-based surfactants are promising candidates to increase drug transport, especially for hydrophilic drugs, through the SC without altering the skin tissue morphology and with the advantage of being non cytotoxic.

In Chapter 4, a series of nonionic and cationic serine-based gemini surfactant were evaluated as skin permeation enhancers for two tetracaine and ropivacaine. The enhancement effects observed were dependent on the penetration modifier and on the drug used. It was observed that the most effectives CPE were the cationic surfactants with longer alkyl chain and shorter spacer $(14Ser)_2N5(+)$ for both drugs. The enhancement flux values observed were higher for RPC (ER=3) and lower in the studies with TC (ER=2). Molecular dynamics simulations provided results in accordance with the experimental observations. Complementary studies such as formulation optimization, cytotoxicity studies on the CPE in HEK and electronic microscopy studies provided valuable information about toxicity to the skin cells and of irritation or morphological changes in the skin tissue. The results obtained showed that the compounds and methodology used are suitable, safe and that these compounds are promising candidates to be used as CPE. Despite that skin integrity evaluation studies did not reveal significant changes in the tissue morphology after the use of the CPE (Chapter 3 and 4), the long term local and systemic toxicity of the chemical enhancers in the final dosage form require further studies and should be carefully assessed.

Regarding Chapter 5, describes the evaluation of liposomes prepared with aminoacid-based surfactants in terms of permeation for topical administration. For this purpose, size, polidispersivity index, potential zeta and encapsulation efficiency of various liposomal formulations containing TC and RPC were assessed and compared. The results obtained indicate that liposomal formulations were able to efficiently co-entrap TC

and RPC providing a reservoir system for long-term administration. This work showed that the efficacy of the liposomes regarding the permeation clearly was improved when using lysine-based surfactants were employed. Generally, the amount of TC and RPC permeated significantly increased and at the lag time decreased. These results are new and significant, confirming that their use as delivery agents, in pharmaceutical formulations especially in the case of ropivacaine hydrochloride.

Chapter 6, addresses the evaluation of a series of previously optimized formulations *in vivo*, using Wistar rats. For this, the *tail-flick* technique showed to be a simple, reliable and useful test for the *in vivo* assessment of local anesthetic effects. The results showed that the analgesic response was found to be dependent on the drug concentration and composition of the systems. The application of the tested formulations did not determine any macroscopic alteration on the skin of the animals. The liposomal formulation containing lysine-based surfactant may constitute a promising formulation for further clinical application in the treatment of acute and chronic pain or before a surgery procedure. Additionally, supplementary *in vivo* experiments involving the *von Frey* fibers should be performed in humans in order to evaluate and determine the therapeutic efficacy of the final formulations containing both drugs.

References

Abraham, M.H., Chadha, H.S., Mitchell, R.C., 1995. The Factors that Influence Skin Penetration of Solutes*. Journal of Pharmacy and Pharmacology 47, 8-16.

Alexander, A., Dwivedi, S., Ajazuddin, Giri, T.K., Saraf, S., Saraf, S., Tripathi, D.K., 2012. Approaches for breaking the barriers of drug permeation through transdermal drug delivery. J. Control. Release 164, 26-40.

Ali, H., Nazzal, S., 2009. Development and validation of a reversed-phase HPLC method for the simultaneous analysis of simvastatin and tocotrienols in combined dosage forms. Journal of Pharmaceutical and Biomedical Analysis 49, 950-956.

Almeida, J.A.S., Faneca, H., Carvalho, R.A., Marques, E.F., Pais, A.A.C.C., 2011. Dicationic Alkylammonium Bromide Gemini Surfactants. Membrane Perturbation and Skin Irritation. PLOS ONE 6, e26965.

Almeida, J.A.S., Marques, E.F., Jurado, A.S., Pais, A.A.C.C., 2010. The effect of cationic gemini surfactants upon lipid membranes. An experimental and molecular dynamics simulation study. Physical Chemistry Chemical Physics 12, 14462-14476.

Alster, T., 2013. Review of Lidocaine/Tetracaine Cream as a Topical Anesthetic for Dermatologic Laser Procedures. Pain and Therapy 2, 11-19.

Amato, M.E., Lipkowitz, K.B., Lombardo, G.M., Pappalardo, G.C., 1998. High-field NMR spectroscopic techniques combined with molecular dynamics simulations for the study of the inclusion complexes of α- and β-cyclodextrins with the cognition activator 3-phenoxypyridine sulphate (CI-844). Magnetic Resonance in Chemistry 36, 693-705.

Arun Rasheed, A.K.C.K., Sravanthi V. V. N. S. S., 2008. Cyclodextrins as Drug Carrier Molecule: A Review. Sci. Pharm. 76, 567-598.

Asbill, C.S., Michniak, B.B., 2000. Percutaneous penetration enhancers: local versus transdermal activity. Pharm Sci Technol To 3, 36-41.

Ashton, P., Walters, K.A., Brain, K.R., Hadgraft, J., 1992. Surfactant effects in percutaneous absorption I. Effects on the transdermal flux of methyl nicotinate. Int. J. Pharm. 87, 261-264.

Babu, R., Mandip, S., Narayanasamy, K., 2005a. Structure-Activity Relationship of Chemical Penetration Enhancers, Percutaneous Penetration Enhancers, Second Edition. Informa Healthcare, pp. 17-33.

Babu, R.J., Mandip, S., Narayanasamy, K., 2005b. Structure?Activity Relationship of Chemical Penetration Enhancers, Percutaneous Penetration Enhancers, Second Edition. CRC Press, pp. 17-33.

Bach, M., Lippold, B.C., 1998. Percutaneous penetration enhancement and its quantification. Eur J Pharm Biopharm 46, 1-13.

Badea, I., Verrall, R., Baca-Estrada, M., Tikoo, S., Rosenberg, A., Kumar, P., Foldvari, M., 2005. In vivo cutaneous interferon-γ gene delivery using novel dicationic (gemini) surfactant–plasmid complexes. The Journal of Gene Medicine 7, 1200-1214.

Banga, A.K., 1998. Percutaneous absorption and its enhancement, in: Group, T.F. (Ed.), Electrically Assisted Transdermal and Topical Drug Delivery. CRC Press.

Bangham, A.D., Standish, M.M., Watkins, J.C., 1965. Diffusion of univalent ions across the lamellae of swollen phospholipids. J Mol Biol 13, 238-252.

Barbero, A.M., Frasch, H.F., 2009a. Pig and guinea pig skin as surrogates for human in vitro penetration studies: A quantitative review. Toxicol In Vitro 23, 1-13.

Barbero, A.M., Frasch, H.F., 2009b. Pig and guinea pig skin as surrogates for human in vitro penetration studies: A quantitative review. Toxicol, in vitro 23, 1-13.

Barenholz, Y., 2001. Liposome application: problems and prospects. Current Opinion in Colloid & Interface Science 6, 66-77.

Barrot, M., 2012. Tests and models of nociception and pain in rodents. Neuroscience 211, 39-50.

Barry, B.W., 1993. Vehicle effect: what is an enhancer?, in: Shah, V.P.M., H. I., Eds. (Ed.), In Topical Drug Bioavailability, Bioequivalence, and Penetration. Plenum, New York, pp. 268-270.

Barry, B.W., 2001. Novel mechanisms and devices to enable successful transdermal drug delivery. Eur. J. Pharm. Sci. 14, 101-114.

Bartek, M.J., Labudde, J.A., Maibach, H.I., 1972. Skin Permeability in vivo: comparison in rat, rabbit, pig and man. J. Invest.Dermatol. 58, 114-123.

Becker, D.E., Reed, K.L., 2012. Local Anesthetics: Review of Pharmacological Considerations. Anesth. Prog. 59, 90-102.

Bennett, W.F.D., MacCallum, J.L., Tieleman, D.P., 2009. Thermodynamic Analysis of the Effect of Cholesterol on Dipalmitoylphosphatidylcholine Lipid Membranes. Journal of the American Chemical Society 131, 1972-1978.

Benson, H.A.E., 2011. Skin Structure, Function, and Permeation, Transdermal and Topical Drug Delivery. John Wiley & Sons, Inc., pp. 1-22.

Berman, B., Flores, J., Pariser, D., Pariser, R., Araujo, T.d., Ramirez, C.C., 2005. Self-Warming Lidocaine/Tetracaine Patch Effectively and Safely Induces Local Anesthesia during Minor Dermatologic Procedures. Dermatol. Surg. 31, 135-138.

Bleck, O., Abeck, D., Ring, J., Hoppe, U., Vietzke, J.-P., Wolber, R., Brandt, O., Schreiner, V., 1999. Two ceramide subfractions detectable in Cer(AS) position by HPTLC in skin surface lipids of non-lesional skin of atopic eczema. Journal Investigative Dermatology 113, 894-900.

Blunk, D., Bierganns, P., Bongartz, N., Tessendorf, R., Stubenrauch, C., 2006. New speciality surfactants with natural structural motifs. New Journal of Chemistry 30, 1705-1717.

Boddé, H.E., Kruithof, M.A.M., Brussee, J., Koerten, H.K., 1989. Visualisation of normal and enhanced HgCl2 transport through human skin in vitro. Int. J. Pharm. 53, 13-24.

Bolzinger, M.-A., Briançon, S., Pelletier, J., Chevalier, Y., 2012. Penetration of drugs through skin, a complex rate-controlling membrane. Current Opinion in Colloid & Interface Science 17, 156-165.

Booij, L.H.D.J., 2009. Cyclodextrins and the emergence of sugammadex. Anaesthesia 64, 31-37.

Borde, C., Nardello, V., Wattebled, L., Laschewsky, A., Aubry, J.-M., 2008. A gemini amphiphilic phase transfer catalyst for dark singlet oxygenation. Journal of Physical Organic Chemistry 21, 652-658.

Bouwstra, J.A., Honeywell-Nguyen, P.L., Gooris, G.S., Ponec, M., 2003. Structure of the skin barrier and its modulation by vesicular formulations. Progress in Lipid Research 42, 1-36.

Brewster, M.E., Loftsson, T., 2007. Cyclodextrins as pharmaccutical solubilizers. Adv. Drug. Deliver. Rev. 59, 645-666.

Brito, R.O., Marques, E.F., Gomes, P., Falcão, S., Söderman, O., 2006. Self-Assembly in a Catanionic Mixture with an Aminoacid-Derived Surfactant: From Mixed Micelles to Spontaneous Vesicles. The Journal of Physical Chemistry B 110, 18158-18165.

Brito, R.O., Marques, E.F., Gomes, P., João Araújo, M., Pons, R., 2008. Structure/Property Relationships for the Thermotropic Behavior of Lysine-Based Amphiphiles: from Hexagonal to Smectic Phases. The Journal of Physical Chemistry B 112, 14877-14887.

Brito, R.O., Marques, E.F., Silva, S.G., do Vale, M.L., Gomes, P., Araújo, M.J., Rodriguez-Borges, J.E., Infante, M.R., Garcia, M.T., Ribosa, I., Vinardell, M.P., Mitjans, M., 2009. Physicochemical and toxicological properties of novel amino acid-based amphiphiles and their spontaneously formed catanionic vesicles. Colloids and Surfaces B: Biointerfaces 72, 80-87.

Brito, R.O., Oliveira, I.S., Araújo, M.J., Marques, E.F., 2013. Morphology, Thermal Behavior, and Stability of Self-Assembled Supramolecular Tubules from Lysine-Based Surfactants. The Journal of Physical Chemistry B 117, 9400-9411.

Bronaugh, R.L., Stewart, R.F., 1985. Methods for in vitro percutaneous absorption studies IV: The flow-through diffusion cell. Journal of Pharmaceutical Sciences 74, 64-67.

Brown, M.B., Martin, G.P., Jones, S.A., Akomeah, F.K., 2006. Dermal and Transdermal Drug Delivery Systems: Current and Future Prospects. Drug Delivery 13, 175-187.

Brun, A., Brezesinski, G., Möhwald, H., Blanzat, M., Perez, E., Rico-Lattes, I., 2003. Interaction between phospholipids and new Gemini catanionic surfactants having anti-HIV activity. Colloid. Surface. A 228, 3-16.

Cappel, M.J., Kreuter, J., 1991. Effect of nonionic surfactants on transdermal drug delivery: I. Polysorbates. Int. J. Pharm. 69, 143-153.

Cardoso, A.M.S., Faneca, H., Almeida, J.A.S., Pais, A.A.C.C., Marques, E.F., de Lima, M.C.P., Jurado, A.S., 2011. Gemini surfactant dimethylene-1,2-bis(tetradecyldimethylammonium bromide)-based gene vectors: A biophysical approach to transfection efficiency. Biochimica et Biophysica Acta (BBA) - Biomembranes 1808, 341-351.

Cargill, C.L., Steinman, J.L., Willis, W.D., 1985. A fictive tail flick reflex in the rat. Brain Res 345, 45-53.

Castronuovo, G., Niccoli, M., 2006. Thermodynamics of inclusion complexes of natural and modified cyclodextrins with propranolol in aqueous solution at 298 K. Bioorgan. Med. Chem. 14, 3883-3887.

Cerezo, J., Zúñiga, J., Bastida, A., Requena, A., Cerón-Carrasco, J.P., 2011. Atomistic Molecular Dynamics Simulations of the Interactions of Oleic and 2-Hydroxyoleic Acids with Phosphatidylcholine Bilayers. The Journal of Physical Chemistry B 115, 11727-11738.

Cevc, G., 2002. Transfersomes, Modified-Release Drug Delivery Technology. Informa Healthcare, pp. 533-546.

Cevc, G., 2004. Lipid vesicles and other colloids as drug carriers on the skin. Advanced Drug Delivery Reviews 56, 675-711.

Cevc, G., Blume, G., 1992. Lipid vesicles penetrate into intact skin owing to the transdermal osmotic gradients and hydration force. Biochimica et Biophysica Acta (BBA) - Biomembranes 1104, 226-232.

Cevc, G., Blume, G., 2001. New, highly efficient formulation of diclofenac for the topical, transdermal administration in ultradeformable drug carriers, Transfersomes. Biochimica et Biophysica Acta (BBA) - Biomembranes 1514, 191-205.

Cevc, G., Blume, G., Schätzlein, A., 1997. Transfersomes-mediated transepidermal delivery improves the regio-specificity and biological activity of corticosteroids in vivo. J. Control. Release 45, 211-226.

Cevc, G., Blume, G., Schätzlein, A., Gebauer, D., Paul, A., 1996. The skin: a pathway for systemic treatment with patches and lipid-based agent carriers. Adv. Drug. Deliver. Rev. 18, 349-378.

Cevc, G., Gebauer, D., Stieber, J., Schätzlein, A., Blume, G., 1998. Ultraflexible vesicles, Transfersomes, have an extremely low pore penetration resistance and transport therapeutic amounts of insulin across the intact mammalian skin. Biochimica et Biophysica Acta (BBA) - Biomembranes 1368, 201-215.

Challa, R., Ahuja, A., Ali, J., Khar, R., 2005. Cyclodextrins in drug delivery: An updated review. AAPS PharmSciTech 6, E329-E357.

Chandak, A., Verma, P., 2008a. Design and development of HPMC based polymeric films of methotrexate - physicochemical and pharmacokinetic evaluations. Yakugaku Zasshi: The Pharmaceutical Society of Japan 128, 1057-1066.

Chandak, A.R., Verma, P.R.P., 2008b. Design and Development of Hydroxypropyl Methycellulose (HPMC) Based Polymeric Films of Methotrexate: Physicochemical and Pharmacokinetic Evaluations. YAKUGAKU ZASSHI 128, 1057-1066.

Chandak, A.R., Verma, P.R.P., 2008c. Development and Evaluation of HPMC Based Matrices for Transdermal Patches of Tramadol. Clinical Research and Regulatory Affairs 25, 13-30.

Chantasart, D., Hao, J., Li, S.K., 2013. Evaluation of Skin Permeation of β-Blockers for Topical Drug Delivery. Pharm. Res. 30, 866-877.

Chao, J., Meng, D., Li, J., Xu, H., Huang, S., 2004. Preparation and study on the novel solid inclusion complex of ciprofloxacin with HP-β-cyclodextrin. Spectrochimica Acta Part A: Molecular and Biomolecular Spectroscopy 60, 729-734.

Chekirou, N.L., Benomrane, I., Lebsir, F., Krallafa, A.M., 2012. Theoretical and experimental study of the tetracain/β-cyclodextrin inclusion complex. J. Incl. Phenom. Macrocycl. Chem. 74, 211-221.

Chilcott, R.P., 2008. Cutaneous Anatomy and Function, Principles and Practice of Skin Toxicology. John Wiley & Sons, Ltd, pp. 1-16.

Clapés, P., Rosa Infante, M., 2002. Amino Acid-based Surfactants: Enzymatic Synthesis, Properties and Potential Applications. Biocatalysis and Biotransformation 20, 215-233.

Colomer, A., Pinazo, A., García, M.T., Mitjans, M., Vinardell, M.P., Infante, M.R., Martínez, V., Pérez, L., 2012. pH-Sensitive Surfactants from Lysine: Assessment of Their Cytotoxicity and Environmental Behavior. Langmuir 28, 5900-5912.

Connors, K.A., Mollica, J.A., 1966. Theoretical analysis of comparative studies of complex formation: Solubility, spectral, and kinetic techniques. J. Pharm. Sci. 55, 772-780.

Cornwell, P.A., Barry, B.W., 1994. Sesquiterpene components of volatile oils as skin penetration enhancers for the hydrophilic permeant 5-fluorouracil. J.Pharm Pharmacol. 46, 261-269.

Cornwell, P.A., Barry, B.W., Bouwstra, J.A., Gooris, G.S., 1996. Modes of action of terpene penetration enhancers in human skin; Differential scanning calorimetry, small-angle X-ray diffraction and enhancer uptake studies. Int. J. Pharm. 127, 9-26.

Cornwell, P.A., Barry, B.W., Stoddart, C.P., Bouwstra, J.A., 1994. Wide-angle X-ray Diffraction of Human Stratum Corneum: Effects of Hydration and Terpene Enhancer Treatment. Journal of Pharmacy and Pharmacology 46, 938-950.

Costa, D., Valente, A.J.M., Miguel, M.G., Queiroz, J., 2011. Gel Network Photodisruption: A New Strategy for the Codelivery of Plasmid DNA and Drugs. Langmuir 27, 13780-13789.

Costa, D., Valente, A.J.M., Pais, A.A.C.C., Miguel, M.G., Lindman, B., 2010. Cross-linked DNA gels: Disruption and release properties. Colloid. Surface. A 354, 28-33.

Covino, B.G., 1987. Toxicity and Systemic Effects of Local Anesthetic Agents, in: Strichartz, G. (Ed.), Local Anesthetics. Springer Berlin Heidelberg, pp. 187-212.

Cross, S.E., Roberts, M.S., 1993. Subcutaneous Absorption Kinetics and Local Tissue Distribution of Interferon and Other Solutes. Journal of Pharmacy and Pharmacology 45, 606-609.

Curtis, E.M., Hall, C.K., 2013. Molecular Dynamics Simulations of DPPC Bilayers Using “LIME”, a New Coarse-Grained Model. The Journal of Physical Chemistry B 117, 5019-5030.

D'AMOUR, F.E., SMITH, D.L., 1941. A METHOD FOR DETERMINING LOSS OF PAIN SENSATION. Journal of Pharmacology and Experimental Therapeutics 72, 74-79.

Dahan, A., Miller, J.M., Hoffman, A., Amidon, G.E., Amidon, G.L., 2009. The solubility-permeability interplay in using cyclodextrins as pharmaceutical solubilizers: Mechanistic modeling and application to progesterone. J. Pharm. Sci.

das Neves, J., Sarmento, B., Amiji, M.M., Bahia, M.F., 2010. Development and validation of a rapid reversed-phase HPLC method for the determination of the non-nucleoside reverse transcriptase inhibitor dapivirine from polymeric nanoparticles. Journal of Pharmaceutical and Biomedical Analysis 52, 167-172.

Davies, H.W., Trotter, M.D., 1981. Synthesis and turnover of membrane glycoconjugates in monolayer culture of pig and human epidermal cells. British Journal of Dermatology 104, 649-658.

Davis, A., Raghavan, S.L., Pellett, M., Hadgraft, J., 2002. The application of supersaturated systems to percutaneous drug delivery, Transdermal Drug Delivery Systems. Informa Healthcare.

Davis, M.E., Brewster, M.E., 2004. Cyclodextrin-based pharmaceutics: past, present and future. Nat Rev Drug Discov 3, 1023-1035.

Del Valle, E.M.M., 2004. Cyclodextrins and their uses: a review. Process Biochemistry 39, 1033-1046.

Diane, O.T., Gerold, M., 2013. Complexation: Cyclodextrins, Encyclopedia of Pharmaceutical Technology, Third Edition. Taylor & Francis, pp. 671-696.

Dittert, L.W., Higuchi, T., Reese, D.R., 1964. Phase solubility technique in studying the formation of complex salts of triamterene. J. Pharm. Sci. 53, 1325-1328.

Doi, T., Kinoshita, T., Kamiya, H., Washizu, S., Tsujita, Y., Yoshimizu, H., 2001. Aggregation of Polypeptide-Based Amphiphiles in Water. Polym J 33, 160-164.

Duangjit, S., Opanasopit, P., Rojanarata, T., Ngawhirunpat, T., 2013. Evaluation of Meloxicam-Loaded Cationic Transfersomes as Transdermal Drug Delivery Carriers. AAPS PharmSciTech 14, 133-140.

Dukhin, S.S., Miller R., Loglio G., 2005. Surface activity of drugs, in: Srivastava, R.C., Nagappa, A.N. (Eds.), Studies in Interface Science. Elsevier, pp. 5-35.

Echezarreta-López, M.M., Perdomo-López, I., Estrada, E., Vila-Jato, J.L., Torres-Labandeira, J.J., 2002. Utility of nuclear magnetic resonance spectroscopy to characterize the structure of dexamethasone sodium phosphate inclusion complexes with cyclodextrins in solution and to analyze potential competitive effects. J. Pharm. Sci. 91, 1536-1547.

Effendy, I., Maibach, H.I., 1995. Surfactants and experimental irritant contact dermatitis. Contact Dermatitis 33, 217-225.

Egelrud, T., 1993. Purification and Preliminary Characterization of Stratum Corneum Chymotryptic Enzyme: A Proteinase That May Be Involved in Desquamation. J Investig Dermatol 101, 200-204.

Egelrud, T., Lundström, A., 1991. A chymotrypsin-like proteinase that may be involved in desquamation in plantar stratum corneum. Archives of Dermatological Research 283, 108-112.

El-Kattan, A.F., Asbill, C.S., Kim, N., Michniak, B.B., 2001. The effects of terpene enhancers on the percutaneous permeation of drugs with different lipophilicities. Int. J. Pharm. 215, 229-240.

El-Kattan, A.F., Asbill, C.S., Michniak, B.B., 2000. The effect of terpene enhancer lipophilicity on the percutaneous permeation of hydrocortisone formulated in HPMC gel systems. Int. J. Pharm. 198, 179-189.

El Maghraby, G.M., Barry, B.W., Williams, A.C., 2008. Liposomes and skin: From drug delivery to model membranes. Eur. J. Pharm. Sci. 34, 203-222.

Elias, P., 2007. The skin barrier as an innate immune element. Seminars in Immunopathology 29, 3-14.

Elias, P.M., 1983. Epidermal lipids, barrier function, and desquamation. Journal of Investigative Dermatology 80, 44s-49s.

Elias, P.M., 1988. Structure and function of the stratum corneum permeability barrier. Drug Dev Res 13, 97-105.

Elias, P.M., 2005. Stratum corneum defensive functions: An integrated view. Journal of Investigative Dermatology 125, 183-200.

Elias, P.M., Tsai, J., Menon, G.K., Holleran, W.M., Feingold, K.R., 2002. The potential of metabolic interventions to enhance transdermal drug delivery. J Investig Dermatol Symp Proc 7, 79-85.

Ellis, R., 2010. Ellis Hematoxylin and Eosin (H&E) Staining Protocol.

Elsayed, M.M.A., Abdallah, O.Y., Naggar, V.F., Khalafallah, N.M., 2007. Lipid vesicles for skin delivery of drugs: Reviewing three decades of research. Int. J. Pharm. 332, 1-16.

EUMODIC, E.M.D.C., 2014. Standard Operating Procedure Title: Tail Flick.

Fartasch, M., Bassukas, I.D., Diepgkn, T.L., 1993. Structural relationship between epidermal lipid lamellae, lamellar bodies and desmosomes in human epidermis: an ultrastructural study. Brit. J. Dermatol. 128, 1-9.

Fernandes, S., Cabeça, L., Marsaioli, A., Paula, E., 2007. Investigation of tetracaine complexation with beta-cyclodextrins and p-sulphonic acid calix[6]arenes by nOe and PGSE NMR. J. Incl. Phenom. Macrocycl. Chem. 57, 395-401.

Finnin, B.C., Timothy M. Morgan, 1999. Transdermal penetration enhancers: Applications, limitations, and potential. J Pharm Sci 88, 955-958.

Fisher, R., Hung, O., Mezei, M., Stewart, R., 1998. Topical anaesthesia of intact skin: liposome-encapsulated tetracaine vs EMLA. British Journal of Anaesthesia 81, 972-973.

Foldvari, M., 2000. Non-invasive administration of drugs through the skin: challenges in delivery system design. Pharm. Sci. Technol. To. 3, 417-425.

Forbes, P., 1969. Vascular supply of the skin and hair in swine. Adv. Biol. Skin 9, 419-432.

Forslind, B., Engström, S., Engblom, J., Norlén, L., 1997. A novel approach to the understanding of human skin barrier function. Journal of Dermatological Science 14, 115-125.

Franco de Lima, R.A., de Jesus, M.B., Saia Cereda, C.M., Tofoli, G.R., Cabeça, L.F., Mazzaro, I., Fraceto, L.F., de Paula, E., 2012. Improvement of tetracaine antinociceptive effect by inclusion in cyclodextrins. J. Drug. Target. 20, 85-96.

Franz, T.J., 1975a. Percutaneous absorption. On the relevance of in vitro data. Journal of Investigative Dermatology 64, 190-195.

Franz, T.J., 1975b. PERCUTANEOUS ABSORPTION. ON THE RELEVANCE OF IN VITRO DATA. J. Invest.Dermatol. 64, 190-195.

Froebe, C.L., Simion, F.A., Rhein, L.D., Cagan, R.H., Kligman, A., 1990. Stratum corneum Lipid Removal by Surfactants: Relation to in vivo Irritation. Dermatology 181, 277-283.

Ganza-Gonzalez, A., Vila-Jato, J.L., Anguiano-Igea, S., Otero-Espinar, F.J., Blanco-Méndez, J., 1994. A proton nuclear magnetic resonance study of the inclusion complex of naproxen with β-cyclodextrin. Int. J. Pharm. 106, 179-185.

Gillet, A., Grammenos, A., Compère, P., Evrard, B., Piel, G., 2009. Development of a new topical system: Drug-in-cyclodextrin-in-deformable liposome. International Journal of Pharmaceutics 380, 174-180.

Glavas-Dodov, M., Goracinova, K., Mladenovska, K., Fredro-Kumbaradzi, E., 2002. Release profile of lidocaine HCl from topical liposomal gel formulation. Int. J. Pharm. 242, 381-384.

Godin, B., Touitou, E., 2003. Ethosomes: new prospects in transdermal delivery. Crit Rev Ther Drug Carrier Syst 20, 63-102.

Godin, B., Touitou, E., 2007. Transdermal skin delivery: Predictions for humans from in vivo, ex vivo and animal models. Adv. Drug. Deliver. Rev. 59, 1152-1161.

Goldburg, W.I., 1999. Dynamic light scattering. American Journal of Physics 67, 1152-1160.

Goll, J.H., Stock, G.B., Determination by photon correlation spectroscopy of particle size distributions in lipid vesicle suspensions. Biophysical Journal 19, 265-273.

Gomes, P., Araújo, M.J., Marques, E.F., Falcão, S., Brito, R.O., 2008. Straightforward Method for the Preparation of Lysine-Based Double-Chained Anionic Surfactants. Synthetic Communications 38, 2025-2036.

Goreti Silva, S., Fernandes, R.F., Marques, E.F., do Vale, M.L.C., 2012. Serine-Based Bis-quat Gemini Surfactants: Synthesis and Micellization Properties. European Journal of Organic Chemistry 2012, 345-352.

Gurtovenko, A.A., Anwar, J., 2007. Modulating the Structure and Properties of Cell Membranes: The Molecular Mechanism of Action of Dimethyl Sulfoxide. The Journal of Physical Chemistry B 111, 10453-10460.

Guy, R.H., Hadgraft, J., 2003. Transdermal Drug Delivery - Second Edition, Revised and Expanded. Marcel Dekker, Inc., New York, Basel.

Guyot, M., Fawaz, F., 2000. Design and in vitro evaluation of adhesive matrix for transdermal delivery of propranolol. International Journal of Pharmaceutics 204, 171-182.

Hachem, J.-P., Man, M.-Q., Crumrine, D., Uchida, Y., Brown, B.E., Rogiers, V., Roseeuw, D., Feingold, K.R., Elias, P.M., 2005. Sustained Serine Proteases Activity by Prolonged Increase in pH Leads to Degradation of Lipid Processing Enzymes and Profound Alterations of Barrier Function and Stratum Corneum Integrity. J Investig Dermatol 125, 510-520.

Hadgraft, J., 1999. Passive enhancement strategies in topical and transdermal drug delivery. Int. J. Pharm. 184, 1-6.

Hadgraft, J., 2001. Skin, the final frontier. International Journal of Pharmaceutics 224, 1-18.

Hadgraft, J., 2004. Skin deep. European Journal of Pharmaceutics and Biopharmaceutics 58, 291-299.

Hadgraft, J., Guy, R.H., 1992. Synthetic membranes as biological models. Adv Phar Sc 6, 43-62.

Hadgraft, J., Peck, J., Williams, D.G., Pugh, W.J., Allan, G., 1996. Mechanisms of action of skin penetration enhancers/retarders: Azone and analogues. Int. J. Pharm. 141, 17-25.

Hadgraft, J., Ridout, G., 1987. Development of model membranes for percutaneous absorption measurements. I. Isopropyl myristate. International Journal of Pharmaceutics 39, 149-156.

Hadgraft, J., Ridout, G., 1988. Development of model membranes for percutaneous absorption measurements. II. Dipalmitoyl phosphatidylcholine, linoleic acid and tetradecane. International Journal of Pharmaceutics 42, 97–104.

Hadgraft, J., Walters, K., 1994. Skin penetration enhancement. J Dermatol Treat 5, 43 - 47.

Hadgraft, J., Walters, K., Wotton, P., 1985. Facilitated transport of sodium salicylate across an artificial lipid membrane by Azone. Journal of Pharmacy and Pharmacology 37, 725-727.

Hess, B., Bekker, H., Berendsen, H.J.C., Fraaije, J.G.E.M., 1997. LINCS: A linear constraint solver for molecular simulations. Journal of Computational Chemistry 18, 1463-1472.

Hess, B., Kutzner, C., van der Spoel, D., Lindahl, E., 2008. GROMACS 4: Algorithms for Highly Efficient, Load-Balanced, and Scalable Molecular Simulation. Journal of Chemical Theory and Computation 4, 435-447.

Heuschkel, S., Goebel, A., Neubert, R.H.H., 2008. Microemulsions - modern colloidal carrier for dermal and transdermal drug delivery. Journal of Pharmaceutical Sciences 97, 603-631.

Higuchi, T., 1960. Physical chemical analysis of percutaneous absorption process from creams and ointments. Journal of the Society of Cosmetic Chemists 11, 85-97.

Honzak, L., Sentjurc, M., Swartz, H.M., 2000a. In vivo EPR of topical delivery of a hydrophilic substance encapsulated in multilamellar liposomes applied to the skin of hairless and normal mice. J. Control. Release 66, 221-228.

Honzak, L., Sentjurc, M., Swartz, H.M., 2000b. In vivo EPR of topical delivery of a hydrophilic substance encapsulated in multilamellar liposomes applied to the skin of hairless and normal mice. J. Control. Release 66, 221-228.

Hoppert, M., 2003. Microscopic techniques in biotechnology, Microscopic techniques in biotechnology. Wiley-VCH, Veinheim, p. 114.

Houk, J., Guy, R.H., 1988. Membrane models for skin penetration studies. Chem Rev 88, 455-472.

Huber, L., 1998. Validation and Qualification in Analytical Laboratories. Taylor & Francis.

Humphrey, W., Dalke, A., Schulten, K., 1996. VMD: Visual molecular dynamics. Journal of Molecular Graphics 14, 33-38.

Hussain, S.H., Limthongkul, B., Humphreys, T.R., 2013. The Biomechanical Properties of the Skin. Dermatol. Surg. 39, 193-203.

ICH, 1996. ICH Harmonized Tripartite Guideline. Validation of analytical procedures. Methodology.

Infante, M.R., Pérez, L., Morán, M.C., Pons, R., Mitjans, M., Vinardell, M.P., Garcia, M.T., Pinazo, A., 2010. Biocompatible surfactants from renewable hydrophiles. European Journal of Lipid Science and Technology 112, 110-121.

Infante, M.R., Pérez, L., Pinazo, A., Clapés, P., Morán, M.C., Angelet, M., García, M.T., Vinardell, M.P., 2004. Amino acid-based surfactants. Comptes Rendus Chimie 7, 583-592.

Jahan, L., Ferdaus, R., Shaheen, S.M., Sultan, M.Z., Mazid, M.A., 2011. In vitro transdermal delivery of metformin from a HPMC/ PVA based TDS-patch at different pH. Journal of Scientific Research 3, 661-667.

Jampilek, J., Brychtova, K., 2012. Azone analogues: classification, design, and transdermal penetration principles. Medicinal Research Reviews 32, 907-947.

Jannin, V., Musakhanian, J., Marchaud, D., 2008. Approaches for the development of solid and semi-solid lipid-based formulations. Adv. Drug. Deliver. Rev. 60, 734-746.

Jianxin Guo, Q.P., Lei Zhang, 2000. Transdermal Delivery of Insulin in Mice by Using Lecithin Vesicles as a Carrier. Drug Delivery 7, 113-116.

Karande, P., Jain, A., Ergun, K., Kispersky, V., Mitragotri, S., 2005. Design principles of chemical penetration enhancers for transdermal drug delivery. Proceedings of the National Academy of Sciences of the United States of America 102, 4688-4693.

Karlsson, L., van Eijk, M.C.P., Söderman, O., 2002. Compaction of DNA by Gemini Surfactants: Effects of Surfactant Architecture. Journal of Colloid and Interface Science 252, 290-296.

Kaszuba, M., McKnight, D., Connah, M., McNeil-Watson, F., Nobbmann, U., 2008. Measuring sub nanometre sizes using dynamic light scattering. Journal of Nanoparticle Research 10, 823-829.

Khan, M.A., Pandit, J., Sultana, Y., Sultana, S., Ali, A., Aqil, M., Chauhan, M., Novel carbopol-based transfersomal gel of 5-fluorouracil for skin cancer treatment: in vitro characterization and in vivo study. Drug Delivery 0, 1-8.

Kirby, A.J., Camilleri, P., Engberts, J.B.F.N., Feiters, M.C., Nolte, R.J.M., Söderman, O., Bergsma, M., Bell, P.C., Fielden, M.L., García Rodríguez, C.L., Guédat, P., Kremer, A., McGregor, C., Perrin, C., Ronsin, G., van Eijk, M.C.P., 2003. Gemini Surfactants: New Synthetic Vectors for Gene Transfection. Angewandte Chemie International Edition 42, 1448-1457.

Kirchner, L.A., Moody, R.P., Doyle, E., Bose, R., Jeffery, J., Chu, I., 1997. The prediction of skin permeability by using physicochemical data. Altern. Lab. Anim. 25, 359–370.

Kitagawa, S., Kasamaki, M., A., I., 2000. Effects of n-Alkyltrimethylammonium on Skin Permeation of Benzoic Acid through Excised Guinea Pig Dorsal Skin. Chem. Pharm. Bull. 48, 1698—1701.

Kokubu, M., Oda, K., Machida, M., Shinya, N., 1990. New lidocaine ester derivatives with a prolonged anesthetic effect. Journal of Anesthesia 4, 270-274.

Korsmeyer, R.W., Gurny, R., Doelker, E., Buri, P., Peppas, N.A., 1983. Mechanisms of solute release from porous hydrophilic polymers. Int. J. Pharm. 15, 25-35.

Krishnaiah, Y.S., Al-Saidan, S.M., 2008. Transdermal Permeation of Trimetazidine from Nerodilol-Based HPMC Gel Drug Reservoir System across Rat Epidermis. Medical Principles and Practice 17, 37-42.

Kukol, A., 2009. Lipid Models for United-Atom Molecular Dynamics Simulations of Proteins. Journal of Chemical Theory and Computation 5, 615-626.

Kyrikou, I., Hadjikakou, S.K., Kovala-Demertzi, D., Viras, K., Mavromoustakos, T., 2004. Effects of non-steroid anti-inflammatory drugs in membrane bilayers. Chemistry and Physics of Lipids 132, 157-169.

Lai-Cheong, J.E., McGrath, J.A., 2009. Structure and function of skin, hair and nails. Medicine 37, 223-226.

Lambert, W., Higuchi, W., Knutson, K., Krill, S., 1989a. Dose-Dependent Enhancement Effects of Azone on Skin Permeability. Pharm. Res. 6, 798-803.

Lambert, W.J., Higuchi, W.I., Knutson, K., Krill, S.L., 1989b. Dose-dependent enhancement effects of azone on skin permeability. Pharmaceutical Research 6, 798-803.

Lauer, A.C., Ramachandran, C., Lieb, L.M., Niemiec, S., Weiner, N.D., 1996. Targeted delivery to the pilosebaceous unit via liposomes. Adv. Drug. Deliver. Rev. 18, 311-324.

Le Bars, D., Gozariu, M., Cadden, S.W., 2001. II. Analyse critique des modèles animaux de douleur aiguë. Seconde partie. Annales Françaises d'Anesthésie et de Réanimation 20, 452-470.

Lee, A.J., King, J.R., Barrett, D.A., 1997. Percutaneous absorption: a multiple pathway model. Journal of Controlled Release 45, 141-151.

Legendre, J.Y., Rault, I., Petit, A., Luijten, W., Demuynck, I., Horvath, S., Ginot, Y.M., Cuine, A., 1995. Effects of β-cyclodextrins on skin: implications for the transdermal delivery of piribedil and a novel cognition enhancing-drug, S-9977. Eur. J. Pharm. Sci. 3, 311-322.

Lipinski, C.A., Lombardo, F., Dominy, B.W., Feeney, P.J., 2001. Experimental and computational approaches to estimate solubility and permeability in drug discovery and development settings. Adv. Drug. Deliver. Rev. 46, 3-26.

Liu, Y., Ye, X., Feng, X., Zhou, G., Rong, Z., Fang, C., Chen, H., 2005. Menthol facilitates the skin analgesic effect of tetracaine gel. Int. J. Pharm. 305, 31-36.

Loftsson, T., Brewster, M.E., 1996. Pharmaceutical applications of cyclodextrins .1. Drug solubilization and stabilization. J. Pharm. Sci. 85, 1017-1025.

Loftsson, T., Brewster, M.E., 2012. Cyclodextrins as functional excipients: Methods to enhance complexation efficiency. J. Pharm. Sci. 101, 3019-3032.

Loftsson, T., Duchêne, D., 2007. Cyclodextrins and their pharmaceutical applications. Int. J. Pharm. 329, 1-11.

Loftsson, T., Friôriksdóttir, H., Ingvarsdóttir, G., Jónsdóttir, B., Sigurôardóttir, A.M., 1994. The Influence of 2-Hydroxypropyl-β-Cyclodextrin on Diffusion Rates and Transdermal Delivery of Hydrocortisone. Drug Development and Industrial Pharmacy 20, 1699-1708.

Loftsson, T., Hreinsdottir, D., Masson, M., 2005. Evaluation of cyclodextrin solubilization of drugs. Int. J. Pharm. 302, 18-28.

Loftsson, T., Masson, M., 2001. Cyclodextrins in topical drug formulations: theory and practice. Int. J. Pharm. 225, 15-30.

Loftsson, T., Masson, M., 2004. The effects of water-soluble polymers on cyclodextrins and,cyclodextrin solubilization of drugs. J. Drug Del. Sci. Tech. 14, 35-43.

Loftsson, T., Masson, M., Brewster, M.E., 2004. Self-association of cyclodextrins and cyclodextrin complexes. J. Pharm. Sci. 93, 1091-1099.

Loftsson, T., Vogensen, S.B., Brewster, M.E., Konradsdottir, F., 2007. Effects of cyclodextrins on drug delivery through biological membranes. J. Pharm. Sci. 96, 2532-2546.

Long, S.A., Wertz, P.W., Strauss, J.S., Downing, D.T., 1985. Human stratum corneum polar lipids and desquamation. Archives of Dermatological Research 277, 284-287.

Lopes, S.C.d.A., Giuberti, C.d.S., Rocha, T.G.R., Ferreira, D.d.S., Leite, E.A., Oliveira, M.C., 2013. Liposomes as Carriers of Anticancer Drugs.

López, A., Llinares, F., Cortell, C., Herráez, M., 2000. Comparative enhancer effects of Span®20 with Tween®20 and Azone® on the in vitro percutaneous penetration of compounds with different lipophilicities. Int. J. Pharm. 202, 133-140.

Loukas, Y.L., 1997. Measurement of Molecular Association in Drug: Cyclodextrin Inclusion Complexes with Improved 1H NMR Studies. Journal of Pharmacy and Pharmacology 49, 944-948.

Loukas, Y.L., Vraka, V., Gregoriadis, G., 1998. Drugs, in cyclodextrins, in liposomes: a novel approach to the chemical stability of drugs sensitive to hydrolysis. Int. J. Pharm. 162, 137-142.

Lundström, A., Egelrud, T., 1991. Stratum corneum chymotryptic enzyme: a proteinase which may be generally present in the stratum corneum and with a possible involvement in desquamation. Acta Derm Venereol 71, 471–474.

Lyklema, J., Overbeek, J.T.G., 1961. On the interpretation of electrokinetic potentials. Journal of Colloid Science 16, 501-512.

Macián, M., Seguer, J., Infante, M.R., Selve, C., Vinardell, M.P., 1996. Preliminary studies of the toxic effects of non-ionic surfactants derived from lysine. Toxicology 106, 1-9.

Madison, K.C., 2003a. Barrier Function of the Skin: "La Raison d'Etre" of the Epidermis. J. Invest.Dermatol. 121, 231-241.

Madison, K.C., 2003b. Barrier Function of the Skin: "La Raison d'Etre" of the Epidermis. J Investig Dermatol 121, 231-241.

Maestrelli, F., González-Rodríguez, M.L., Rabasco, A.M., Mura, P., 2006. Effect of preparation technique on the properties of liposomes encapsulating ketoprofen-cyclodextrin complexes aimed for transdermal delivery. Int. J. Pharm. 312, 53-60.

Maghraby, G.M.M.E., Williams, A.C., Barry, B.W., 2001a. Skin delivery of 5-fluorouracil from ultradeformable and standard liposomes in-vitro. Journal of Pharmacy and Pharmacology 53, 1069-1077.

Maghraby, G.M.M.E., Williams, A.C., Barry, B.W., 2001b. Skin hydration and possible shunt route penetration in controlled estradiol delivery from ultradeformable and standard liposomes. Journal of Pharmacy and Pharmacology 53, 1311-1322.

Maghraby, G.M.M.E., Williams, A.C., Barry, B.W., 2006. Can drug-bearing liposomes penetrate intact skin? Journal of Pharmacy and Pharmacology 58, 415-429.

Malde, A.K., Zuo, L., Breeze, M., Stroet, M., Poger, D., Nair, P.C., Oostenbrink, C., Mark, A.E., 2011. An Automated Force Field Topology Builder (ATB) and Repository: Version 1.0. Journal of Chemical Theory and Computation 7, 4026-4037.

Manosroi, A., Kongkaneramit, L., Manosroi, J., 2004. Stability and transdermal absorption of topical amphotericin B liposome formulations. Int. J. Pharm. 270, 279-286.

Marangoci, N., Mares, M., Silion, M., Fifere, A., Varganici, C., Nicolescu, A., Deleanu, C., Coroaba, A., Pinteala, M., Simionescu, B.C., 2011. Inclusion complex of a new propiconazole derivative with β-cyclodextrin: NMR, ESI–MS and preliminary pharmacological studies. Results in Pharma Sciences 1, 27-37.

Marjukka Suhonen, T., A. Bouwstra, J., Urtti, A., 1999. Chemical enhancement of percutaneous absorption in relation to stratum corneum structural alterations. J. Control. Release 59, 149-161.

Marques, H.M.C., Hadgraft, J., Kellaway, I.W., 1990. Studies of cyclodextrin inclusion complexes. I. The salbutamol-cyclodextrin complex as studied by phase solubility and DSC. Int. J. Pharm. 63, 259-266.

Másson, M., Loftsson, T., Másson, G.s., Stefánsson, E., 1999. Cyclodextrins as permeation enhancers: some theoretical evaluations and in vitro testing. J. Control. Release 59, 107-118.

Matsuda, H., Arima, H., 1999. Cyclodextrins in transdermal and rectal delivery. Adv. Drug. Deliver. Rev. 36, 81-99.

McCAFFERTY, D.F., WOOLFSON, A.D., BOSTON, V., 1989. IN VIVO ASSESSMENT OF PERCUTANEOUS LOCAL ANAESTHETIC PREPARATIONS. British Journal of Anaesthesia 62, 17-21.

McClellan, K., Faulds, D., 2000. Ropivacaine. Drugs 60, 1065-1093.

McCormack, B., Gregoriadis, G., 1994a. Drugs-in-cyclodextrins-in liposomes: a novel concept in drug delivery. Int. J. Pharm. 112, 249-258.

McCormack, B., Gregoriadis, G., 1994b. Entrapment of Cyclodextrin-Drug Complexes into Liposomes: Potential Advantages in Drug Delivery. J. Drug. Target. 2, 449 - 454.

McCormack, B., Gregoriadis, G., 1998. Drugs-in-cyclodextrins-in-liposomes: an approach to controlling the fate of water insoluble drugs in vivo. Int. J. Pharm. 162, 59-69.

McCrae, A.F., Jozwiak, H., McClure, J.H., 1995. Comparison of ropivacaine and bupivacaine in extradural analgesia for the relief of pain in labour. British Journal of Anaesthesia 74, 261-265.

McGrath, J.A., Uitto, J., 2010. Anatomy and Organization of Human Skin, Rook's Textbook of Dermatology. Wiley-Blackwell, pp. 1-53.

Meisner, D., Mezei, M., 1995. Liposome ocular delivery systems. Adv. Drug. Deliver. Rev. 16, 75-93.

Menger, F.M., Keiper, J.S., Azov, V., 1999. Gemini Surfactants with Acetylenic Spacers. Langmuir 16, 2062-2067.

Menger, F.M., Littau, C.A., 1991. Gemini-surfactants: synthesis and properties. Journal of the American Chemical Society 113, 1451-1452.

Menger, F.M., Littau, C.A., 1993. Gemini surfactants: a new class of self-assembling molecules. Journal of the American Chemical Society 115, 10083-10090.

Menon, G.K., 2002. New insights into skin structure: scratching the surface. Adv. Drug. Deliver. Rev. 54, Supplement, S3-S17.

Mezei, M., 1993. Liposomes and the skin, in: Gregoriadis, G., Florence, A.T., Patel, H. (Eds.), Liposomes in drug delivery. Harwood Academic, NewYork, pp. 125–137.

Michaels, A.S., Chandrasekaran, S.K., Shaw, J.E., 1975. Drug permeation through human skin: Theory and invitro experimental measurement. AIChE Journal 21, 985-996.

Michniak, B., Thakur, R., Wang, Y., 2005. Essential oils and terpenes, Percutaneous Penetration Enhancers, Second Edition. Informa Healthcare, pp. 159-173.

Michniak, B.B., Player, M.R., Godwin, D.A., Lockhart, C.C., Sowell, J.W., 1998. In vitro evaluation of azone analogs as dermal penetration enhancers: V. Miscellaneous compounds. International Journal of Pharmaceutics 161, 169-178.

Michniak, B.B., Player, M.R., Godwin, D.A., Phillips, C.A., Sowell, J.W., 1995. In vitro evaluation of a series of azone analogs as dermal penetration enhancers: IV. Amines. International Journal of Pharmaceutics 116, 201-209.

Möckel, J., Lippold, B., 1993. Zero-Order Drug Release from Hydrocolloid Matrices. Pharm. Res. 10, 1066-1070.

Moran, M.C., Pinazo, A., Perez, L., Clapes, P., Angelet, M., Garcia, M.T., Vinardell, M.P., Infante, M.R., 2004. "Green" amino acid-based surfactants. Green Chemistry 6, 233-240.

Moser, K., Kriwet, K., Naik, A., Kalia, Y.N., Guy, R.H., 2001. Passive skin penetration enhancement and its quantification in vitro. European Journal of Pharmaceutics and Biopharmaceutics 52, 103-112.

Mosher, G., D. O. Thompson, 2002. Complexation and cyclodextrins, in: Boylan, I.S.a.I.C. (Ed.), Encyclopedia of Pharmaceutical Technology, 2nd edition ed. Marcel Dekker, New York, pp. 531-558.

Motta, S., Sesana, S., Ghidoni, R., Monti, M., 1995. Content of the different lipid classes in psoriatic scale. Archives of Dermatological Research 287, 691-694.

Mowafy, M., Cassens, R.G., 1975. Microscopic structure of pig skin. Journal of Animal Science 41, 1281-1290.

Mura, P., Bettinetti, G., Melani, F., Manderioli, A., 1995. Interaction between naproxen and chemically modified β-cyclodextrins in the liquid and solid state. Eur. J. Pharm. Sci. 3, 347-355.

Naik, A., Kalia, Y.N., Guy, R.H., 2000a. Transdermal drug delivery: overcoming the skin's barrier function. Pharm Sci Technol To 3, 318-326.

Naik, A., Kalia, Y.N., Guy, R.H., 2000b. Transdermal drug delivery: overcoming the skin's barrier function. Pharm. Sci. Technol. To. 3, 318-326.

Nancy, A.M.-R., 2005. Structure and Function of Skin, Dermal Absorption Models in Toxicology and Pharmacology. CRC Press, pp. 1-19.

Nastruzzi, C., Esposito, E., Pastesini, C., Gambari, R., Menegatti, E., 1993. Comparative study on the release kinetics of methyl nicotinate from topical formulations. International Journal of Pharmaceutics 90, 43-50.

Nemes, Z., Steinert, P.M., 1999. Bricks and mortar of the epidermal barrier. Exp Mol Med 31, 5-19.

Neubert, R., Bendas, C., Wolfgang, W., Gienau, B., W., F., 1991. A multilayer membrane system for modelling drug penetration into skin. International Journal of Pharmaceutics 75, 89-94.

Neubert, R., Wohlrab, W., Bendas, C., 1995. Modelling of drug penetration into human skin using a multilayer membrane system. Skin Pharmacol Physi 8, 119-129.

Nilsson, M., Valente, A.J.M., Olofsson, G., Söderman, O., Bonini, M., 2008. Thermodynamic and Kinetic Characterization of Host−Guest Association between Bolaform Surfactants and α- and β-Cyclodextrins. J. Phys. Chem. B 112, 11310-11316.

Nokhodchi, A., Shokri, J., Dashbolaghi, A., Hassan-Zadeh, D., Ghafourian, T., Barzegar-Jalali, M., 2003. The enhancement effect of surfactants on the penetration of lorazepam through rat skin. Int. J. Pharm. 250, 359-369.

Notman, R., Noro, M., O'Malley, B., Anwar, J., 2006. Molecular Basis for Dimethylsulfoxide (DMSO) Action on Lipid Membranes. Journal of the American Chemical Society 128, 13982-13983.

Nuria Perez-Cullell, L.C., Alfonso de la Maza, Jose L. Parra, Joan Estelrich, 2000. Influence of the Fluidity of Liposome Compositions on Percutaneous Absorption. Drug Delivery 7, 7-13.

O'Brien, J., Wilson, I., Orton, T., Pognan, F., 2000. Investigation of the Alamar Blue (resazurin) fluorescent dye for the assessment of mammalian cell cytotoxicity. European Journal of Biochemistry 267, 5421-5426.

O'Brien, L., Taddio, A., Lyszkiewicz, D., Koren, G., 2005. A Critical Review of the Topical Local Anesthetic Amethocaine (Ametop™) for Pediatric Pain. Paediatr. Drugs. 7, 41-54.

Papadopoulou, V., Kosmidis, K., Vlachou, M., Macheras, P., 2006. On the use of the Weibull function for the discernment of drug release mechanisms. Int. J. Pharm. 309, 44-50.

Pellett, M.A., Watkinson, A.C., Hadgraft, J., Brain, R., 1994. An ATR-FTIR investigation of the interactions between vehicles and a synthetic membrane, Proceedings of the International Symposium of Controlled Released Bioactive Materials, pp. 439-440.

Perez, N., Perez, L., Infante, M.R., Garcia, M.T., 2005. Biological properties of arginine-based glycerolipidic cationic surfactants. Green Chemistry 7, 540-546.

PermeGear, I., 2012. Franz diffusion cells.

Piel, G., Piette, M., Barillaro, V., Castagne, D., Evrard, B., Delattre, L., 2006. Betamethasone-in-cyclodextrin-in-liposome: The effect of cyclodextrins on encapsulation efficiency and release kinetics. Int. J. Pharm. 312, 75-82.

Piggot, T.J., Piñeiro, Á., Khalid, S., 2012. Molecular Dynamics Simulations of Phosphatidylcholine Membranes: A Comparative Force Field Study. Journal of Chemical Theory and Computation 8, 4593-4609.

Poger, D., Mark, A.E., 2009. On the Validation of Molecular Dynamics Simulations of Saturated and cis-Monounsaturated Phosphatidylcholine Lipid Bilayers: A Comparison with Experiment. Journal of Chemical Theory and Computation 6, 325-336.

Polishchuk, A.Y., Zaikov, G.E., 1997. Multicomponent transport in polymer systems for controlled release. CRC Press.

Ponec, M., Weerheim, A., Kempenaar, J., Mommaas, A.M., Nugteren, D.H., 1988. Lipid composition of cultured human keratinocytes in relation to their differentiation. Journal of Lipid Research 29, 949-961.

Ponec, M., Weerheim, A., Lankhorst, P., Wertz, P., 2003. New acylceramide in native and reconstructed epidermis. Journal of Investigative Dermatology 120, 581-588.

Potts, R.O., Guy, R.H., 1992. Predicting skin permeability. Pharmaceutical Research 9, 663-669.

Pugh, W.J., Hadgraft, J., 1994. Ab initio prediction of human skin permeability coefficients. International Journal of Pharmaceutics 103, 163-178.

Ragsdale, D., McPhee, J., Scheuer, T., Catterall, W., 1994. Molecular determinants of state-dependent block of Na+ channels by local anesthetics. Science 265, 1724-1728.

Rajewski, R.A., Stella, V.J., 1996. Pharmaceutical applications of cyclodextrins. 2. <I>in vivo</I> drug delivery. J. Pharm. Sci. 85, 1142-1169.

Reifenrath, W.G., Chellquist, E.M., Shipwash, E.A., Jederberg, W.W., 1984. Evaluation of animal models for predicting skin penetration in man. Fund. Appl. Toxicol. 4, S224-S230.

Reimer, K., Fleischer, W., BrÃ¶gmann, B., Schreier, H., Burkhard, P., LanzendÃ¶rfer, A., GÃ¼mbel, H., Hoekstra, H., Behrens-Baumann, W., 1997. Povidone-Iodine Liposomes An Overview. Dermatology 195, 93-99.

Rieger, M., Rhein, L.D., 1997. Surfactants in Cosmetics, Second Edition. Taylor & Francis.

Riviere, J., Heit, M., 1997. Electrically-Assisted Transdermal Drug Delivery. Pharm. Res. 14, 687-697.

Riviere, J.E., 2006. Dermal absorption models in toxicology and pharmacology. CRC Press, Boca Raton,.

Roberts, M., Mueller, K., 1990. Comparisons of in Vitro Nitroglycerin (TNG) Flux Across Yucatan Pig, Hairless Mouse, and Human Skins. Pharm. Res. 7, 673-676.

Roberts, M.S., Pugh, W.J., Hadgraft, J., 1996. Epidermal permeability: Penetrant structure relationships. 2. The effect of h-bonding groups in penetrants on their diffusion through the stratum corneum. Int. J. Pharm. 132, 23-32.

Robson, K.J., Stewart, M.E., Michelsen, S., Lazo, N.D., Downing, D.T., 1994. 6-Hydroxy-4-sphingenine in human epidermal ceramides. Journal of Lipid Research 35, 2060-2068.

Romsing, J., Henneberg, S.W., Walther-Larsen, S., Kjeldsen, C., 1999. Tetracaine gel vs EMLA cream for percutaneous anaesthesia in children. British Journal of Anaesthesia 82, 637-638.

Roy, D., Semsarilar, M., Guthrie, J.T., Perrier, S., 2009. Cellulose modification by polymer grafting: a review. Chemical Society Reviews 38, 2046-2064.

Russeau, W., Mitchell, J., Tetteh, J., Lane, M.E., Hadgraft, J., 2009. Investigation of the permeation of model formulations and a commercial ibuprofen formulation in Carbosil® and human skin using ATR-FTIR and multivariate spectral analysis. International Journal of Pharmaceutics 374, 17-25.

Ryman-Rasmussen, J.P., Riviere, J.E., Monteiro-Riviere, N.A., 2006. Penetration of Intact Skin by Quantum Dots with Diverse Physicochemical Properties. Toxicological Sciences 91, 159-165.

Sadlej-Sosnowska, N., 1997. Fluorometric determination of association constants of three estrogens with cyclodextrins. J. Fluoresc. 7, 195-200.

Sanchez, L., Mitjans, M., Infante, M.R., Vinardell, M.P., 2004. Assessment of the Potential Skin Irritation of Lysine-Derivative Anionic Surfactants Using Mouse Fibroblasts and Human Keratinocytes as An Alternative to Animal Testing. Pharm. Res. 21, 1637-1641.

Sanchez, L., Mitjans, M., Infante, M.R., Vinardell, M.P., 2006. Potential irritation of lysine derivative surfactants by hemolysis and HaCaT cell viability. Toxicology Letters 161, 53-60.

Scalia, S., Villani, S., Casolari, A., 1999. Inclusion Complexation of the Sunscreen Agent 2-Ethylhexyl-p-dimethylaminobenzoate with Hydroxypropyl-β-cyclodextrin: Effect on Photostability. Journal of Pharmacy and Pharmacology 51, 1367-1374.

Schecter, A.K., Pariser, D.M., Pariser, R.J., Ling, M.R., Stewart, D., Sadick, N.S., 2005. Randomized, Double-Blind, Placebo-Controlled Study Evaluating the Lidocaine/Tetracaine Patch for Induction of Local Anesthesia prior to Minor Dermatologic Procedures in Geriatric Patients. Dermatol. Surg. 31, 287-291.

Scheindlin, S., 2004. Transdermal Drug Delivery: PAST, PRESENT, FUTURE. Mol Interv 4, 308-312.

Scheuplein, R.J., 1967. Mechanism of Percutaneous Absorption. The Journal of Investigative Dermatology 48, 79-88.

Scheuplein, R.J., Blank, I.H., 1971. Permeability of the skin. Physiol. Rev. 51, 702-747.

Scheuplein, R.J., Ross, L.W., 1974. MECHANISM OF PERCUTANEOUS ABSORPTION. V. PERCUTANEOUS ABSORPTION OF SOLVENT DEPOSITED SOLIDS. J Investig Dermatol 62, 353-360.

Schmid, M.H., Korting, H.C., 1996. Therapeutic progress with topical liposome drugs for skin disease. Adv. Drug. Deliver. Rev. 18, 335-342.

Schmitz, G., Müller, G., 1991. Structure and function of lamellar bodies, lipid-protein complexes involved in storage and secretion of cellular lipids. Journal of Lipid Research 32, 1539-1570.

Schmook, F.P., Meingassner, J.G., Billich, A., 2001. Comparison of human skin or epidermis models with human and animal skin in in-vitro percutaneous absorption. Int. J. Pharm. 215, 51-56.

Schneider, H.-J., Hacket, F., Rüdiger, V., Ikeda, H., 1998. NMR Studies of Cyclodextrins and Cyclodextrin Complexes. Chem. Rev. 98, 1755-1786.

Schott, H., 1985. Surfactant systems: Their chemistry, pharmacy and biology. By D. Attwood and A. T. Florence. Chapman & Hall, London EC4P 4EE, United Kingdom. 1983. 794 pp. Journal of Pharmaceutical Sciences 74, 1140-1141.

Schreier, H., Bouwstra, J., 1994. Liposomes and niosomes as topical drug carriers: dermal and transdermal drug delivery. Journal of Controlled Release 30, 1-15.

Schuler, L.D., Daura, X., van Gunsteren, W.F., 2001. An improved GROMOS96 force field for aliphatic hydrocarbons in the condensed phase. Journal of Computational Chemistry 22, 1205-1218.

Schuttelkopf, A.W., van Aalten, D.M.F., 2004. PRODRG: a tool for high-throughput crystallography of protein-ligand complexes. Acta Crystallographica Section D 60, 1355-1363.

Shabir, G.A., 2003. Validation of high-performance liquid chromatography methods for pharmaceutical analysis: Understanding the differences and similarities between validation requirements of the US Food and Drug Administration, the US Pharmacopeia and the International Conference on Harmonization. Journal of Chromatography A 987, 57-66.

Sheihet, L., Chandra, P., Batheja, P., Devore, D., Kohn, J., Michniak, B., 2008. Tyrosine-derived nanospheres for enhanced topical skin penetration. International Journal of Pharmaceutics 350, 312-319.

Shin, S.-C., Cho, C.-W., Oh, I.-J., 2001. Effects of non-ionic surfactants as permeation enhancers towards piroxicam from the poloxamer gel through rat skins. Int. J. Pharm. 222, 199-203.

Shin, S.-C., Cho, C.-W., Yang, K.-H., 2004. Development of lidocaine gels for enhanced local anesthetic action. International Journal of Pharmaceutics 287, 73-78.

Shokri, J., Nokhodchi, A., Dashbolaghi, A., Hassan-Zadeh, D., Ghafourian, T., Barzegar Jalali, M., 2001. The effect of surfactants on the skin penetration of diazepam. Int. J. Pharm. 228, 99-107.

Shukla, D., Tyagi, V.K., 2006a. Gemini surfactants: A review. Journal of Oleo Science 55, 381-190.

Shukla, D., Tyagi, V.K., 2006b. Gemini Surfactants: A Review. J Oleo Sci 55, 381-190.

Siepmann, J., Peppas, N.A., 2001. Modeling of drug release from delivery systems based on hydroxypropyl methylcellulose (HPMC). Adv. Drug. Deliver. Rev. 48, 139-157.

Siepmann, J., Peppas, N.A., 2011. Higuchi equation: Derivation, applications, use and misuse. Int. J. Pharm. 418, 6-12.

Silva, S.C., Sousa, J.S., Marques, E., Pais, A.C.C., Michniak-Kohn, B., 2013a. Structure Activity Relationships in Alkylammonium C12-Gemini Surfactants Used as Dermal Permeation Enhancers. AAPS J. 15, 1119-1127.

Silva, S.G., Alves, C., Cardoso, A.M.S., Jurado, A.S., Pedroso de Lima, M.C., Vale, M.L.C., Marques, E.F., 2013b. Synthesis of Gemini Surfactants and Evaluation of Their Interfacial and Cytotoxic Properties: Exploring the Multifunctionality of Serine as Headgroup. European Journal of Organic Chemistry 2013, 1758-1769.

Silva, S.G., Rodríguez-Borges, J.E., Marques, E.F., do Vale, M.L.C., 2009. Towards novel efficient monomeric surfactants based on serine, tyrosine and 4-hydroxyproline: synthesis and micellization properties. Tetrahedron 65, 4156-4164.

Silva, S.M.C., Hu, L., Sousa, J.J.S., Pais, A.A.C.C., Michniak-Kohn, B.B., 2012. A combination of nonionic surfactants and iontophoresis to enhance the transdermal drug delivery of ondansetron HCl and diltiazem HCl. European Journal of Pharmaceutics and Biopharmaceutics 80, 663-673.

Simonsson, C., 2011. New insights in contact allergy and drug delivery : a study of formulation effects and hapten targets in skin using two-photon fluorescence microscopy. Gothenburg: Department of Chemistry.

Skelly, J., Shah, V., Maibach, H., Guy, R., Wester, R., Flynn, G., Yacobi, A., 1987. FDA and AAPS Report of the Workshop on Principles and Practices of In Vitro Percutaneous Penetration Studies: Relevance to Bioavailability and Bioequivalence. Pharm. Res. 4, 265-267.

Smith, V., Ndou, T., Muñoz De La Peña, A., Warner, I., 1991. Spectral characterization of β-Cyclodextrin : Triton X-100 complexes. J. Inclus. Phenom. Mol. 10, 471-484.

Sriamornsak, P., Sungthongjeeh, S., 2007. Modification of theophylline release with alginate gel formed in hard capsules. AAPS PharmSciTech 8, E1-E8.

Srinivasan, V., Higuchi, W.I., Su, M.-H., 1989. Baseline studies with the four-electrode system: The effect of skin permeability increase and water transport on the flux of a model uncharged solute during iontophoresis. J. Control. Release 10, 157-165.

Stella, V.J., Rajewski, R.A., 1997. Cyclodextrins: Their Future in Drug Formulation and Delivery. Pharm. Res. 14, 556-567.

Stewart, M.E., Downing, D.T., 1999. A new 6-hydroxy-4-sphingenine-containing ceramide in human skin. Journal of Lipid Research 40, 1434-1439.

Sudo, S., Ohtomo, T., Otsuka, K., 2013. Easy measurement and analysis method of zeta potential and electrophoretic mobility of water-dispersed colloidal particles by using a self-mixing solid-state laser. Journal of Applied Physics 114, -.

Suzuki, Y., Nomura, J., Koyama, J., Horii, I., 1994. The role of proteases in stratum corneum: involvement in stratum corneum desquamation. Archives of Dermatological Research 286, 249-253.

Szejtli, J., 1998. Introduction and General Overview of Cyclodextrin Chemistry. Chem. Rev. 98, 1743-1754.

Szejtli, J., 2005. Cyclodextrin Complexed Generic Drugs are Generally not Bio-equivalent with the Reference Products: Therefore the Increase in Number of Marketed Drug/Cyclodextrin Formulations is so Slow. J. Incl. Phenom. Macrocycl. Chem. 52, 1-11.

Tan, E.L., Lid, J.-C., Chien, Y.W., 1993. Effect of Cationic Surfactants on the Transdermal Permeation of Ionized Indomethacin. Drug Development and Industrial Pharmacy 19, 685-699.

Tehrani-Bagha, A.R., Oskarsson, H., van Ginkel, C.G., Holmberg, K., 2007. Cationic ester-containing gemini surfactants: Chemical hydrolysis and biodegradation. Journal of Colloid and Interface Science 312, 444-452.

Teixeira, R.S., Cova, T.F.G.G., Silva, S.M.C., Oliveira, R., Araújo, M.J., Marques, E.F., Pais, A.A.C.C., Veiga, F.J.B., Lysine-based surfactants as chemical permeation enhancers for dermal delivery of local anesthetics. Int. J. Pharm.

Teixeira, R.S., Cova, T.F.G.G., Silva, S.M.C., Oliveira, R., Araújo, M.J., Marques, E.F., Pais, A.A.C.C., Veiga, F.J.B., 2014a. Lysine-based surfactants as chemical permeation enhancers for dermal delivery of local anesthetics. Int. J. Pharm. 474, 212-222.

Teixeira, R.S., Veiga, F.J.B., Oliveira, R.S., Jones, S.A., Silva, S.M.C., Carvalho, R.A., Valente, A.J.M., 2014b. Effect of Cyclodextrins and pH on the permeation of tetracaine: Supramolecular assemblies and release behavior. Int. J. Pharm. 466, 349-358.

Thomas, B.J., Finnin, B.C., 2004. The transdermal revolution. Drug Discov Today 9, 697-703.

Tojo, K., 1987. Random brick model for drug transport across stratum corneum. Journal of Pharmaceutical Sciences 76, 889-891.

Torchilin, V.P., 2001. Structure and design of polymeric surfactant-based drug delivery systems. J. Control. Release 73, 137-172.

Touitou, E., Dayan, N., Bergelson, L., Godin, B., Eliaz, M., 2000. Ethosomes — novel vesicular carriers for enhanced delivery: characterization and skin penetration properties. Journal of Controlled Release 65, 403-418.

Touitou, E., Junginger, H.E., Weiner, N.D., Nagai, T., Mezei, M., 1994. Liposomes as carriers for topical and transdermal delivery. Journal of Pharmaceutical Sciences 83, 1189-1203.

Trommer, H., Neubert, R.H.H., 2006. Overcoming the Stratum Corneum: The Modulation of Skin Penetration. Skin Pharmacology and Physiology 19, 106-121.

Tsai, J.C., Guy, R.H., Thornfeldt, C.R., Gao, W.N., Feingold, K.R., Elias, P.M., 1996. Metabolic approaches to enhance transdermal drug delivery. 1. Effect of lipid synthesis inhibitors. Journal of Pharmaceutical Sciences 85, 643-648.

Turesson, I., Thames, H.D., Repair capacity and kinetics of human skin during fractionated radiotherapy: Erythema, desquamation, and telangiectasia after 3 and 5 year's follow-up. Radiotherapy and Oncology 15, 169-188.

Uekama, K., Hirayama, F., Irie, T., 1998. Cyclodextrin Drug Carrier Systems. Chem. Rev. 98, 2045-2076.

van den Bergh, B.A.I., Wertz, P.W., Junginger, H.E., Bouwstra, J.A., 2001. Elasticity of vesicles assessed by electron spin resonance, electron microscopy and extrusion measurements. Int. J. Pharm. 217, 13-24.

van der Spoel, D., van Maaren, P.J., Caleman, C., 2012. GROMACS molecule & liquid database. Bioinformatics 28, 752-753.

Van Santvliet, L., Caljon, K., Pieters, L., Ludwig, A., 1998. Physicochemical properties, NMR spectroscopy and tolerance of inclusion complexes of antazoline and tetracaine with hydroxypropyl- β -cyclodextrin. Int. J. Pharm. 171, 147-156.

Veiga, F.J., eacute, Baptista, Fernandes, C.M., Carvalho, R.A., Geraldes, C.F.G.C., 2001. Molecular Modelling and ¹H-NMR: Ultimate Tools for the Investigation of Tolbutamide: β-Cyclodextrin and Tolbutamide: Hydroxypropyl-β-Cyclodextrin Complexes. Chemical and Pharmaceutical Bulletin 49, 1251-1256.

Vemuri, S., Rhodes, C.T., 1995. Preparation and characterization of liposomes as therapeutic delivery systems: a review. Pharmaceutica Acta Helvetiae 70, 95-111.

Ventura, C.A., Giannone, I., Paolino, D., Pistarà, V., Corsaro, A., Puglisi, G., 2005. Preparation of celecoxib-dimethyl-[beta]-cyclodextrin inclusion complex: characterization and in vitro permeation study. European Journal of Medicinal Chemistry 40, 624-631.

Ventura, C.A., Tommasini, S., Falcone, A., Giannone, I., Paolino, D., Sdrafkakis, V., Mondello, M.R., Puglisi, G., 2006. Influence of modified cyclodextrins on solubility and percutaneous absorption of celecoxib through human skin. Int. J. Pharm. 314, 37-45.

Verma, D.D., Verma, S., Blume, G., Fahr, A., 2003a. Liposomes increase skin penetration of entrapped and non-entrapped hydrophilic substances into human skin: a skin penetration and confocal laser scanning microscopy study. European Journal of Pharmaceutics and Biopharmaceutics 55, 271-277.

Verma, D.D., Verma, S., Blume, G., Fahr, A., 2003b. Particle size of liposomes influences dermal delivery of substances into skin. Int. J. Pharm. 258, 141-151.

Verma, P.R.P., Murthy, T.E.G.K., 1997. Transdermal flurbiprofen delivery using HPMC matrices: design, in vitro and in vivo evaluation. Drug Development and Industrial Pharmacy 23, 633-638.

Vieira, D.B., Carmona-Ribeiro, A.M., 2006. Cationic lipids and surfactants as antifungal agents: mode of action. Journal of Antimicrobial Chemotherapy 58, 760-767.

Viscardi, G., Quagliotto, P., Barolo, C., Savarino, P., Barni, E., Fisicaro, E., 2000. Synthesis and Surface and Antimicrobial Properties of Novel Cationic Surfactants. The Journal of Organic Chemistry 65, 8197-8203.

Vitorino, C., Almeida, J., Gonçalves, L.M., Almeida, A.J., Sousa, J.J., Pais, A.A.C.C., 2013. Co-encapsulating nanostructured lipid carriers for transdermal application: From experimental design to the molecular detail. J. Control. Release 167, 301-314.

Vives, M.A., Infante, M.R., Garcia, E., Selve, C., Maugras, M., Vinardell, M.P., 1999. Erythrocyte hemolysis and shape changes induced by new lysine-derivate surfactants. Chemico-Biological Interactions 118, 1-18.

Vives, M.A., Macián, M., Seguer, J., Infante, M.R., Vinardell, M.P., 1997. Hemolytic Action of Anionic Surfactants of the Diacyl Lysine Type. Comparative Biochemistry and Physiology Part C: Pharmacology, Toxicology and Endocrinology 118, 71-74.

Vollmer, U., Müller, B.W., Peeters, J., Mesens, J., Wilffert, B., Peters, T., 1994. A Study of the Percutaneous Absorption-enhancing Effects of Cyclodextrin Derivatives in Rats. Journal of Pharmacy and Pharmacology 46, 19-22.

Vyas, A., Saraf, S., Saraf, S., 2008. Cyclodextrin based novel drug delivery systems. J. Incl. Phenom. Macrocycl. Chem. 62, 23-42.

Walters, K.A., 2002a. Dermatological and Transdermal Formulations. Marcel Dekker, New York.

Walters, K.A., 2002b. Dermatological and transdermal formulations, New York ed.

Walters, K.A., Bialik, W., Brain, K.R., 1993a. The effects of surfactants on penetration across the skin. Int J Cosmetic Sci 15, 260-271.

Walters, K.A., Bialik, W., Brain, K.R., 1993b. The effects of surfactants on penetration across the skin*. International Journal of Cosmetic Science 15, 260-271.

Weiner, N., Lieb, L., Niemiec, S., Ramachandran, C., Hu, Z., Egbaria, K., 1994. Liposomes: A Novel Topical Delivery System for Pharmaceutical and Cosmetic Applications. J. Drug. Target. 2, 405 - 410.

Wertz, P.W., 2000. Lipids and barrier function of the skin. Acta Derm Venereol Supp 208, 7-11.

Wertz, P.W., Miethke, M.C., Long, S.A., Strauss, J.S., Downing, D.T., 1985. The composition of the ceramides from human stratum corneum and from comedones. Journal of Investigative Dermatology 84, 410-412.

Wertz, P.W., Swartzendruber, D.C., Abraham, W., Madison, K.C., Downing, D.T., 1987. ESsential fatty acids and epidermal integrity. Archives of Dermatology 123, 1381-1384.

Wickett, R.R., Visscher, M.O., 2006. Structure and function of the epidermal barrier. American journal of infection control 34, S98-S110.

Williams, A.C., Barry, B.W., 1989. Essential oils as novel human skin penetration enhancers. Int. J. Pharm. 57, R7-R9.

Williams, A.C., Barry, B.W., 1991. The enhancement index concept applied to terpene penetration enhancers for human skin and model lipophilic (oestradiol) and hydrophilic (5-fluorouracil) drugs. Int. J. Pharm. 74, 157-168.

Williams, A.C., Barry, B.W., 2004. Penetration enhancers. Advanced Drug Delivery Reviews 56, 603-618.

Williams, A.C., Barry, B.W., 2012. Penetration enhancers. Adv. Drug. Deliver. Rev. 64, Supplement, 128-137.

Williams, A.C., Shatri, S.R.S., Barry, B.W., 1998. Transdermal Permeation Modulation by Cyclodextrins: A Mechanistic Study. Pharmaceutical Development and Technology 3, 283-296.

Woodford, R., Barry, B.W., 1986. Penetration Enhancers and the Percutaneous Absorption of Drugs: An Update. Cutaneous and Ocular Toxicology 5, 167-177.

Woodley, D.T., 1987. Importance of the Dermal-Epidermal Junction and Recent Advances. Dermatology 174, 1-10.

Yang, P., Singh, J., Wettig, S., Foldvari, M., Verrall, R.E., Badea, I., 2010. Enhanced gene expression in epithelial cells transfected with amino acid-substituted gemini nanoparticles. European Journal of Pharmaceutics and Biopharmaceutics 75, 311-320.

Yuan, C., Du, L., Jin, Z., Xu, X., 2013. Storage stability and antioxidant activity of complex of astaxanthin with hydroxypropyl-β-cyclodextrin. Carbohyd. Polym. 91, 385-389.

Zana, R., 2002a. Dimeric (gemini) surfactants: Effect of the spacer group on the association behavior in aqueous solution. Journal of Colloid and Interface Science 248, 203-220.

Zana, R., 2002b. Dimeric and oligomeric surfactants. Behavior at interfaces and in aqueous solution: a review. Advances in Colloid and Interface Science 97, 205-253.

Zana, R., Benrraou, M., Rueff, R., 1991. Alkanediyl-.alpha.,.omega.-bis(dimethylalkylammonium bromide) surfactants. 1. Effect of the spacer chain length on the critical micelle concentration and micelle ionization degree. Langmuir 7, 1072-1075.

Zana, R., Talmon, Y., 1993. Dependence of aggregate morphology on structure of dimeric surfactants. Nature 362, 228-230.

Zhang, Y.-T., Xu, Y.-M., Zhang, S.-J., Zhao, J.-H., Wang, Z., Xu, D.-Q., Feng, N.-P., 2014. In vivo microdialysis for the evaluation of transfersomes as a novel transdermal delivery vehicle for cinnamic acid. Drug Development and Industrial Pharmacy 40, 301-307.

Zink, W., Graf, B., 2004. Benefit-Risk Assessment of Ropivacaine in the Management of Postoperative Pain. Drug Safety. 27, 1093-1114.

Appendix

A. Simultaneous quantification of tetracaine and ropivacaine using a rapid reversed-phase HPLC method

The characterization of the formulations in terms of drug content described in the previous Chapters followed a suitable and validated method.

In this appendix, it is reported the development and validation of a simple new HPLC method for simultaneous quantification of tetracaine and ropivacaine. The validated method was used to determine both the content of TC and RPC incorporated in the liposomes.

1.A. Materials

TC and ammonium acetate were acquired from Sigma Aldrich (St. Louis, MO, United States of America**)**. HP-*β*-CD with 97% of purity, with an average degree of substitution of 2 to 6 units of 2-hydroxypropyl (C_3H_7O) per glucose unit, and with an average molecular weight of 1380 g/mol, was purchased from Acros Organic (Geel, Belgium). RPC was a gift from AstraZeneca (London, United Kingdom). MeOH and ACN HPLC grade were purchased from LiChroSolv Merck (Darmstadt, Germany). Grade A volumetric flasks were purchase from Fisher (Loughbrough,UK). Clear glass HPLC vials (2 ml) and 0.350 mL inserts were acquired from Supelco - Sigma Aldrich (St. Louis, MO, United States of America**)**. All reactants were used as received.

2.A. Instrumentation and chromatographic conditions

The HPLC analysis of TC and RPC was carried out using a Shimadzu LC-2010C HT apparatus (Shimadzu Co., Kyoto, Japan) equipped with a quaternary pump, a vacuum degasser, an autosampler unit, and a L2450 UV/visible dual wavelength detector and the chromatographic analysis were conducted in isocratic mode. The quantification of both drugs was carried out using a Phenomenex® reverse phase C_{18} column Luna (Torrance, CA, USA) with 5 µm particle size and 250 mm x 4.6 mm length with a SecurityGuard™ cartridge Phenomenex® (Torrance, CA, USA) as the stationary phase, at 25°C. The results were processed using Shimadzu LC-solution software version 1.12. The mobile phase was prepared by mixing methanol, acetonitrile and ammonium acetate solution on the proportions 7:7:6 respectively. The solution was subsequently filtered using a 0.45 µm Nylon membrane (Supelco Analytical, Bellefonte, USA) and sonicated for 1 h prior to use. The detection was carried out at 311 nm for TC and 210 nm for RPC. The injection volume used was 25 µL for all standards and samples and the mobile phase flow rate was set to 1.0 mL min^{-1}. In these conditions the run time was established for 15 min to allow the separation of all compounds (Table 7-1).

Table 7-1 Standard HPLC conditions for the analysis of tetracaine and ropivacaine.

Conditions	Tetracaine	Ropivacaine
mobile phase (acetonitrile: methanol: amonium acetate)	35:35:30	
flow rate (mL/min)	1	
temperature (°C)	25 ± 2	
injection volume (µl)	25	
UV detection wavelength (nm)	311	210
detection sensitivity	0.025	0.025
run time	ca. 6.9	ca. 9.1
quantitative method	Total peak area	

3.A. Preparation of stock solutions, calibration standards and quality controls

Three stock solutions were prepared. TC and RPC together were prepared in a final concentration of ca. 1 mg/mL. The drugs were accurately weighed (5 mg) and added to 5 mL of mobile phase in a Grade A volumetric flask. Eight standard solutions containing TC and RPC (0.1, 0.5, 1, 5, 10, 50 and 100 µg/mL) were obtained by diluting each initial stock solution with PBS. The calibration standards were run in series. Six injections of 0.1, 1 and 10 µg/mL standards were prepared and were considered as quality control (QC). For determination of the limit of detection (LOD) and limit of quantitation (LOQ) of the method, three runs were completed on a single day with the same set of standards, followed by two further runs completed on two separate days with a fresh set of standards on each day. The standard HPLC conditions were set constant throughout the set of experiments. All stock solutions were stored at -20 ºC.

4.A. Method validation

The HPLC method was developed and validated according to US Food and Drug Administration (FDA) regulations (das Neves et al., 2010; Huber, 1998). The linearity, precision, limits of detection and quantification parameters were calculated.

4.1.A. System suitability

The standard solution containing TC and RPC at concentration 10 µg/mL was injected 6 times to determine the system suitability. The capacity factor (k'), resolution (Rs) tailing factor (T) and theoretical plate number (N) were also considered (Shabir, 2003) (Table 7-2). The capacity factor is a measure of where the peak of interest is located with respect to the void volume, i.e., corresponds to the elution time of the non-retained components. R is a measure of the degree of separation of two peaks. The tailing factor is a measure of the peak symmetry, and the theoretical plate number is a measure of the column efficiency, that is, how many peaks can be located per unit run-time of the chromatogram.

Table 7-2 System suitability test parameters.

	Tetracaine (10 µg/mL)		**Ropivacaine (10 µg/mL)**	
	Retention time	**Peak area**	**Retention time**	**Peak area**
Mean (n = 6)	6.88	1744801	9.15	859807.5
S. D.	0.05	28974	0.05	16592.3
% RSD	0.72	1.64	0.54	1.93
Theoretical plates (N)	5495.501		7123.755	
Capacity factory (K)	1.696		2.814	
Tailing factor (T)	1.681		1.559	
Resolution (Rs)	15.467		2.710	

According to results the RSD of peak area and retention time for both drugs were lower than 2 % that is the acceptance limit according to the guidelines (Table 7-2). These values indicate that the two compounds can be analyzed simultaneous for the same system. The tailing factor (T), resolution (R_s) and capacity factor (k') show that the peaks were symmetric and generally well resolved indicating optimal column efficiency.

4.2.A. Linearity

Calibration curves from different stock solutions were constructed over the concentration range 0.1-50 mg/mL for TC (Figure 7.1) and RPC (Figure 7.2). The regression equation and the determination coefficient (R^2) obtained from the least squares method was estimated. Linearity of the peak area of eight standard solutions as a function of TC and RPC concentration was determined through the calculation of a regression line analysis using Origin® graphing and analysis (OriginLab Corp, Northampton, USA).

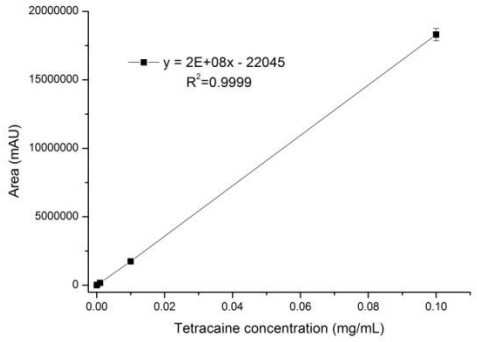

Figure 7.1 Linearity studies for the developed HPLC method: calibration curves obtained for tetracaine.

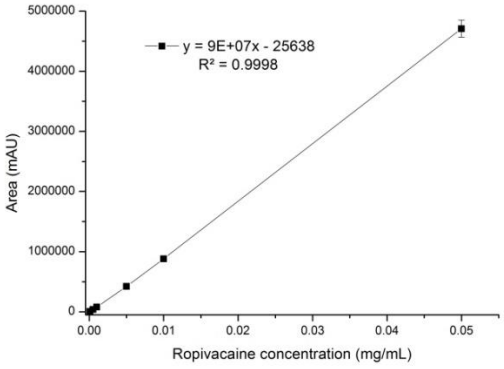

Figure 7.2 Linearity studies for the developed HPLC method: calibration curves obtained for ropivacaine.

Table 7-3 Results obtained from the regression analysis by the least squares method for TC and RPC.

Analyte	Mean R^2 ± S.E.	Mean slope.	Mean intercept
Tetracaine	0.9999 ± 0.0003	$2x10^8$	22045
Ropivacaine	0.9998 ± 0.0005	$9x10^7$	25638

a *Intercept is expressed in mg/mL.*

Each calibration curves has a correlation higher than 0.999 indicating a good linearity confirming that the method as linear between 0.1 and 50 µg/mL. This complies with recommendations e.g. from references (das Neves et al., 2010; Shabir, 2003) (Table 7-3).

4.3.A. Specificity

The specificity of the method was obtained analyzing the solutions in the Franz diffusion cells medium (PBS). The specificity is the capability of the method to accurately measure the analyte in the presence of all potential sample components. As shown, the medium supernatant did not exhibit any peaks interfering with analytes retention times, thus indicating that the method is specific (Figure 7.3).

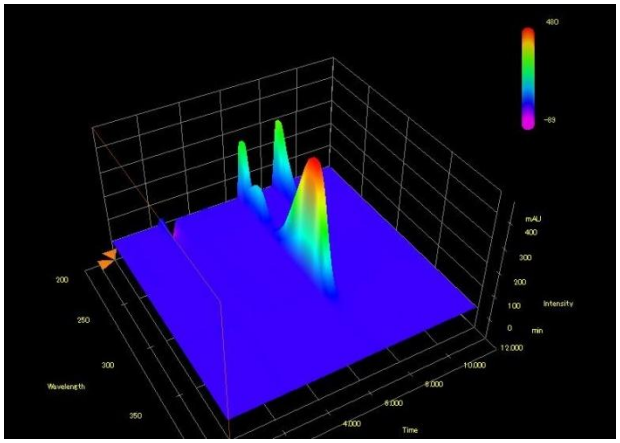

Figure 7.3 Chromatograms 3D of TC and RPC determined in the receptor medium (PBS pH = 7.4).

4.4.A. Limits of detection and quantification

The limits of detection and quantitation were determined based on different calibration curves obtained from different standard solutions. The limit of detection of an analytical procedure (LOD) is defined as the lowest amount of an analyte in a sample that can be

quantitatively determined with suitable precision and accuracy (International Conference on Harmonisation of Technical Requirements for Registration of Pharmaceuticals for Human Use 1996) (ICH, 1996). The LOD and LOQ of the system were determined using Eq. 7.1 and 7.2, respectively, from peak area data pooled over three days

$$LOD = Y_B + 3S_B \quad (7.1)$$

$$LOQ = Y_B + 10S_B \quad (7.2)$$

where Y_B is the Y intercept from regression equation and S_B the standard error of the Y estimate.

Table 7-4 Detection limit and quantification detection for the analytical procedure

	Limits of detection (µg/mL)	Limits of quantification (µg/mL)
Tetracaine	0.706	2.353
Ropivacaine	0.101	0.791

The limits of detection and quantification were calculated using a summation of the data from five calibration curves (shown in Figure 7.1 and Figure 7.2). The estimated LOD was 0.706 µg/ml and LOQ 2.353 µg/ml for the tetracaine method. The estimated LOD and LOQ found for ropivacaine were 0.101 and 0.791 µg/mL, respectively (Table 7-4).

4.5.A. Precision

Precision indicates the degree of scatter between a series of measurements obtained from multiple sampling of the same homogeneous sample. Three standard solutions (quality controls), 0.1, 1 and 10 µg/mL, respectively were prepared six times each and analyzed. Inter-day and intra-day variation were compared using three runs on a single day with one set of standards and three individual sets of standards analysed on three separate days. The relative standard deviation (RSD) determined at each concentration level should not exceed 15%, except for the lower limit of quantitation, where it should not exceed 20 % (Ali and Nazzal, 2009).

Precision for the quality controls in the intra-day and inter-day run are shown in Table 7-5. The intra- and inter-day RSD values did not exceed 10% which is in agreement with acceptance recommendations. These data indicate that the developed method is reliable and reproducible.

Table 7-5 Intra-day and inter-day precision and accuracy results for TC and RPC

	Intraday (n=6)		Interday (n=18)	
Nominal concentration (µg/mL)	**Measured Concentration (µg/mL) Mean±SD**	**Precision % RSD**	**Measured Concentration (µg/mL) Mean±SD**	**Precision % RSD**
TC - 0.1	0.21 ± 0.01	3.24	0.22 ± 0.01	1.61
TC – 1	0.95 ± 0.04	4.14	0.96 ± 0.02	1.53
TC -10	8.84 ± 0.32	3.60	8.82 ± 0.14	1.58
RPC – 0.1	0.355 ± 0.001	0.08	0.356 ± 0.001	0.27
RPC – 1	1.13 ± 0.01	1.29	1.56 ± 0.05	4.14
RPC – 10	9.83 ± 0.18	1.87	10.13 ± 0.60	5.99

5.A. Conclusion

A specific, linear, suitable, reliable and reproducible new method for the simultaneous quantitation of TC and RPC was developed and validated over the range 0.1-100 µg/mL. The method was successfully applied to measure the drug content in LPS formulation after preparation.

"Sentes que um tempo acabou
Primavera de flor adormecida
Qualquer coisa que não volta, que voou
Que foi um rio, um ar, na tua vida

E levas em ti guardado
O choro de uma balada
Recordações do passado
O bater da velha cabra

Sabes que o desenho do adeus
É fogo que nos queima devagar
E no lento cerrar dos olhos teus
Fica esperança de um dia aqui voltar

Capa negra de saudade
No momento da partida
Segredos desta cidade
Levo comigo p'ra vida"

Balada de despedida – Fado de Coimbra

Coimbra – Paço das escolas 31 Julho 2014

O espírito do vencer está no acreditar